Qualitative and quantitative analysis of MRI data from patients with ~~chronic partial~~ epilepsy

by

Sanjay Mull Sisodiya

A thesis submitted to

The University of London

in partial fulfilment of the requirements

for the degree of PhD.

1996

Department of Clinical Neurology

Institute of Neurology

London

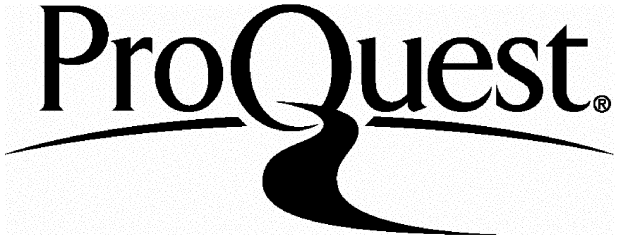

ABSTRACT

Cerebral dysgenesis is the second commonest cause of refractory epilepsy, but its identification and the definition of its anatomical boundaries, though clinically important, remain problematical. This thesis investigates new methodologies for analysis of structural MRI data in normal subjects and patients with partial epilepsy due to known or suspected focal abnormalities and examines the following hypotheses:

- informative structural patterns and proportionalities in the normal brain should be quantitatively demonstrable.

- structural abnormalities in the brain affected by cerebral dysgenesis may extend beyond visualised boundaries of the apparently focal lesion itself.

- postprocessing of MRI data should reveal more abnormalities, qualitative and quantitative, than are found by visual inspection alone, including abnormalities in apparently normal scans of some patients with focal epilepsy.

Subjects studied were: healthy controls (33); patients with: dysgenesis (35); focal epilepsy and apparently normal scans (45); patients with a different cause for epilepsy, without obvious dysgenesis (hippocampal sclerosis; 16).

Qualitative analysis was performed by reconstruction of data into three-dimensional surface renderings and inspection for surface gyral pattern abnormalities. Novel methodologies (grey, white matter volume distributions; surface areas; callosal areas; surface-volume relationships) were devised for the quantitative analysis of cerebral anatomy. Methodological problems and biases are considered.

Extensive quantitative structural order was found in

brains from normal subjects; using the chief methodology devised, evidence supporting the hypothesis of widespread structural abnormality was found in 70% of patients with dysgenesis, no controls and no patients with isolated hippocampal sclerosis. More subtle abnormalities were also revealed in all patient groups using measures of surface-volume proportionalities. Using all methods some abnormality of structure was revealed in 56% of patients with apparently completely normal scans.

The biological basis and clinical relevance of these findings is discussed. Extensive abnormalities in dysgenesis may be due to widespread alteration in the normal pattern of connections in the brain.

TABLE OF CONTENTS

LIST OF TABLES

LIST OF FIGURES

GLOSSARY

CCA cross-sectional area of corpus callosum

CH cerebral hemisphere/cerebral hemispheric

CPS complex partial seizure(s)

CSF cerebrospinal fluid

E_A extra subcortical matter surface area

ECC ratio of E_A to CCA

EEG electroencephalogram

EGM ratio of E_A to GM volume

ESM ratio of E_A to SM volume

GM grey matter (includes neocortex, archicortex and paleocortex, but excludes basal ganglia)

GMV volume of GM

HS hippocampal sclerosis

L left (alone, suffix or prefix)

MRI magnetic resonance imaging

P_A predicted SM surface area

PR ratio of volumes of a pair of blocks

R right (alone, suffix or prefix)

ROI region-of-interest

S.D. standard deviation

SEH subependymal heterotopia

SGS secondary generalised seizure(s)

SM subcortical matter (includes all hemispheric white matter, thalamus and basal ganglia except caudate)

SM_A surface area of subcortical matter

SMV volume of SM

SPS simple partial seizure(s)

TRAT ratio of volume of left CH to volume of right CH

> value greater than upper limit of normal range

< value lower than lower limit of normal range

STATEMENT OF ORIGINALITY

The methodologies used to examine the hypotheses were all devised solely by the author: these include the derivation of measurement of total hemispheric volume ratio (TRAT) and the block technique of regional volume distribution analysis, the measurement of surface areas by voxel counting and the derivation of surface area measure ratios. The use of fractal dimension analysis to determine whether surface voxel counting could be used on any segmented brain was also devised by the author, as was the method of exclusion of brains from analysis by consideration of degrees of rotation.

The boundaries used for segmentation were all devised by the author. All segmentations used to generate and test hypotheses were performed by the author. Recording of all data and statistical and mathematical analyses were all performed by the author.

The interpretation of the data was originated by the author. This thesis was written entirely and solely by the author.

The program used to count voxels in surface contours was partly already present within the software of the Allegro workstation and was modified by Dr.S.Free, who also wrote and applied the program used to measure surface contour fractal dimension by dilation logic. Dr. Free also performed segmentations for interrater analysis, but these segmentations were not used for analysis of patients with respect to the biological hypotheses tested and postulated and are not reported in the Result (Chapter 4).

ACKNOWLEDGEMENTS

I would like to thank Professor Simon Shorvon for giving me a job, for his unfailing enthusiasm and support, and for the experience of his vision and humanity; Dr David Fish for his perspicacity, precision and demanding standards - leavened with wit; and both for their inspiring examples and kindness; Dr John Duncan for permission to study his patients; Dr John Stevens for always being willing to look at films and having a cheering anecdote in difficult times - διδασκαλος germanus; and Dr Samantha Free who gave so much and without whom none of this could ever have happened.

I would like to thank Dr. Raymond Ali whose dedication and hard work I have tried to emulate; Dr. Ley Sander for arranging things financial and always smiling; the radiographers at St. Mary's Hospital for their kind cooperation at all times; all the Fellows in the Epilepsy Research Group and Department of Neurophysiology with whom I have shared experiences and who gave their time to listen; Dr Louis Lemieux who helped with computing problems; ISG Technologies who tried their best to help when computers failed; the audiovisual department, and in particular Mr George Kaim, for hundreds of pictures, slides and the illustrations in this thesis.

I would like to thank The Wellcome Trust and the National Society for Epilepsy for the opportunities their support gave me; anonymous reviewers for robust criticisms; the staff at Chalfont and Queen Square for their assistance.

I would like to thank my parents to whom I owe most everything.

The greatest example was that of patients I have had the privilege to see over these three years.

For all the people I love and who all gave

CHAPTER ONE: INTRODUCTION

1.1. Epilepsy and cerebral dysgenesis

Epilepsy is the commonest serious neurological condition. About one person in fifty will have one or more afebrile seizures during their lifetime and one in two hundred will endure chronic epilepsy (Cockerell et al.,1994). In Great Britain alone, this means that there are some 350,000 people with chronic epilepsy (Binnie et al.,1991). This is a major handicap for the sufferers, with associated social, psychological and financial handicaps and an increased standardised mortality rate (Cockerell et al.,1994). The control or abolition of seizures are the major goals for all physicians concerned with the care of patients with epilepsy.

Identifying the cause of epilepsy is becoming crucial for management and prognostication (Sander, 1993). The individual causes of epilepsy are legion: they may be divided into developmental (or dysgenetic), traumatic (birth, accidental, anoxic cerebral injury), sclerotic (hippocampal sclerosis), tumoural, infective (meningitic, encephalitic), vascular, metabolic (disturbances and diseases), degenerative, and perhaps the largest group (60-70%), cryptogenic: those for whom there is no apparent cause (Cockerell et al.,1995). The proportion of cases attributable to each of these causes varies with age (Sander et al.,1990), geography (Placencia et al.,1992) and also, now, history: as modern neuroimaging allows detailed study of the brain in vivo, it is likely that the large number of patients in whom no cause could previously be found will diminish.

In the majority (some 60-70%) of patients, epilepsy can be controlled or remits spontaneously (Cockerell et al.,1995). In the remainder, however, seizures become intractable to medical therapy. For these cases, surgical removal of the

cause of the epilepsy is being increasingly considered (Binnie et al.,1991). Histopathological studies have shown that hippocampal sclerosis (HS), a condition of unknown aetiology, is the commonest cause of chronic partial epilepsy in patients who undergo surgical treatment (Duncan and Sagar, 1987; Bruton, 1988; Wolf et al.,1993). It is not clear whether such studies accurately reflect the epidemiology of causes of refractory epilepsy in the population, as cases were usually selected, with selection criteria not always published.

Magnetic resonance imaging (MRI) has revolutionised the understanding of epilepsy (Shorvon et al.,1994). It enables detailed examination of the structure of the brain *in vivo* providing a degree of spatial resolution and imaging flexibility that is just beginning to be exploited, as witnessed by a number of recent workshops on imaging in epilepsy (London, 1992; Cleveland, 1994; Yale, 1994). With different and advancing MR techniques, different aspects of brain structure may be visualised and quantified. Serial and cohort studies can be performed, without the risks inherent in X-ray based imaging. MRI provides the means to perform epidemiological neuroimaging studies that may provide a more accurate picture of the causes of epilepsy in the population.

It is in the study of patients with refractory epilepsy that MRI has been most extensively applied to date. MRI can reliably detect and predict the presence of hippocampal sclerosis (Li et al.,1995) and is now recognised as a very important, if incompletely explored, presurgical investigation in patients with refractory epilepsy thought to arise from the mesial temporal structures (Spencer, 1995). In addition, use in a research environment has increased our understanding of the nature of this condition and its associations and progression (Cendes et al.,1993; Trenerry et al.,1993; Kuks et al.,1993).

Preliminary work in selected groups of patients shows

that there are other detectable causes of refractory epilepsy in the adult population. Selection bias should be acknowledged: the cost of MRI has limited its use so far mainly to patients referred to tertiary centres with intractable epilepsy. In such patients, MRI has shown that whilst HS remains the commonest underlying diagnosis, abnormal development of the cerebral cortex (cerebral dysgenesis) may be the second commonest cause in adult patients (Li et al.,1995). In the majority of such patients, CT scanning fails to reveal the underlying pathology - indeed, often even early MRI failed to reveal such changes (Stevens, 1995).

1.2. The clinical problem

Cerebral dysgenesis has long been recognised as a cause of epilepsy. It first featured in postmortem studies on human fetuses and infants; these revealed pachygyria, polymicrogyria, schizencephaly and other dysgenetic changes (Yakovlev and Wadsworth, 1946; Dekaban, 1965; Richman et al.,1974; Barth, 1987). Subsequently, the use of resective surgery as a treatment for refractory epilepsy provided further evidence that dysgenesis might be culpable (Taylor et al.,1971). The ability to demonstrate dysgenesis in vivo - preoperatively - using MRI, and its association with other neurological illnesses in the adult population (Barth, 1987), has stimulated research into dysgenesis.

Understanding of dysgenesis, however, remains limited. In particular, the detailed structural changes associated with dysgenesis at cellular, subcellular and molecular levels are only now beginning to be unravelled (eg Reiner et al.,1993; Duong et al.,1994). In most cases, it is not yet possible to define even the *extent* of dysgenesis in an individual brain antemortem. Postmortem studies are still few, and the extent of lesions is rarely addressed with detailed histological studies. Not only is the definition of the extent of the

lesion fundamental to understanding dysgenesis, but it is also probably of pivotal importance to the surgical management procedures that provide the samples themselves (Awad et al.,1991; Palmini et al.,1995).

Thus, there is surgical evidence showing that when dysgenesis is present in resection specimens, the extent of resection is a critical factor in outcome with respect to freedom from seizures postoperatively. Palmini et al. (1991) studied outcome in 20 patients with proven dysgenesis amongst a larger number of patients undergoing surgical treatment for epilepsy: they determined that the only significant prognostic factor was extent of lesional resection, 78% of those with a greater than 50% resection having a good outcome in comparison to none of the remainder. It is not clear how the extent of resection was judged in individual patients. Awad et al. (1991) also reported that having complete resection of a lesion (dysgenetic in 20/47 of their cases) was associated with a higher chance of becoming seizure-free than if there was incomplete resection, though even complete resection was not necessarily associated with seizure-freedom. They postulated that in patients with proven dysgenesis (eg tubers, "cytoarchitectural dysmorphism") there might be "widespread nonvisualised histopathology". Unfortunately, their results do not allow outcome to be correlated for specific underlying histopathologies and resection extents. Surgical removal of an electrically-determined epileptogenic zone rather than a (complete removal of the) lesion is known to be associated with a poor outcome for a wide variety of lesional pathologies (Fish et al.,1991). It is now accepted that complete removal of a lesion is in general the best policy when operating for epilepsy on a patient with a lesion (Fried and Cascino, 1993).

The problem remains that the definition of the complete extent of a lesion is difficult when that lesion is dysgenetic. Rarely, such lesions appear to be genuinely focal, especially in the case of dysembryoplastic neuroepithelial

tumours (Daumas-Duport et al.,1988); even in these cases, however, lesionectomy alone is associated with a smaller chance of rendering the patient seizure-free than if a wider excision is performed (Raymond et al.,1995). In most other types of dysgenetic pathology, the anatomical extent of the lesion is difficult to define (Fried and Cascino, 1993; Andermann, 1994). That there are few studies of cortical histology beyond the visualised lesional margins, and that apparently normal adjacent (or distant) cortex is unlikely to be removed at operation, make it more difficult to study this problem. With the increasing revelation of dysgenesis as a probable underlying cause of refractory epilepsy and an increasing use and recommendation of surgery for treatment in these cases, it is important that the problem be addressed, especially if complete lesion excision is indeed the optimum surgical strategy.

This was the clinical impetus for the thesis, the hypothesis being that the extent of structural abnormalities associated with cerebral dysgenesis in patients with partial epilepsy was greater than the visible extent of such lesions. If evidence for this were available, a more rational approach to clinical investigation and management might become possible.

The possibility of addressing this question has been raised only because MRI has proved such a useful tool in the investigation of cerebral structure. Methods are required to demonstrate the existence of abnormalities outside a clearly visualised lesion where none are visible to the naked eye on MRI.

Qualitative and quantitative postprocessing of MRI data might provide an answer. For example, reformatting - qualitative postprocessing - of data may reveal abnormalities in some apparently normal scans (Raymond et al.,1993; Barkovich et al.,1995). MRI data can quantify structures that

previously could not even be seen. The example *par excellence* is that of quantitative analysis of the hippocampal formation. It has been shown by numerous studies that quantitation of hippocampal MRI data is of importance in the clinical management of patients with mesial temporal sclerosis (Jack, 1994). Quantitative postprocessing of data already acquired can furnish information that is not detected by inspection alone (Reutens et al.,1995; Van Paesschen et al.,1995). Currently, even with high resolution scanning and experienced neuroradiological review, 25% of *all* scans in refractory epilepsy cases may appear completely normal (Li et al.,1995), though it is likely from a biological standpoint that the majority of cases of partial epilepsy seen in adults are due to underlying structural cerebral abnormalities. Further quantitative postprocessing has not been applied extensively to the study of the cerebral hemispheres in epilepsy. Given the nature of dysgenesis and MRI, quantitative analysis of cerebral structure outside the hippocampus promises to be useful.

In order that methodologies appropriate to the MRI technology and the problem in hand be devised, further consideration of both the biological circumstances (see below) and the methodological and technological limitations is required (see Chapter 2).

1.3. Normal cerebral development

The study of abnormalities in human biology has always been richly rewarding in the understanding of normality, both in terms of structure and function. Quantitative analysis of cerebral structure for the investigation of abnormalities associated with development and epilepsy may cast light on normal structural properties of the cerebral hemispheres.

Histologically, the adult human neocortex is essentially

uniform in cellular structure, being composed of six layers, with local variations in fine detail that are related to function. The outermost, subpial layer is composed mainly of fibres (axons and dendrites), with some synapses and very few cells: it is called the molecular layer, or layer 1. Passing progressively further inwards, five cellular layers are discernible on the grounds of cellular morphology and disposition: they are numbered 2 to 6 respectively. In certain regions, some layers are more prominent than others, but the essential laminar structure is always preserved in the normal brain.

Normal cerebral development is well described in many texts (see Sarnat, 1992) and is not repeated in detail here. Three salient features will be highlighted.

1. The inside-out gradient of normal development. A general principle of the development of neuronal structures is that neurons are generated at a distance from their final resting positions, to which they migrate along sometimes extensive pathways. Four pathways are recognised in human brain development: the cerebral, from the subventricular zone to the cortical plate; the corpus pontobulbare, forming the pontine and medullary nuclei; the corpus gangliothalamicus, forming the corpus striatum, globus pallidus and thalamus; and the cerebellar migrations (Sidman and Rakic, 1973). In the case of the development of the cortical plate, that gives rise to the adult neocortex, cells migrate in waves, each successive wave passing through previous migrations to lie more pial, so that layer 2 cells are those that migrated last and those of layer 6 migrated first (Angevine and Sidman, 1961). Neurons in the developing hemispheres migrate along radial glial fibres. It appears that migration may be disturbed at any stage, leading to ectopic neuronal positioning (see below).

2. Precocious connectivity. The large amount of interneuronal connectivity in the mature brain will be

emphasised below (1.4.). Connectivity appears to be not only prolific, but also precocious. Axodendritic synapses between primordial corticopetal fibres from the mesencephalic tegmentum and Cajal-Retzius cells in the primordial molecular layer (layer 1) can be seen as early as day 43. Invading thalamic afferents synapse with subplate neurons (that underlie and predate the neurons migrating from the subventricular zone to the cortical plate) before they synapse on their eventual neocortical targets. The importance of such primordial connections to the final synaptic organisation of the neocortex is shown, for example, by selective ablation of cells regionally in the subplate leading to the failure of local thalamic afferents to pass eventually into the overlying cortical plate, even though their predestined targets are in their correct positions (Ghosh et al.,1990). Precocious and mature synaptic connectivity may not only be a fundamental cortical property, but also a cerebral morphogen (Purves et al.,1992).

3. Complexity of development. The published accounts of cerebral development are continuously overtaken by novel findings demonstrating its intricacy. For example, the mechanism of neuronal migration along pathways is complex, involving cell adhesion molecules, transmembrane signalling and cytoskeletal changes (Rakic et al.,1994). Disruption in any of these processes may affect migration, causing cerebral dysgenesis. In addition, neuroblast migration in the cortical plate may not be purely radial. Tangential migration of neurons from the subventricular zone may occur (Walsh and Cepko, 1993; Tan and Breen, 1993), requiring the pure radial unit hypothesis (see Rakic, 1988) to be modified. In fact *precursor* cells within the ventricular zone move along the axis of the embryo, but the clonal progeny from a single daughter cell produced at each stage of division is still likely to migrate in a limited radial fashion (Reid et al.,1995). Such subtlety of development, much of which remains incompletely established, confounds interpretation of

experimental results.

1.4. Normal cerebral structural properties: proportionalities

The magnitude of the achievement of normal cerebral development should not be underestimated. Stereological estimation suggests that there are at least fourteen billion neurons present in a single human hemisphere (Braendgaard et al.,1990), with up to four thousand synapses on a given neuron (Cherniak, 1990). However, the entire human genome is thought to contain fewer than 100,000 genes (McKusick, 1979). Therefore general principles determining the structure and development of the cortex must exist. There is little knowledge of such rules for human brains. The study of the abnormal and, often, obscure, has provided much of the available information. The most widely held theory for cortical gyrogenesis, for example, arose from analysis of two brains affected by extensive dysgenesis (Richman et al.,1975).

Based on quantitative MRI work, it has been postulated that some regulation ensures that the two cerebral hemispheres are of very similar total volume (Filipek et al.,1994). Other structural principles have been noted in the adult cortex. Neurons are ordered into functional columns (Mountcastle, 1978), thought to be the basic processing units of the neocortex. Local variations in cerebral anatomy, which may be large enough to enable definition of regions on the basis of cytoarchitecture, are thought to be due to modulation of this basic functional element rather than to an alteration in its fundamental pattern (O'Leary, 1989). Phylogenetic neocortical expansion is also thought to have occurred as a result of an increase in the number of such units rather than by an alteration in the fundamental building blocks (Rakic, 1995).

Rockel et al. (1980) explored this, by counting the total number of neuronal cells beneath a fixed area of cortical pial

surface. They found that across species and for different regions of the cortex, the total number of neurons in the entire cortical thickness under a given area was fixed. They suggested a constant surface packing density is perhaps a fundamental developmental principle, (extensive) local variations in cytoarchitecture being produced by alteration in connections (the neuropil), maintaining the fundamental organisation, whilst explaining limited local differences in cortical thickness. They suggested that estimation of surface area might allow determination of the number of underlying neurons. On the grounds of developmental regularity, their propositions and findings remain tantalising. However, there are two major problems with their analysis. Firstly, the cortex is known to be heterogeneous in its composition: examination of a slice of cortex passing through a crown and an adjacent sulcal fundus shows that even on inspection, cell density differs in these two regions (Welker, 1990). Rockel et al. do not state which part of the gyrus their samples were taken from: crown, fundus or both. Secondly their cell counting technique is not specified: depending on the size of their counting volume, some cells may have been more likely to have been counted than others, thus biasing their results. However, although the validity of Rockel et al.'s (1980) data is questionable, their ideas need to be explored further: *mean* cell density across the entire surface of the hemisphere may be relatively constant. Unbiased quantification techniques have since been popularised (Gundersen, 1986; Mayhew, 1992). Haug (1987) used unbiased, stereological techniques to determine the surface density of neurons in man in five Brodmann regions. Whilst within a region there appeared to be a constant cell surface density across subjects, it varied between regions. Braendgaard et al. (1990), also using stereological techniques, showed that mean neuron number *per unit volume* was relatively constant in randomly sampled regions of frontal, parietal and temporal cortex, at 4.4×10^7 neurons/cm^3 (standard deviation 0.6×10^7). The mean cell density is higher in the occipital lobe (7.1×10^7). Total cell number

related to brain volume in man (Braendgaard et al.,1990) and across species (Haug, 1987), providing a surrogate for total neuron number in the normal brain. Thus, if a (grey) surface parameter can be shown to relate to a (grey) volume parameter, then total neuronal number in the *normal* brain should relate to the surface measure, as suggested by Mountcastle (1978).

Rockel et al. (1980) also suggested that the proportion of neurons in a given functional category for a given surface area was also constant. This proposition is less affected by the use of nonstereological methodology, and remains useful (O'Leary, 1989). It has also been shown that the proportions of pyramidal and nonpyramidal cells in widely differing cortical areas of different species are of the same order of magnitude (Winfield et al.,1980). Reliable determination of cortical surface area might thus provide a means of estimating total, regional and function-specific neuronal numbers. Such knowledge would further increase understanding of normal cerebral anatomy and its disruption in dysgenesis.

The number of fibres passing through the corpus callosum correlates with its cross-sectional area (Tomasch, 1954; Aboitiz et al.,1992). As the proportion of the total number of neurons extending interhemispheric axons is probably constant (Rockel et al.,1980), and the mean number of neurons underlying a given area of cortex in the normal brain may be fixed, then the cross-sectional area of the corpus callosum ought to correlate with a surface measure of the cortex, this measure estimating the total number of neurons.

Ordered structures supporting normal function are likely to arise from ordered development. Genetic studies of individuals with abnormal brains may reveal details of the general principles governing normal development; structural study of such brains may show further quantifiable abnormalities of development that can be related to genetic defects. Thus the revelation of a single gene defect

responsible for the occurrence of a specific and extensive structural change (Reiner et al.,1993) allows further dissection of the structural developmental process, and the genetic control underlying its components. In order for such studies to be possible and directed, structural changes in the brain must first be detected, examined and quantified. The varieties of such disruption will now be discussed.

1.5. The abnormal adult brain: cerebral dysgenesis

Developmental structural changes in the brain are of many different pathological varieties, known collectively as cerebral dysgenesis (Sarnat, 1992). Before MRI, dysgenesis in the adult brain was considered to be rare. MRI, however, has demonstrated that cerebral dysgenesis (CD) occurs not only in severely affected children, but also that adults may have many forms of CD, possibly manifesting only as epilepsy (Raymond et al.,1995) or relatively minor developmental abnormality, such as dyslexia (Galaburda and Kemper, 1979). The prevalence of CD in the adult population is largely unknown. Only postmortem studies are available; the largest series suggests that CD may occur in 1.5% of normal adult brains, and in 14% of brains from individuals with epilepsy (Meencke and Veith, 1992). One population that has been studied in vivo is that of individuals with refractory epilepsy. In a large study from this institution, CD was seen in 12% of 341 such patients (Li et al.,1995); this is likely to be a minimum estimate.

The spectrum of CD in the adult population is more restricted than that in infants. Polymicrogyria, pachygyria/agyria, schizencephaly, heterotopia, focal cortical dysplasia, tuberous sclerosis and hamartomatous malformations have all been detected, histopathologically or on neuroimaging (Raymond et al.,1995). A brief description of CD follows (for thorough surveys see Barth, 1987 & Sarnat, 1992).

Agyria or lissencephaly describes a brain in which gyration is absent and the cortical surfaces are smooth. Failure of migration affects extensively all but one of the four pathways: the corpus gangliothalamicus is unaffected, so that the thalamus and corpus striatum are singly uninvolved in the developmental disruption. There are at least two distinct histopathologies. In type I the affected cortex is four-layered: there is a subpial molecular layer, then a disorganised outer cellular layer (containing cells normally in layers 3,5 and 6), a cell-sparse zone and finally an inner cellular layer with numerous cells whose migration is believed to have been arrested and which normally would have constituted mainly layers 2 and 3. In type II lissencephaly there is little discernible layering, neurons instead being grouped in clusters and columns. In the underlying white matter, heterotopic neurons form nodules.

Pachygyria is the presence of broader and fewer gyri than normal. Histologically identical to agyria, the two often occur in different regions of the same brain (Friede, 1975). Macrogyria is a purely descriptive term, applied to gyri that appear broadened, on inspection or imaging. It carries no histopathological implications, and indeed may be due to at least six different pathologies (Raymond et al.,1995).

Polymicrogyria is the presence of a large number of narrowed, thinned gyri. A cobblestone appearance may be discernible, though fusion of adjacent molecular layers may give the impression of macrogyria. Histologically, there are layered and unlayered varieties. In the layered form, there is believed to be *postmigrational* ischaemic necrosis of neurons, mainly in lamina 5. This is associated with an increased convolution of the overlying laminae, with the generation of small gyri of reduced thickness and width. Unlayered polymicrogyria is macroscopically indistinguishable, but a cell-sparse layer suggestive of laminar destruction is absent. The distinction between the two varieties may, however, be

blurred, especially in terms of the timing of the cause.

Schizencephaly is the presence of a cleft extending across the wall of the hemisphere, from pia to ependyma. The cleft walls are lined by grey matter, which may be polymicrogyric. It is believed to result from a destructive influence that in less dramatic cases produces polymicrogyria. There may be abnormal cortex around the cleft; this is usually polymicrogyric. Recently, there has been a trend away from the use of the term "schizencephaly", in favour of a more complete description of the abnormality with the use of "cleft" instead (Sarnat, 1992; Raymond et al.,1995).

Dysgenesis may be due to abnormal positioning of neurons (heterotopia). Heterotopic tissue may be described in terms of its extent, morphology and position. Subependymal heterotopia (SEH) is the presence of ectopic grey matter lying underneath the ventricular ependyma in the post-developmental brain. Overlying cortex appears normal. It may be due to a failure of migration or of apoptosis. SEH appears to be a distinct type of dysgenesis as judged by clinical phenotype (Raymond et al.,1994a). Females appear to be affected more commonly than males; an X-linked mode of inheritance with prenatal lethality for males has been postulated for the familial form of the condition (Huttenlocher et al.,1994).

Subcortical heterotopia is the presence of aggregations, in either laminar, band or nodular form, of neurons in the white matter, commonly in the centrum semiovale. It may be associated, especially if extensive, with abnormal gyration of the overlying cortical ribbon. It is believed to be due to a premature arrest of neuronal migration.

Focal cortical dysplasia is the presence of abnormally large and dysmorphic neurons in many layers of an otherwise normally laminated cortex (Taylor et al.,1971). It is a specific histological diagnosis, though macroscopically it may

be diffuse and extensive, mimicking the appearance of macrogyria or even hemimegalencephaly (Harding, 1992).

Of other forms of dysgenesis, two will be studied. Agenesis of the corpus callosum may be seen in association with other dysgenetic abnormalities of cerebral structure, such as polymicrogyria, focal migrational disorders, tuberous sclerosis or as part of a recognised syndrome. Transcallosal axons originate mainly from layer 3 of the mature cortex (Innocenti, 1986): their interhemispheric passage requires the programmed cell death of glia in the dorsum of the lamina terminalis. In the presence of cells in layer 3, but without glial apoptosis, transcallosal axons are redirected within the hemisphere of origin, forming the longitudinal bundles of Probst. The presence of this bundle suggests that callosal agenesis is a secondary phenomenon.

Hypothalamic hamartoma is an uncommon dysgenesis, not neocortical, but which is associated with widespread functional changes in the hemispheres as manifest by retardation, epilepsy, behavioural disturbances and cognitive decline (Breningstall, 1985; Berkovic et al.,1988).

This survey of dysgenesis has highlighted abnormalities seen histopathologically in some forms of cerebral maldevelopment. Entities may occur together, and sometimes a single diagnosis cannot be made in vivo. Thus gyral abnormalities, subependymal heterotopia and full-thickness clefts may be seen in association. Such cases show that causative agents may act diffusely in time and space, and that it is the time at, and for, which such insults occur that dictates the resulting abnormalities, rather than the particular nature of the insult.

1.6. Abnormalities in dysgenesis: localised or widespread?

There are numerous descriptions of the appearance,

clinical features and relevance of each of the various types of dysgenesis. However, the detailed anatomy and pathophysiology of the diseases are rarely documented, and rarely too are clues available as to the actual cause of the anomaly (Raymond et al.,1995), though many possible causes are recognised (Barth, 1987). Thus although the associations with epilepsy, developmental delay, neurological abnormalities and mental retardation are well documented, the pathogenesis remains mysterious.

Many reports of dysgenesis describe it as a localised abnormality of brain anatomy, for example as perisylvian polymicrogyria (Kuzniecky et al.,1994). This is based on visual inspection alone, whether on neuroimaging, at surgery or at postmortem. It is often inferred that structural abnormalities are limited solely to the visible extent of the lesion. Such localisation is unlikely, however, both because of the nature of the insults causing symptomatic dysgenesis, which are likely to act widely, and because of the high degree of connectivity in the human cerebrum, resulting in secondary disruption of cerebral structure. These factors will now be discussed in some detail.

1.6.1. Evidence for extensive abnormalities in dysgenesis: connectivity

In older postmortem studies, a macroscopic description of the lesional area was often accompanied by a statement that other areas of the brain appeared normal (eg Richman et al.,1974). These regions were rarely studied histopathologically, although often a gradual change from normal to abnormal cytoarchitecture at the edges of the visualised abnormality was noted (Stewart et al.,1975). The genuine normality of the rest of the brain cannot, therefore, be determined from these reports.

There is, on the other hand, evidence to suggest that structural and functional abnormality is more extensive than the boundaries of a lesion seen by eye alone. This comes from animal and human data. Barron (1950) reported experiments performed to examine gyrogenesis. Having destroyed various parts of the fetal sheep brain, he examined it after further intrauterine development. He showed that when the developing hemispheres were transected in the coronal plane, the caudal portion degenerated; the fissural pattern of the anterior remnants differed from comparable areas on unoperated fetuses. Unfortunately, there was no histological examination of the lesioned brains. Goldman and Galkin (1978) performed prenatal prefrontal corticectomies in monkeys and subsequently compared gyral patterns with those in postnatally-operated monkeys and controls. The gyral pattern was altered not only in the operated area, but also in distant regions (eg occipital lobe) of both the same hemisphere and the contralateral hemisphere. Such changes were not seen in animals operated postnatally. Prolongation of neurogenesis and interference with neuronal migration were excluded as possible explanations for their findings. The adjacent precentral gyrus of the dorsolateral convexity was unaffected arguing against non-specific mechanical or vascular effects of surgery as these would be more marked next to the lesioned area than in distant areas. The prefrontal cortex is associational, projecting in the rhesus monkey to the occipital lobe. Thus, altered connectivity between these regions is likely to be the explanation of the findings (Goldman-Rakic, 1980), this altered connectivity allowing normal function in the prenatally-operated monkeys despite cortical loss. Rakic (1988) reported similar results with manipulation of thalamocortical input. Bilateral enucleation, when performed in the first half of gestation, led to the development of gyri in the normally smooth occipital convexity. This was due to an expansion of adjacent associational cortex into the region normally accommodating input from the lateral geniculate nucleus, without significant excess cell death.

Extensive changes in cerebral constitution following a focal neocortical lesion have also been shown in the fetal cat (Loopuijt et al.,1995). Changes in gyral patterns were seen in both the ipsilateral and contralateral hemispheres. In addition, there were volume reductions in the ipsilateral hemisphere, attributed to alterations in neuronal number outside the lesion. The alterations were thought to have been mediated by connectivity as targets for remaining neurons and projections from ablated neurons were both removed. Interestingly, *volume* reduction was associated with proposed connectional abnormalities.

In general, gyral changes are likely to reflect underlying changes in structural and functional cytoarchitecture (Rademacher et al.,1993), the greater proportion of the volume of gyri being connectional in nature (Haug, 1956). In all these animal experiments, interneuronal connectivity is altered and shown to have morphogenetic potency. Dysgenesis, in these cases experimental rather than accidental, in one area is seen to have effects on distant areas of the brain.

"Experimental" evidence for the probable extensive nature of human CD comes from surgery for refractory epilepsy. Surgery is aimed at the removal of a lesion postulated to be involved, and revealed on neuroimaging. In patients in whom isolated hippocampal sclerosis is the lesional abnormality, the prognosis for cessation of seizure activity following removal of the diseased hippocampus is good (Berkovic et al.,1995). When CD is found in resected tissue, the prognosis is considerably worse, provided patients are followed for an adequate period postoperatively (Palmini et al.,1991 and 1995; Bruton, 1988; Salanova et al.,1994). Awad et al. (1991) and Andermann (1994) have proposed that this is because CD is extensive; this is supported by more detailed electrographic studies (Palmini et al.,1995). The persistence of seizures postoperatively in cases of gelastic seizures associated with

hypothalamic hamartomata (Cascino et al.,1993), often with unchanged semiology, also supports this, and further evidence comes from reoperation series (Salanova et al.,1994). These observations suggest that functional abnormality, whatever its basis, extends over more of the brain than the lesion itself appears to.

Connectivity is an important quality of the human brain. There may be of the order of 50,000 billion synapses in the cerebral cortex alone. In areas of cerebral dysgenesis, abnormalities in the cellular apparatus of connectivity have been seen, though few studies have been performed. Bordarier et al. (1986) examined the orientation of pyramidal neurons in agyric cortex post-mortem in a child with abnormality of chromosome 17. The cortex was four-layered. In the superficial neuronal layer 80% of pyramidal cells were radially inverted: their apical dendrites were directed centripetally rather than centrifugally. Whilst axons so diverted can adjust their trajectory completely, dendrites cannot (Sarnat, 1992), so that abnormal connectivity may result. Unfortunately, whilst neuronal abnormality was demonstrated, no assessment of connectivity was possible. Takada et al. (1994) studied dendritic development quantitatively in agyric visual cortex using Golgi staining. They demonstrated a significant reduction in the total apical dendritic length, the number of orders of branching of apical dendrites, the number of branches themselves and their complexity, for pyramidal neurons in both superficial and deep cellular layers of the four-layered cortex. As the development of dendrites depends on the axonal microenvironment in which they find themselves (Pinto-Lord and Caviness, 1979), this finding argues for abnormal connectivity beyond a simple inversion of orientation, and more towards an extensive miswiring (quantitatively and possibly in terms of complexity). Sadly, there are very few similar quantitative analyses. In one qualitative report (Ferrer, 1984), changes in dendritic morphology and orientation were also found in a polymicrogyric

brain.

Cowan et al. (1984) have demonstrated that cells in the central nervous system are unlikely to remain alive unless they are connected. Areas of CD are alive and functional (eg Palmini et al.,1995); thus, given the high degree of connectivity in the brain and the presence of abnormalities in the apparatus of this connectivity in CD, it would seem likely that there might be abnormalities in other regions in dysgenetic brain, in particular of those areas that are connected to the obviously dysgenetic region. This is postulated to be the explanation for the findings of Goldman and Galkin (1978), and of Barron (1950). It forms the theoretical ultrastructural background for the opinion that extensive structural abnormality explains failure of surgical treatment in some cases of human epilepsy caused by dysgenesis.

1.6.2. Evidence for extensive abnormalities in dysgenesis: causes of dysgenesis

There are many recognised causes of cerebral dysgenesis (Barth, 1987; Sarnat, 1992), many of which are syndromes with a probable genetic basis. Aetiological abnormalities in these syndromes are poorly understood. For many genetic disturbances, however, most neurons are likely to be affected, for example in the trisomies and Miller-Dieker syndrome. In cases of dysgenesis thought to be caused by environmental insults, a diffuse effect on development is also probable, given the nature of causative agents. Thus methylmercury poisoning is associated with extensive migrational defects, and in vitro damages the membranes of growth cones, that are common to all neurons. Whilst dysgenesis will be apparent where the largest number of neurons are most affected, depending on the amount and duration of exposure, most developing neurons are likely to be affected to some extent, producing extensive dysgenesis. The same is likely to apply to

other exogenous agents, such as X-irradiation and ethanol.

Based on this diverse evidence, it would seem likely that structural and functional abnormalities in brains with apparently focal CD should be extensive and spread beyond the boundaries of the visualised lesion alone. This is in terms of the lesion itself, most causes of which are likely to have a diffuse effect, and in terms of areas connected to the lesion, which are likely to be additionally disrupted because they are connected to the dysgenetic area.

1.7. Aims of thesis

The aims of the thesis were to test the following hypotheses, based on the clinical problem and the anatomical facts presented above:

1. That structural abnormalities in the human brain affected by cerebral dysgenesis should extend beyond the visualised boundary of the apparently focal lesion itself.

2. That the existence of structural order in the normal brain should be quantitatively demonstrable:
(a) measures of cortical surface area should correlate with grey matter volume, if cortical thickness is limited in its variability and
(b) cortical surface area measures should correlate with callosal cross-sectional area.

3. That there may be disruption of any such correlations in brains of patients with epilepsy.

4. That by further processing of MRI data, more abnormalities, qualitative and quantitative, should be detected than are found by visual inspection alone.

5. That patients with subependymal heterotopia should be quantitatively different from patients with other sorts of dysgenesis associated with epilepsy, because of the clinical differences seen (Raymond et al.,1994a).

Possible mechanisms underlying structural disorder in the dysgenetic brain are suggested on the basis of the results and their interpretation. Other, unsuspected, findings are also discussed.

It should be emphasised that the hypotheses are applied only to the patient groups studied and are not intended to be applied to all patients with epilepsy. The causes of epilepsy are varied and may, for argument's sake, be due to abnormalities in ion channels: in such cases, although structural abnormalities exist, they need not necessarily be detectable by MRI or the methods devised in this thesis.

CHAPTER 2: MAGNETIC RESONANCE IMAGING OF THE BRAIN

2.1. Application of hypotheses to MRI data

In order to test the hypotheses, it is necessary to be able to determine whether there are cerebral structural abnormalities present where none can be seen on routine inspection of MRI scan data. New ways are required of extracting more of the data present in high resolution scans.

From the biological perspective, according to the hypotheses put forward in the previous chapter, subtle alterations in cerebral structure associated with cerebral dysgenesis, but not visible to the eye, should be associated with alterations in the neuropil beyond the visualised boundaries of the lesion itself. Neuropil alterations may be qualitative, as they are in some visible CD lesions (for example with blurring of the grey-white interface), or quantitative, with more or less neuropil than expected. Qualitative or quantitative neuropil changes might be associated with gyral changes, as local cytoarchitecture is one factor affecting gyral structure (Rakic, 1988; Rademacher et al.,1993). Subtle gyral changes may easily be missed if the complex three-dimensional cortex is sliced and viewed in two dimensions. Three-dimensional visualisation of a three-dimensional object may increase comprehension of that object (Fig 2.1).

High resolution MRI data may be reconstructed into three-dimensional representations, allowing in vivo visualisation of the surface gyral pattern. Abnormalities of the surface pattern may then be detected by comparison with normal subjects' patterns. There are a number of ways of achieving such comparisons, and these are critically reviewed below.

Neuropil alterations may also be determined quantitatively, if normal ranges for neuropil volume, shape

Figure 2.1. Serial 1.5mm thick images of half a melon scanned using a volumetric protocol (see 3.2 for details). An alphanumeric character has been carved into the cut face of the melon. On inspection of the two-dimensional images, it is difficult to determine what this character is: reconstruction, however, reveals the character (overleaf).

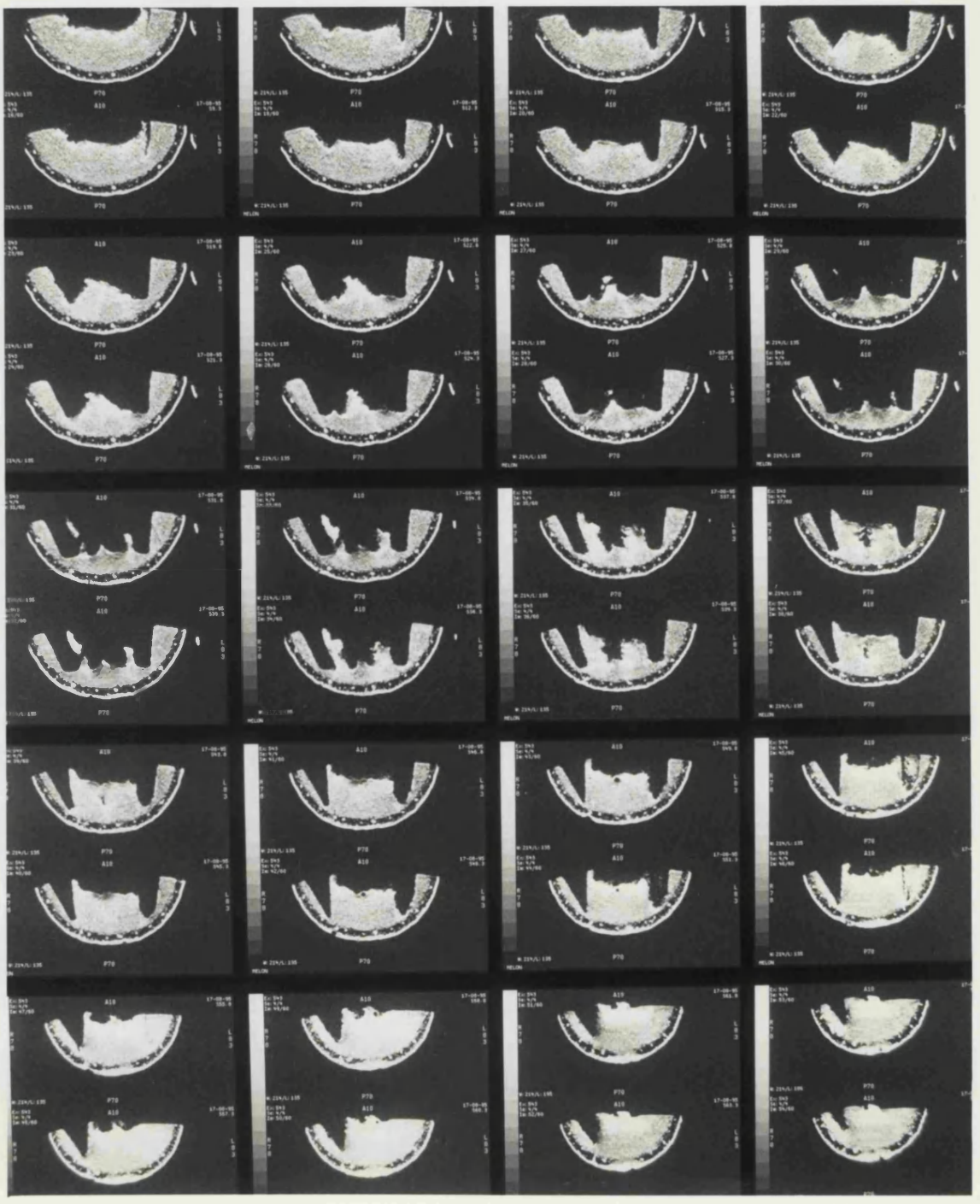

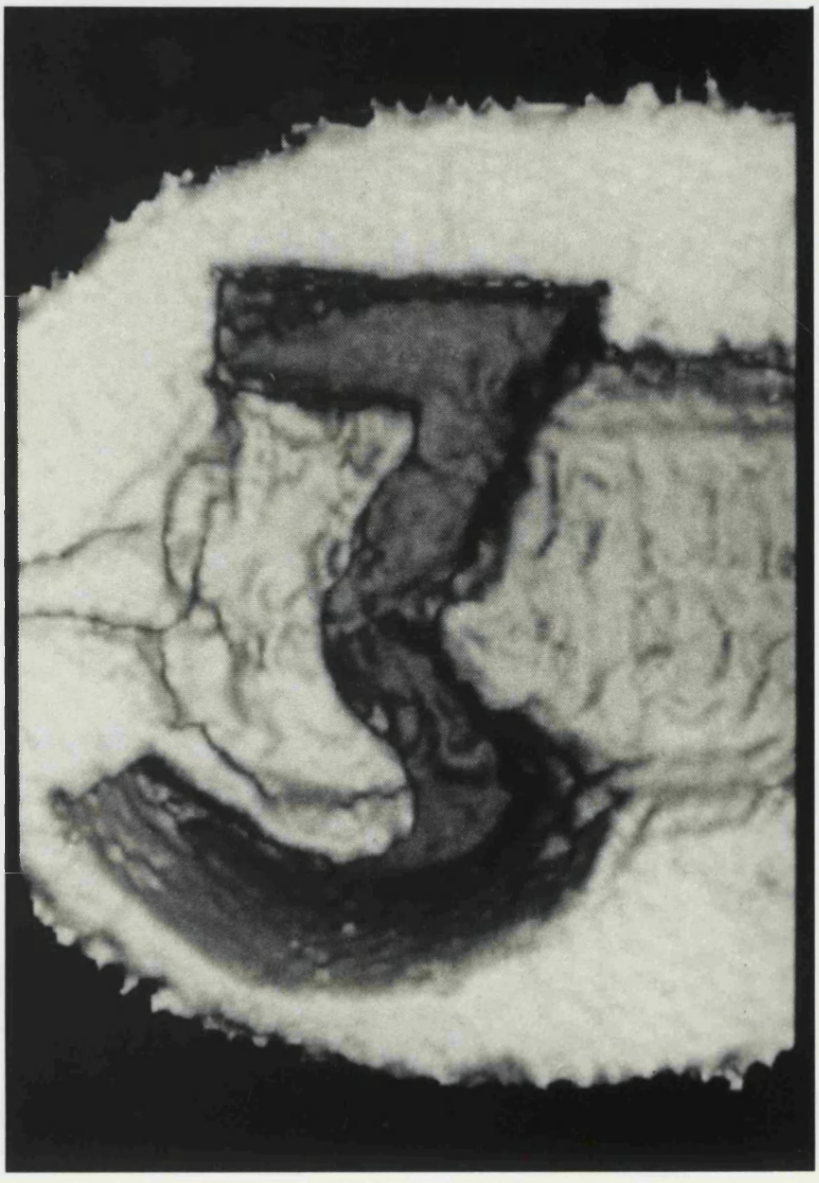

and relative signal intensity can be determined. Alterations in any of these parameters, if localisable, might determine whether the postulated hypotheses are tenable. The determination of these characteristics of the neuropil requires that it be identifiable on MRI data and that spatial measurement be possible. The presence of "abnormal" neuropil outside the visible boundaries of the lesion would be in support of the hypothesis that CD is an extensive disorder of brain structure.

In order for these aims to be achieved, data from MRI must first be analysed so that different tissues of interest are identified and treated separately. On routinely viewed images, CSF, grey matter, white matter and any other particular regions of interest (ROI's) must be isolated. This process is known as segmentation and is the basis of most quantitative MRI-based analysis. Segmentation is required even for visual inspection of three-dimensional reconstructions of the cerebral surface. In view of the fundamental importance of the segmentation process to this thesis, some time will be spent considering it, before methods of using the information it produces are contemplated.

2.2. Segmentation

MRI scanning converts information about the spatial distribution of certain biological characteristics (density and environment of paramagnetic particles) into spatially distributed voxels, whose intensities depend on the biological tissue and the scanning parameters. There are many different ways of acquiring MRI data, in which the three main biologically-governed variables, T_1-, T_2- and proton density-weighting, are changed. Sequences may be prepared in various ways in order to elicit specific tissue characteristics. In most cases, the acquisition of data is a compromise between many conflicting requirements, such as scanning time

(determined by cost and the need for patient compliance), spatial resolution within images, the number of slices and their separation and tissue contrast. Different tissues can appear very different under altered imaging parameters; the choice of parameters is governed by the requirements of the study.

Data presented in this report were acquired so that hemispheric anatomy could be examined in detail whilst minimising scan duration. A key requirement was the ability to clearly image the hippocampus so that its volume could be measured with minimum partial volume effects and greatest accuracy. A high resolution T_1-weighted volume scan was used. The scan generated 124 coronal slices each 1.5mm thick with in-plane display resolution of 0.9mmx0.9mm. This sequence proved ideal for the measurement of the volume of the hippocampus (Cook et al.,1993) and for detailed examination of the hemispheres in patients with cryptogenic partial epilepsy. It also allowed the data to be reformatted, increasing the yield of structural abnormalities (Raymond et al.,1993). So that all studies were comparable, no changes were made in the sequence parameters during the course of the study. When this study was started, the majority of the data reported had already been acquired, limiting the segmentation and postprocessing methods that could be employed.

Voxels in a three-dimensional data set from an MRI scan contain both spatial information (with respect to their neighbours) and intensity information. The process of segmentation is the classification of voxels on the basis of intensity information modified specifically by spatial information. Many techniques have been devised, all with the ultimate aim of automating the procedure as far as possible, to minimise subjectivity through operator interaction and to accelerate processing. Some methods will now be discussed.

2.2.1. Intensity Thresholding

The commonest method of segmentation of one region from another depends on identifying voxels of chosen intensity and linking them in certain ways in order to produce a spatial boundary between groups of voxels of different intensity characteristics (Kennedy et al.,1987). Boundaries may be closed to form a region-of-interest (ROI) containing voxels with intensities lying within certain bounding values (thresholds).

The process usually involves an operator visually identifying a border and setting a threshold parameter to the intensity level of voxels in the identified border. Automatic algorithms then create a closed connected boundary within the image by reference to this threshold and rules that govern the growth of the boundary. The encompassed area is the ROI. Further thresholds higher or lower than the initial one may also be set to limit voxel inclusion within the ROI more precisely. Various modifications of this fundamental process have been devised. One such is that new areas, satisfying threshold requirements, to be considered for inclusion within an ROI should be connected to the existing ROI by a given minimum number of voxels. This criterion helps limit the spread of the ROI into areas of an intensity falling between the chosen thresholds but which are not biologically part of the ROI, thus aiding distinction, for example, of meninges from the surface of the grey matter.

Other modifications of the thresholding algorithm are essentially more sophisticated methods of identifying the threshold or boundary voxel intensity. One such method uses voxel intensity histograms to identify statistically the value of the threshold that is most likely to correctly separate different tissues. DeCarli et al. (1992) found that, using such techniques, they were able to obtain volume measurements for whole brain that were within 7% of volumes determined on

the same postmortem brains by fluid displacement methods. The technique requires calculations to be performed for each study to be segmented. It can account for slice-by-slice voxel intensity changes due to radiofrequency (RF) inhomogeneity. However, it cannot account for within-slice RF inhomogeneity, which was present in the data used in this thesis: it was therefore unsuitable for this work.

2.2.2. Multispectral analysis

This was first introduced for MRI in 1985 by Vannier et al. It is a powerful method of automatic segmentation, unaffected by RF inhomogeneity even within slices. When pixel intensities from two tissue types (eg brain and CSF) from T_2-weighted and proton density scans are plotted on a two-dimensional histogram (called bifeature space), the resulting points cluster into two regions representing the two original tissues. The clusters are the pattern formed by a two-dimensional population distribution of voxel intensities produced by the two sequences. The information from this histogram can be used to classify all the pixels in the original image into either brain or CSF (in this example). Blatter et al. (1995) have recently provided a normative database of MRI-determined grey, white and CSF volumes using multispectral analysis available in a commercial package. In their report, manual interaction was still required to remove extracerebral soft tissues from the automatically segmented images. Automation reduces the need for operator interaction and must reduce some operator-generated variability, but does not eliminate it. Presumably it also speeds the processing of data, but this is not stated. In addition, interrater and intrarater reliabilities, though found to be high for CSF compartments and the brain as a whole, were the lowest of all for the grey matter and the white matter (mean interrater correlation coefficient 0.590 for grey matter and 0.599 for white matter). It can only be presumed that this variability, which is not discussed by the authors, but which pertains to

tissues that constitute the bulk of the segmented areas, is largely due to manual interaction. A further major problem with multispectral analysis is that current scanners may not allow the acquisition of volumetric (thin slice, contiguous) scans using the sequences required for cluster analysis: Blatter et al. used 5mm thick slices with 2mm gaps, which entail a loss of resolution when compared with the 1.5mm thick contiguous slices used in this thesis.

Feature map segmentation with clusters separated using nonparametric techniques was reported by Jackson et al. (1994). They found volumes comparable with those produced by groups using other techniques, including intensity thresholding and direct postmortem volume measurements. They commented that "for optimal reproducibility, all data should be analysed by a single observer", but acknowledged that this is not usually feasible for longer term and larger studies. For such studies, training of observers and easily applied rules for manual interaction are important. Whilst both operator training and rule usage were explored in this thesis, the results presented derive from segmentation performed by the author alone.

Yet more sophisticated means of segmentation are continually being devised. Amongst these are the application of neural network theory to "train" automated segmentation processes and the extension of cluster analysis to three classification dimensions using coregistered T_1-, T_2- and proton-density-weighted scans. All these clustering methods require specific programming and could not have been used on the data available.

2.2.3. Choice of segmentation method for this study

Intensity thresholding, with an additional connectivity variable that was set by the operator, was used for segmentation in this thesis. Each slice was edited and

thresholds were changed as required between and regionally within slices to account for RF inhomogeneity. Other ways of correcting for RF inhomogeneity, such as the use of flood phantoms, though apparently satisfactory, cannot represent the real brain and its complexity and loading characteristics (Harris et al.,1994).

Intensity thresholding with semi-automated, manually-supervised, segmentation was used for this thesis because:
(i) it is simple and easy to use: no additional programming or help was required to achieve segmentation using a intensity-thresholding based dedicated workstation
(ii) it is reliable (see below)
(iii) it ensures each slice of data has to be examined
(iv) it is flexible and leaves control with the operator (unlike some automated packages) and allows compensation for RF inhomogeneity
(v) it allows the specification and application of user-defined boundaries.

Multispectral analysis may appear to provide the best means of *automating* segmentation. Whilst automation of segmentation may seem to be desirable, this is only so if the resulting data are more reliable and valid (see also 3.6.). Visual identification, rather than automated choice, of the grey-white interface is only less desirable because it is labour-intensive. It is not, however, any less valid because of the nature of the "real" grey-white interface. Ultimately, this interface can only be determined at a subcellular microscopic level, being the sum of all the junctions of axon hillock and axon. This is an impossible task and surrogates must be employed. Any other contour "identifying" the grey-white interface will be method-specific: it may be the position of a colour change if histological stains are used, for example, and this can only approximate the "real" interface. On MRI, it is the position where signal of white matter intensity begins to predominate. For this reason, one

cannot compare the "accuracy" of automated determinations of the grey-white interface with that of visually-guided determination: this would require a gold standard which does not exist. In these circumstances, the critical issue becomes less one of microscopic precision, provided the choice is anatomically sensible, and instead one of reproducibility, within and between subjects and operators. Reproducibility using multispectral analysis is not necessarily higher: in fact, interrater reliability of segmentation in the current study, using intensity thresholding, was comparable with segmentation using multispectral analysis (as reported by Blatter et al.,1995; note that some operator interaction was still required in their report), and intrarater reliability was much higher (see section 3.13.). Also for cluster analysis, the use of relatively thick slices would have been necessary (see above), with an associated price with respect to overprojection errors. The segmented images produced in this study were of a quality sufficient for both further quantitative analyses and visual inspection. In addition, this study was undertaken on data most of which had already been acquired, in a form unsuitable for multispectral analysis.

The price of using intensity thresholding is that the process is time-consuming and labour-intensive; over 1000 hours of operator interaction was required for collection of the data reported here. The original data were segmented using a proprietary package that was, however, very user-friendly and did not require additional programming by experts in image processing or computer software. For more general utility, these are important considerations.

Once each image has been segmented, the ROI's can be stacked to produce three-dimensional representations (surface renderings). Further analysis, such as volume and surface area measurement of a given representation, can then be undertaken.

2.3. Post-segmentation processing

2.3.1. Visualisation of surface-rendered images

Having generated suitable surface renderings, the normal range of variation of surface gyral patterns needs to be determined so that abnormal gyri may be identified.

The human brain is an anisotropic shape, variable in detail between individuals. Even monozygotic twins may have discordant gyral patterns (Steinmetz et al.,1994). The precise amount of intersubject variability has not been formally determined in the population, though large control series have examined the amount of variation in three-dimensional shape in about 300 subjects. All quantitative attempts at comparison of brain shapes require the presence in the brain of some reference frame which can be used to align different brains so that they may be compared. In most of the literature, the aim of the work has been to allow registration of a brain either to itself (imaged in different modalities or over time) or to a model "normal" brain (Collins et al.,1994). The doyen in this field, Bookstein, has produced a method of aligning brains using statistical deformation techniques (see Bookstein, 1991). For midsagittal MR images of the brain, alignment satisfying various requirements is achieved by identification of (at least) four midsagittal landmarks and then deformation of an individual brain to maximally align these landmarks to a template derived from the statistical alignment of the same landmarks from a number of individuals. This allows a "normalised" midsagittal image to be generated for each individual. Evans et al. (1992) have taken coregistration further and generated a three-dimensional "average" shape from 250 normal subjects. It should be noted that their average brain has very few identifiable sulci.

Such work of course is not designed to examine shape, rather to register and "normalise" brains. Indeed, shape is

specifically distorted during the registration process, so that individual regional distribution of volume is disturbed or lost. Such individual detail relates closely to cytoarchitectonic fields and may provide a better guide to functional localisation than does reference to an idealized brain (Rademacher et al.,1993). In addition, intersubject registration presupposes that some degree of homogeneity exists between the averaged brains - or if not present initially, that it can be produced by preliminary deformation. Brains with CD associated with gyral anomaly may have unique gyral patterns that are radically different from most normal brains, making coregistration with a normal (or "average") brain difficult. For the purpose of identification of abnormal gyri, the end result is unhelpful, though quantification of the process required in an individual, less distorted, case to *achieve* registration with the average brain might give some idea of the specific shape of that brain. This possibly useful and sophisticated technique for gyral analysis was not available to the author.

Visual determination of gyral abnormalities from three-dimensional images, on the other hand, does not suffer from these problems of averaging out valuable information. Allowances can more easily be made for differing brain and hemisphere sizes (which can be quantified subsequently), and for torques in the major brain axes (Kertesz et al.,1990), in the same sophisticated way that human visual processing can, for example, identify many differently shaped, stylised and incomplete forms of letters as those letters (eg a: A a α ɑ....). This is achieved, however, at the expense of introducing subjectivity and increased processing time. Depending on the specific surface rendering model chosen, variation apart from that due to biology may also be introduced by such banalities as the position of on-screen lighting by computer-generated sources. These problems may be overcome given adequate processing time. That of subjectivity can to some extent be overcome by blinding raters to the

identity and class of the subject being examined. By viewing all three-dimensional representations from all perspectives, specific projection biases can be addressed. Provided that a large enough control group is available for visual comparison, this technique should allow detection of gyral abnormalities.

Nevertheless, there may be better ways of examining surface-rendered images. Curvature-based models can overcome problems generated by external lighting models, surface voxels on the reconstruction having, for example, brightness values according to local curvature determined with respect to the position of neighbouring voxels (Andreasen et al.,1994). Such models may prove useful in the future, as areas identified visually as being abnormal can be located precisely from the data and be described quantitatively based on spatial coordinates and local curvature indices.

2.3.2. Quantitative analyses

The interdependence of structure, as measured by cerebral whole and part volumes, and function has long been a topic of interest - both scientific and political. Functional localisation in the brain has been shown to relate to some extent to local cytoarchitecture (von Economo, 1929; Rakic, 1988; Rademacher et al.,1993). On this basis, many workers have sought to relate malfunction to specific quantified changes in cerebral volume. For studies using MRI data, volumes are almost invariably estimated using the Cavalieri principle (Gundersen and Jensen, 1987; Mayhew and Olsen, 1991). In essence, this stereological device allows the estimation of the volume of an irregular three-dimensional object by calculation of the cross-sectional areas of a number of parallel slices through the object, if the thickness of the slices is known. It has been shown that the use of as few as ten slices through an irregular object produces an estimate with an expected coefficient of error of less than 5% (Gundersen and Jensen, 1987). In fact, the coefficient of

error varies approximately inversely with the number of slices (Henery and Mayhew, 1989). The use of one single slice is therefore associated with a large error, whilst the use of 120 or so slices (for whole hemispheres), as in this study, is associated with a very small expected coefficient of error. This number of slices is not necessary to estimate hemispheric volume to a small predicted error, but is required to maintain the same small degree of error when *regions* of the hemisphere are examined; detailed surface renderings also benefit from the use of a large number of thin slices.

The area measured on any given MRI slice will suffer from overprojection error increased by slice thickness, such that slices thicker than 4mm generate errors of at least 5% in volume measures in phantoms (Filipek et al.,1989). Hennig (1969) showed that for spherical objects in histological preparations, the "correction coefficient" for volume estimation due to finite section thickness is

$$1/\{1 + 1.5(\text{section thickness}/\text{object diameter})\}$$

This formula is not strictly applicable to MRI, but approximates to the error found by Filipek et al. (1989) for 4mm slices. Measurements using thicker slices of smaller objects (eg 5mm slices of the hippocampus) would be associated, on this basis, with errors of the order of 80%. Therefore data must be cautiously interpreted when inadequately thin slices are employed. For 1.5mm slices of the cortex, the overprojection error is of the order of 1.5%, an acceptable figure given the degree of volume change being studied.

Conditions in which volume measurements have received much interest include normal development and aging, Alzheimer's disease, schizophrenia, HIV infection and Down's syndrome. Various methods have been used to determine variation and abnormality of volume in these studies and to

relate them to clinical findings. Some of these will now be reviewed.

Normal cerebral anatomy and volumes have been extensively studied. The measurement of the volumes of whole brain have been discussed above (see methods of segmentation). Regional analyses have also been performed. Kertesz et al. (1990) made several claims about cerebral asymmetry based on linear and area measurements of lobar extents. This work is significantly flawed as there are numerous biases introduced by their methodology: in particular the use of single transverse slices through complex objects to determine their extent and shape is invalid - a single slice, not chosen randomly, cannot be representative of the entire three-dimensional structure to within an acceptable coefficient of error.

MRI-based measures using the Cavalieri principle are now commonly reported. Three recent studies demonstrate the issues of importance (Pfefferbaum et al.,1994; Blatter et al.,1995; Filipek et al.,1994). Pfefferbaum et al. (1994) report a study of changes in brain volumes with growth from infancy to late adulthood. However, there were major problems with data acquisition and analysis. Data was acquired differently for older and younger subjects; for the older group, slices were 5mm thick with an interslice gap of 2.5mm. In slices of this thickness, overprojection errors are likely to be higher (see above). Reliability of segmentation methods depends in part on the complexity of the object being processed (Kikinis et al.,1992); the grey and white matter are much more complex than the hippocampus, in the mensuration of which such thick slices and large interslice gap create large errors. The younger age group was also scanned with variable interslice gaps and different fields of view. The authors "arithmetically adjusted" their data from the younger age group for comparison with the older age group - no details of this are given. Having acquired their data, Pfefferbaum et al. analyse only selected slices. Certain slices were not used because of

marked partial volume effects (exaggerated by their thick slices and slice orientation), whilst other slices were excluded because the automatic segmentation algorithm did not work in them. The amount of brain thus excluded from their analysis is not determined; given the anisotropic structure of the brain, this introduces a bias for which no correction is possible (or attempted). Further bias is introduced by their regional analysis. In the slices they have selected for analysis, they measure grey and white matter volumes in only the outer 45% of tissue on any given slice; the inner 55% could not be analysed reliably by their automated segmentation method. If some individuals have deeper - or more shallow - sulci than others, different proportions of grey and white matter will be excluded in different individuals, making them incomparable. Undetermined amounts of grey and white matter are thus nonrandomly excluded from selected slices and segmented by a method that does not appear to be robust. Their extensive discussion, founded on unreliable data, can be given little weight. This paper illustrates the many pitfalls to which volumetric MRI analysis is prone. It is not an encouraging standard for automated segmentation; the advantage gained in time and ease of analysis would seem to be entirely lost by the unreliability of the results obtained.

Blatter et al. (1995) provide a large database of normative volumetric data from MRI studies. In contrast to the report by Pfefferbaum et al., they use what would appear to be a more robust segmentation method, that is commercially available and which allows them to use all the data available in each study. They also acknowledge the need to account for inhomogeneity in data acquisition. They determined interrater and intrarater reliability coefficients for their technique. These are high except for repeat segmentations of the grey and white matter (the majority of the volume of the hemispheres!). Their *intrarater* coefficients for these tissues are 0.763 (grey) and 0.842 (white). They do not describe the anatomical boundaries used for grey and white matter; this may account at

least partly for these comparatively low intrarater reliability coefficients and illustrates the importance of rigorous definition of boundaries independently of their specific positioning by segmentation.

The report by Filipek et al. (1994) is the most rigorous of these studies of the normal brain. However, there are a number of issues that should be discussed. The first is that prior to analysis of their data, they performed positional "normalisation" and resampling. As no regional estimations were performed and the entire data set analysed and volumes calculated by the Cavalieri principle, the need for this is not clear. That the normalised data were resampled prior to segmentation introduces interpolational changes that cannot be quantified and are not mentioned. Secondly, an entirely automatic segmentation is performed, within defined anatomical boundaries (that are given in some detail). It is said that this reduces the error produced by visual choice of interfaces. This of course is true, as the choice is not visual. However, that the choice is automated does not imply that it is necessarily any more accurate or valid (see above and section 3.6.). Curiously, these authors do not discuss the reliability of their technique.

Regional analyses of brain volumes have been performed by other workers in attempts to find local structural abnormalities underlying functional changes. Whilst many of these studies are rigorous in their methodology, nevertheless some issues remain unaddressed. Raz et al. (1995) report on regional cerebral volumes from a group of individuals with Down's syndrome and compare these with normal controls. They define a number of regions in each individual by manually tracing defined boundaries; correlation is then shown, for example, between parahippocampal gyral volume in affected individuals and performance intelligence quotient. Their analysis of brain volumes, however, assumes that brain shape is the same in individuals with Down's syndrome and control

subjects, so that their boundary definitions of many regions, that are governed by anatomical landmarks, are equally applicable to both groups of subjects. However, individuals with Down's syndrome have many anthropometric abnormalities: they are, for example, usually much shorter than controls. The authors attempt to adjust for this for this particular discrepancy statistically. They do not provide any evidence, however, that brain shapes are not different between the groups or that any differences in shape might be completely accounted for by adjustment for height (unlikely *a priori*, as shape is three-dimensional), so that one cannot be confident of all their conclusions. Some of their results may simply be a measure of brain shape dissimilarity; these may well relate to underlying cytoarchitectural disruption and be what Raz et al. are actually measuring. In addition, Raz et al. "correct" their original data for the effects of head tilt, pitch and rotation by using standard neuroanatomical landmarks and bringing each brain into a unified system of coordinates: all of this assumes, as above, that all the brains have shapes similar enough for this to be meaningful.

The criticism that brain shapes are assumed to be the same applies to all studies in which regional rule-based measurements are performed, especially if entire volume is not measured or adequately defined. It applies, for example, to a study of regional brain volumes in schizophrenia by Breier et al. (1992). The frontal cortex is defined as that volume lying between the most anterior slice in which frontal cortex was visible and, posteriorly, the first slice in which the genu of the corpus callosum became visible. This *assumes* that all subjects brains compared were of similar shape and that rotation (for example around a coronal left-right axis) was irrelevant. They did not provide any proof of the first assumption, nor any quantification of the errors generated by the second. Thus their measures may have been not only of frontal volumes but also of frontal shapes: it cannot be concluded that real differences in volume alone necessarily

exist. In another study of the brains of individuals with schizophrenia, Schlaepfer et al. (1994) again use a model-based regional volume estimation technique without either discussing or quantifying the errors possibly generated. Whilst their implicit assumptions that brain shapes are similar may be true, it cannot be assumed that exclusion of regions of grey and white matter from the analysis, in the same way that Pfefferbaum et al. (1994) did, has no significantly different effect on the groups compared. Reiss et al. (1993) published data on regional grey and white matter loss in children suffering from a neurodegenerative condition called Rett syndrome. Each segmented brain was divided into 16 regions by 5 planes defined by anatomical landmarks. This division itself assumes - without any proof or estimation of variation - that landmarks are comparable between control and disease brains, and that brain shape is comparable, again without any proof. Subsequently, component volumes within a given region were divided by total brain volume within that region to correct for "the possible influence of slight variations in head tilt and slice location". Again, this assumes that regional distribution of total brain volume in different brains is identical, which remains unproven. Their results are therefore an estimate of brain shape combined with the effects of tilt and positioning, and not just of regional grey and white distribution. Sometimes, poor definition and unexplored assumptions may even generate dangerous data. Andreasen et al. (1993) report results showing significant correlations between regional brain volumes and various measures of IQ in normal individuals. However, they do not define the boundaries for their regions of interest at all; in the case of the hippocampal formation (which they measure), boundary definition is well known to be difficult (Bergin et al.,1994). This is confirmed in their own report by a figure quoted for interrater reliability of 0.53 for test-retest (undefined statistic) repeats: this is said to be "within the acceptable range" but is well outside figures that can be achieved (Bergin et al.,1994). There is a large body of such

flawed work, especially in the psychiatric literature, where the search for quantitative biological "validation" of preexisting concepts and theories often seems to lead to the publication of work in which assumptions cannot be true, premises are unsustainable and results and conclusions incredible. Once published, such results often become accepted as scientific fact and misused (Gould, 1989).

From this review, it is apparent that there are a number of ways of determining various volumes in healthy and diseased brains, but that none is perfect. Problems with methodology are rarely discussed or even raised. Most importantly, the assumption of brain shape comparability is usually unproven (and rarely even raised). Rather than assuming that brains are the same shape, or forcing brains of different shapes artificially into a common reference frame and thereby losing information, an alternative approach is to explore brain anatomy from a structural viewpoint by examining the differences in brain shape between individuals, accepting that this is what is actually being measured (at the very least) and that alterations in brain shape are due to composite alterations in underlying structures at various as yet inaccessible levels, from the laminar organisational and macroscopic aggregate to the individual cytoskeletal. These alterations may be the local and distant effects of cerebral dysgenesis that are partly the subject of this thesis.

Having explored the issues and concerns with regard to data acquisition and analysis in cases of refractory epilepsy associated with cerebral dysgenesis from the twin perspectives of the structural biology of the lesion and the pitfalls of image analysis, the management of these issues in this thesis can now be addressed.

CHAPTER 3: METHODS

3.1. Subjects: patient and control selection

Thirty-three neurologically normal volunteer subjects, 11 female and 22 male were studied. Their age range was 19 to 52 years. All gave informed consent for the scanning procedure. Twenty-seven subjects were right-handed and five left-handed; handedness could not be ascertained for one subject.

Patients were all were drawn from clinics at the National Hospital and the Chalfont Centre for Epilepsy. They were selected for the following groups:

1. Patients with definite cerebral dysgenesis previously identified on routine visual inspection of their printed films by an experienced neuroradiologist (n = 22).
2. Patients with chronic partial (usually refractory) epilepsy in whom routine visual inspection had failed to reveal any specific neocortical lesion (n = 45). Three of these patients had had surgery elsewhere without relief from seizure activity.
3. Patients with only subependymal heterotopia seen on routine inspection (n = 13).
4. Patients with only hippocampal sclerosis (HS) identified on quantitative analysis of MRI data (n = 16). This was a disease control group, chosen because they had a focal cause for their epilepsy (as shown in the 10 quantitatively analysed who were all seizure-free postoperatively and because none had any other abnormalities seen on inspection: 85% of cases of HS are known to have no evidence of other lesions on MRI; Raymond et al.,1994b). Other possible disease controls groups, eg patients with epilepsy due to focal cerebral damage, were not available in sufficient numbers, nor could the focal nature of their lesions be guaranteed.

Of these 96 patients, 19 (13 from group 2, including the three postoperative cases and 6 from group 4 who were less than a year postoperatively, the other ten having been followed up for more than 2 years) were studied by reconstruction only because of time limitations; all the others were further analysed using other techniques. In addition, nine studies were segmented more than once by a single observer, and eight were segmented by a second observer to assess intrarater and interrater stability. Four individuals were scanned repeatedly (two twice, two three

times) in different positions, allowing an assessment to be made of the effect of head position on the results. For those subjects analysed quantitatively, there was no significant difference in age between any group and the controls or between any group and any other group.

3.2. MRI data acquisition

Magnetic resonance imaging was performed on a 1.5T GE Signa unit (General Electric, Milwaukee, USA). A coronal SPGR (spoiled gradient recalled) sequence was used for image analysis (echo time, TE 5ms, repetition time, TR 35ms, flip angle 35 degrees, acquisition matrix 256x128, number of excitations, NEX, 1, field of view 24cm, producing 124 contiguous slices each 1.5mm thick). Sagittal T_1-weighted (TR/TE/NEX 500/10/2), and axial proton density (2800/30/1) and T_2-weighted (2800/90/1) images were also routinely acquired. Scans were acquired from 1991 to 1994.

3.3. Image visual review

All the images used in this study were reviewed by an experienced neuroradiologist, with a specific remit to examine for hippocampal sclerosis and cerebral dysgenesis, with knowledge of available localising electroclinical information. All scans were scrutinised specifically for abnormalities of the pattern of gyration, sulcal depth and cortical thickness and the pattern of the grey-white interface. These are amongst the commonest manifestations of dysgenetic lesions (Barkovich et al.,1987, 1992a & 1992b; Raymond et al.,1995). In addition, scans of 20 patients, initially reported as normal, were reexamined by the neuroradiologist in blinded fashion in random mixture with scans of 20 normal control subjects; no abnormalities were reported. The scans of the patients with hippocampal sclerosis were reviewed with a view to detection

of additional cerebral dysgenesis (Raymond et al.,1994b): none had any additional dysgenetic lesions. No neocortical gliosis was reported on T_2-weighted imaging.

3.4. Image analysis

3.4.1. Segmentation

A dedicated image processing workstation (Allegro, ISG Technologies, Toronto, Canada), designed for the reconstruction of slice data into three-dimensional images using thresholding and region-growing, was used. All MRI data processed by the Allegro is converted to an isotropic voxel format (cubic voxels, edge length 0.46875mm).

Although blinding to the subject's identity is possible, blinding to the MRI data is not because segmentation is manually supervised. Because familiarity with cerebral anatomy is required to interpret the rules for the definition of the boundaries of the regions-of-interest, the operator is likely to identify lesions visible on inspection of two-dimensional images, such as cerebral dysgenesis and hippocampal sclerosis. However, patient clinical data were not known by any operator prior to segmentation so that observer bias was minimised.

Images were displayed on screen with operator-controlled width and level settings. Image brightness is known to affect segmentation (Harris et al.,1994). The process used by Harris et al. to correct for brightness was not available on the Allegro. Data brightness is fixed: display parameters (width and level) need alteration to produce images suitable for viewing. Preliminary assessment showed image display width and level had an effect on threshold choice in this work too. In the majority (75%) of cases, width and level were both set to 100; in 14 of the remaining 29 subjects, either width or level differed in magnitude by only 20 points from this 100/100

setting. The effect of this range of settings on the choice of threshold for segmentation of grey and white matter was explored in one subject whose ideal settings for both width and level were 100 (Table 3.1). Because of the reliability of segmentation overall (see 3.7 below), the issue of threshold variation changing with image display parameters is in fact unimportant.

Table 3.1. Lower threshold chosen for white and grey matter segmentation at various level and width settings for a single slice in a subject whose ideal level and width settings are 100/100. Entries are for white/grey thresholds. Visually acceptable settings for segmentation are outlined in the central box.

Level / Width	60	70	80	90	100	110	120	130
60	*	*	*	*	*	108/ #	108/ #	110/ #
70	*	*	*/ 64	*/ 68	*/ 74	108/ #	108/ #	110/ #
80	*	*/ 60	104/ 68	104/ 68	104/ 68	104/ 68 #	104/ #	104/ #
90	*	*/ 64	104/ 68	104/ 68	104/ 68	104/ 68	104/ #	104/ #
100	104/ 64 #	*/ 60	104/ 68	104/ 68	104/ 68	104/ 68	104/ 68 #	104/ #
110	104/ 64 #	104/ 64	104/ 68	104/ 68	104/ 68	104/ 68	104/ 68 #	104/ #
120	104/ 64 #	104/ 64	104/ 68	104/ 68	104/ 68	104/ 68	108/ 68 #	104/ #
130	104/ 64 #	104/ 64 #	104/ 68	104/ 68	104/ 68	108/ 68	108/ 68 #	108/ 64 #
140	104/ 64 #	104/ 64 #	104/ 64 #	104/ 68 #	104/ 68 #	108/ 68 #	108/ 64 #	108/ 64 #
200	104/ 64 #	104/ 64 #	104/ 64 #	104/ 64 #	104/ 64 #	108/ 64 #	108/ 64 #	108/ 64 #

Symbols: * grey and white matter cannot be distinguished
grey matter becomes invisible or indistinct

From these data, it can be seen that the lower threshold for the grey or white matter needs to be changed only for relatively large (~30%) level and width changes; most commonly at these window settings, grey-white separation becomes impossible or the grey matter vanishes, so that such settings are not chosen. Small windowing changes of up to 20 points either side of the ideal for either level or window have no effect on the chosen threshold.

In some cases images were not visible at these settings; ideal values were chosen by adjustment of image width and level on an analogue scale on screen such that the appearance of slice 30 in the data set (always the first slice segmented) was similar to images in other studies. For 100 subjects, the choice of width and level was repeated without knowledge of the previous choice to assess reliability (see section 3.6.).

Once images were suitably displayed, the upper and lower threshold limits for segmentation for each ROI were set. For all ROI's except the ventricles, the upper threshold was always set at the upper limit available (4095). The lower limit was chosen by the operator, initially using an analogue sliding cursor on screen for gross adjustment. The choice was then fine-tuned digitally by application of a mask with the threshold choices on screen and then adjustment of the lower threshold until optimal coverage of the ROI by the mask was achieved as judged by the operator on visual correspondence between the mask and the visually-determined ROI (Fig 3.1). Because of RF inhomogeneity, which is smooth and progressive, the optimal threshold may vary both within and between slices. The threshold was therefore altered between slices for a given ROI as necessary; this usually meant altering the initial lower threshold value by increments of 2 to 4%. Thresholds were changed as often as required within a single study. Each mask with its defined threshold limits is called a seed and ROI's are outlined automatically by the growth of the seed until it covers all the relevant area. The seed is positioned

Figure 3.1. In the upper figure, a mask has been applied to the image to cover the cerebral hemispheres and match the grey matter-CSF boundary as closely as possible. The lower threshold for the CH seed is thus set and the CH can be segmented out from the image. In the lower figure, the threshold for the mask has been raised so that it covers the white matter thus enabling a seed to isolate this region of interest. Note the incomplete inclusion of the thalamus, which was added to the SM ROI subsequently (see Appendix 1).

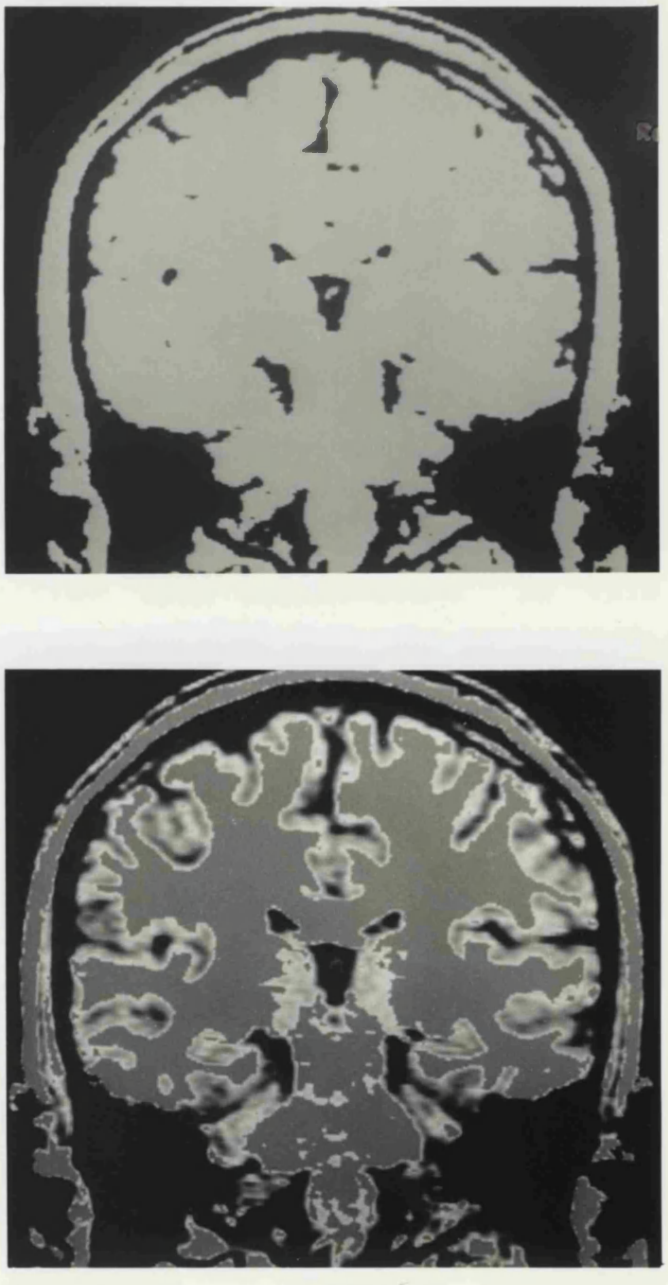

Figure 3.2. Seeding of the left temporal lobe white matter occasionally required the setting up of a separate seed with a slightly reduced lower threshold. In this case, seed 71 has a lower threshold of 100, whilst seed 72 has a lower threshold of 96. Both are required to ensure complete segmentation of the left SM.

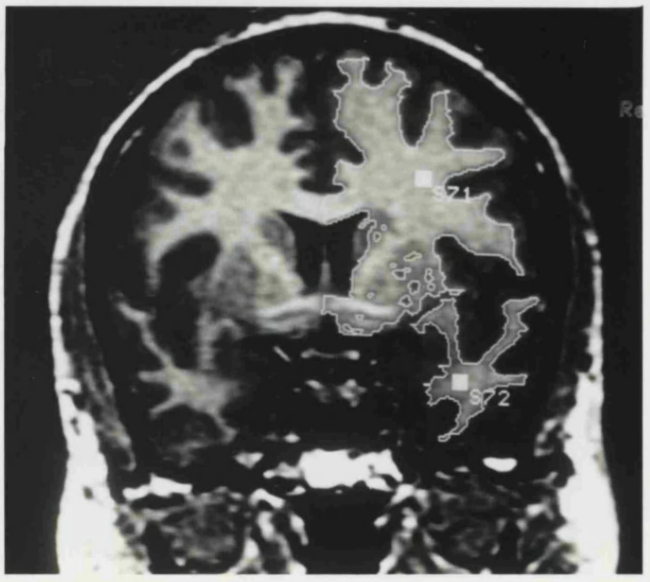

Figure 3.3. This figure demonstrates the importance of manual supervision of the segmentation process: unsupervised, discontinuous areas all belonging biologically to the same ROI might be omitted from segmentation. In this image, the automatic process isolated only the peripheral component of the ROI: manual placement of a seed in the larger unsegmented ipsilateral SM was required.

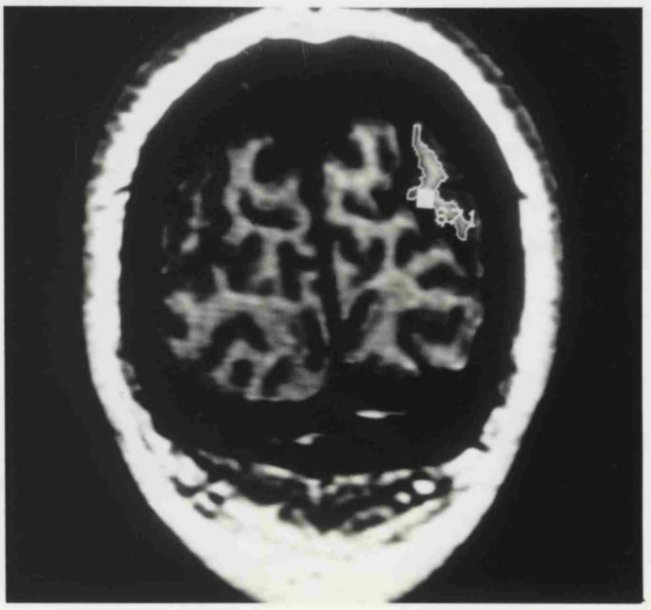

within a chosen ROI by the operator. Due to RF inhomogeneity specific to a scanner, separate seeds were occasionally needed for the left temporal lobe, with the lower threshold usually 4 to 5% lower than that for the main body of the SM (Fig 3.2 and Appendix 1). Manual editing was required to ensure that the ROI isolated on each slice was biologically valid; thus extracerebral soft tissues occasionally needed removal. Additional seeds for a given ROI also needed to be placed when the plane of imaging made isolated islands of the ROI (eg white matter cores of gyri separated from the main body of white matter because they were discontinuous within a given slice; Fig 3.3). Because such continuity was easier to judge from the centre of the brain than from one end, and because shifts in threshold requirements also occurred at the poles on the coronal images, segmentation was started in every case in image 30 and proceeded first posteriorly to the occipital pole, then anteriorly from image 30 to the frontal pole until the entire brain had been analysed.

In the case of the ventricles, the lower threshold value was fixed at 0 and at the subcortical matter lower threshold for the upper value. This ensured that when the ventricle was incorporated into the SM for the estimation of SM surface area (see below and Appendix 1), it was completely abolished as a separate ROI.

3.4.2. Regions-of-interest boundary definitions

Regions-of-interest were defined on slices according to rules devised to ensure both maximum biological relevance and operator reproducibility. Separate region-of-interest seeds were set up for right and left cerebral hemispheres (CH), subcortical matter and ventricles; the caudate and, where present, hamartomatous tissue or subependymal heterotopia, were also isolated with separate manually-drawn ROI's. The details of the boundaries are given in Appendix 1.

ROI's were stacked automatically by the Allegro in the reconstruction process generating three-dimensional representations. Volumes were automatically calculated from the sum of the areas of each ROI in each slice according to the Cavalieri principle (see 2.3.2).

Hippocampal volumes were measured according to the method previously described from our centre and in regular use at this institution (Cook et al.,1993). These measurements were made using a GE Independent console at St. Mary's Hospital.

3.5. Statistics

The normality of distribution of every parameter in the control group was assessed using normal probability plots and Kolmogorov-Smirnov (or Shapiro-Wilks) statistics. Normal ranges for normally distributed variables were then defined as within three standard deviations from the mean for a given variable. For variables for which it was significantly unlikely that nonnormal samples had been drawn from a normally distributed population, or for small sample numbers, nonparametric statistics were used. The individual statistical test used in each case is noted. Significance was taken at the 0.01 level.

Reliability was assessed for repeat measures using the intraclass correlation coefficient (Snedecor and Cochran, 1967). This measure does not require normal distribution of variables, and accounts for different variances, means and ranges in separate comparison groups. A value of 1 for this coefficient implies that there is no intrasubject variability for a given measure that is repeated, whilst a value of 0 means that differences between measures obtained on the same subject on repeated testing tend to be as large or larger than those between subjects.

All statistics were performed using SPSS for Windows, Version 6.1 (SPSS Inc, Michigan, Chicago).

Up to 116 quantitative parameters were examined in each subject. Testing of the normality of the distribution of each of these parameters in controls revealed that in only one case (left/right SM ratio in block position 3) was a variable that did not appear normally distributed on a frequency histogram unlikely to have been sampled from a normally distributed population. However, as 116 variables were tested and the significance level for the Kolmogorov-Smirnov (or Shapiro-Wilks) statistic set at $p = 0.01$, one variable satisfying this criterion would be expected to be found by chance alone. Given the high degree of interconnectivity in the cortex, that all the other variables were probably normally distributed suggests that the finding for this one variable is indeed due to chance alone.

3.6. Validity

A valid measure unbiasedly reflects reality. Ideally, the validity of a measure is determined against a gold standard, against which the new measure can be compared. Unfortunately, for many of the measures described here, such standards do not exist, or are not truly comparable; for some of the measures, MRI is the *only* way they can be obtained. The possible biases of the postprocessing analyses are considered in sections 3.10. and 3.13.1; the validity of segmentation is considered further below.

Validation of segmentation is usually assessed against phantoms. Such phantoms may be "complex", with multiple internal components as described by Kohn et al. (1991). Their models were not intended to be "anthropomorphic" yet "were intended to simulate conditions problematic for the segmentation of brain and CSF from MR images". Neither did

their phantoms "model T_1 and T_2 relaxation properties of brain and CSF". Yet their view of an "optimal phantom" was one that modeled both relaxation properties and structural boundaries. Other authors attempt to assess the validity of their segmentation methods with "realistic brain phantom images" (Schlaepfer et al.,1994), having previously stated that no phantom is really complex enough (Harris et al.,1994). The author's experience is that the macroscopic features of the brain, for example the abuttal of gyral walls in the depths of sulci, create many of the problems in segmentation: these are likely to be insuperable using any technique for in vivo analysis.

Validity has been assessed by comparison of results with those obtained by measurement of grey and white volumes using other techniques, almost invariably on fixed tissues. Such methods bring their own problems and, without accurate assessment of method-specific errors, comparison can only be limited (DeCarli et al.,1992). Comparison of five studies with results from this study are made in Table 3.2 (WM = white matter; the results of Blatter et al.,1995 presented are the mean of their means for males and females across all age groups; for Miller et al.,1980, the mean of young male and female hemispheres - side unspecified - have been averaged and are presented in the right hemisphere column).

Table 3.2. Comparison of volume results

Study	Whole brain GM	Whole brain WM	Right GM	Right WM	Left GM	Left WM
Kohn 1991	-	-	677 (GM+WM)		671.9 (GM+WM)	
Jackson 1994	753.6	621.7	-	-	-	-
Filipek 1994	688.8	443.8	346.2	221.8	342.6	221.1
Blatter 1995	679	652	-	-	-	-
Miller 1980	-	-	586		-	-
Current study	513	487	250	250	263	237

The results, though all of the same order of magnitude are clearly different and reflect the wide differences in changing methodologies, segmentation, ROI boundaries and, possibly, populations. For some measures (eg the SM surface area), comparable results may not exist or the methods may be biased: validation is then more difficult to perform. However, comparison of data obtained using identical techniques should still be useful, provided that bias, if present, does not affect different individuals differentially. This is addressed further below.

3.6. Reliability

As all aspects of the thesis are dependent on segmentation, the reliability of all aspects of this process were tested.

The choice of windowing and threshold have an effect on segmentation. The effect of windowing has been addressed (section 3.4.1.). The effect of thresholding was investigated in 3 subjects, by segmenting samples of slices using an imposed range of thresholds for the SM from the grossly overinclusive to the grossly underinclusive: the extreme thresholds required the use of the lasso function to encompass areas that were clearly part of the SM. The results are shown in Tables 3.3 and 3.4.

Table 3.3. Effect of threshold choice on resulting area segmented in a control subject (slice 60, right SM seed).

Threshold	Area segmented	Ratio actual/ideal threshold	Inverse of threshold ratio	Ratio area for set threshold/ area for ideal threshold
78*	4020	0.85	1.18	1.45
80*	3790	0.87	1.15	1.37
82*	3570	0.89	1.12	1.29
84*	3360	0.91	1.10	1.21
86*	3180	0.94	1.07	1.15
88	3060	0.96	1.05	1.10
90	2940	0.98	1.02	1.06
92 (ideal)	2770	1	1	1
94	2640	1.02	0.98	0.95
96	2490	1.04	0.96	0.90
98*	2280	1.07	0.94	0.82
100*	2090	1.09	0.92	0.76
102*	1700	1.11	0.90	0.62
104*	1180	1.13	0.89	0.43
106*	985	1.15	0.87	0.36

Symbol: * segmentation inaccurate as judged by visual inspection.

Table 3.4. Changes in total right SM area across brain with change in lower threshold value.

Threshold ratio(actual/ideal)	Inverse ratio of thresholds	Ratio of summed areas segmented
Control subject, right SM ROI's summed over 20 equally spaced slices		
0.85	1.18	1.70
0.92	1.09	1.39
1.00	1.00	1.00
1.02	0.98	0.92
1.09	0.92	0.64
Patient 4, right SM ROI's summed over 20 equally spaced slices		
0.90	1.12	1.56
0.94	1.07	1.33
1.00	1.00	1.00
1.06	0.94	0.74
1.13	0.89	0.43

It can be seen that the resulting areas (and hence volumes) are sensitive to the choice of threshold; the appearance of reconstructed images is not (Kohn et al.,1991). Fortunately, however, the lower threshold choices for both CH and SM are highly reproducible, and windowing has little effect on the reliability of the choice of threshold (see below).

Repeat segmentation of either CH or SM in a given slice showed that the choice of the position of the seed within the region-of-interest had no effect on the resulting area encompassed provided that all appropriate tissue was seeded. Thus repositioning of a seed in a single discontinuous area without the placement of a seed in other areas could lead to erroneous results (Fig. 3.3).

To assess the reproducibility of the entire segmentation process for CH and SM, four studies were segmented five times each by the author, who was blinded to previous segmentations; five other studies were segmented twice each, also blindly, and in these the block volumes were compared. The choice of reformatting plane and seeding of the cross-section of the corpus callosum (section 3.7.2) were repeated over an interval of 18 months. The resulting areas and maximum callosal length on the reformats were compared. Eight studies were resegmented by a second operator, blinded to the segmentation of the first operator. The volumes of the resulting structures were compared (Table 3.5).

Table 3.5. Interrater correlation coefficients

(Number of subjects studied)	Interrater correlation coefficient			
Level (7)	0.833			
Width (7)	0.790			
	Right		Left	
	CH	SM	CH	SM
Threshold (8)	0.999	0.968	0.999	0.989
Volume (8)	0.918	0.731	0.919	0.600

The windowing correlations between raters are not high. However, whilst a more rigorous approach requiring preprocessing of data as performed by Harris et al. (1994) might be preferable from this point of view, the system used for determination of image brightness in fact had little effect on the choice of the threshold for segmentation. Despite similar choice of threshold, however, the interrater correlation coefficient for the SM volume do not seem high. In fact values are equal to or higher than those reported by Blatter et al. (1995) who used, as the basis of their segmentation, multispectral analysis (see section 3.2.2), in which interrater reliability depends on boundary rule application and not choice of threshold. It would appear therefore that the application of boundary rules is the major factor causing interrater differences. For the results in this thesis, this finding is not important as all the results are based on the author's segmentations (the ideal situation, as suggested by Jackson et al.,1994): the intrarater correlation coefficients are all very high (see Table 3.6). For larger or longer term studies, improved interrater performance (by training) would be necessary.

Table 3.6. Intrarater correlation coefficients

Parameter	Right		Left	
Level (n=100)	0.936			
Width (n=100)	0.992			
Threshold (SM, n=82)	0.999		-	
Threshold (CH, n=80)	0.999		-	
Volume, SM (n=4, 5 complete resegmentations)	0.998	min/max 0.974	0.998	min/max 0.964
Volume, GM (n=4, 5 complete resegmentations)	0.996	min/max 0.987	0.999	min/max 0.988
Surface areas (n=4, 5 complete resegmentations)	0.997		0.997	
Blocks on repeat segmentation of same scan (n=80 blocks)	0.999			
Blocks on repeat segmentation of different scans of 3 individuals (n=120 blocks)	0.999			
CCA (n=42)	0.987			
L (maximum callosal length on reformats, n=35)	0.984			

min/max is the mean ratio across the group of minimum to maximum volumes from repeat segmentations of a single subject.

3.8. Visualisation

Reconstructed images were visualised on screen, rotated, magnified and cut as desired. Once reconstructed, CH, caudate nucleus, SM and blocks from each hemisphere were separately viewed to check that segmentation had been complete, in particular to ensure that all contralateral hemispheric tissue had been excluded and that all extracerebral soft tissue had been removed. On-screen computer-generated sources lit images; shifting their position could alter the appearance of reconstructions and was always performed for thorough inspection of the gyral pattern. Screen images could be saved for future inspection, comparison and photography. All three-dimensional representations were also compared with a standard atlas of sulcal patterns (Ono et al.,1990).

3.9. Whole volume analysis

The volume of the entire left CH (grey matter, subcortical matter and caudate nucleus, with any dysgenetic regions) was compared with the volume of the right CH to generate a total ratio, TRAT.

3.10. Regional analysis of volume

3.10.1. Method

The shape of an object is the regional distribution of its volume in space. Measurement of this distribution is therefore a quantitative description of the shape of an object, though there may be simpler ways of describing regular objects (such as a sphere). The regional distribution of volume in a highly complex object, such as the cerebral hemisphere, is biologically determined by the amount and position of its various component tissues, primarily the white

and grey matter. The mechanisms governing this distribution are not known. In certain cases, there is frank and visually-detectable maldistribution of these tissues with well-recognised changes in the constitution and construction of the grey or white matter (cerebral dysgenesis). The detection of regional alterations in the distribution of grey and white matter volumes in reconstructions beyond the visualised lesion would support the hypothesis that structural changes in patients with dysgenesis are extensive. Any technique that allows the examination of the shape of the hemisphere should be suitable for this purpose; some methods may be more amenable and suitable for the data available than others.

A novel and conceptually simple technique was devised for shape analysis for this thesis, attempting to take problems defined in Chapter 2 into account. Potential biases in the method were explored. The method was developed from the observation that whole hemisphere volume symmetry was often significantly disrupted in patients with dysgenesis. It determined whether such asymmetry was due to unequally distributed volume changes or diffusely spread symmetry disruption within each hemisphere. Whilst total hemispheric volumes and TRAT are independent of hemisphere shape, regionalised volume asymmetries or simply regional volume measurements within a single hemisphere are in fact a measure of hemispheric shape. Thus the technique not only allows determination of regional volume distribution within the hemisphere, but at the same time quantifies hemispheric shape.

The method for regional analysis was as follows. Hemispheric GM and SM reconstructions were divided into smaller volumes, called blocks: these were defined independently in each hemisphere in each brain to span one tenth of the total anterior-posterior extent of the hemisphere from which they were derived (Fig 3.4). The anterior-posterior extent was defined by the first and last slices on which grey matter was visible on the original data set. Rotation of the

Figure 3.4. View from above of segmented cerebral hemispheres divided into blocks. The occipital pole is at the top of the picture. Each block extends for one-tenth of the the entire extent of the hemisphere that contains it. Blocks (or ratios) are numbered 1 to 10 as shown.

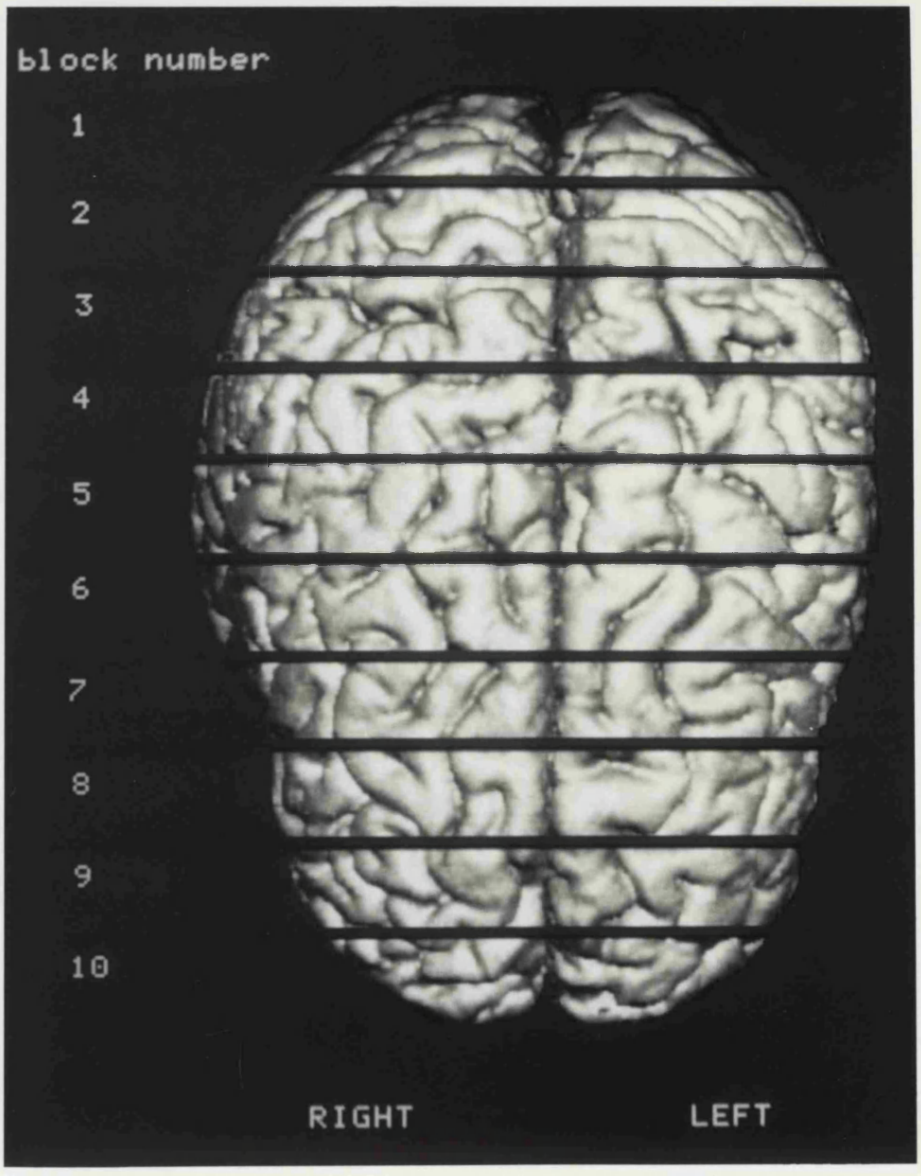

brain in the scanner may affect this extent, but no correction for rotation was undertaken, because this requires landmark identification and there are not always enough indisputable landmarks for brains, and those that are used assume that all brains are the same shape (see section 2.3.2). Inspection of routine images from some patients with dysgenesis showed that such "landmarks" indeed do not always exist. In addition, even isotropic correction into some defined, but arbitrary, framework requires the reformatting of data that of necessity involves interpolations from the original data. The effects of these interpolations are thought to be minimal when thin-slice data is used, but are still present and could not have been quantified with certainty. The inestimable bias introduced would have had effects on surface voxel counts and volume measurements through its effect on segmentation and on the application of boundary rules used in isolating regions-of-interest on each slice. Thus data was not corrected for rotation in the scanner. It should be stressed that gross rotation is unlikely because the range of variation of slice orientation with respect to major landmarks usually apparent (eg the long axis of the corpus callosum) was limited by (i) the nature of scanning brains *in vivo* in the long tunnels of MRI machines, as subjects are required to lie supine and comfortably within the scanner and (ii) the need to produce images that are readily comparable between subjects by visual inspection by a neuroradiologist. In order to be rigorous and exclude patients in whom rotation may have been excessive, however, the following analysis of rotation was undertaken.

3.10.2. Effects of head orientation on regional volume measures

Rotation affecting measurement of regional volume distribution can be resolved into component rotations around sagittal, axial and coronal axes. Because blocks were created in the coronal imaging plane (ie with end-faces parallel to the coronal imaging plane), rotation in this plane (around the

sagittal axis) has no effect on the volume distribution measured using the block divisions, so that this rotation is irrelevant. On the other hand, components of rotation around the coronal and axial axes will affect the results of the estimation of regional volume distribution: these effects were studied.

In order to compute the degree of rotation of any object in three-dimensional space, its orientation in this space must be known. This requires the unambiguous determination of features intrinsic to the object that vary in spatial position with rotation of the object, so that determination of the relative position of these features with respect to coordinate axes of the containing volume enables calculation of the rotation of the original object. Consider the plan below. The lines AB and EF are some identifiable features (landmarks) of the brain.

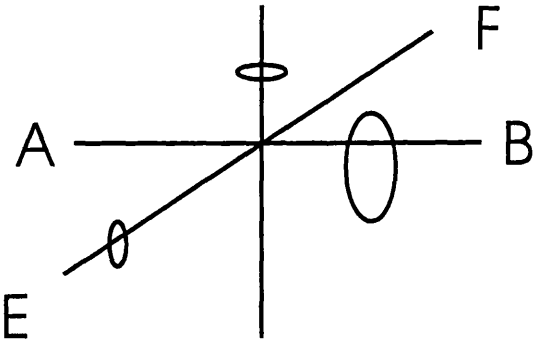

This brain is then imaged using a thin-slice protocol. The relative orientation of the brain can be determined by the changes in the slices in which AB is present and the change in apparent length of EF (measured/real ratio) with rotation: that is to say that angles ß and γ may be determined. Angle α has to be more than 60 degrees before it affects the slice position of the ends of the line AB (see Appendix 2). This degree of rotation about an anterior-posterior axis is uncomfortable to achieve and impossible to maintain over the period of a volume acquisition scan (9 minutes). The range of rotations for a group of scanned brains can thus be determined from the maximum and minimum values of ß and γ.

If all brains were the same shape, then the range of variation of the block variables (or the coefficient of variation of these parameters) in given block positions would describe the shape of the brain, within the range of rotations over which the brains were scanned. If all brains were perfectly spherical, for example, then the range of variation of block volumes (corrected for brain size) would be zero and independent of rotations (because a sphere has an infinite number of axes of symmetry).

For nonspherical objects such as real brains, if shape varies in a limited way but lines AB and EF bear the same relationship in different brains to individual brain shape, then they can be used to estimate relative rotation between brains. For those brains whose rotation in the scanner falls within the range of rotations of the control subjects forming the normal ranges, these ranges can still be applied to the patient brain and abnormalities of regional volume distribution determined. If a brain is grossly rotated, regional volume analysis may be confounded by the rotations, and the results measure both alterations in shape and changes due to rotation.

However, the more wayward the shape of the brain, the less likely it becomes that the lines AB and EF will retain a "normal" relationship to that shape. In this case, the degree of relative rotation of the scan (of the abnormally shaped brain with respect to the normal controls) may not be as easily calculated, although the line segment EF can still be used to estimate the relative rotations of the same individual between scans (provided the relationship of EF to the brain as a whole does not change between scans or with brain orientation). In the limiting case, lines AB and EF may not exist at all in a given subject's brain and landmark-based orientation analysis may fail. In this limiting situation a still more robust means of analysis is required. When brains without gross dysgenesis are considered, these factors may

appear less significant, and thus may not have been considered extensively thus far by workers in this field (eg Talairach and Tourneux, 1988; Rohlf and Marcus, 1993; Collins et al.,1994).

In this thesis, landmarks are used only to determine whether shape analysis can be applied. One cranial and one cerebral landmark have been used to determine relative brain position. The cranial landmark is the most posterior slice in which the posterior wall of the internal auditory meati (IAM's) appear on the coronal images. This is equivalent to line AB. There is no evidence to suggest that in the dysgeneses studied, associated skull base abnormalities exist distorting the IAM's. The difference in slice of appearance of the right and left IAM is a measure of the rotation of the skull (and by extrapolation the brain) about the axial axis (angle γ), relative to the ideal in which the two IAM's appear in the same slice. The degree of rotation associated with each slice difference is given in Appendix 3. The maximum slice difference seen was 5. Because each slice is 1.5mm thick, even if IAM's appear in the same slice, there may still be a rotation about the axial axis.

That the most posterior slice in which the IAM appears is noted for the purposes of estimation of rotation means that the length of the IAM itself (approximately 1cm; Williams et al.,1989) does not confound the determination, and that the IAM can effectively be treated as a point at the most lateral extent of the internal auditory canal. The line between the two IAM's can then be used as line segment AB.

There are no absolutely invariant cerebral landmarks: some, however, are relatively invariant in most brains. The landmark used (equivalent to line EF) is the length of the corpus callosum: in the majority of the cases, on visual inspection of the slice data, the midsagittal reformat and the three-dimensional reconstructions, this bears a regular

relationship to the hemispheres. In the original coronal data set, the maximum anterior-posterior extent of the corpus callosum (M) was calculated (M = number of slices occupied x 1.5mm). The data set was then reformatted on the Allegro: from the coronal images, an axial plane was picked that passed through the forceps major and minor; through the resulting axial image, a sagittally-disposed line (oblique or, if necessary, curved) was chosen that passed through the middle of the genu, trunk and splenium; a reformatted image of the corpus callosum was produced along this plane. With the reformat in this place, the line cursor on the coronal data set was moved up and down to check whether the sagittally-oriented line chosen passed through the middle of the callosum (as judged visually) in all axial cuts, and the chosen sagittal line was adjusted if necessary. If satisfactory, the sagittal reformat was then saved. On the reformatted image, the maximum true anterior-posterior extent of the corpus callosum (L) was determined by inspection and measured using the Statistics/Angle/Line tool. The ratio of the lengths of the callosum (M/L) is the product of the cosines of angles γ and ß. As the axial rotational component angle γ is known, ß can be determined. Thus, the angles through which the brain had been rotated prior to scanning could be determined for controls and patients (except the two patients with callosal dysgenesis).

The relative importance of the issue of landmark invariance must be seen in perspective. The landmarks were *only* required to determine whether an individual subject's brain might have been excessively tilted with respect to the controls. On visual inspection by an experienced neuroradiologist, in 107 out of 129 brains examined in this work, no neocortical abnormalities at all were seen: disruption of the structural relationship between the landmark sets and the hemispheres is therefore extremely unlikely. In the remaining 22 patients with cerebral dysgenesis revealed by routine inspection, gross abnormalities of the shapes of the

hemispheres, possibly invalidating the use of the landmarks to determine the degree of rotation, were not reported. Some hemispheres were noted to be smaller than their counterparts, but none were felt to have gross shape changes, as might be seen, for example, in holoprosencephaly. No patients with such gross structural changes were included. Indeed, the major aim of the thesis was to detect occult changes in either apparently "normal" scans or "normal" areas on scans with focal dysgenesis. The callosum was absent in two patients with dysgenesis. Inspection of the sagittal scout images in these two suggested that there was not a large degree of pitch. These two patients were therefore retained for analysis. Thus no patients were rejected from analysis because the relative rotation at scanning could not be determined.

The range of rotations at which the controls were scanned is shown graphically in Fig 3.5. The extreme points form an envelope of rotations: block analysis of shape can be legitimately applied to patients whose own rotations fall within this envelope. For patients whose rotations fall outside this plot, rotation itself may confound block volume and ratio measures, which can no longer be considered to be examining cerebral shape alone within restricted rotation limits.

Analysis reveals that only four patients had been scanned at a combination of rotations around coronal and axial axes outside the controls' envelope for these rotations: they did not have block analyses. These four patients are shown on Fig 3.5 (marked 1 to 4).

Three controls were rescanned at different values of ß and γ. Their original and repeat positions on the rotation graph (Fig 3.5) are shown. Analysis of repeat scan data did not alter initial block results.

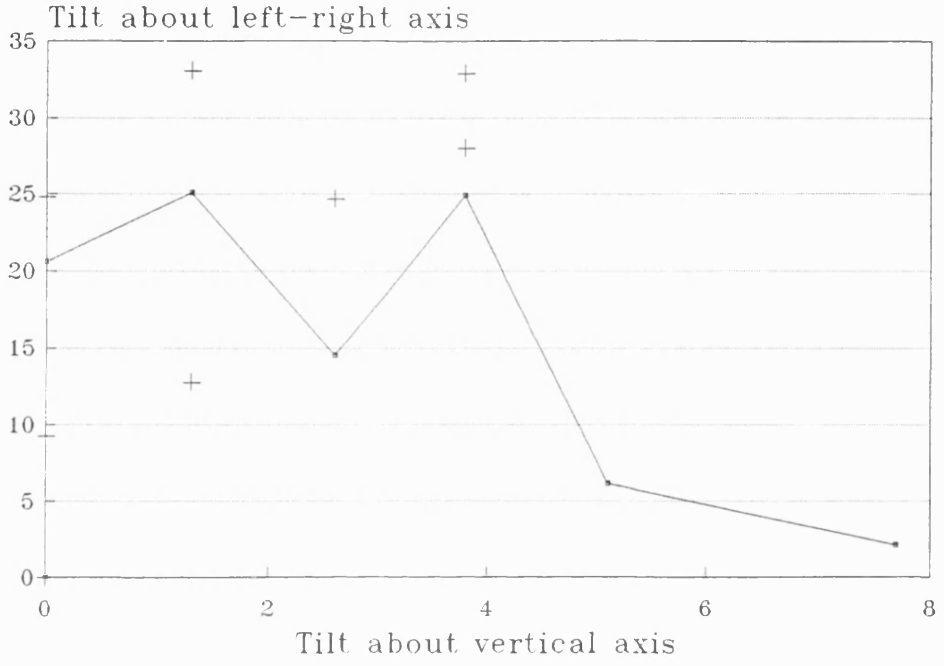

Figure 3.5. The maximum rotations (ß and γ) at which control subjects' brains were scanned are shown in the plot above and form an envelope of rotations, subjects falling within which can be analysed by the block technique. Points 1 to 4 represent the values of ß and γ at which the brains of four patients were scanned; they fall outside the envelope of permissible rotations. Points labelled C are the positions of the repeat scans of three control subjects (see text for details).

For any three-dimensional object in space, there are six degrees of freedom; the three rotational ones have been considered. Translations have no significant effect on volume measurements (given that partial volume effects are minimised by thin slice volume acquisitions in large objects; see 2.3.2.), though they may have an effect on surface area measurements (see section 3.10.).

The regional volumes measured were of CH in each block, SM in each block and caudate volume in blocks in which the caudate was present. The GM volume in a given block was obtained by subtraction of SM and caudate volumes from CH volume in each block. Total segmented volume was the sum of all 20 CH block volumes; total GM or SM volume for a given hemisphere was the sum of all 10 GM or SM blocks in that hemisphere.

The measured volume of each block for a given subject (40 in all per subject, 10 SM blocks and 10 GM blocks in each hemisphere) was then divided by the total segmented volume (sum of right and left CH blocks) for that subject in order to normalise for total brain volume (DeCarli et al.,1992; Murphy et al.,1993) and allow comparison of volume distribution measurements *between* subjects. In addition, to further investigate the symmetry noted in control subjects, the following ratios were also calculated: the volume of a given left-sided block of GM or SM compared with its right-sided homologue (see Fig 3.6) and the volume of a given block of GM compared with its ipsilateral underlying SM block (Fig 3.7). Thus in total each brain yielded 80 volumetric (block or block ratio) variables.

Figure 3.6. Derivation of GM/GM and SM/SM block volume ratios. In the upper figure is shown a homologous pair of grey matter blocks from position 9 in a control subject: the GM/GM ratio is derived by division of the volume of the left-sided block by the volume of the right-sided block. In the lower figure is shown a homologous pair of SM blocks; the SM/SM ratio is derived in an identical fashion.

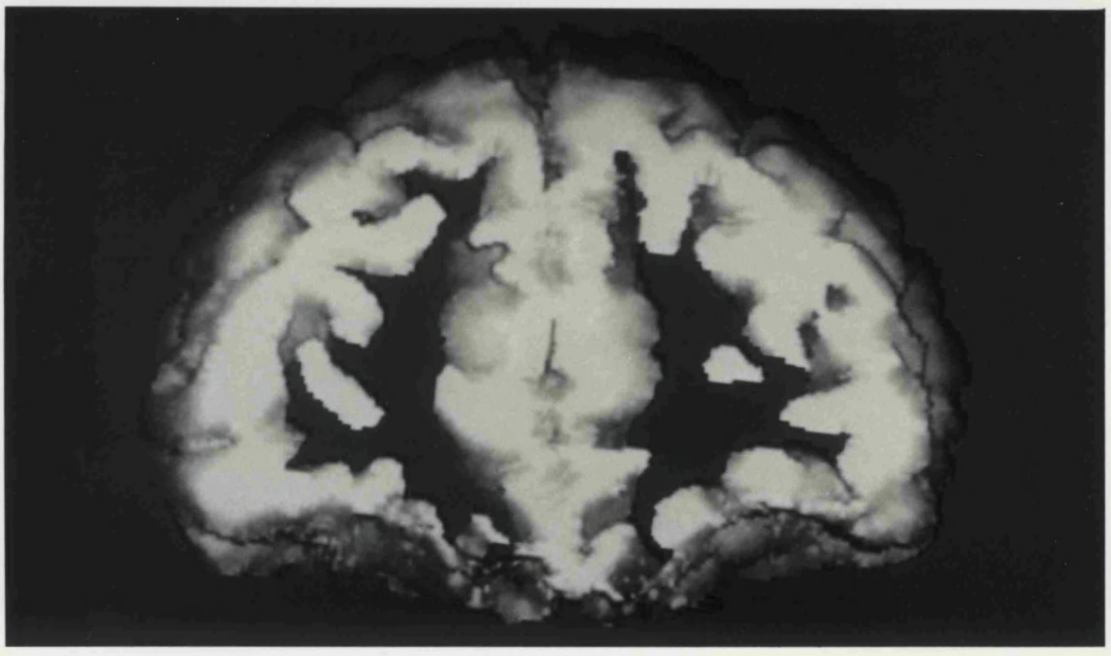

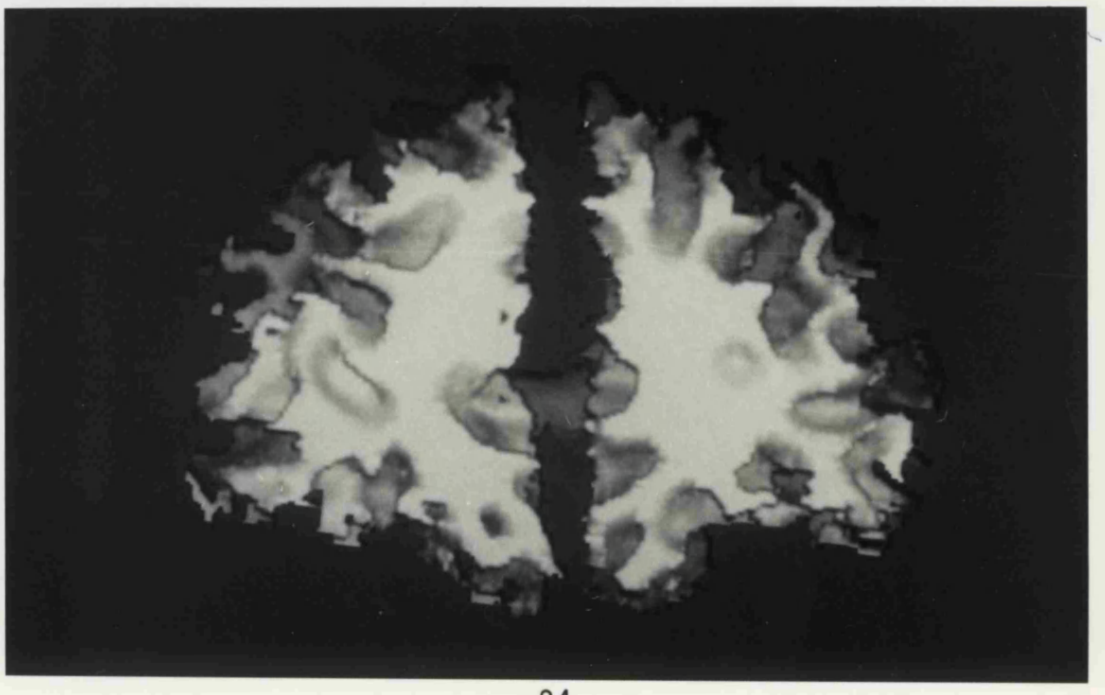

Figure 3.7. Derivation of the GM/SM ratio. The volume of a given grey matter block (in this case from position 5 in the right hemisphere) is divided by the volume of the SM block in the same position, producing a GM/SM ratio.

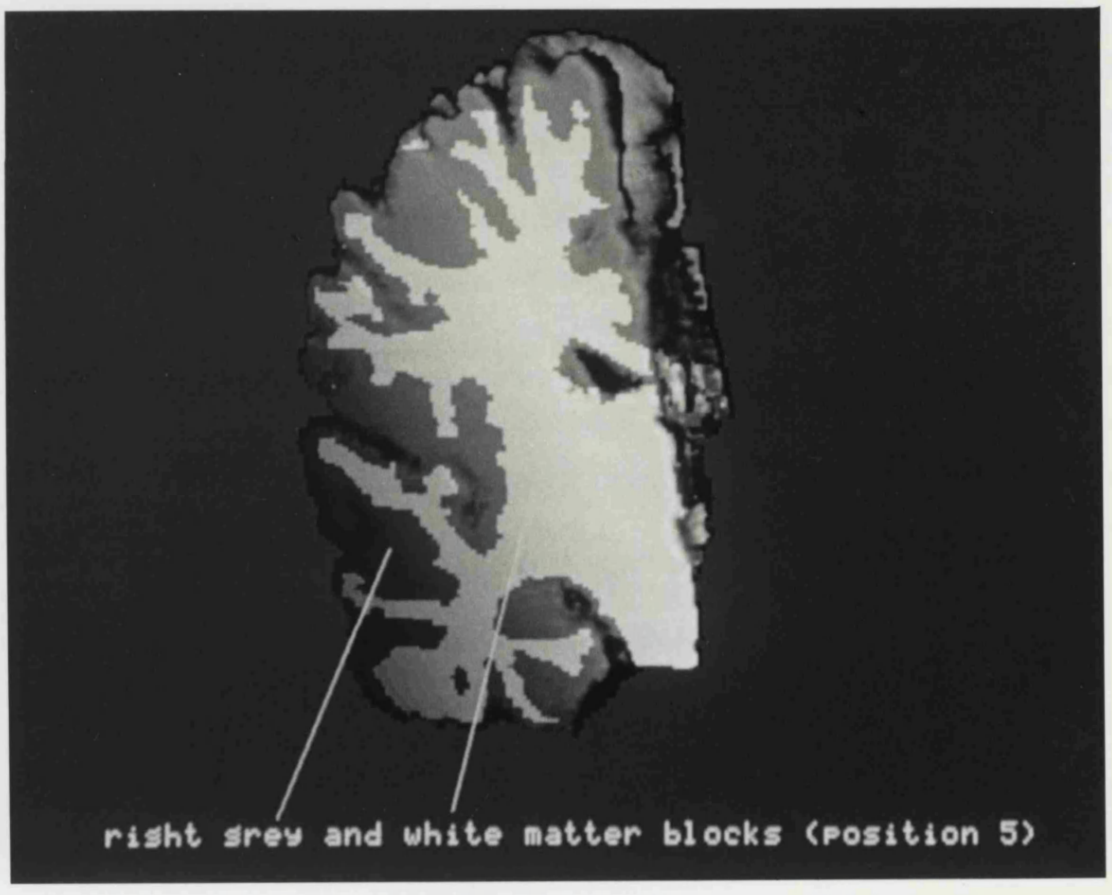

These variables provide quantitative regionalising information about the shape of the brain, though a particular combination does not describe a unique shape. Normal ranges from control subjects establish the amount of shape variation and shape symmetry that exists in neurologically-normal subjects within the ranges of rotation through which these subjects were scanned. Abnormal shapes of brains scanned within this range may manifest with abnormalities of these variables, and shape and symmetry changes can be localised.

Blocks one tenth of the anterior-posterior extent of a hemisphere were chosen as they are conveniently calculated and provide more localising information than, say, fifths, and smaller coefficients of variation resulting from the caprice of gyral anatomy in the normal brain, than, say, twentieths (see Appendix 4).

3.11. Corpus callosum cross-sectional area

The area of the corpus callosum (CCA) was measured in all subjects by creating an ROI in the corpus callosum on reformatted images created as described in section 3.10.2.

3.12. Block pair analysis

To explore interregional connectivity, the relationship of the volumes of non-homologous GM block pairs in controls was examined by calculation of (Pearson) correlation coefficients between these volumes. For pairs of blocks in which the correlation was highly significant ($p \leq 0.001$), a block pair ratio, PR, was calculated for each control subject such that:

$$PR = \frac{\text{volume of grey matter block Xi}}{\text{volume of grey matter block Yj}}$$

where X = R or L; Y = R or L and i≠j. Normal ranges for each ratio were calculated from the 33 control subjects.

3.13. Surface area measures and derivatives

The surface area of the cerebral hemispheres has been measured in a number of ways in the past. Amongst the more ingenious methods was one quoted in Blinkov and Glezer (1968), of covering the surface as well as possible with thin foil, and then measuring the area of foil used, effectively unfolding the surface. For objects as complex as the hemispheres, however, only stereological methods (Gundersen, 1986) can provide unbiased, model-free estimates efficiently. The use of vertical sectioning as devised by Baddeley et al. (1986) provides an efficient way of estimating the surface area of arbitrary objects, like the hemispheres, but was not applicable to the data available for analysis (see below). Although almost all previously published data on cortical areas concern the free surfaces (eg Schlaug et al.,1995), usually of postmortem brains (Blinkov and Glezer, 1968; Henery and Mayhew, 1990), the grey-CSF surface cannot always be reliably identified on MRI, especially where gyri abut. The inner GM surface, effectively the grey-white interface, can be defined with greater precision globally on MR images. Surface area measurements were therefore performed on this interface, or outer SM surface, by counting the number of voxels in the surface contours of the SM reconstructions.

3.13.1. Justification and head orientation effects

The grey-white interface is a convoluted three-dimensional contour, with a finite thickness. It will occupy a certain configuration of voxels in the MRI data, depending on both the biology of the real interface (its 'thickness' and anatomy) and the orientation of this interface in the scanner.

Orientation was not precisely fixed, though it was limited (see 3.10.1. and 3.10.2.). One might imagine that more voxels will be occupied by the same interface in certain orientations than in others.

Consider a small regular surface contour the size and shape of a single voxel (edge length 1 unit) in a space composed of identical voxels. The number of voxels that the surface contour even partly occupies is counted. Minimally, this surface could be orientated to occupy a single voxel of its containing space. On the other hand, it could be rotated and translated in three dimensions to intrude on 12 voxels. Thus, orientation alone could make a difference of 12-fold to the observed voxel count that would quantify this surface. Consider extending the surface contour so that whilst it remains cubical, its edge is now 1.1 units long. Minimally, this surface occupies (at least partly) 8 voxels in the original voxel space, whilst maximally it can still only intrude upon 12. Thus the impact of orientation in voxel space on this slightly more "complex" (with regard to its embedding space) surface is reduced. If the surface in question is now made into a rectangular cuboid composed of two unit voxels with one common face, the ratio of maximum to minimum voxel occupation produced by orientation changes will be less than 12-fold, as all voxels even partly intruded upon by the common face of one voxel will already have been intruded upon by the other voxel through this common face. Thus, increasing complexity of the surface contour will reduce the effect of orientation of the contour in voxel space.

For surfaces which are any more complex, such thought experiments become very difficult, and the bias introduced by orientation (rotation and translation) can only be estimated empirically. For this reason, four individuals rescanned (two subjects twice each, two subjects three times) in different orientations, without attempting to align the brain to previous scanning positions, were studied. One of these

subjects was scanned lying in a tilted prone and two different supine positions, effecting radical alterations in imaging slice angle with respect to major brain axes. These scans were then segmented as usual and the relative intraindividual rotation in each case was estimated using the ratio M/L. The brains were assumed to be rigid bodies: for small changes in orientation, this is known to be effectively the case (Hajnal et al.,1995).

For the six pairs of repeat segmentations, the minimum value of the ratio of the surface voxel counts for a given hemisphere was 0.947 for the right hemisphere and 0.948 for the left hemisphere. The intraclass correlation coefficient for all repetitions was 0.993. The full results, including the estimate of head rotation, M/L, are given in Appendix 5. The repeat segmentations were not included in the results.

Thus, even for radical changes in orientation (in the subject who was scanned supine and tilted prone), the change produced in the voxel count is small, and less than the volume variation produced by repeat segmentation of the same study alone (see section 3.7.). Empirically, therefore, for these four brains, it would appear that whilst orientation does have an effect on the voxel count, the complex nature of the SM surface with respect to the slices imaging it is such that this effect is small, and much smaller than the range of measured surface voxel counts across the entire subject group.

To extrapolate this finding to all the brains in the study would presuppose that all the brains are of equal complexity. Such assumptions may be the downfall of model-based, as opposed to stereological, design-based, derivations of structural parameters (Gundersen, 1986). Estimation of the complexity of the hemispheric SM surfaces for all the control subjects was performed in this report using three-dimensional fractal analysis of the SM surface (see next section). This analysis shows that the complexity of the SM surfaces - in an

orientation, size and shape-independent analysis - of the normal subjects is in fact remarkably similar (see 4.1.7.). Therefore, the assumption that all the control SM surfaces are approximately of equal complexity is not unfounded. Thus the voxel counts obtained are not invalidated by the methodology used in their derivation; they are robust to the impact of orientation in the scanner. This applies also to all patients for whom the estimate of fractal dimension falls within the normal range. Patients with abnormal SM fractal dimension were not analysed with respect to surface areas: this was the case for 7/77 patients.

Stereological quantitation of surface areas is possible from parallel slices as revealed by Baddeley et al. (1986). Ideally, the elegant methodology propounded by these workers and employed already in the estimation of surface areas from postmortem data (Henery and Mayhew, 1989) would have been used. However, there are a number of restraints on data acquisition that prevents this methodology being used. Most importantly, the data was not collected with random (isotropic) orientation of imaging planes with respect to an arbitrary horizontal plane. Isotropic orientation is possible with current MRI technology (though not as yet for volumetric acquisitions); the plane of acquisition may be made isotropic random with respect to an arbitrary horizontal plane without the subject needing to be moved, and is indeed one of the great advantages of MRI. But all the scans were acquired for clinical analysis in the first instance, requiring that they were all as far as possible comparable, particularly with respect to neocortical structure and the hippocampus. Isotropic sectioning would greatly reduce the clinical value of scans analysed, almost invariably, by eye. For any large series of brains imaged for clinical reasons, visual analysis is likely to remain the favoured methodology for some time to come. Reformatting of the data is possible, but this will not create a new isotropic data set: the grey-white interface has already been demarcated and converted into voxels (under

clinical imperatives) and reformatting cannot now make it randomly *acquired*.

Gundersen (1986) states that biased, non-stereological analyses are hampered because experimenters need to deal with "only a vague idea about the significance of the bias which cannot be estimated in any non-trivial case". In this thesis, detailed analysis has allowed an attempt to estimate the bias of the method used here. It is small with respect to biological variability, presumably a result of the complexity and resultant isotropicity of the grey-white interface.

As discussed above, the exact numerical characteristics of the "real" grey-white interface cannot currently be analysed. All estimates will depend on part at least on the method used to derive those estimates - including visual assessment on macroscopic slices. The grey-white interface in our data is composed of a number of voxels: how these relate to the "real" interface cannot be determined, and will depend on the variables of biological interest - the anatomy of the interface and its thickness - and head orientation. The error that orientation may generate has been estimated and is small. Thus the voxel count is an estimate of the anatomy of the "real" interface, and given its normal thickness in all except one case, more particularly a measure of the surface extent of the grey-white interface. In the one case with thickening of the grey-white interface on the images detected by an experienced neuroradiologist (case 6), fractal dimension of the SM surfaces was abnormally low, so that surface area measures could not be performed in any case. The blurring of the grey-white interface did not have a significant effect on volume or block analysis (see section 3.4.2.)

3.13.2 Predicted and extra subcortical matter surface areas

The area of the grey-white interface was determined from

the original segmentation of the SM modified to include the ventricle entirely within the SM, so that ventricular size or ventriculomegaly would not increase the voxel count spuriously (Fig 3.8). This voxel count was called SM_A, corresponding to the subcortical volume, SM_V, measured excluding the ventricle. Two other surfaces were derived: predicted and extra subcortical matter areas.

Predicted area: for each hemisphere individually, SM_V was considered to be spherical. From simple geometric considerations, it can be shown that the surface area of a sphere of volume SM_V is P_S such that:

$$P_s = 4\pi \left(\frac{3SM_V}{4\pi}\right)^{\frac{2}{3}}$$

P_S was converted into a voxel count (P_A) enabling its manipulation and comparison with the voxel-counted surface area measured directly ($P_A = P_S/0.2197$, this constant factor being calculated from the surface area ($0.46875^2 mm^2$) of one face of the cubic voxels constituting the SM surface contour in the proprietary imaging software).

Extra subcortical matter area: the extra SM surface area, E_A, is the additional surface area of the SM produced by the folding (invagination and drawing out) of its surface and was defined as:

E_A = (measured surface area) - (predicted surface area)

= $SM_A - P_A$

Figure 3.8. Spurious effects on the measured surface voxel count due purely to the ventricle (including ventriculomegaly) are eliminated by inclusion of a separate ventricular seed in a modified SM reconstruction made specifically and only for surface voxel count estimation. Filling in of the ventricle in this way ensures that the voxel count obtained is only of those voxels in the outer SM surface, that is the surface of interest and of biological relevance in this context. The segmentation of the ventricle (in this extreme example, S1 is the ventricular seed) is shown in the upper figure; when this is included in the SM reconstruction, a cross-section of the resulting object would appear as shown by the dark line in the manually annotated lower figure.

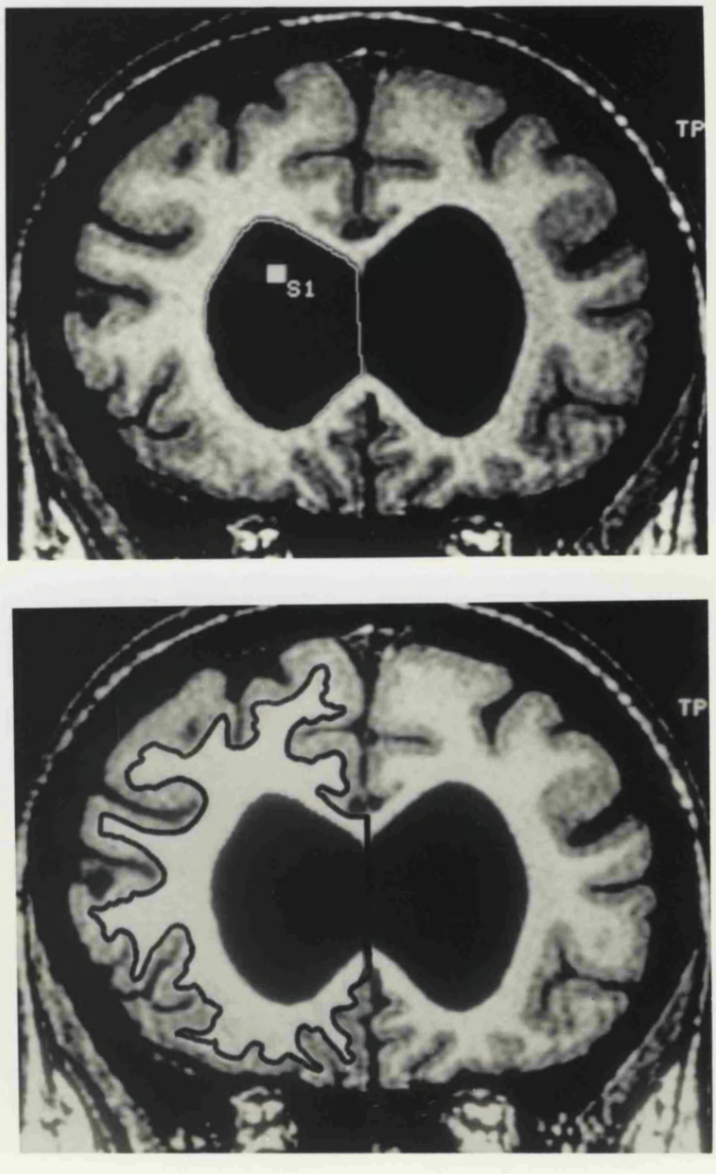

An estimate of the contribution to the surface voxel count made by the white matter cores of gyri was assessed in ten subjects. This was performed by manual editing of the initial segmentation in each slice from right SM block 3 (see Fig 3.4). In this block gyral white matter cores lay mostly parallel to the coronal slices, minimising overprojection and maximising their distinction: it would have been difficult to perform a similar experiment elsewhere. The block constituted an approximately cylindrical portion of the hemisphere. The segmentation was completely edited using a template (Fig 3.9) so that all white matter protrusions less than an arbitrary 3mm in diameter were removed (Figure 3.10). The volume and surface voxel number of these SM objects before and after this editing were measured. In addition, the surface area of a cylinder of the same volume as the original block was calculated. The extra surface area present on the original block as a result of folding of the SM within this region was determined by subtraction of the predicted surface area of this isovolumic object from the measured surface area of the original block. This real measured extra area was compared to the loss of surface area produced by pruning of the same regions as described.

3.13.3 Calculation of mean cortical grey matter thickness

Mean cortical thickness for each entire hemisphere was calculated according to:

$$\text{Thickness (mm)} = \frac{\text{GM volume}}{\text{SM surface area}}$$

where the GM volume is in mm^3 and the area is SM_A voxels x $0.2197 mm^2$/voxel.

Figure 3.9. This is the template placed on screen to guide the pruning of gyral white matter cores; all cores less than 3mm across (on screen) were manually cut from the segmented ROI, generating the images shown below.

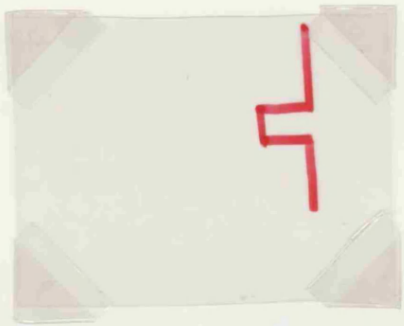

Figure 3.10. The picture on the left shows the SM block in position 3 from the right hemisphere of a control subject; the picture on the right is the same block reconstructed from images in which gyral cores were pruned from the original SM segmentation using the template shown in Fig.3.9.

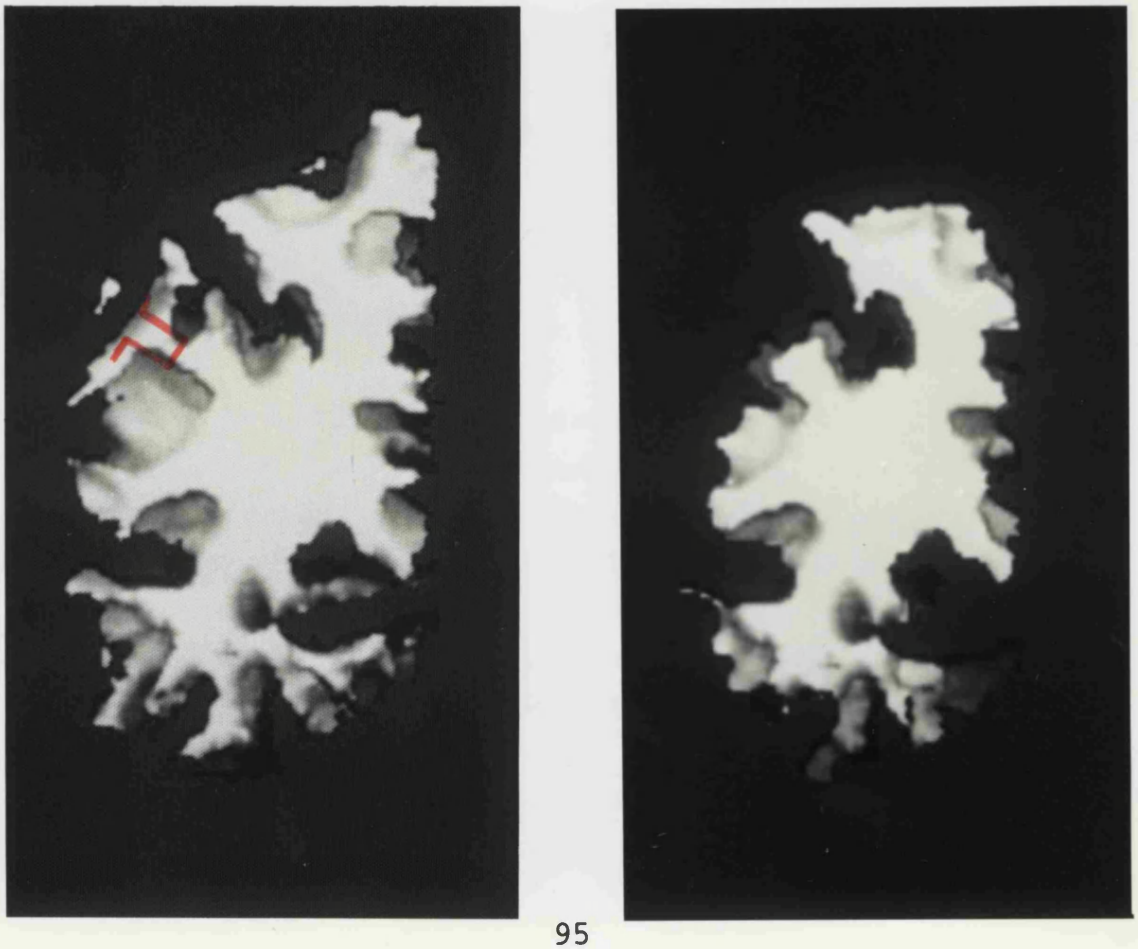

3.13.4. Surface area derivatives

Based on E_A and GM and SM volumes, and CCA, the following relational parameters were derived:

-for the relationship between GM volume (GMV, in cm^3) and E_A (in voxels),

$$EGM = E_A/GMV$$

-for the relationship between SM volume (SMV, in cm^3) and E_A,

$$ESM = E_A/SMV$$

-for the relationship between E_A and CCA (in cm^2),

$$ECC = E_A/CCA$$

3.14. Fractal dimension estimation

The fractal dimension of a structure is a measure of its complexity and self-similarity (see Mandlebrot, 1982, for a full review). The grey-white interface has been shown to be a fractal structure on two-dimensional analysis (Cook et al.,1995).

For this study, fractal dimension was estimated in three dimensions using an automated procedure. The process was performed on the surface contour of the three-dimensional renderings of the SM. Fractal dimension was estimated by a dilation technique. This is illustrated in Figure 3.11. If each point on the line is replaced by a circle with its centre on the line, this line can be transformed into a two-dimensional shape with an area. If circles of progressively larger diameter are used, the resulting area increases. If the area is plotted against the diameter of the dilating element,

an estimate of the length of the original line is obtained. The technique is more useful when the line is not straight and therefore may not be measured easily otherwise. For fractal structures, there is overlap of the areas of the dilating circles. The degree of overlap, and hence the change in measured area with increasing size of the dilating circles, increases with the complexity of the line, according to a power law in which the power relates to fractal dimension (or more precisely 1-fractal dimension). Essentially a similar procedure was applied to the SM surface contour, using approximately spherical dilating elements of various diameters.

Examples of dilation of the hemispheric SM surface are shown in Fig 3.12. The fractal dimension can be estimated by plotting measurements of the logarithm of resulting surface area against the logarithm of the size of the measuring element. The sensitivity of the technique to changes in the structure of the SM was tested by manually altering (smoothing; a process similar to the pruning of blocks described above in section 3.10.2.) the original SM segmentation in blocks. It was shown that pruning of the last SM digitations (within the gyral cores) over the entire extent of the block produced alterations in the fractal dimension irrespective of whether or not the pruning was extensive enough to produce visible changes in the appearance of the SM block (Free et al.,unpublished results).

The program calculating fractal dimension was written and applied by Dr.S.Free, who also kindly gave permission to reproduce Figures 3.11 and 3.12. Fractal results provided here are only on those subjects segmented by the author. The fractal results are used only to comment on the high degree of structural order in control brains and to exclude certain patients from other analyses devised by the author (see above).

Figure 3.11. Principle of dilation logic for estimation of fractal dimension. In the upper figure, circles of diameter d are placed with their centres on a line, dilating it to an area. For the line on the left, line length and area of the dilated line are directly related. As the complexity of the line increases (upper centre and right), the degree of overlap of the circles changes. If circles of increasing diameter are used (lower figure), then the area of the resulting dilated "lines" is related to the diameter of the dilating circles used (so-called structuring elements) by a power relationship. Estimation of the value of the exponent gives a value for the fractal dimension of the line, a measure of its self-similarity or complexity.

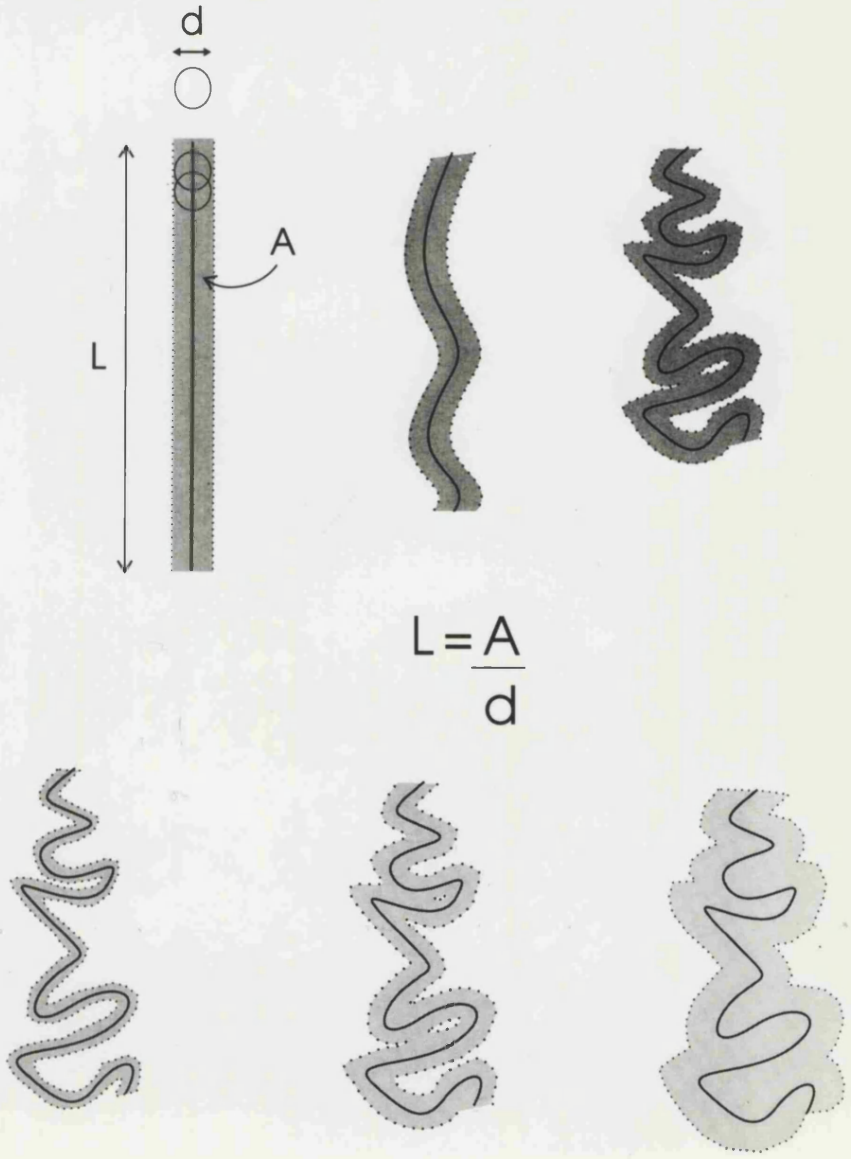

Figure 3.12. Application of dilation logic to the three-dimensional SM surface. The upper image is the surface of the SM of a left hemisphere. This *surface* is dilated in three dimensions using spheres rather than circles as structuring elements, so that a resulting *volume* is produced: the volume of the dilations is related to the size of the structuring element and allows calculation of the fractal dimension of the SM surface contour.

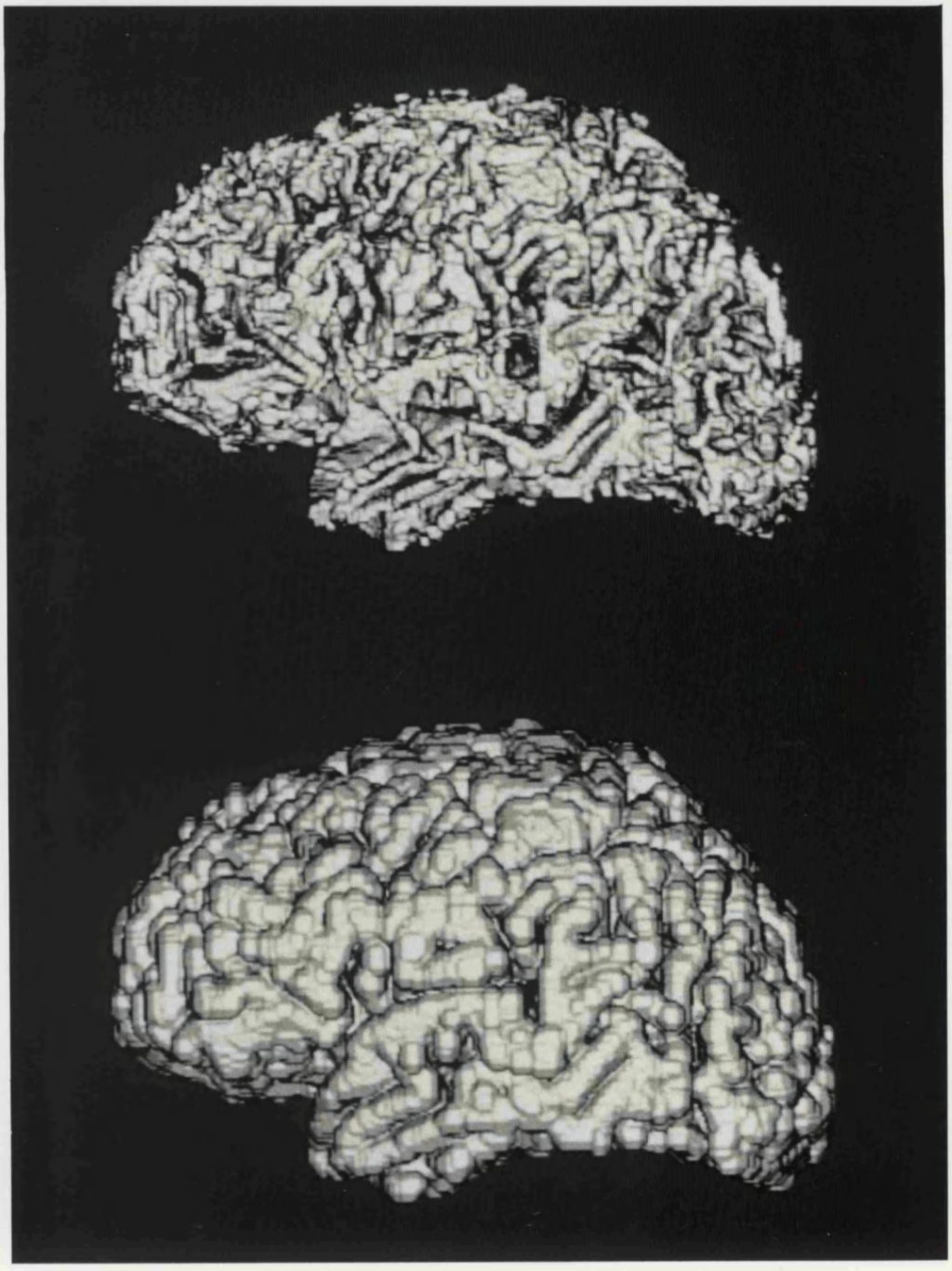

CHAPTER 4: RESULTS

4.1. Controls
- 3D visualisation
- Whole hemispheric volumes and areas
- Block volumes and symmetry
- Block pair ratios
- Corpus callosum cross-sectional area (CCA)
- Surface area derivatives
- Fractal dimension

4.2. Patients with cerebral dysgenesis on routine inspection
- Three-dimensional visualisation
- Whole hemispheric volumes
- Block volumes and symmetry
- Block pair ratios
- CCA
- Surface area derivatives
- Fractal dimension

4.3. Patients with normal scans on routine inspection
- Three-dimensional visualisation
- Postprocessing results
- Surface area derivatives and fractal dimension

4.4. Patients with subependymal heterotopia
- Clinical and MRI details
- Postprocessing results
- Surface area derivatives and fractal dimension

4.5. Patients with hippocampal sclerosis
- Clinical details
- Postprocessing results

4.6. Mean cortical thickness

4.7. Summary of results across groups by analytic technique

4.1. Controls

4.1.1 Three-dimensional visualisation

The control subjects were used to establish a normal range of variation for gyral anatomy, in conjunction with a published atlas of sulcal anatomy (Ono et al.,1990). No gyral malformations were identified on reconstruction in the control subjects.

Inspection of the reconstructed images revealed that in certain areas the surface rendering did not allow gyri to be easily distinguished because they could not be adequately separated at segmentation (the gyri abut closely). Whilst this does not have a significant effect on volume measures, it precludes proper examination of the gyral pattern in the posterior parietal, occipital and posterior temporal aspects of the dorsolateral convexity, and the mesial and inferior aspects of the hemispheres. Thus only the dorsolateral convexity of the frontal, anterior parietal and temporal lobes were examined and compared in the thesis.

4.1.2. Whole hemispheric volumes and surface areas

For all quantitative results, standard deviations are given in brackets after mean values.

Values for hemispheric volumes and surface areas are given in Table 4.1. Mean TRAT was 0.999 (0.013). There was no significant difference between right- and left-handers or between the sexes. Only one subject had a volume ratio outside the normal range (actual value, 1.042).

Table 4.1. Mean (s.d.) measured hemispheric surface areas and volumes for males and females.

Males	R	L
Surface area (SM_A, number of voxels)	390000 (24300)	378000 (23400)
GM volume (cm^3)	263 (28)	272 (28)
SM volume (cm^3)	261 (25)	245 (21)
Females	**R**	**L**
SM_A	346000 (37500)	337000 (32300)
GM volume	225 (21)	235 (24)
SM volume	229 (36)	222 (31)

There was no significant difference between right- and left-handers as separate groups for the following variables in isolation: right SM_A, E_A, P_A; right SM, GM, total hemispheric volume; left SM_A, E_A, P_A; left SM, GM, total hemispheric volume (Mann-Whitney).

For right-handers, SM_A, E_A, and P_A were bigger on the right than on the left (Mann-Whitney, $p<0.00005$). A similar pattern was not significant for left-handers ($p=0.2249$). For right-handers, grey matter volume is significantly higher, and subcortical matter volume significantly lower, on the left compared to the right (Wilcoxon, $p<0.00005$). For left-handers, the difference is nonsignificant (Wilcoxon, $p=0.0431$ for GM and SM pairings).

Values of total cerebral volume, right and left hemispheric volume, right and left GM volume, and right and left SM surface voxel counts are significantly higher for male subjects than for female subjects (Mann-Whitney, $p<0.001$).

However, SM_A corrected (by division) for total cerebral volume or for hemispheric GM volume is not significantly different between the sexes.

4.1.3. Block volumes and block symmetry ratios

The derivation of the 80 block variables corrects for entire segmented volume; separation of data from male and female subjects is not necessary (Mann-Whitney for males and females as independent groups, $p>0.01$ for 80 variables).

The tightness of the distributions of the variables changes across the anterior-posterior extent of the hemisphere (as shown graphically in Fig. 4.1).

Only two values from the entire control group's 2640 values (33 controls x 80 variables) fell outside the appropriate normal range. If each variable were considered to be independent then, by chance alone, there would be 7.1 abnormal values (0.27%).

The two abnormal variables were in two subjects. No one subject had more than one abnormal variable. On this basis, a structurally abnormal brain, in terms of the (proportional) regional distribution of grey and white matter, was defined as a brain in which more than 1/80 block variables had a value outside the normal range. This quantitates abnormal brain shape within the limits of rotation at which the controls' brains were scanned.

4.1.4. Block pair ratios

In the normal subjects, 22 pairs of non-homologous GM blocks have significantly correlated volumes (Pearson correlation coefficient, $p\leq0.001$), out of a total possible number of pair combinations (as opposed to permutations) of 180.

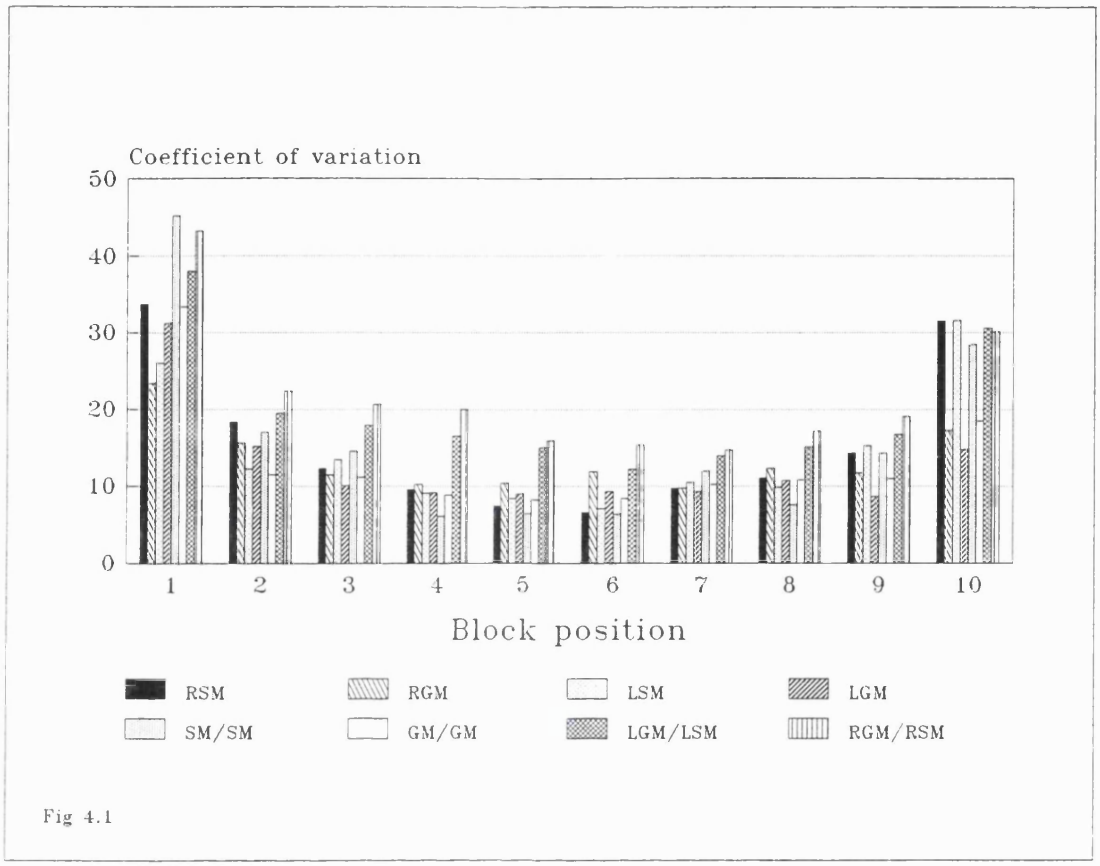

Fig 4.1

Figure 4.1. Composite plot of coefficients of variation for each of the eight block variables in each position. Note that the coefficients are lowest in the central blocks and highest at the poles.

Figure 4.2. *Schematic representation of grey matter blocks* with highly correlated volumes. Each arrow represents a pair of blocks in nonhomologous positions for which the volumes are significantly related

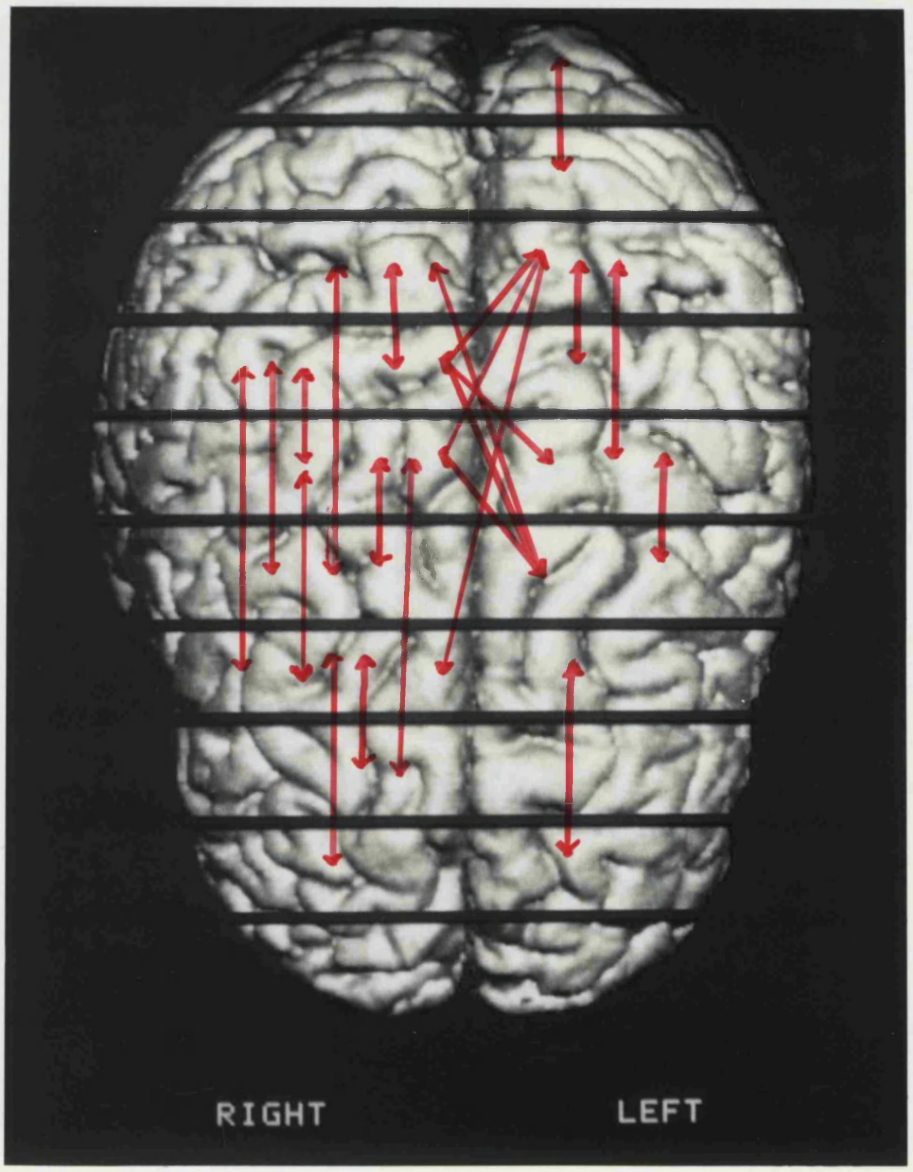

For homologous blocks, six of ten GM block pairings (Rj with Lj, j = 1 to 10, Fig. 3.4) had significant correlation coefficients for their volumes ($p \leq 0.001$). The 22 blocks pairs are shown schematically in Fig. 4.2. Some blocks have many more significantly correlated relationships than others. There are more links in the right hemisphere than in the left (27 as opposed to 17).

Of the ratios, PR, for the 33 control subjects together, only 2/726 values fell outside normal ranges (expected number by chance alone assuming that PR are independent, 1.96/726). There was one abnormal pair ratio in each of only two subjects. The remaining 31 subjects did not have any block pair abnormalities. The presence of more than one abnormal PR value was therefore considered to pick out an abnormal brain in terms of PR, interpreted as abnormal in terms of interregional connectivity (see Discussion).

4.1.5. Cross-sectional area of the corpus callosum

The mean area of the corpus callosum (CCA) was 696mm^2 (73mm^2), with no significant sex or handedness difference. Across the group, CCA correlated highly with the R extra SM surface (E_A) area (Pearson, r=0.5404, p=0.002) and with L E_A (Pearson, r=0.4844, p=0.004).

4.1.6 Surface areas derivatives and volume relationships

Predicted (P_A) and extra (E_A) subcortical matter surface areas

There is no significant sex difference for these measures when corrected for ipsilateral hemispheric grey matter volume. Hence male and female subjects are grouped, as there is no effect of sex independent of brain size and subsequent analyses compare surface areas measured with those expected given hemispheric volumes. The mean values (in voxels) are:

P_A right 75900 (6640), left 73300 (5570); E_A right 299000 (31000), left 291000 (28200).

The proportion of the measured SM surface area (SM_A) that is extra surface area (E_A) is high and significantly different (Mann-Whitney, $p=0.001$ for the right and $p=0.002$ for the left) for the sexes. For males, mean E_A/SM_A is 80.0% (0.8%) for the RSM and 80.2% (0.9%) for the LSM; for females, the values for RSM and LSM are 79.1% (0.4%) and 79.2% (0.5%) respectively. There is no significant difference between the hemispheres for either right- or left-handers.

For the blocks of SM edited such that all white matter protrusions less than 3mm in diameter were removed, the percentage loss in surface area (mean 41%) was significantly greater (Mann-Whitney, $p<0.0005$) than the percentage loss in volume (mean 22%). The measured loss of surface voxel count by editing correlated highly with the calculated extra surface area of each block due to folding of the surface of the block (Spearman correlation coefficient 0.95, $p<0.0005$).

Correlation between GM volumes and SM surface area measures

For the group as a whole, the coefficients for the correlations (Pearson) between GM volume and SM_A or E_A were: for the right hemisphere GM volume-SM_A 0.51 ($p=0.002$), GM volume-E_A 0.54 ($p=0.001$); for the left hemisphere GM volume-SM_A 0.66 ($p<0.0005$), GM volume-E_A 0.69 ($p<0.0005$). Thus for both R and L hemispheres, there is significant correlation between the measured SM surface area and the volume of the GM, marginally increased when the extra SM surface area is considered. A plot of SM_A against GM volume for the left hemisphere is shown in Fig. 4.3.

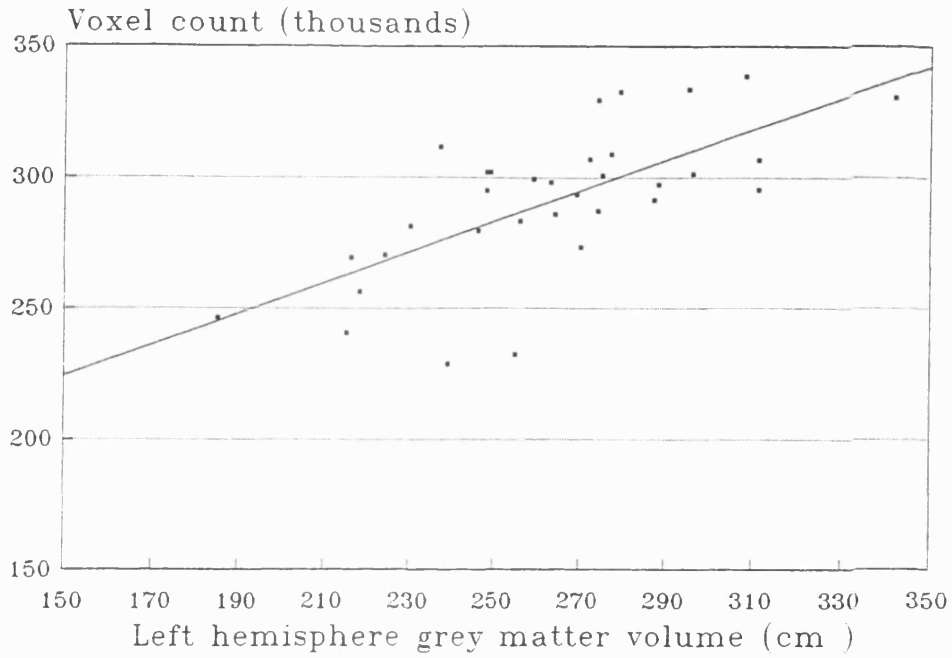

Figure 4.3. Correlation between subcortical matter surface area, as measured by surface voxel count, and grey matter volume for the left hemisphere for 33 normal subjects. The correlation coefficient is 0.66 ($p<0.0005$).

Surface area derivatives

The results across the whole group are: for the right hemisphere, EGM 1200 (140), ESM 1200 (78.3), ECC 435 (44.7); for the left hemisphere, EGM 1120 (104), ESM 1230 (81.2), ECC 424 (44.8). There is no significant effect of handedness or sex for these results (Mann-Whitney). No control subject fell outside the normal ranges.

Mean cortical grey matter thickness

The mean value for cortical thickness of the R hemisphere was 3.0mm (0.37) and for the L, 3.3mm (0.32). There is no significant sex or handedness difference for hemispheric cortical thickness. The left cortex is significantly thicker than the right (paired t-test, $p<0.0005$).

4.1.7. Fractal dimension analysis

There was no significant sex or handedness group effect for whole hemisphere SM fractal dimension estimation. The mean value of fractal dimension for R SM was 2.298 (0.009), and for L SM 2.297 (0.007). No control subject had a fractal dimension outside the normal range.

4.2. Patients with cortical dysgenesis on routine inspection

Clinical details of the 22 patients studied, with the MRI diagnosis from visual inspection of the two-dimensional images, are given in Appendix 6.

4.2.1. Three-dimensional visualisation

Inspection of the three-dimensional reconstructions revealed gyral abnormalities beyond the lesion(s) seen on visual inspection of the routine images (by an experienced

neuroradiologist) in 6/22 patients.

In patient 1, polymicrogyria was noted on routine inspection in the right frontal and parietal lobes. Reconstruction revealed that macrogyria extended below the Sylvian fissure to include the superior and middle temporal gyri (Fig. 4.4).

Additional gyral anomalies were apparent on reconstruction in patient 9. In addition to the bilateral clefts, the pattern of gyration of the left superior and middle frontal gyri was altered anterior to the cleft (Fig. 4.5).

Right parietal macrogyria was noted on routine inspection in patient 14. Reconstruction revealed macrogyria extending all the way to the right frontal pole, in obvious comparison to the gyral widths in the left lobe (Fig. 4.6).

Bilateral clefts were also associated with further unreported gyral abnormalities in patient 16. Abnormalities of the left superior and middle frontal gyri well anterior to the cleft were again noted (Fig. 4.7).

Increased gyral complexity in the right frontal lobe, affecting particularly the right middle frontal gyrus, was seen in patient 13, who on routine inspection was noted to have an isolated hypothalamic hamartoma (Fig. 4.8).

Patient 20, with a right-sided cleft and associated subependymal and subcortical heterotopia, has an abnormal unusually positioned oblique gyrus in the left frontal lobe (Fig. 4.9).

Figure 4.4. Lateral view of surface rendering of right hemisphere in patient 1. There is atrophy of gyri in the perisylvian area posteriorly; surrounding broadened gyri are outlined in the schematic.

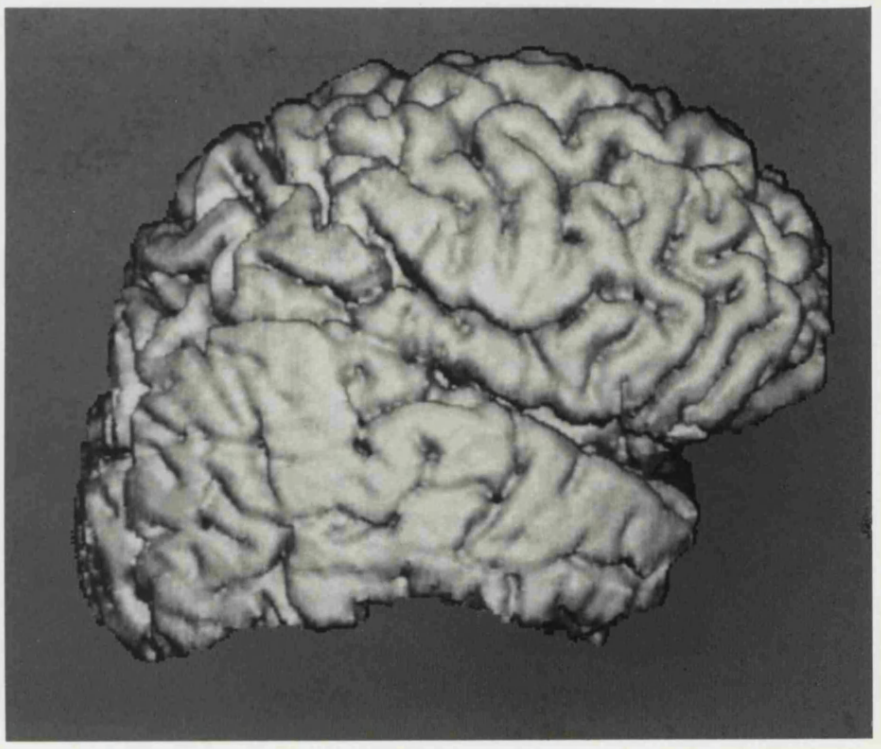

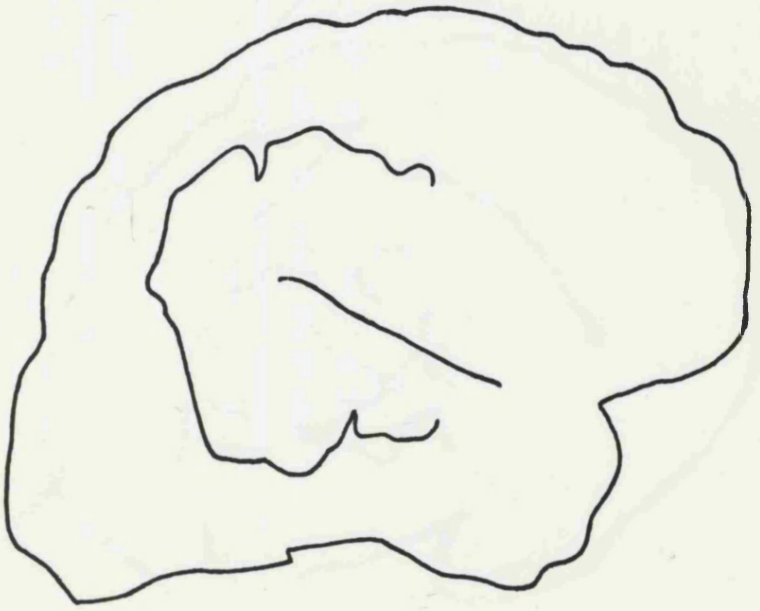

Figure 4.5. Left anterior oblique view of surface rendering of brain for patient 9. The left superior and middle frontal gyri are abnormally disposed, most markedly near the frontal pole, with loss of the normal sinuous meandering pattern and thinned parallel gyri as highlighted in the schematic. The position of the cleft is also shown in the schematic (**c** - **c**).

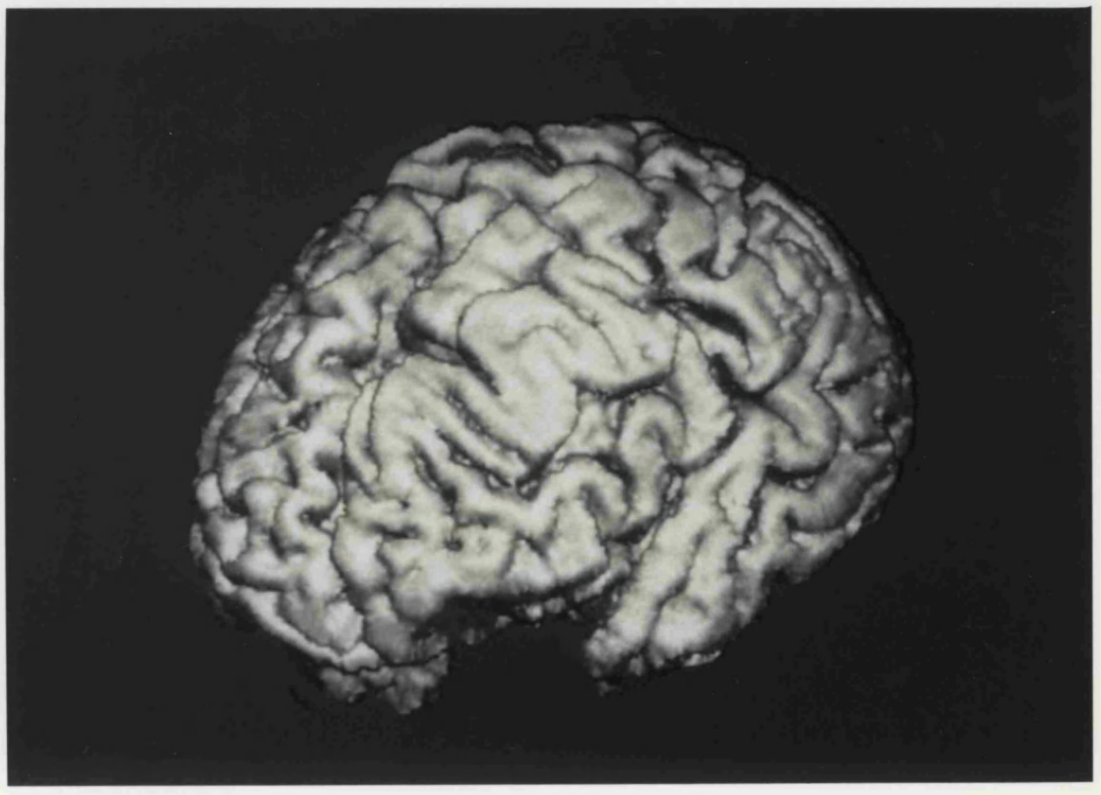

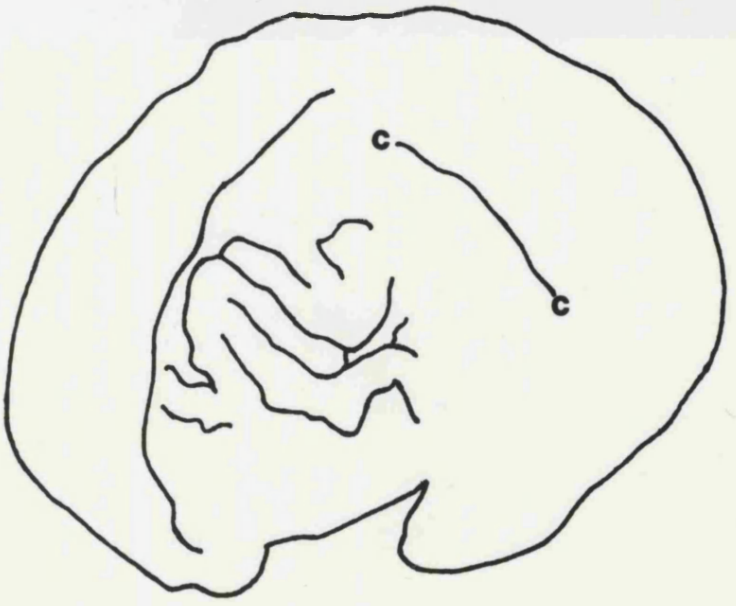

Figure 4.6. Frontal view (right hemisphere on left of picture) of surface rendering of patient 14. Note that the gyri are broader and the sulci shallower all the way to the frontal pole on the right when compared to the left.

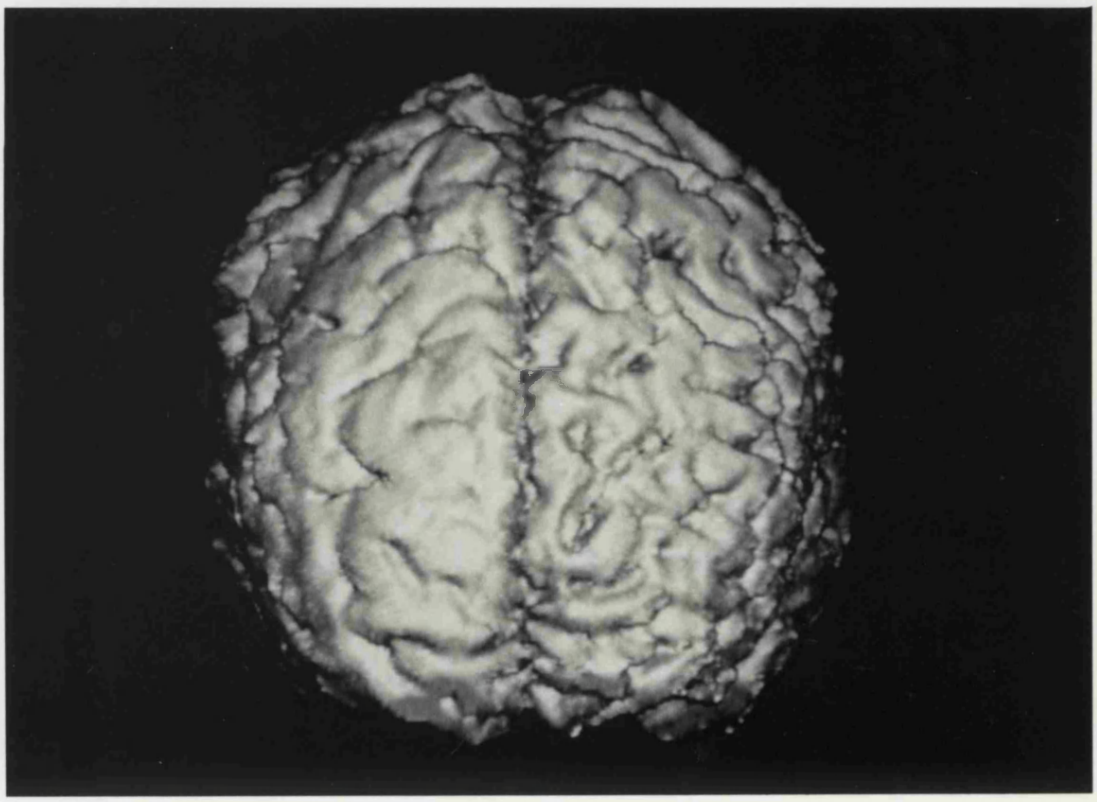

Figure 4.7. Left anterior oblique view of surface rendering of brain for patient 16. Note again the abnormal disposition of the left frontal gyri near the frontal pole. In this patient, the left-sided cleft is visible posteriorly (**c** - **c**).

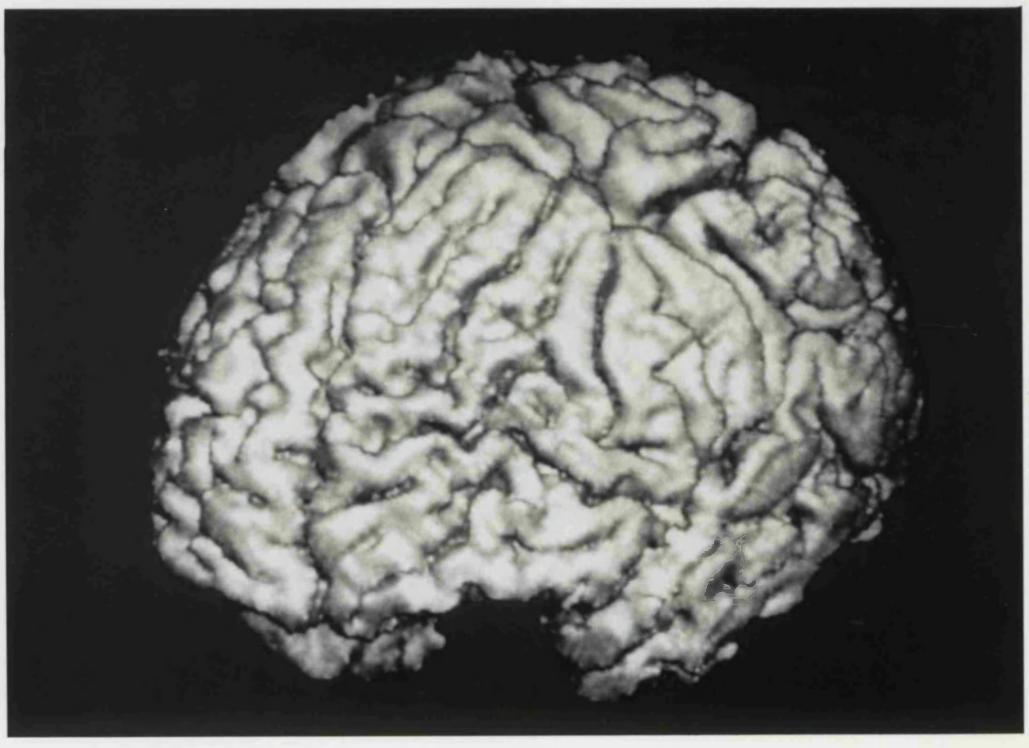

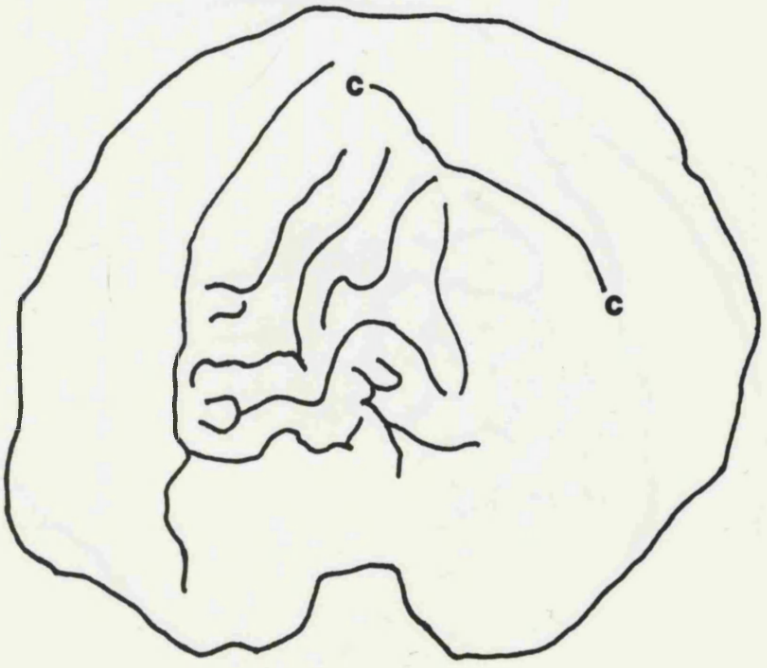

Figure 4.8. Right anterior oblique view of surface rendering in patient 13. There is increased complexity of the right middle frontal gyrus, as highlighted in the schematic. Such complexity was not seen in the controls or the published atlas.

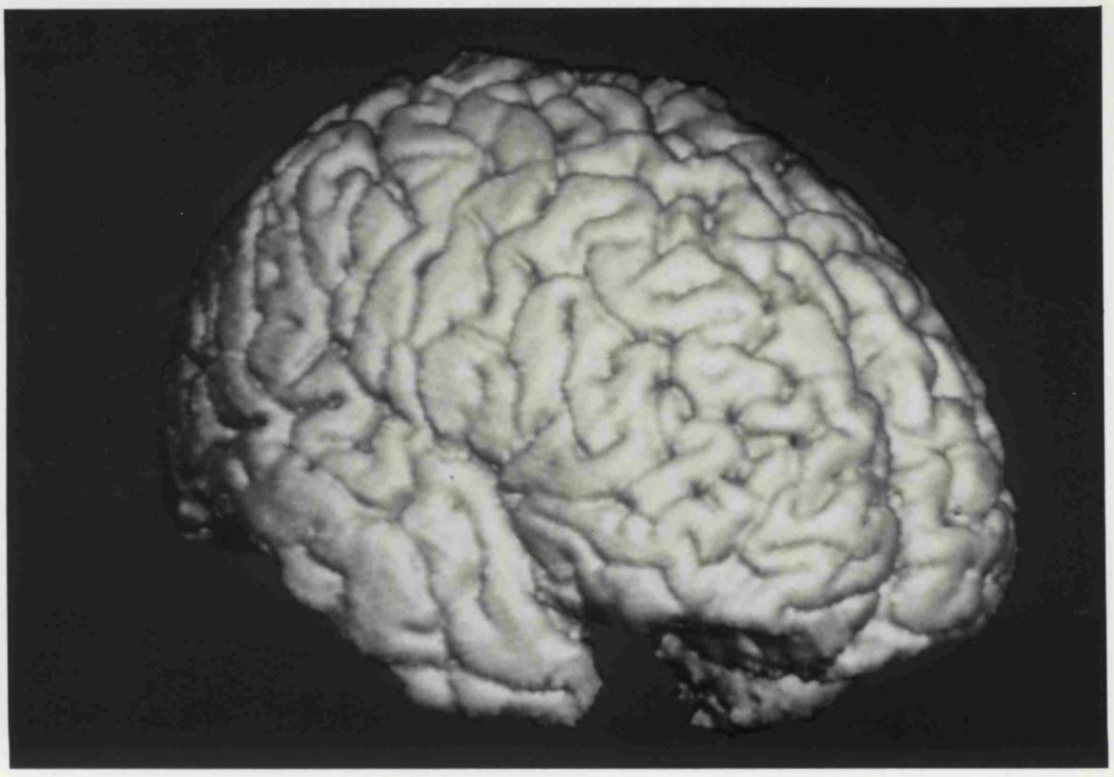

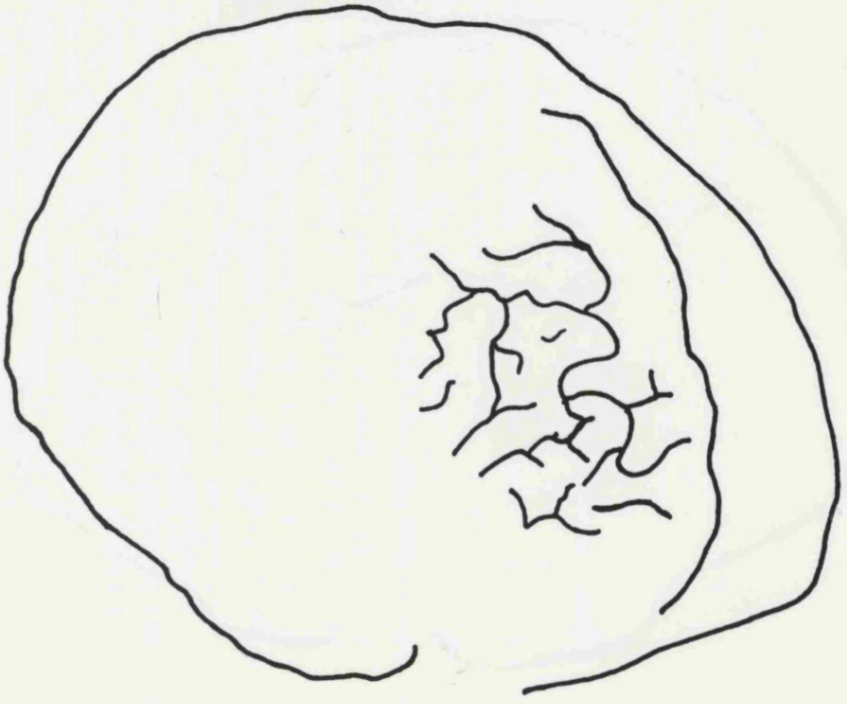

Figure 4.9. Left anterior oblique view of reconstruction for patient 20. The abnormal sulcus in the left frontal lobe of this patient with right-sided dysgenesis is marked in the schematic.

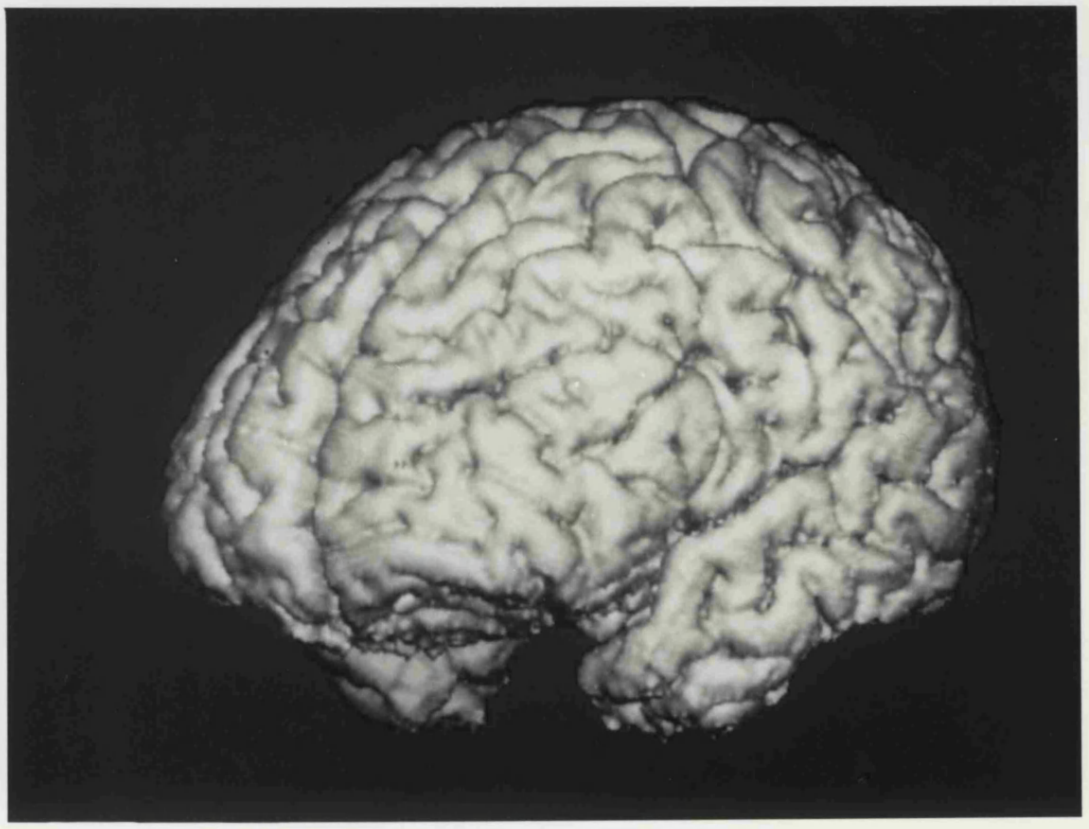

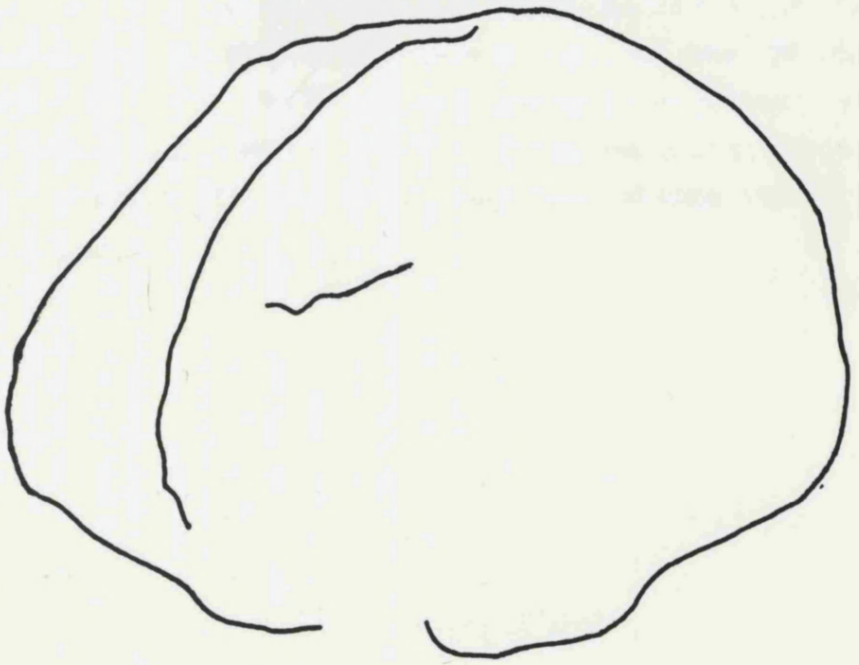

4.2.2. Whole hemispheric volumes

9/22 patients had significantly asymmetrical cerebral hemispheres, reported on inspection alone in only three (patients 3, 4 and 21). Seizures arose from the smaller hemisphere in 5/9; lateralisation was not possible for one subject.

Left SM volume was significantly smaller than normal (for males or females separately) in patients 6, 7, 9, 15 and 21. Right SM volume was smaller in patients 3, 6 and 9, and larger than normal for patient 4. Right GM was abnormally small in patient 9 and abnormally large in patient 4.

4.2.3. Block volume and block symmetry

Patient 21 was rotated to an extent that placed her outside the envelope of rotations for the controls: block analyses were not performed in this patient.

Of the remaining twenty-one patients, 19 had more than 1/80 abnormal values. The block results are summarised in Table 4.2. It should be noted that the majority of the SM changes were falls, and that the majority of the GM changes were rises. All the GM/SM changes were also rises. 57/126 ratio abnormalities (GM/GM, SM/SM, GM/SM) were not associated with abnormalities of underlying component blocks (GM or SM).

Table 4.2. Summary of block or ratio changes

Change in value	>	<		>	<
Patient group					
CEREBRAL DYSGENESIS (n=21)					
block or ratio			ratio		
GM	49	1	GM/GM	6	1
SM	1	49	SM/SM	14	4
GM/SM	101	0			
Patient group					
NORMAL SCANS (n=32)					
block or ratio			ratio		
GM	16	1	GM/GM	4	1
SM	2	3	SM/SM	3	2
GM/SM	50	0			

Abbreviations: > greater than upper, < less than lower, limits of normal range

The block extent(s) of the visible lesion(s) was also determined on the original coronal images. Blocks or ratios which are abnormal can be further classified in terms of their position with respect to the block extent of the lesion: abnormal blocks positioned outside this spatial extent are termed "extralesional". For abnormal ratios (GM/GM or SM/SM) in which one of the two blocks is within the lesion, the abnormal ratio is not considered to be extralesional. The total number of abnormal values per subject is shown in Table 4.3. Only two individuals had no abnormal values. Of the remaining 19 patients, dysgenesis was seen to affect the entire anterior-posterior extent of the cortex in two (patients 6 and 15): thus the presence of extralesional abnormalities cannot be defined in these cases. Of the remaining 17 patients with apparently focal lesions, extralesional abnormal values were present in 15. Of the extralesional abnormal blocks and ratios, 66/74 were *not* contiguous with the block extent of the lesion(s). The magnitude of the abnormality for abnormal blocks (number of standard deviations from the mean value for that block or ratio: Z-score) did not differ between intralesional and extralesional abnormal blocks.

Table 4.3. Abnormalities in patients with dysgenesis

Patient number	Number of block abnormalities	Number of extralesional abnormalities	Number of contiguous extralesional abnormalities	Surface area derivatives
1	2	1	0	none
2	4	2	0	ECCR, ECCL,ESMR>
3	17	4	0	ECCL>
4	4	2	1	none
5	2	0	0	ECCR,ECCL>
6	54	n/a	n/a	n/a
7	31	4	3	EGMR,EGML ECCR,ECCL<
8	10	0	0	none
9	4	1	0	ESMR,ESML>
10	0	n/a	n/a	ECCR,ECCL>
11	0	n/a	n/a	none
12	16	9	0	ECCR,ECCL ESMR,ESML>
13	8	8	0	none
14	9	4	1	ECCR,ECCL>
15	22	n/a	n/a	n/a
16	6	2	0	none
17	16	16	0	ECCR,ECCL ESML>
18	3	3	0	none
19	3	3	0	none
20	4	3	3	ECCR,ESMR ESML>
21	n/a	n/a	n/a	ECCR,ECCL ESMR,ESML>
22	12	12	0	none

Abbreviations: n/a: not appropriate; surface area derivatives, see 3.10.4.

The distribution of the abnormal values in these 21 patients is shown in Fig.4.10. It can be seen that the majority of the abnormal values were located in block positions 3 to 5: in comparison, these blocks in the control subjects have a tight volume distribution as shown by the small coefficients of variation over these blocks (see Fig. 4.1). Visual reinspection of the original images did not reveal any abnormality of structure or volume in the slices within extralesional abnormal blocks.

4.2.4. Block pair ratios

More than one abnormal PR was found in 8/21 patients. Of the 36 abnormal PR values in these 8 patients, neither block of a pair was located within the lesion in 10.

4.2.5. Corpus callosal cross-sectional area

This is abnormally low in patients 3, 5 and 21. The callosum is grossly attenuated and associated with a lipoma in patient 17 and completely absent in patient 12.

4.2.6. Fractal dimension in patients with dysgenesis

Whole hemisphere SM fractal dimension was bilaterally abnormal for patients 6 (both lower than normal) and 15 (both greater than normal): these patients were omitted from surface area analyses.

4.2.7. Surface area derivatives

Results are given in Table 4.3. On calculation, mean cortical thickness was abnormal only in patient 7. Calculation was not performed for patient 6, in whom the cortex was visibly thickened (see 4.2.6.). Some patients (9/20) with dysgenesis have no abnormalities in any surface area derivatives.

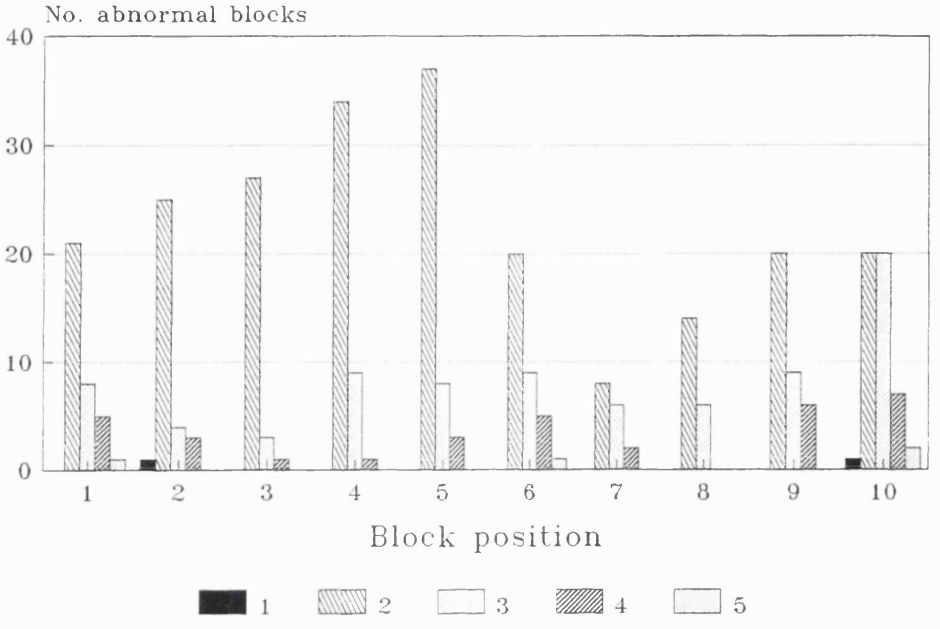

Figure 4.10. Distribution of positions of abnormal block variables. Note that the patients with frank dysgenesis have the largest number of abnormal blocks and that these are located mainly in the central regions (blocks 3 to 5), where the coefficients of variation for the block variables in control subjects are small. Group 1, control subjects; group 2, patients with dysgenesis; group 3, patients with normal scans; group 4, patients with subependymal heterotopia; group 5, patients with hippocampal sclerosis.

4.3. Patients with normal scans on routine inspection

Forty-five patients with chronic partial epilepsy were studied in whom routine inspection of the volumetric scan had failed to reveal any neocortical abnormalities (other than surgical resections in 3). In 13/45, only the surface renderings of the grey matter were created; in the other 32, some quantitation was also performed.

4.3.1. Three-dimensional visualisation

Three-dimensional reconstruction of the scan data revealed gyral abnormalities in 17/45 patients (38%). Electroclinical details of these patients and the abnormalities seen on reconstruction are shown in Figures 4.11 to 4.27.

The remaining 28 patients (including two who had had surgery) also had focal seizure semiology or focal EEG abnormalities or both; all had seizures that were thought to arise outside the mesial temporal structures. None had any gyral abnormalities in the dorsolateral convexity of the frontal, parietal or anterior temporal lobes (other than any resections).

4.3.2. Postprocessing results

Quantitative analysis was performed in 32/45 patients. Hemispheric asymmetry was seen in four: epilepsy was thought to arise from the smaller side in three (34, 35 & 46); localisation was not possible on electroclinical grounds in one (27). SM volume was abnormally low bilaterally in three patients (37, 51 and 55). No other hemispheric volume or callosal area abnormalities were found.

Figure 4.12. Patient 29. Male, 23 at scan, 7 at seizure onset. Fetal cyanosis at birth. Seizures: jerking of right arm and leg; occasional SGS. Continuous slow and sharp wave activity over L temporal and parietal lobes; ictal EEG unhelpful, postictal activation of left-sided abnormality. Reconstruction shows attenuation of the left superior temporal gyrus (arrowed), with possibly some enlargement of the left middle temporal gyrus.

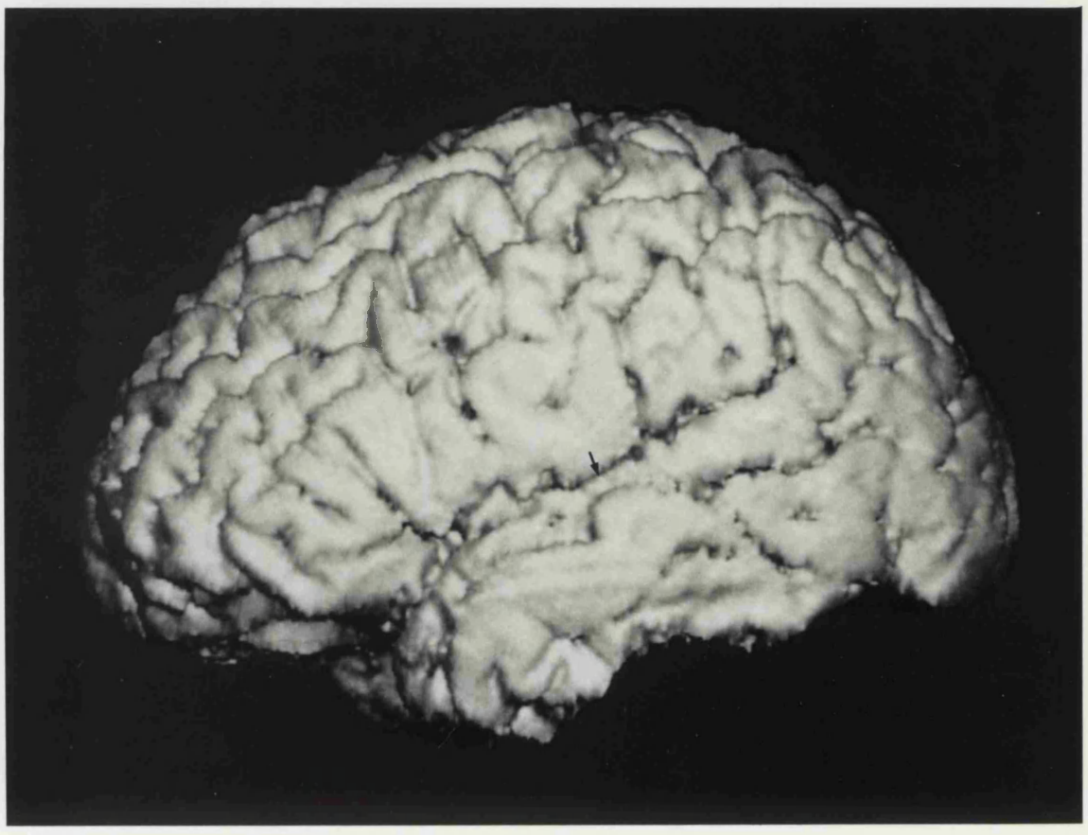

Figure 4.13. Patient 32. Female, 35 at scan, 7 at seizure onset. Mild left hemiparesis. Typical frontal lobe seizures: brief, frequent, nocturnal, with bilateral arm dystonic posturing (L>R), grimacing, lower limb stiffening and clonic left-sided movements. No significant EEG changes. Focal widening of right middle frontal gyrus on surface rendering (arrowed).

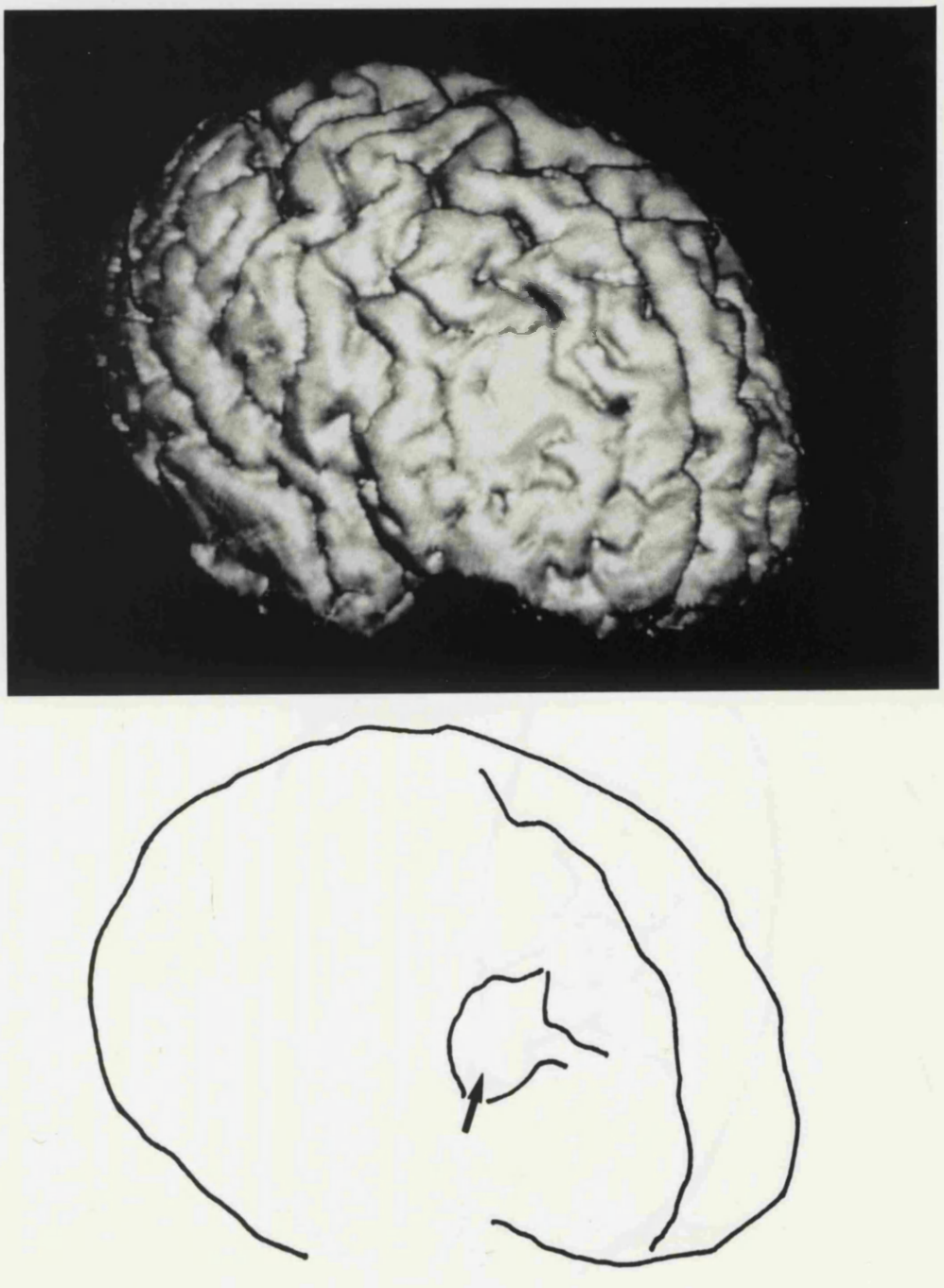

Figure 4.14. Patient 34. Male, 29 at scan, 3 at seizure onset. Episodes of simple partial status since age 13: left visual field obscuration by flashing lights; progression to CPS/SGS. Right occipital ictal discharge; giant phase-locked spikes on photic stimulation. Abnormal right parietal sulcation on reconstruction marked on schematic.

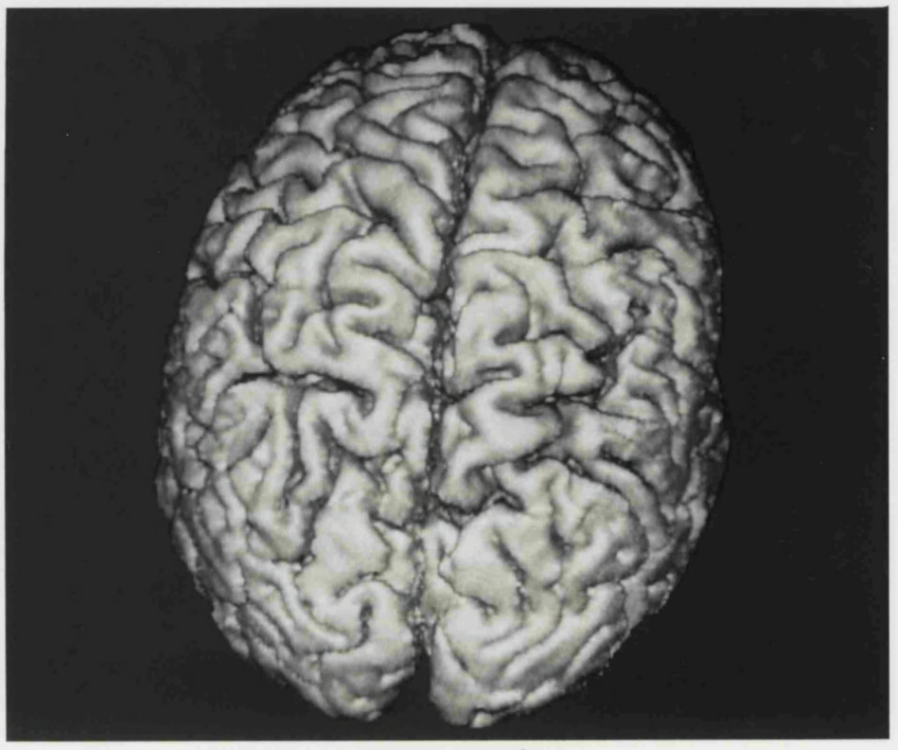

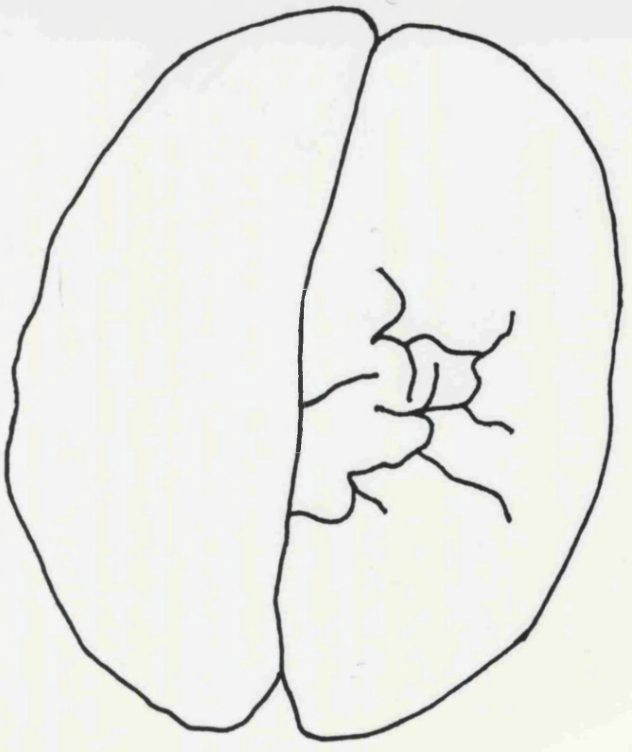

Figure 4.15. Patient 36. Male, 24 at scan, 7 at seizure onset. Frequent nocturnal seizures with extension and dystonic posturing of both arms and bicycling movements of legs. No significant EEG changes. Reconstruction shows abnormal sulcation right frontal lobe (arrowed).

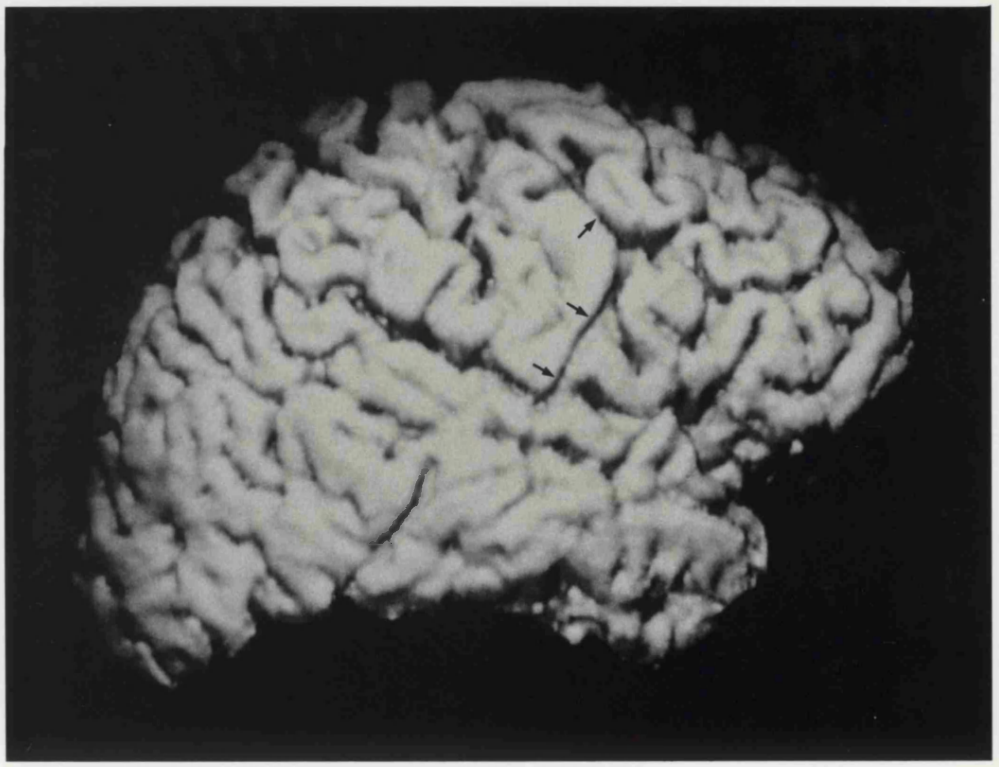

Figure 4.16. Patient 41. Female, 44 at scan, 12 at seizure onset.Frequent, brief, nocturnal attacks with stretching of legs and scissor movements and verbalisation. Interictal EEG shows bilateral frontotemporal spikes and sharp waves; ictal recordings unhelpful. Increased complexity over left middle frontal gyrus (marked) on reconstruction.

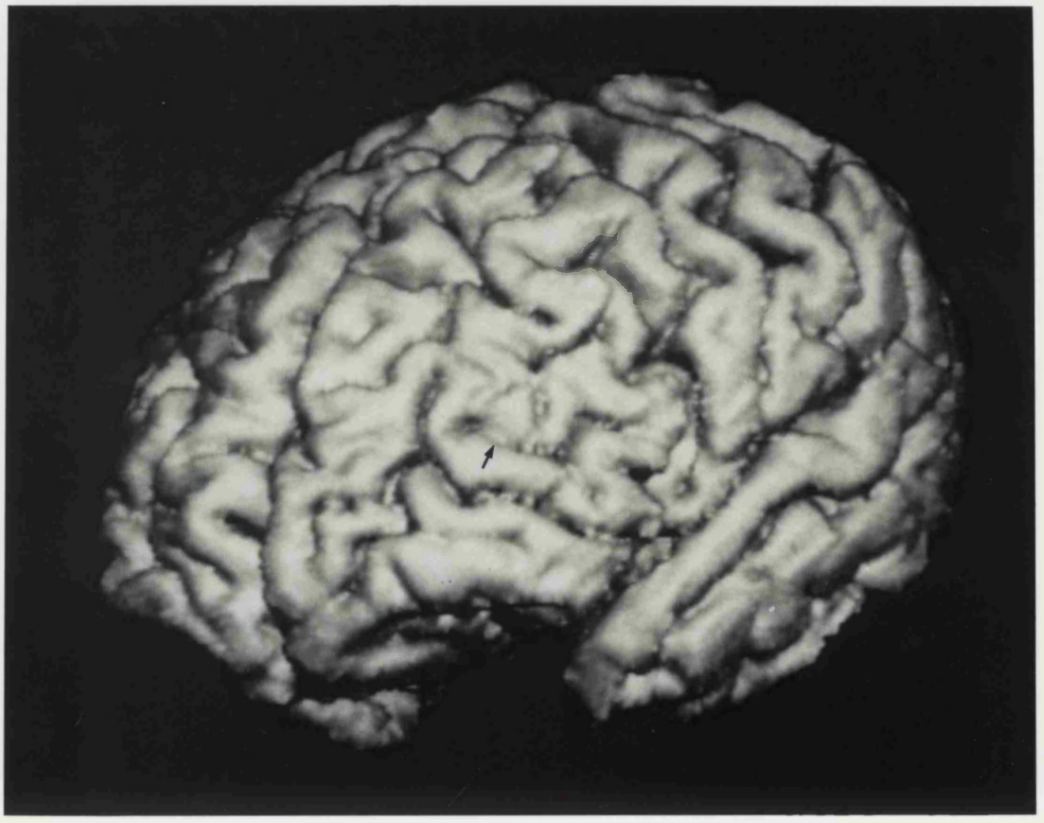

Figure 4.17. Patient 42. Male, 63 at scan, 40 at onset. Very frequent (200/day), brief attacks with dazed expression, head turning and shuffling movements of the left leg; immediate recovery. Frequent sharp waves or sharp-slow wave complexes maximal on frontopolar recording (F3)& bilateral synchronous sharp/slow wave complexes. Ictal EEG unhelpful. Reconstruction confirms atrophy and reveals abnormal gyral pattern in the left frontal lobe, with a stellate gyral appearance (outlined).

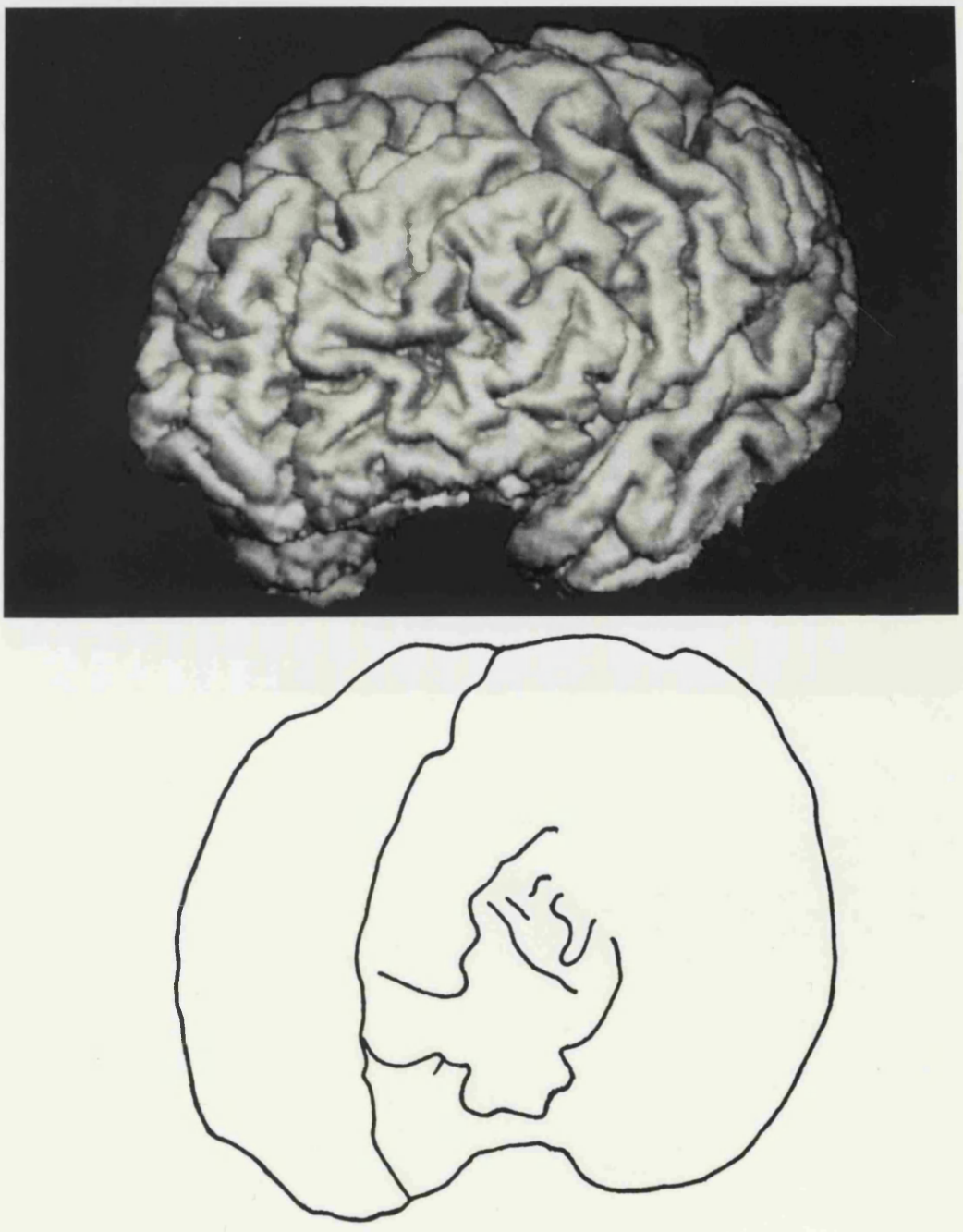

Figure 4.18. Patient 43. Male, 21 at scan, 12 at seizure onset. Complex partial seizures with extension of left leg; infrequent nocturnal SGS. Interictal vertex epileptic activity, field suggestive of horizontal dipole, often seen with small lesions; first ictal changes in R central region, where postictal slow also predominant. Reconstruction shows small area of abnormal gyral complexity in the right middle frontal gyrus (arrowed).

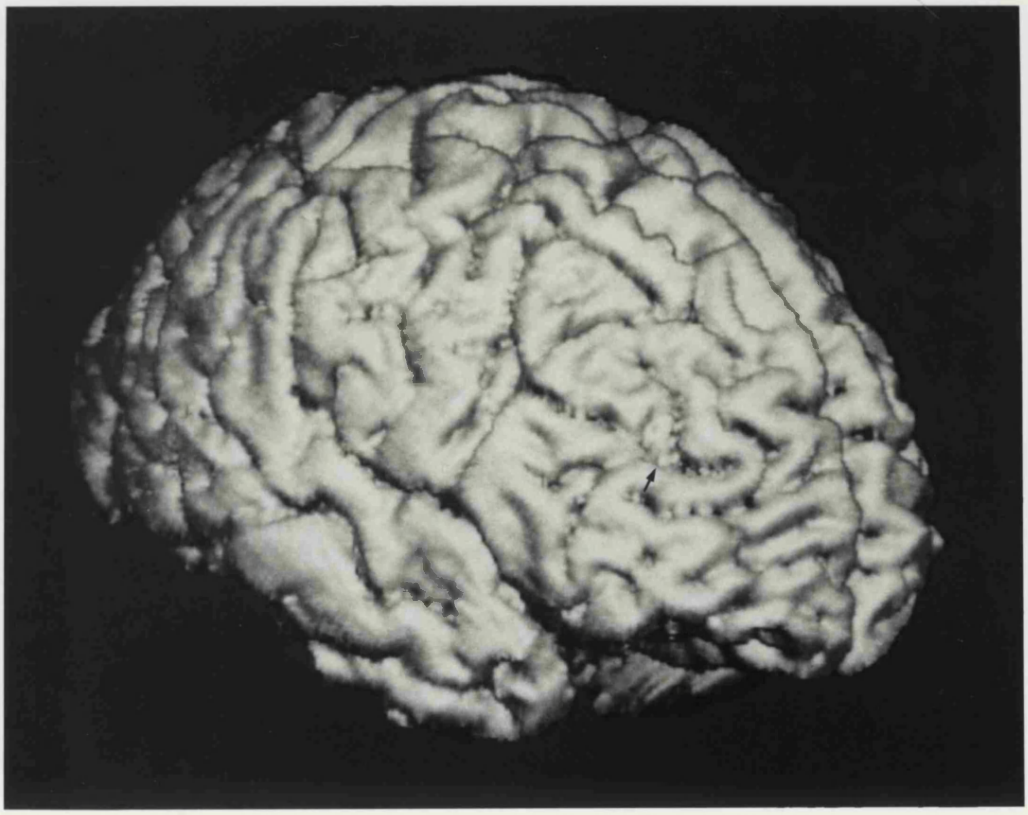

Figure 4.19. Patient 44. Male, 18 at scan, 9 at seizure onset. Left hemiatrophy. Frontal lobe seizures: frequent nocturnal complex partial with grimacing and bilateral arms elevation. Interictal EEG shows bilateral frontal parasagittal sharp and slow waves; ictal EEG: generalised attenuation. Reconstruction shows abnormal ring-like gyral configuration right frontal lobe (outlined).

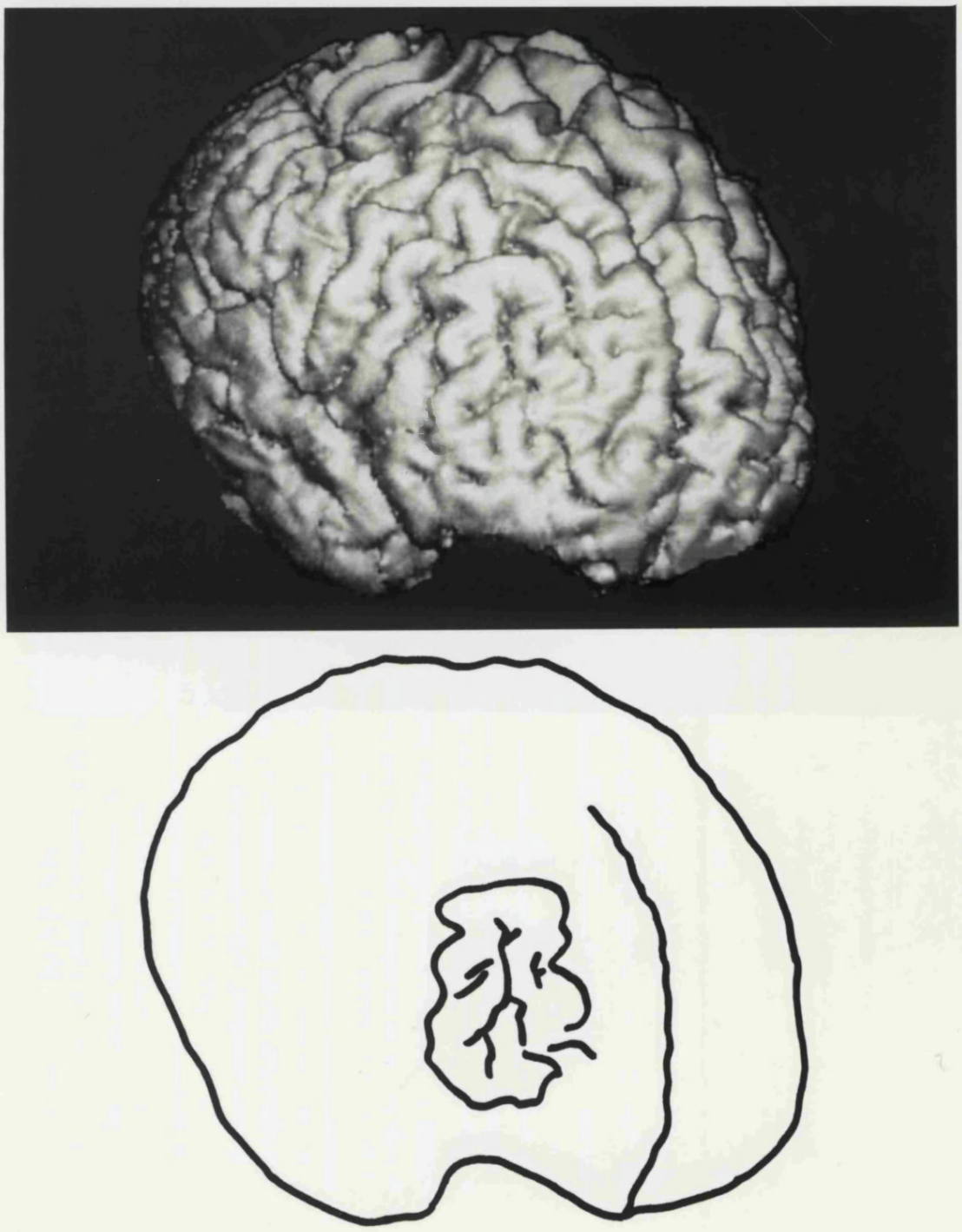

Figure 4.20. Patient 46. Female, 44 at scan, 6 at onset. Complex partial seizures with right arm posturing and left arm automatisms. Predominantly left anterior temporal spikes interictally, with occasional bilaterally synchronous spikes. Ictal EEG unhelpful. Reconstruction shows abnormal gyral configuration left middle frontal gyrus, (ring-like) with central island gyrus (arrowed).

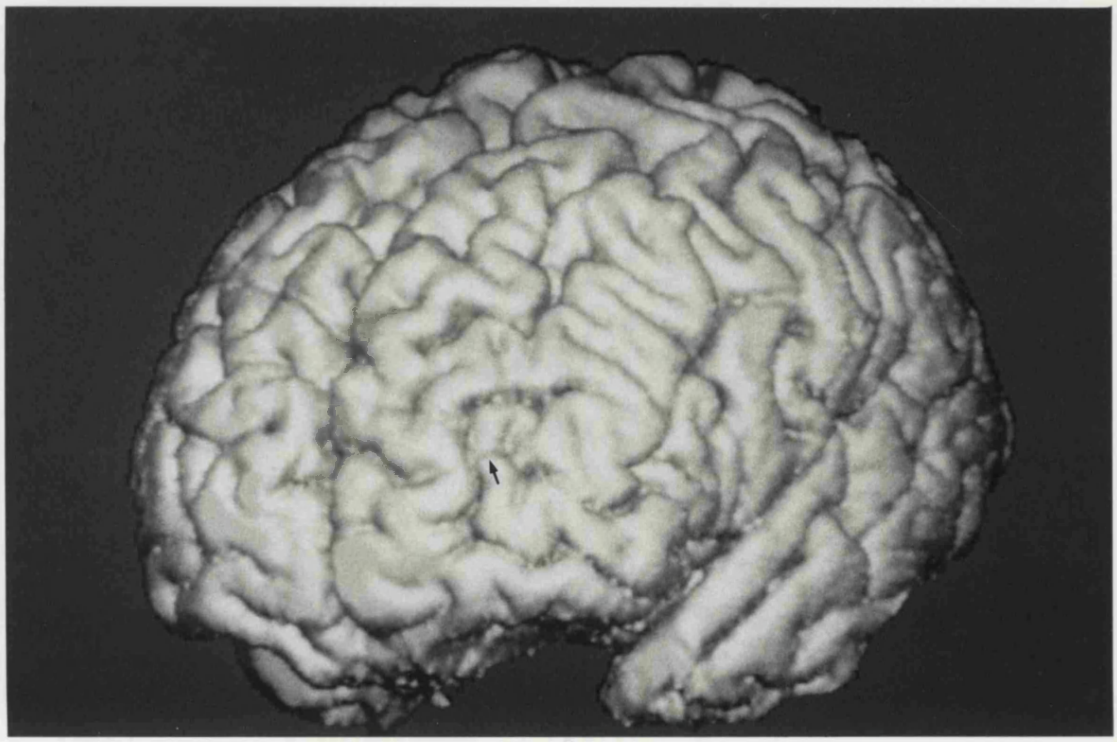

Figure 4.21. Patient 49. Female, 18 at scan, 3 at onset. Frequent seizures; bilateral arm extension and automatisms. Interictal EEG shows bifrontal spikes more marked on left. Ictal EEG unhelpful. Reconstruction shows gyral abnormality left frontal lobe (outlined).

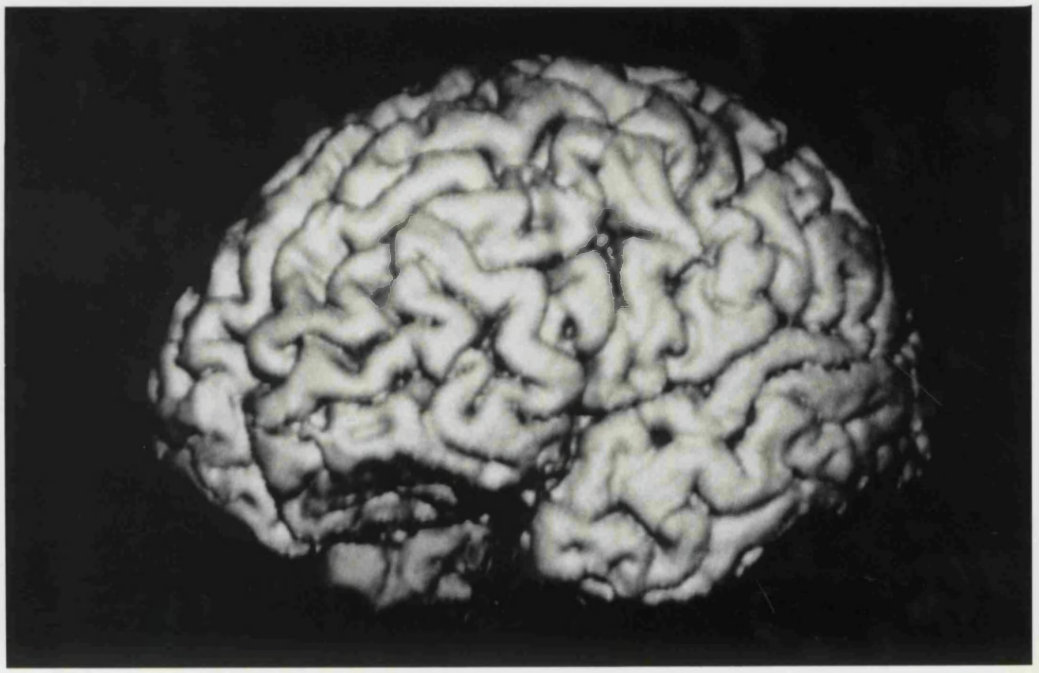

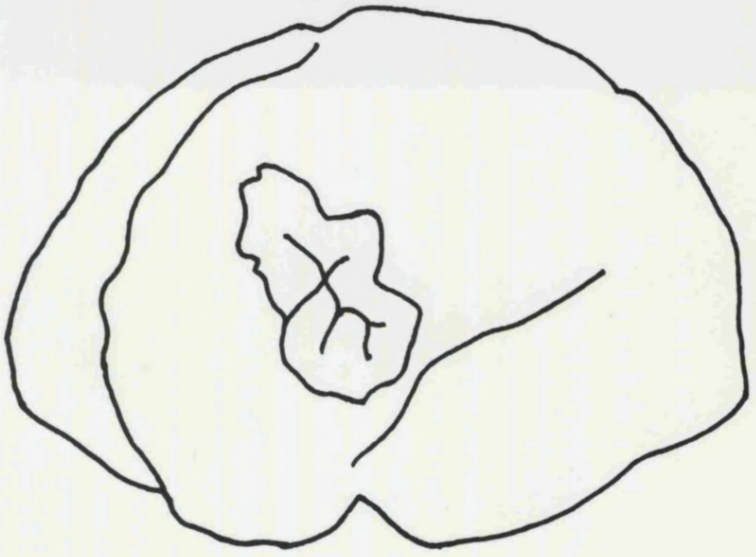

Figure 4.22. Patient 53. Female, 36 at scan, 8 at onset. Frequent nocturnal attacks; bilateral limb dystonic posturing and late jerking; immediate recovery. Daughter with identical attacks since age 6. Interictally, bilateral slow waves, more marked on left than right; ictal EEG unhelpful. Increased gyral complexity in the left middle frontal gyrus (marked) on reconstruction.

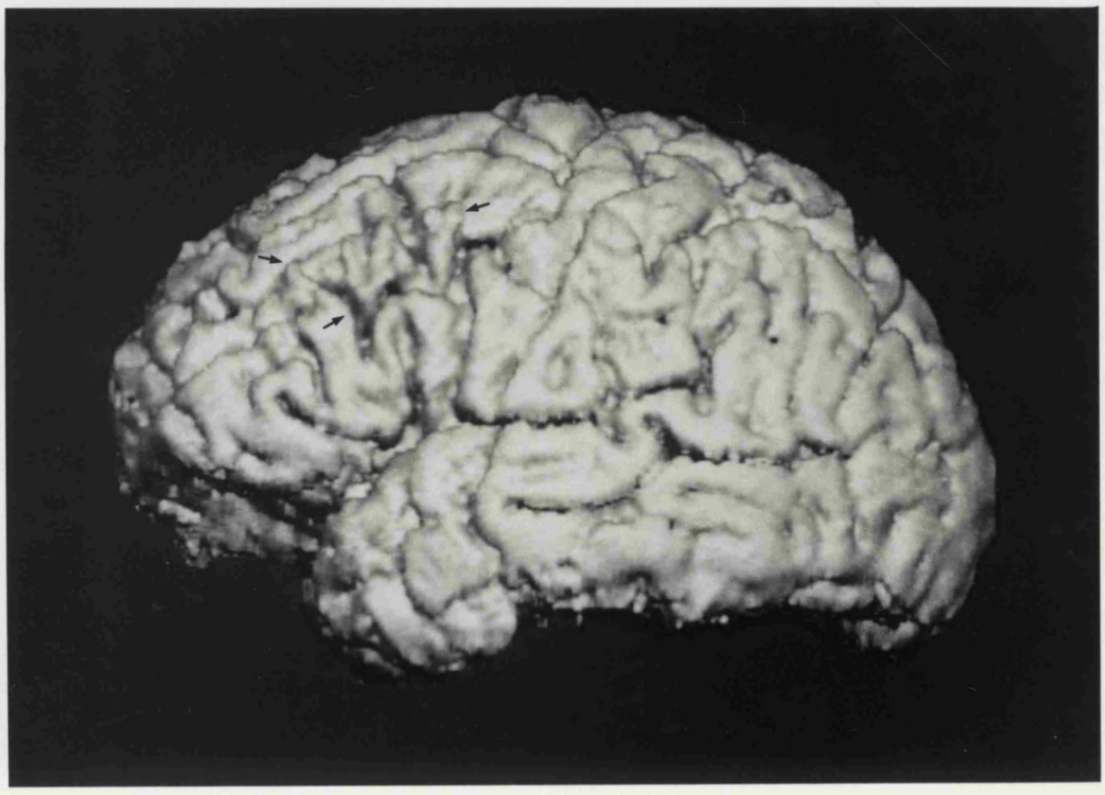

Figure 4.23. Patient 54. Female, 27 at scan, 4 at onset. Frequent seizures: rhythmic jerking of whole body and dystonic posturing of right arm. Interictal EEG shows infrequent abnormality over left frontal region (F3); no ictal changes, postictal left anterior slow wave activity. Reconstruction shows stellate abnormality of disposition of gyri in left frontal lobe (outlined).

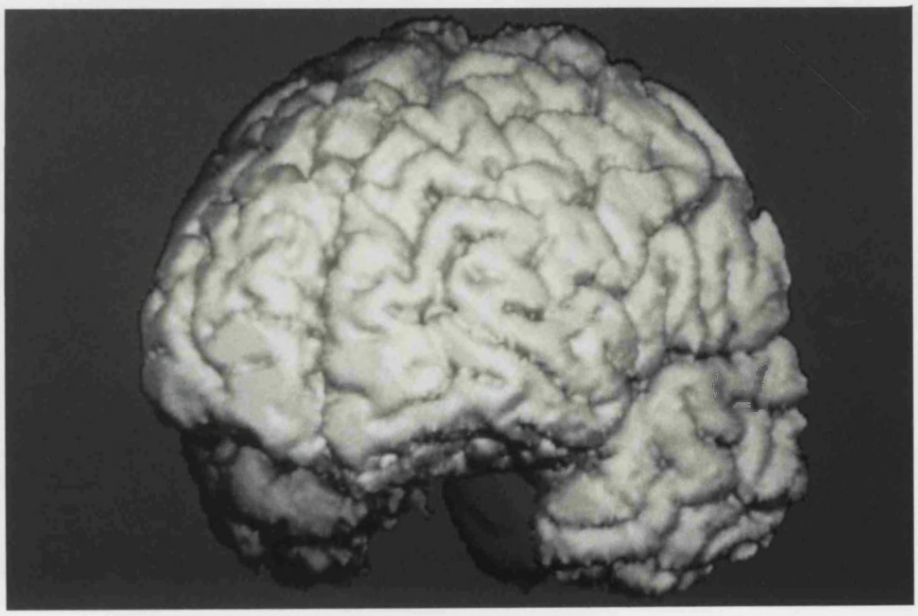

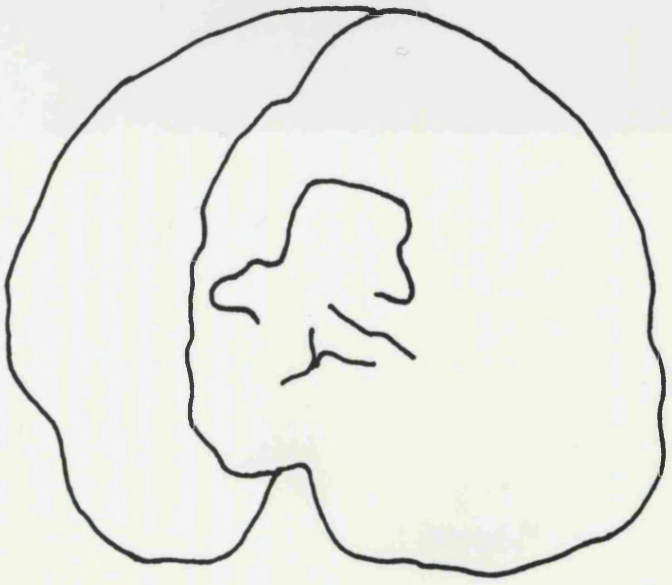

Figure 4.24. Patient 55. Male, 30 at scan, 14 at onset. Born 10 weeks premature; bacterial meningitis at 8/12. Complex partial seizures with blurring of vision, shouting of names, then tonic stiffening of all limbs. Interictal EEG shows sharp-slow wave complexes in both temporal regions; ictal EEG unhelpful. On reconstruction, sulci are shallow in the right frontal lobe.

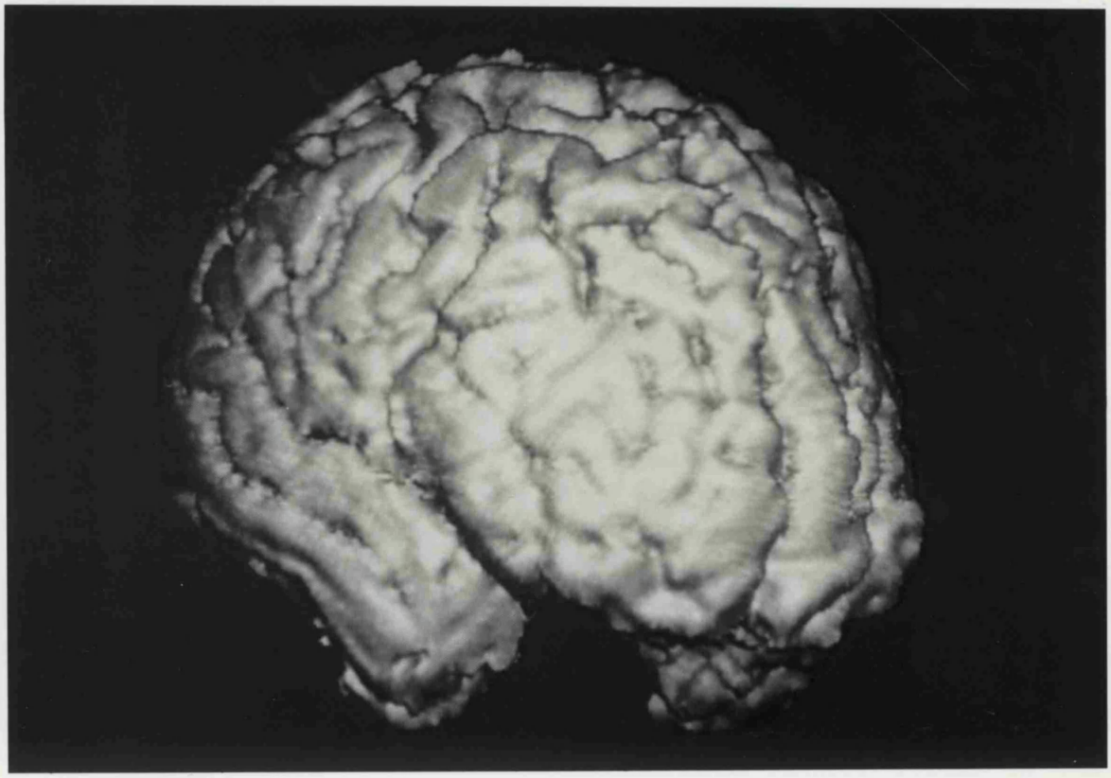

Figure 4.25. Patient 56. Male, 32 at scan, 7 at seizure onset. Complex partial seizures; groaning, grunting, shaking of arms (R predominantly). After one cluster, right Todd's paresis. Bursts of high frequency activity right frontal region (maximal at F4), less frequent sharp waves or spikes on left, equipotential at F7 and T3; rarely runs of fast activity in the left inferior frontal regions. On reconstruction, altered gyral patterns both frontal regions (more marked on right), without clear termination of middle frontal gyrus in either hemisphere.

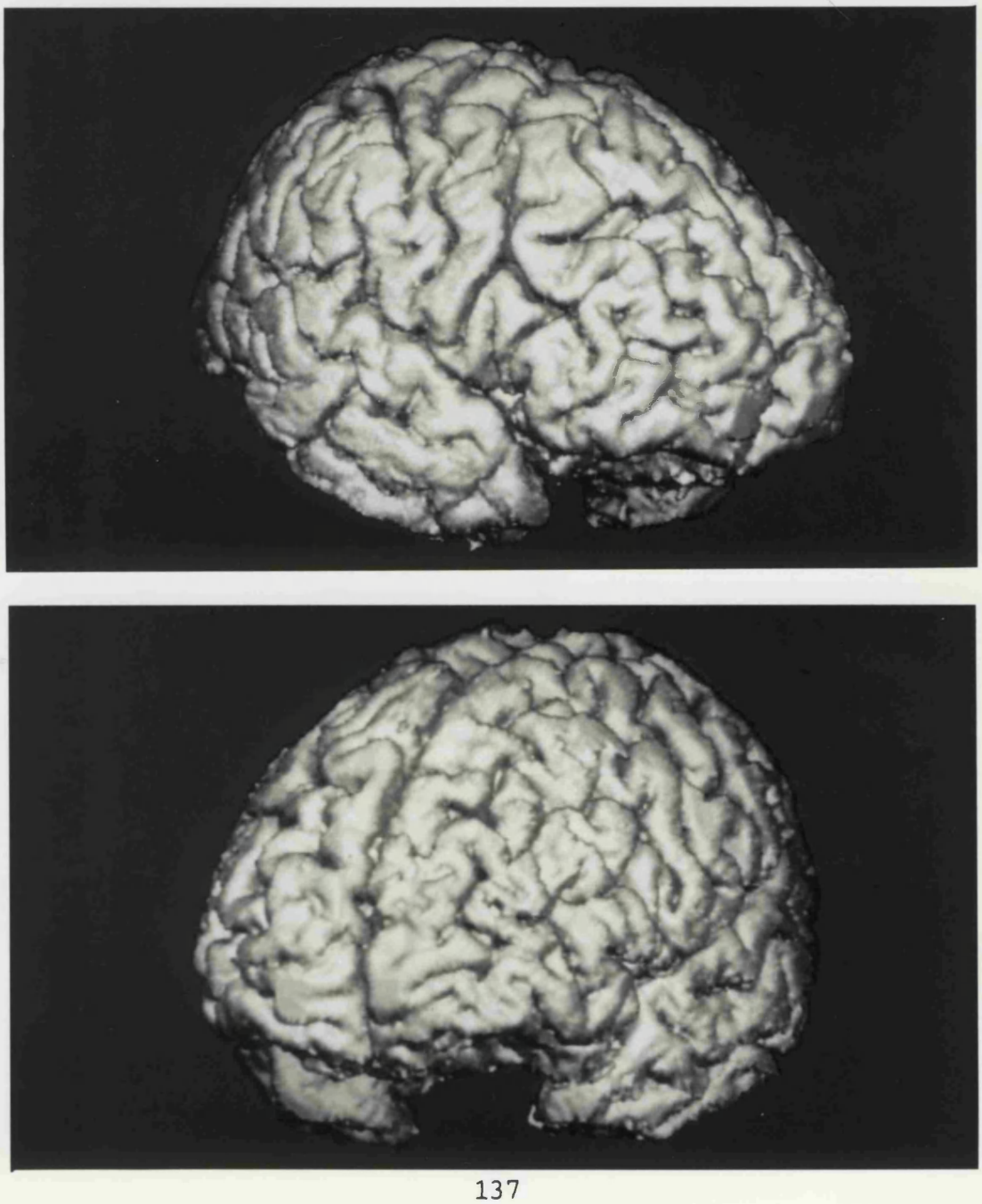

Figure 4.26. Patient 59. Male, 48 at scan, 18 at onset. Multiple seizure types; complex partial with epigastric aura, orofacial automatisms, face and eye deviation to the left; or with trembling of left-sided limbs; comlex partial status once a month; secondary generalised seizures every three to six months. EEG shows posterior right temporal focus. On reconstruction, abnormal gyrus R middle frontal gyrus (outlined).

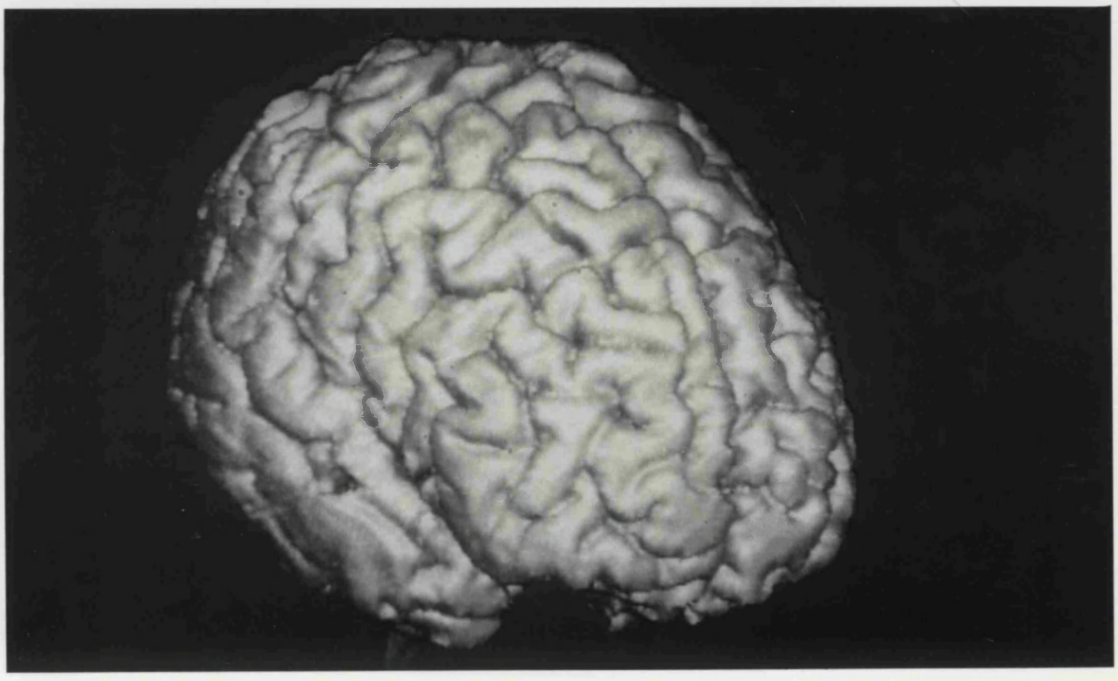

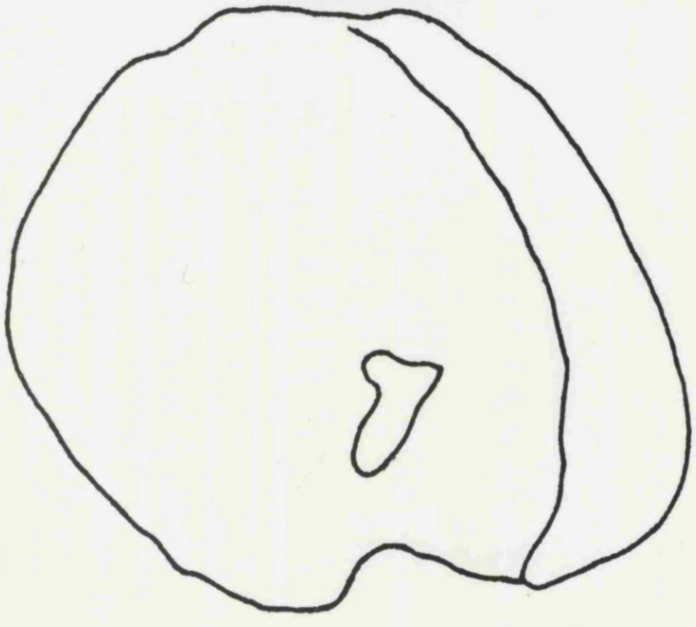

Figure 4.27. Patient 60. Male, 18 at scan, 6 at onset. Familial frontal lobe epilepsy. Frequent tonic extension of right-sided limbs. No EEG localisation. On reconstruction, gyri of L hemisphere seen to be narrower than those of R hemisphere.

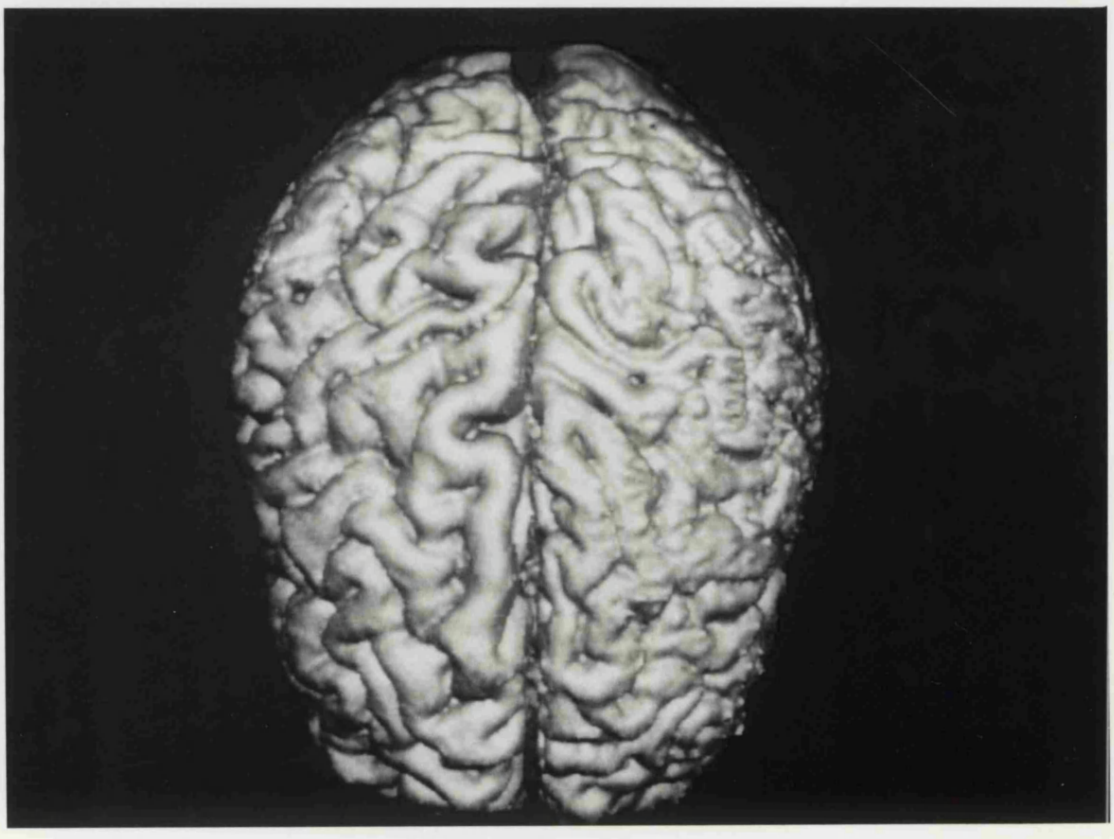

Figure 4.28. Patient 61. Male, 27 at scan, 9 at seizure onset. Previous R temporal lobectomy; seizures returned after 4 years, unchanged semiology: frequent brief attacks with fidgeting of all limbs and complex automatisms. Depth electrode studies confirmed seizure onset in the right frontal dorsolateral convexity. On reconstruction, abnormal gyral pattern in the inferior margin of the right frontal lobe (marked).

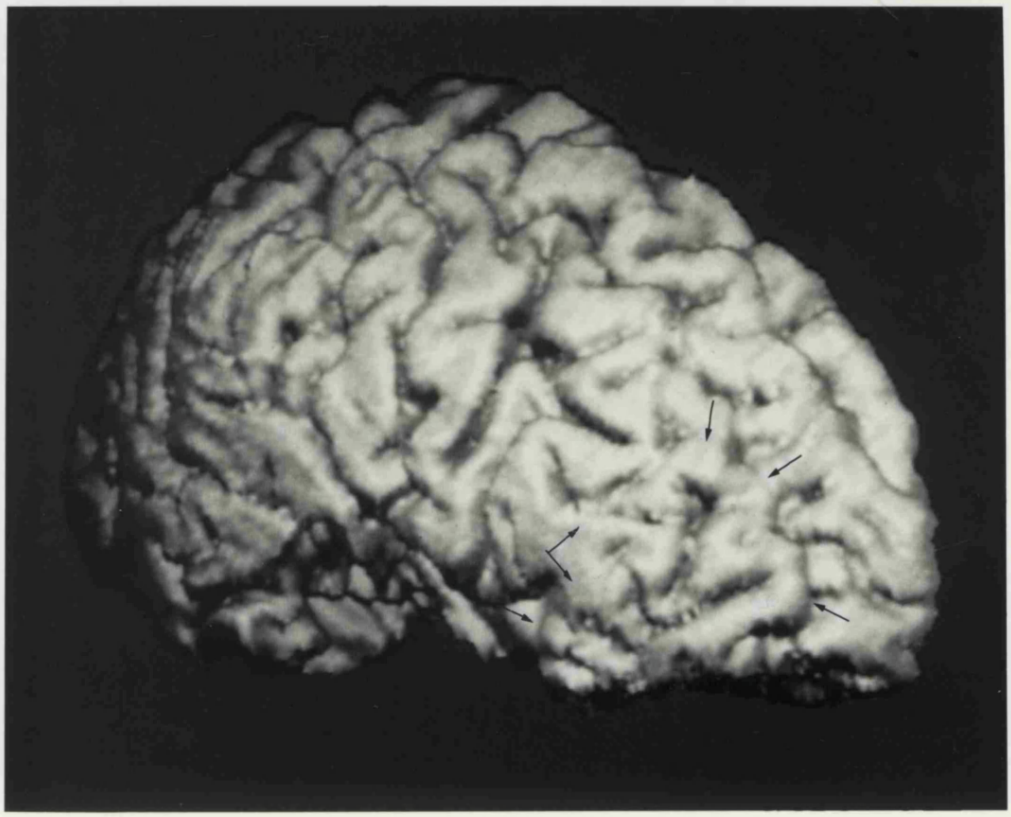

Block analysis was not performed in patient 43 because of excessive rotation. In the remaining 31 patients, 16 had structurally abnormal brains as defined (>1 abnormal value of 80/brain). For these 16, the mean number of abnormal values was 4.94. Across all 31, there were a total of 82 abnormal values (expected by chance alone: 6.70). The spatial distribution of these abnormal values is shown in Fig. 4.10 and the distribution in terms of type of block abnormality in Table 4.2. Only 7 of the 16 patients with quantitatively abnormal brains on block analysis have gyral abnormalities on three-dimensional reconstruction.

By definition, no lesions were seen on routine inspection of the two-dimensional images in these patients: in this sense, all the abnormal blocks were "extralesional". If this assessment is related to gyral abnormalities revealed on reconstruction, in the 14 patients with such abnormalities and who had also had block analysis performed, extralesionally abnormal blocks not contiguous with the lesion were seen in 10.

Analysis of non-homologous block pairs showed 5/32 patients had more than one abnormal pair ratio; two of these (42 & 46) have gyral abnormalities revealed on reconstruction.

4.3.3. Surface area derivatives and fractal dimension

Fractal dimension was abnormal in the right hemisphere in 1 patient and on the left in 4 (see Appendix 6 for details). These hemispheres in these patients were omitted from surface area analyses.

Abnormal surface area derivatives were seen in 6 patients. EGMR and EGML were normal in all patients. ESMR was elevated in 5 patients (27, 47, 50, 54 and 55); ESML was elevated in 3 (46, 47 and 55). Only patient 55 had low SM volume (bilaterally). ECCR was abnormal in one patient (50),

who had normal whole cerebral volumes but many abnormal block volumes. This patient, with borderline intellectual deficit, has refractory partial seizures, poorly localised on electroclinical grounds. Patient 47 also has a partial seizure disorder, with onset over the posterior head region.

The results for this group are summarised in Appendix 6.

4.4. Patients with only subependymal heterotopia

4.4.1. Clinical and MRI details

On routine inspection, the only neocortical structural abnormality visible in these patients was subependymal heterotopia. Clinical details of the patients are given in Appendix 6.

Patient 81 had hippocampal asymmetry noted on measurement and confirmed on histology after temporal lobectomy (with no intention of removing SEH). Postoperative scanning revealed that the SEH was intact on inspection. Seizures of unchanged semiology returned after an interval of a year.

4.4.2. Postprocessing results

Three-dimensional reconstruction did not reveal gyral abnormalities in any of the 13 patients.

All GM and SM volumes were within the normal ranges. TRAT was abnormal in 2/13: the left hemisphere was larger than the right in both (cases 77 and 81) and in both the SEH was left-sided only.

The degree of rotation of patient 77 fell outside the envelope of rotations for the controls; she was excluded from

block analyses. None of the remaining 8 female patients had more than one abnormal value on block analysis. Thus none had a structurally abnormal brain as defined above. All 4 male patients had more than 1/80 abnormal values (mean/subject 7.5; actual values 3, 8, 8 and 11): all thus had structurally abnormal brains. All four males had noncontiguous extralesional abnormal blocks. Inclusion of the heterotopic tissue in either the subcortical matter or the grey matter did not alter either total volume or block analysis results in any way. Results are given in full in Appendix 6.

Block pair analysis for the patients with SEH revealed that only one subject had more than one abnormality (patient 76, two abnormal values). By chance alone, there would be 0.77 abnormalities in the group as a whole. CCA was normal in all 13.

4.4.3. Surface area derivatives and fractal dimension

No patients had abnormal SM fractal dimension.

In one patient (83), ESM was bilaterally increased; it was reduced on the right in patient 77. ECCR was elevated in patient 75. There were no other abnormalities.

4.5. Patients with hippocampal sclerosis only

4.5.1. Clinical and MRI details

Ten patients had hippocampal sclerosis (HS) demonstrated histologically following surgery; none had any evidence on preoperative MRI of any other lesions (Raymond et al.,1994b). All had become seizure-free postoperatively (minimum follow up one year); all were studied using all the quantitative methods. The data from six other patients with hippocampal sclerosis shown either on MRI alone or who had had surgery

with less than 12 months follow up were also reconstructed, but not studied quantitatively. Brief clinical details are given in Appendix 6.

There was no significant difference between the patients with isolated hippocampal sclerosis and those with CD in terms of history of secondarily generalised seizures or duration of epilepsy (Mann-Whitney, two-tailed, $p>0.1$).

4.5.2. Postprocessing results

On 3D reconstruction, none of the sixteen patients had detectable gyral abnormalities in comparison to the control group or the published atlas.

Analysis of total volumes revealed that the left hemisphere was significantly larger than the right in one patient (100), and significantly smaller than the right in two others (101, 107). The smaller hemisphere was ipsilateral to the side of the removed sclerosed hippocampus, and therefore the side of epileptogenesis, in all three cases. Absolute hemispheric grey and white matter volumes were within the normal range in all ten cases.

Estimation of rotation showed that patient 100 fell outside the envelope of rotations for the controls: block analysis was not performed on this patient.

As a group, the patients with HS had only 4 abnormal variables out of 720 in total (all raised GM/SM ratios). By chance alone, 1.94 abnormal variables would be expected. No patient had more than one abnormal value: thus none had a structurally abnormal brain as defined.

Only one patient had more than one abnormal block pair ratio (two abnormal pairs; patient 102). CCA was abnormally small in only one individual (100), with a value of 409mm^2.

The fractal dimension of the grey-white interface was not abnormal in any case. ECCL was abnormally high in two patients (100 and 102).

4.6. Mean cortical thickness

This value was calculated for all hemispheres quantitatively analysed except those with an abnormal SM fractal dimension, for whom surface area derivatives, and therefore cortical thickness, could not be estimated. Cortical thickness was normal in all controls; of 70 patients in whom it was calculated, thickness was only abnormal in one (patient 7), in whom the mean thickness of the cortex was abnormally high bilaterally.

4.7. Summary of results across groups by analytic technique

In Table 4.4(a), all the results are summarised, giving proportions of subjects in each group with abnormalities in a given test. In 4.4(b), the proportion of patients in the various groups with structurally abnormal brains, as defined by block analysis, is compared using the χ^2 statistic (after application of Bonferroni correction for multiple comparisons, so that only p values < 0.00048 are considered significant). When all 13 patients with SEH are considered as a group, they are not significantly different (χ^2) from any other group, thus disproving the hypothesis postulated in section 1.7. However, in view of the marked difference in block analysis between male and female patients with SEH (see 4.4 above), male and female patients were treated *post hoc* as separate subgroups in the table (see also Discussion).

Table 4.4(a). Summary of results: proportion with abnormalities on each test

Test	Controls	Dysgenesis	Normal scans on 2D inspection		SEH		Hippocampal Sclerosis
			Abnormality on reconstruction	Normal on reconstruction	Male	Female	
Reconstruction	0/33	6/22	17/17	0/27	0/4	0/9	0/16
TRAT	1/33	9/22	3/13	1/19	1/4	1/9	3/10
Whole hemispheric volumes	0/33	7/22	1/13	2/19	0/4	0/9	0/10
Number with>1 abnormal block	0/33	19/21	8/12	8/19	4/4	0/8	0/9
PR	0/33	8/21	2/12	3/19	0/4	2/8	0/9
CCA	0/33	5/22	0/13	0/19	0/4	0/9	1/10
Fractal dimension	0/33	2/22	2/13	2/19	0/4	0/9	1/10
Surface area derivatives	0/33	11/20	4/11	2/17	1/4	2/9	2/10

(b) Significance for χ^2 values (see text)

	Controls	Dysgenesis	Normal scans on 2D inspection		SEH		HS
			Abnormality on reconstruction	Normal on reconstruction	Male	Female	
Controls	-	S	S	S	S	n/a	n/a
Dysgenesis	-	-	NS	NS	NS	S	S
Abn. on recon.	-	-	-	NS	NS	NS	NS
Normal on recon.	-	-	-	-	NS	NS	NS
SEH, male	-	-	-	-	-	S	NS
SEH, female	-	-		-	-	-	n/a

Abbreviations: S = significant; NS = nonsignificant; n/a is entered if no individuals in either group has a structurally abnormal brain as defined by blocks. Abn. = abnormalities; recon. = reconstruction.

CHAPTER 5: DISCUSSION

The first three sections centre on the aims of the thesis as stated in section 1.7; the particular case of subependymal heterotopia, the functional significance of the findings and future directions are then considered.

5.1. The extensive nature of structural abnormalities in dysgenesis

It has been postulated that human cerebral dysgenesis is likely to be an extensive disorder, with structural abnormalities beyond the visualised lesion alone (see Chapter 1). Whilst there is much evidence in favour of this in animals and some circumstantial evidence in humans, direct evidence has not been available in humans. The difficulties involved in showing such extralesional abnormalities have been described previously. In summary, *in vivo*, brain outside a lesion may appear normal on visual inspection alone (of MRI or at operation), and there is usually no justification for its excision at surgery. Postmortem, the effort needed to detect areas of abnormality in normal-looking brain is, if anything, greater, requiring extensive sampling and tedious techniques (eg Golgi staining; Huttenlocher, 1974). As some abnormalities may be purely quantitative (cell counts), histopathology would be further complicated by stereological considerations, which have seldom been addressed in postmortem studies. Lastly, few brains with dysgenesis are available postmortem to centres with the interest and ability to examine them adequately. Hence other methods were devised to address the question in vivo.

Using MRI technology and a novel methodology based on biological consideration of the nature of dysgenesis, results from this work show that there are abnormalities of cerebral structure, associated with frank dysgenesis, in regions well beyond the visually-determined lesion in 79% of cases.

Cerebral tissue within extralesionally abnormal block variables appears to be normal on visual inspection alone of MRI data. In these cases, cerebral structure is extensively disrupted: there are quantifiable changes in shape (regional volume distribution) that are not apparent to the human eye on inspection alone, and are not present in control subjects.

Such changes are not present in patients whose epilepsy is due to hippocampal sclerosis alone (as judged by seizure-freedom postoperatively and the absence of other lesions identified on routine inspection or reconstruction). In terms of the occurrence of secondarily generalised seizures or duration of epilepsy, there is no difference between the patients with hippocampal sclerosis and those with dysgenesis. Thus epilepsy need not produce the block abnormalities seen: these are more likely to be associated with the cause of the epilepsy.

Examination of the patients with visually normal scans and chronic partial epilepsy confirms the finding that structural abnormalities of the cortex may be present where none can be seen on inspection alone. These patients had no neocortical abnormalities detected even when the images had been examined by an experienced neuroradiologist with an interest in dysgenesis, and when the images had been previously reformatted by another, independent, researcher examining the utility of reformatting (Raymond et al.,1993). In 52% of these patients there were abnormalities of the regional distribution of volume (see section 4.3.2). Thus structural abnormality may exist in brains in which inspection fails to reveal any abnormalities, dysgenetic or otherwise. The revelation of abnormalities by quantitation is also seen in the study of the hippocampus (Reutens et al.,1995; Van Paesschen et al.,1995) and may be seen as a natural extension of the original hypothesis: abnormalities are present in visually normal areas of scans with definite dysgenesis and in visually normal scans of other patients with partial epilepsy.

That the majority of extralesional abnormalities in the group with visible dysgenesis are noncontiguous (see 4.2.3) suggests that changes may not only be locally extensive (as now shown by Palmini et al.,1995), but also multifocal, as postulated by Awad et al. (1991). This may be because the cause of the dysgenesis itself - not investigated at all in this work - acts diffusely or because of extensive interneuronal connectivity (see section 1.6.). The latter is discussed further below. Note that Palmini et al. (1995) show that dysgenesis may be demonstrable histologically in areas that are normal on inspection.

Visualisation of the three-dimensional surfaces of the cerebral hemispheres is another way in which the spread of dysgenesis may be shown to extend beyond the lesion visualised on two-dimensional images. Given that gyral morphology is affected by cortical architecture (Rademacher et al.,1993), additional gyral abnormalities are likely to represent additional areas of structural disruption. Three-dimensional reconstruction has revealed additional gyral abnormalities in 6/22 patients with obvious dysgenesis and in 18/45 patients in whom no abnormalities were seen at all on routine inspection (see 4.2.1 and 4.3.1). It should be emphasised that the patients in the latter group did not all have quantitative abnormalities, and those with quantitative abnormalities did not all have gyral changes: the techniques explore different aspects of cerebral structure and are complementary. In both cases the changes may be due to CD. It may be that if gyral volumes, rather than arbitrary (but strictly defined) regions, were examined, then the two techniques might reveal changes in similar locations, although problems of measuring the volumes of specific gyri, and comparing them between individuals, are daunting, especially given the unique gyral patterns sometimes seen in CD (see 2.3.1.).

Clinically, these findings are important. Firstly, they provide a possible explanation for the poor outcome after

surgical resection of apparently focal dysgenetic lesions in patients with refractory epilepsy. To explore this further, a cohort of patients undergoing surgery for epilepsy ought to be studied prospectively using these techniques, and the outcome compared to the quantitative preoperative findings and lesional histopathology, as is being done for hippocampal volumetry and mesial temporal epilepsy (Spencer, 1995). If the presence of extralesional abnormalities is associated with a poor outcome, then quantitative preoperative analysis may prevent lesional surgery in patients doomed to a poor outcome. Secondly, the findings demonstrate that areas of scans and whole scans that appear normal may harbour quantifiable abnormalities, so that the large number of patients with partial epilepsy said to be cryptogenic may in the future decline.

There is evidence therefore in support of the hypothesis that there may be abnormalities of cerebral structure beyond the visualised lesion in brains affected by dysgenesis.

5.2. The normal human brain

The results demonstrate significant relationships between various aspects of hemispheric structure - confirming the presence of order in cerebral organisation at this level of analysis. Thus the cerebral hemispheres are highly symmetric in terms of volume, confirming others' results (Filipek et al.,1994; Klekamp et al.,1987). There are many volumetric relationships between different parts of the brain, that are not necessarily contiguous, even though the volumes defined are arbitrary (see 4.1.3 to 4.1.6). Given the range of orientations at which the normal brains were scanned, this suggests that the distribution of grey and subcortical matter in the hemispheres is regulated, such that the brain in normal caucasian individuals has a limited range of shapes.

There are also relationships between various surface area measures and neocortical volume and callosal area. These findings support the second hypothesis postulated in the introduction and extend, at a macroscopic level, the findings of Rockel et al. (1980), Winfield et al. (1980) and Haug (1987), suggesting that there are indeed proportional relationships between cortical surface area and neuronal number in normal subjects (see below). Such average relationships could enable general principles to generate gross structure without this having to be specifically prescribed in each individual: less genetic information is therefore required, reconciling the complexity of the adult brain with the total amount of DNA available to define it. In theory, this carries with it the risk that small genetic changes may have extensive effects on cerebral development, as seen in practice in the Miller-Dieker syndrome (Reiner et al.,1993).

5.2.1. Hemispheric surface area measures

Surface area measures of the cortex are important because they reflect cytoarchitectural organisation. Current thinking attributes the size of the cortical surface mainly to the growth of the neocortex due to expansion of its neuropil (Armstrong et al.,1991 & 1995). In ontogeny and phylogeny, this expansion is limited very largely to a tangential direction by replication of a basic columnar multicellular element, which is repeated and locally elaborated rather than fundamentally changed (Richman et al.,1975; Rockel et al.,1980; Rakic, 1995): there is hardly any increase in cortical thickness even across species (Welker, 1990). Cortical folding allows a large surface area to be contained in a comparatively small volume and is an efficient organisation (Ruppin et al.,1993). As a consequence of this organisation, the surface density of neurons in the cortex has been postulated to be constant, so that determination of a cortical surface area measure might provide a means of

estimating total and regional neuronal numbers and function-specific neuronal proportions (see 1.4).

For reasons given in section 3.13, the cortical surface area measure used was the SM surface, a boundary created by the spatial dominance of intergyral arcuate (or "U" fibres) and aggregating projectional fibres passing through this interface. Such projectional fibres are most plentiful in the walls and at the crowns of gyri and least numerous in the depths of the sulci (Welker, 1990).

The white matter cores within gyri, underlying the crown and walls, increase SM surface area significantly more than they increase its volume. Measurement of the surface area of a block of SM before and after arbitrary but defined pruning supports this proposition: the removal of all protruding white matter cores 3mm or less in diameter leads to a large loss of surface area, but significantly less volume loss. The observed loss of surface area correlates significantly with the calculated extra surface area of the block generated by its surface folding. That the observed loss and calculated extra surface area are not identical may simply be because an arbitrary (though defined) white matter core size of 3mm was specified; real gyral cores have various diameters and shapes, and a more sophisticated method might have been to remove cores depending on individual brain size. The aim, however, was to demonstrate a principle, which is also supported by the finding that the ratio of extra SM area to the total SM area (the ratio E_A/SM_A) is high. The experiment shows that E_A, the extra surface area generated by folding of the SM, may also be taken as an estimate of the surface area of the gyral cores, that is the area directly overlain by cortical grey matter in gyral crowns and walls rather than in sulcal depths. Both E_A and SM_A correlate, in normal brains, with GM volume, and thus with total neuronal number (Braendgaard et al.,1990). However, given the nonuniform density of projectional (afferent and efferent) fibres crossing the grey-white interface, E_A better

reflects projectional axon numbers than does the total SM area, SM_A, and may be considered to be more biologically relevant (Sisodiya et al.,1996). In brains where, for example, the cortex is pathologically thickened (for example as a result of lissencephaly), E_A may be a better measure of projectional axonal numbers that either SM_A, grey matter volume (Haug, 1987; Braendgaard et al.,1990) or even the free GM surface (Rockel et al.,1980).

The surface area derivatives quantify mean structural properties of entire hemispheres. The parameters assess the relationship between the extra SM area, E_A, and GM and SM volume and CCA. These ratios are independent of brain size and may identify changes in structural proportions even though the underlying variables (surface areas and volumes) fall within the normal range. Values all fall within three standard deviations of the mean for control subjects, suggesting that there is order in normal cerebral structure. In patients, small areas of disproportion, due to structural abnormality, may be averaged out by larger areas of proportion (structural normality) within the same hemisphere. If abnormal values for these parameters are found, then the pathological process present in the hemisphere must be quantitatively dominant.

The ratio ECC is perhaps most simply interpreted. In control subjects, E_A is a measure of the number of projectional axons and the amount of neuropil/neuron causing tangential growth of the neocortex (Fig 5.1). CCA is a measure of the number of interhemispheric fibres (Tomasch, 1954; Aboitiz et al.,1992). ECC is a function of these quantities. An increase in ECC implies either (1) that the proportion of (noninterhemispheric) projectional axons is increased and the proportion of interhemispheric fibres is reduced (or that they are thinner on average) or (2) that the mean amount of neuropil/neuron is increased (or some combination of these findings). In any case, there must be an alteration in the normal pattern of interneuronal connectivity (as mediated by

Figure 5.1

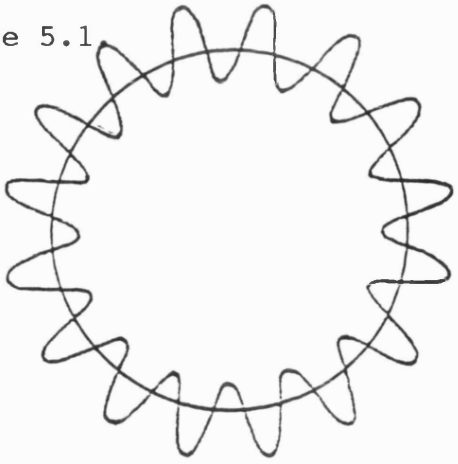

Schematic demonstration of generation of SM surface. In the top figure, the predominantly outer folded line represents the real SM surface in cross-section; the circular outline encompasses the same area but is unfolded; the difference in the perimeters of the two regions is the extra length (area in three dimensions) generated by the folding of the surface of the SM. This is termed E_A, the extra area and is defined by:

$$E_A = SM_A - 4\pi(3SMV/4\pi)^{2/3}$$

where SM_A is the measured SM surface area and SMV the measured SM volume.

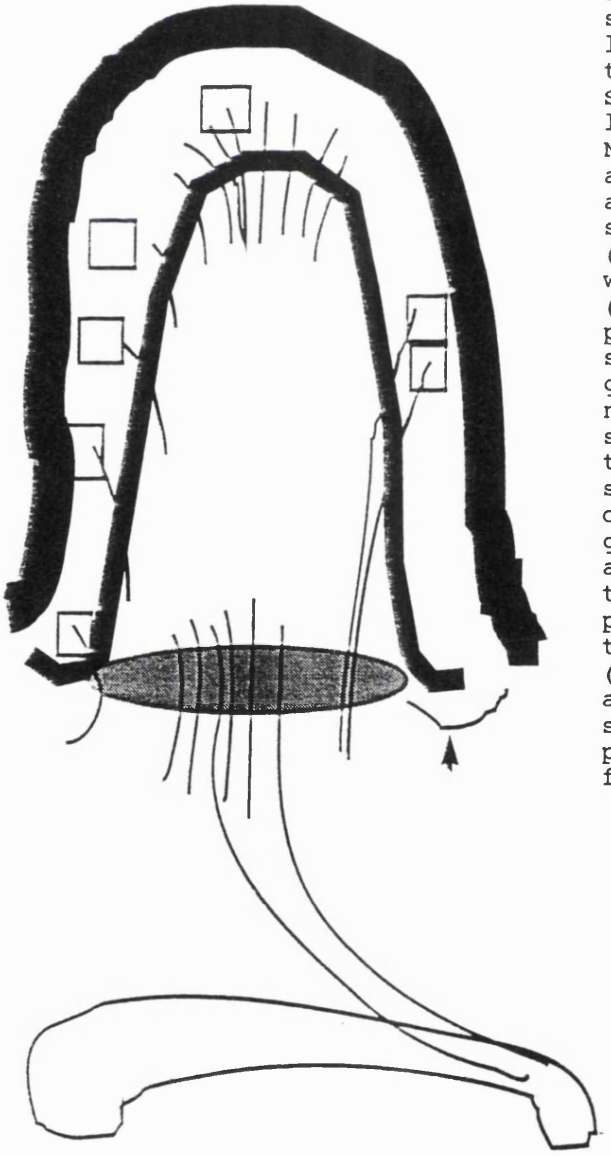

The bottom figure represents a single gyrus; the outer thick line is the grey-CSF surface, the inner thick line is the GM-SM interface. The numerous thin lines are projectional axons. Note their density is highest at the gyral crown and lowest at the gyral base; in the sulcus, they form U fibres (marked ↑). The base of the white matter core of the gyrus (shaded grey) is composed of projectional axons; these are separated in the body of the gyrus by the growth of the neuropil (represented by the squares). E_A is a measure of the inner thick line, ie the surface of gyral white matter cores, and is therefore generated by both projectional axons and neuropil growth (see text). A fixed proportion of projectional axons pass through the corpus callosum (represented in cross-section and not to scale), the cross-sectional area of which is proportional to the number of fibres passing through it.

axons, synapses and dendrites), given that the proportion of neurons belonging to a given functional class is thought to be fixed (Winfield et al.,1980) and that the mean amount of neuropil/neuron in normal brains is also relatively constant (see above). The specific nature of average changes in cortical structure probably cannot be determined solely from a change in ECC, but a better idea might be gained if changes in EGM, ESM and hemispheric volumes were also taken into account. A reduction in ECC has the converse implications with respect to changes in cerebral structure, and also implies extensive alteration in averaged interneuronal connectivity.

EGM is a function of E_A as above and GM volume. GM volume depends on neuronal numbers and, predominantly, on neuropil volume (Haug, 1956), gross gliosis being excluded in this study by the negative T_2 findings (see section 3.3). Any change in neuropil is equivalent to a change in connectivity; changes in neuronal numbers, given the finite volume of the GM and that all neurons have neuropil, must be accompanied by neuropil volume change and therefore alteration in connectivity. A reduction in EGM therefore implies (some combination of) either (1) a reduction in the mean amount of neuropil/neuron or the proportion of projectional axons or (2) a disproportionate increase in the GM volume, that again necessitates a fall in projectional axon number.

Geometrically, grey matter volume is a function of grey matter surface area and thickness. Changes in grey matter thickness are very limited (Rakic, 1995; and section 4.6). It has been suggested that this is because of biophysical constraints acting on the apical dendrites of pyramidal cells (Prothero and Sundsten, 1984). An equally valid reason may be that if an abnormal number of neurons are stacked vertically and yet maintain normal dendritic expansions, then the tangential area available for the passage of the increased number of afferent and efferent axons required to keep the increased number of neurons connected is, perversely, reduced,

limiting the number of neurons that can be supported in such a stack. This is essentially a more pial and smaller scale application of the gyral window concept of Prothero and Sundsten (1984). Therefore in abnormally thick cortex, if the number of neurons is increased, then the proportion of axons that cross the grey-white interface must be reduced; if the number of neurons is unchanged or reduced, then in the absence of gross gliosis (normal T_2 findings), the mean amount of neuropil per neuron must increase. Abnormal cortical thickness therefore implies that connectivity within it is likely to be abnormal.

ESM is a function of E_A and SM volume. The biological correlate of SM volume is the product of the number of all extracortical projectional axons of various diameters and the mean volume of axons of a given diameter. If ESM is increased, then *either* E_A must be disproportionately large (ie. there are more projectional axons, demanding a reduced mean volume per axon in the SM, or more neuropil/neuron - but this cannot be associated with increased extracortical projection as then SM volume would rise - so that local connectivity, without axons entering and contributing to the SM, must rise), *or* there is simply reduced volume per axon in the SM (with or without a reduction in their number). In either case (or with some combination of the two possibilities), the reduced mean volume per projectional axon implies altered connectivity as axons must be shorter and/or thinner than normal: the latter possibility is likely to be associated with reduced terminal arborization of the axon (Mitchison, 1991). Shorter axons would suggest a tendency to increased local connectivity at the expense of more distant connectivity. In this group of patients, if ESM is abnormal, it is always increased. In no case is an increase in ESM associated with an abnormally high value of E_A itself; indeed, in one case, an abnormally high ESM is associated with an abnormally low E_A (patient 7).

5.2.2. Cortical thickness

Calculated mean cortical thickness is abnormal in only one patient, and not at all in controls (mean thickness was also obviously increased in one other patient, number 6, in whom calculation was precluded by abnormal hemispheric fractal dimension). This supports the view that cerebral structure develops by the increase of the number of fundamental elements rather than by alteration in the structure of these elements and emphasises the importance of limited cortical thickness (Rakic, 1995), possible reasons for which have been discussed above.

5.2.3 Hemispheric symmetry

In contrast to symmetry of hemispheric volume, hemispheric function is known to be asymmetric. Asymmetry of hemispheric gyral patterns in normal subjects has been well documented (Ono et al.,1990; Falk et al.,1991; Steinmetz et al.,1994). These asymmetries have been shown to relate to underlying cytoarchitecture (Galaburda and Kemper, 1979; Rademacher et al.,1993) - supporting the view that cellular structures govern cerebral shape rather than the other way around (Bok, 1959). Asymmetry of the hemispheric surface areas may allow reconciliation of gyral pattern differences and hemispheric volume identity.

Henery and Mayhew (1989) examined postmortem brains of six males and six females using stereological techniques and determined that there was no asymmetry of either cerebral volume or cortical free surface area. In this report, a larger number of individuals has been studied. For right-handers alone, there is a difference between the surface area of the subcortical matter between the right and left hemispheres (independent of sex). There is a similar, non-significant, asymmetry for the left-handers, though few of these were studied and cerebral dominance was not addressed.

In the right-handed control subjects, E_A is larger on the right than on the left, whilst grey matter volume is greater on the left than on the right. Asymmetry therefore extends to hemispheric component volumes. Similar nonsignificant trends are seen in the left-handers.

If the hypothesis that the proportion of neurons allocated to a given function is fixed (Rockel et al.,1980; Winfield et al.,1980) is correct, then the asymmetry of E_A and GM volumes suggests that there are more neurons in the normal right hemisphere than the normal left but that the quantity of neuropil/neuron is on average greater in the left hemisphere than on the right for right-handers (see Appendix 7 for deduction). Unfortunately, most reports of histological assessment of cell densities and numbers do not state which hemisphere measurements were taken from; the most rigorous report sampled only the right hemisphere (Braendgaard et al.,1990). Cortical thickness is greater on the left than on the right (see 4.1.6): thickness differences have been attributed to differing amounts of neuropil (Rakic, 1995). This is compatible with evidence to suggest that there is more intrahemispheric processing in the left hemisphere than in the right (Gur et al.,1980). None of the analyses are affected by handedness, with similar, but non-significant, trends for left-handers as are found at a significant level in right-handers: thus separate analysis of surface area derivatives for right and left handers is not necessary.

Functional asymmetry associated with gyral asymmetry may therefore be associated with different underlying neuropil quantity and organisation in the two hemispheres. Regionalisation of the surface area measures would clearly be of value, especially if the area of grey-white interface underlying specified regions of the cortex could be measured and compared between individuals. Then it might be possible to determine that specific gyral asymmetries were associated with different local cortical thicknesses and differing amounts of

neuropil. Regional asymmetry in surface area (of the planum temporale) has recently been documented and related to specific cortical function (Schlaug et al.,1995).

Perhaps the more surprising fact, then, is that the hemispheres are so symmetrical in terms of total volume. The biological basis for this remains obscure. However, that volume symmetry is important is shown by the asymmetry seen in patients. Whilst only 1/33 (3%) of controls has a TRAT outside the normal range, 20/77 (26%) patients do. It is possible that this reflects an early insult to the developing brain that is somehow lateralised and results in overall volume asymmetry of the hemispheres: lateralised DNA abnormalities have been found in hemimegalencephalic dysgenesis (Manz et al.,1979).

5.3. Interpretation of altered quantitative measures in patients

Abnormal structural parameters, including extralesional changes, have been shown in the majority of the patients with CD (see section 4.2). The possible basis for these findings is now explored.

5.3.1. Blocks

Block analysis sheds light on the possible nature of extensive structural abnormality in CD. For the patients with cerebral dysgenesis, there are many abnormal GM/SM block ratio values (101/440): all, notably, are above the upper limit of the normal range. An abnormally high GM/SM ratio may be explained in a number of ways. Firstly, it may be due to a pure increase in the non-neuronal component of the grey matter i.e. the glia and blood vessels. However, given the paucity of available information, there is limited histopathological support for this idea, it being reported with any frequency only in focal cortical dysplasia and polymicrogyria with focal

scarring (Barth, 1987). In some such cases, Barkovich et al. (1992a) report increased signal on T_2-weighted images in the lesional areas. This was not seen in our cases and certainly not in the extralesional sites. Secondly, it may be due to a pure increase in the number of neurons in lesional and extralesional abnormal areas: however, the increase in grey matter is associated with a relative decrease in the accompanying white matter and thus it would be necessary to postulate either (1) that the proportion of nonprojectional neurons was increased, implying altered local connectivity or (2) that the increased number of neurons projected thinner axons. Such axons might have altered terminal arborization as compared to unthinned, normal axons (Mitchison, 1991), and thus terminal connectivity would have to be altered. Thus a pure change in the number of neurons alone without altered connectivity is also unlikely to explain the results. However, if neuropil volume is considered altered in the first place, then the results can be more readily explained, whether the number of neurons is altered or not. Alteration in neuropil volume must be due to (any combination of) changes in axon, dendritic or synaptic content, necessarily implying some change in connectivity. Thus interneuronal connectivity changes may underlie the findings of regionally altered GM and SM block volumes and ratios. The local apparatus of connectivity (eg dendrites) in CD lesions has been shown to be abnormal histologically in the limited published literature (Ferrer, 1984; Bordarier et al.,1986; Takada et al.,1994). Histological evidence of pathologically increased local circuit neuron numbers, necessarily associated with altered local neuropil and interneuronal connectivity, was reported in a pathogenic CD lesion by Ferrer et al. (1992). Sadly, there are very few studies in which this possibility is even addressed. Local (Jones et al.,1982) and widespread (Goldman-Rakic, 1980) alteration of connectivity is seen in animal experiments involving the disruption of corticogenesis. These animals, however, were not epileptic. Altered connectivity as inferred from dendritic changes is seen in humans with

epilepsy and, for example, mental retardation. Volumetric analysis of scans of such patients would be of considerable interest, especially as these scans are often normal on inspection.

Of the 31 patients with chronic focal epilepsy and apparently normal scans studied quantitatively, 16 had a significant number of abnormal block values (see 4.3.2). As with the patients with dysgenesis apparent on routine imaging, all the GM/SM ratio abnormalities were increases. This is interpreted as above as indicating an abnormality of connectivity - in the absence of visible evidence of cerebral dysmorphogenesis on routine inspection. The latter is therefore not necessary for epileptogenesis, whilst abnormal connectivity (neuropil volumes) is associated with epileptogenesis (see 5.5. for further discussion). Some of these patients also had gyral abnormalities - but not gross neuronal malpositioning - revealed on reconstruction only: however, not all those with block abnormalities had gyral changes and vice versa. This may be because of the arbitrary nature of the regional volume analysis which may reduce its sensitivity as larger areas of normality within a block swamp smaller areas of abnormality.

Block pair measures assess another aspect of connectivity. The majority of the GM volume in the human cerebrum is composed of neuropil (Haug, 1956). Therefore, that the volumes of two GM blocks correlate highly suggests that the volumes of neuropil in these two blocks also correlate highly. The relationship between the volumes of a given pair of blocks is a statistical finding: biologically, the correlation is probably due to stereotyped patterns of corticocortical interneuronal connectivity, though whether this is directly from one block to the other or via more complex circuits across the hemispheres or even via subcortical structures cannot be determined with the available data. This may also be an explanation for the limited range of

shapes of normal brains revealed on quantitation by block analysis.

Amongst the patients with dysgenesis, 9/21 (43%) have more than one pair abnormality, though neither underlying GM block of a pair is abnormal in 72%. In addition, in the group of patients with no apparent change on routine imaging, 5/31 have more than one abnormal pair ratio. In both these groups of patients, this is further evidence for abnormal corticocortical (intra- and inter-hemispheric) connectivity, with or without visible dysmorphogenesis.

In routine usage, the term "dysgenesis" commonly conjures up impressions of macrogyria, clefts and so forth. Imaging and histological advances have detected other forms of cerebral structural change that are likely to be developmental in origin and therefore dysgenetic by definition. Dysgenesis at the synaptic level is well recognised (Becker, 1991) and, though quantifiable, may not be visible even on (routine) microscopy (Huttenlocher, 1974; Purpura, 1974). Quantitation is also used in the definition of megalencephalic dysgenesis, such that brains weighing more than 2.5 standard deviations above the mean are considered abnormal (Dekaban and Sakuragawa, 1977). The scale of application of quantitation is irrelevant, so that if more or less neuropil (axons, dendrites or synapses), for example, is present in a local region than should be the case (as seen with block analysis), then this too may be considered dysgenetic. Extensive, including "extralesional", structural changes in the brains of patients with chronic partial epilepsy, may therefore be considered 'dysgenetic', and may arise as a result of abnormal interneuronal connectivity, as suggested in section 1.6.1.

5.3.2. Surface area measures

The interpretation of surface area derivative abnormalities is exemplified by consideration of changes in

patients with known pathological abnormalities. Patients with full thickness clefts of the neopallium commonly have polymicrogyria in the surrounding and distant neocortex, possibly with additional subependymal heterotopia (Dekaban, 1965) and reduction in the subcortical white matter and cross-sectional area of the corpus callosum (Levine et al.,1974). In cases of layered polymicrogyria, as seen in association with pallial clefts, very few axons or dendrites traverse the astroglial scar seen in the deeper layers of the neocortex (Williams et al.,1976). Extracortical projection from neurons pial to the scar and projections from lost neurons that would have been in the position of the scar are reduced leading to reduced subcortical white matter volume and callosal area, as reported by Levine et al. (1974). Histological (Richman et al.,1974), including Golgi (Williams et al.,1976), analysis has shown, however, that the number of neurons in remaining layers and the amount of neuropil need not be attenuated. In patients with full thickness clefts revealed by MRI in this study, similar structural and histological abnormalities might be predicted.

In two patients with full thickness clefts, there is indeed reduction of SM volume (patients 9 and 21), with a reduction in CCA in one (patient 21). Additional abnormalities of connections are revealed by the surface area derivatives. One might predict that in these patients interhemispheric connections would be fewer than expected for a given brain size, and that extracortical projection would be reduced, as axons and dendrites would not cross the astroglial layer in the polymicrogyric cortex. However, the remaining neuropil is normal (see above), so that this contribution to E_A may be normal. As a result of these changes, from the interpretation of surface area derivatives given above, both ECC and ESM should be abnormally high. In 4/6 patients with cleft(s), there are precisely such abnormalities of the surface area derivatives. ESM is increased bilaterally in a patient with bilateral full thickness clefts (patient 9), and also

bilaterally in patients 12, 20 and 21, who have only unilateral clefts on routine inspection of the MRI. ECC is also abnormally high in 3 of these cases. Therefore the measured surface area changes, interpreted as revealing some combination of (i) increased mean neuropil/neuron and (ii) reduced extracortical projection (specifically including reduced interhemispheric projection), correlate with the presumed histopathology. Patients 9, 12 and 20 also have abnormal GM/SM ratios, in support of the suggestion that interneuronal connectivity may be altered in favour of increased local (nonextracortical) connectivity (see above).

It should be noted that in these cases perilesional polymicrogyria was not obvious or definite on routine inspection, but is presumed to be present. Quantitation shows that structural disproportion compatible with polymicrogyria is present in 66% of such cases and may be found in hemispheres that are completely normal on routine inspection. This lends further support to the hypothesis that structural abnormalities in CD may extend beyond visualised boundaries, and be associated with abnormalities of connections (eg interhemispheric axons).

Two patients with clefts, patient 16 with bilateral full thickness clefts and patient 4 with unilateral partial thickness clefts, do not have any abnormalities of the surface area derivatives. This is possibly because the extent of presumed structural abnormality (polymicrogyria) around a cleft is variable (Dekaban, 1965; Levine et al.,1974), such that quantitative normality of the rest of the hemisphere swamps localised quantitative abnormality. This may also be the case for patient 1 who is known to have polymicrogyria. These patients highlight a limitation of the method and suggest that regionalisation of surface area derivatives is required.

Agenesis of the corpus callosum is associated with

hemispheric dysgeneses other than merely the radial rearrangement of gyri on the mesial surfaces (Friede, 1975; Barkovich and Norman, 1988), such as polymicrogyria (Billette de Villemeur et al.,1992) and pyramidal tract hypoplasia (Parrish et al.,1979). The ratio ECC should be and is abnormal bilaterally in these cases, as interhemispheric projection is obviously reduced. In both cases, additional abnormalities of ESM are found, bilaterally in patient 12 and on the left only in patient 17. As interpreted above on the basis of analysis of brains with clefts, this implies some combination of increased mean neuropil/neuron and reduced mean extracortical projection (supported in both patients by the finding of 9 elevated GM/SM ratios), associated with the presence, though not necessarily exclusively, of polymicrogyria. It is therefore possible that the gyral abnormality (see Figure 5.2) seen in patient 12, who has a cleft, callosal agenesis and specific surface area derivative abnormalities, is polymicrogyria, though this is not the only MRI diagnosis. Patient 17 has the expected abnormalities of gyral disposition on the mesial surfaces of the hemispheres; the quantitative results suggest that there may also be extensive polymicrogyria in the left hemisphere, though this was not seen on routine inspection. Polymicrogyria may be occult on macroscopic inspection or imaging and revealed only on histology (Galaburda and Kemper, 1979; Kuzniecky et al.,1994).

Therefore in some cases, quantitative changes in postprocessed MRI data and expected histology can be directly correlated, raising the possibility of predicting histopathology when this is not directly apparent from routine inspection alone of the MRI. The nature of the dysgenesis in the right hemisphere of patient 2 is unclear, though polymicrogyria is a possible diagnosis (see Figure 5.3). Analysis of the surface area derivatives shows a pattern similar to that in patients with known or probable polymicrogyria, with elevation of ECC and ESM in the dysgenetic hemisphere, suggesting that the underlying

Figure 5.2. Right anterior oblique view of surface rendering for patient 12. Note the broad abnormal gyrus in the superolateral aspect of the temporal lobe. Macrogyria may be due to many different histopathologies (see text for discussion)

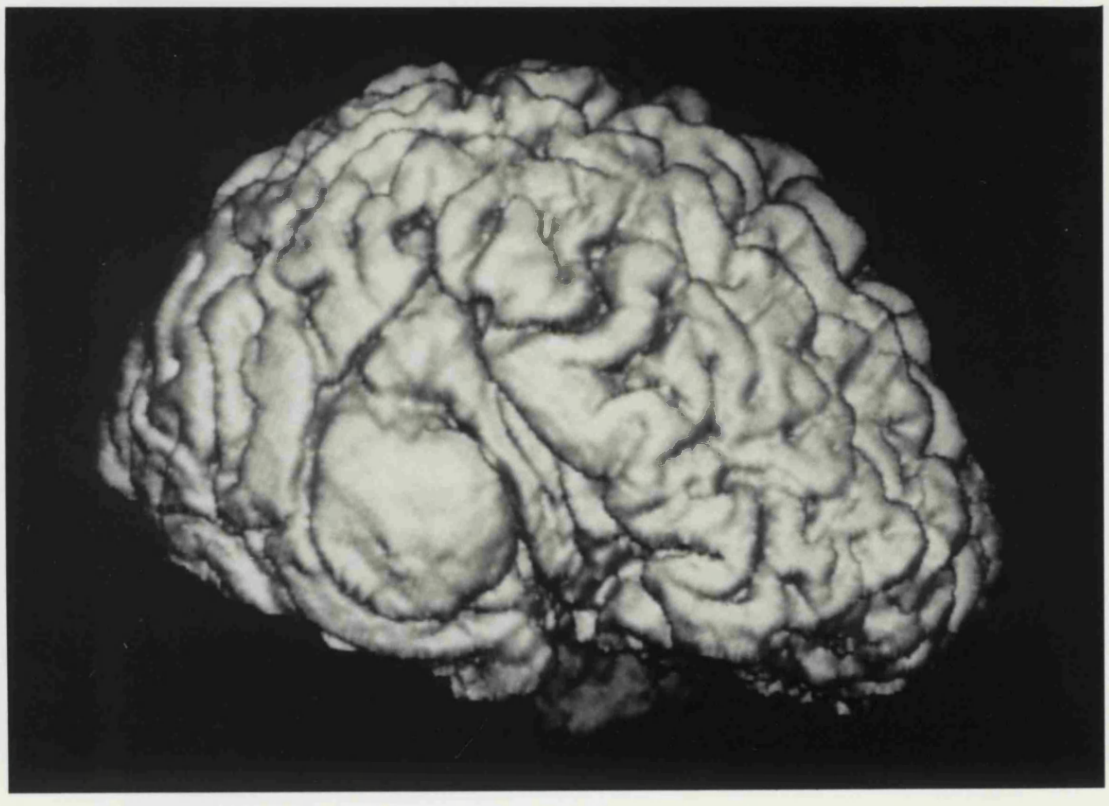

Figure 5.3. Coronal SPGR image from patient 2. The presence of dysgenesis in the right hemisphere is obvious, but its nature is unclear.

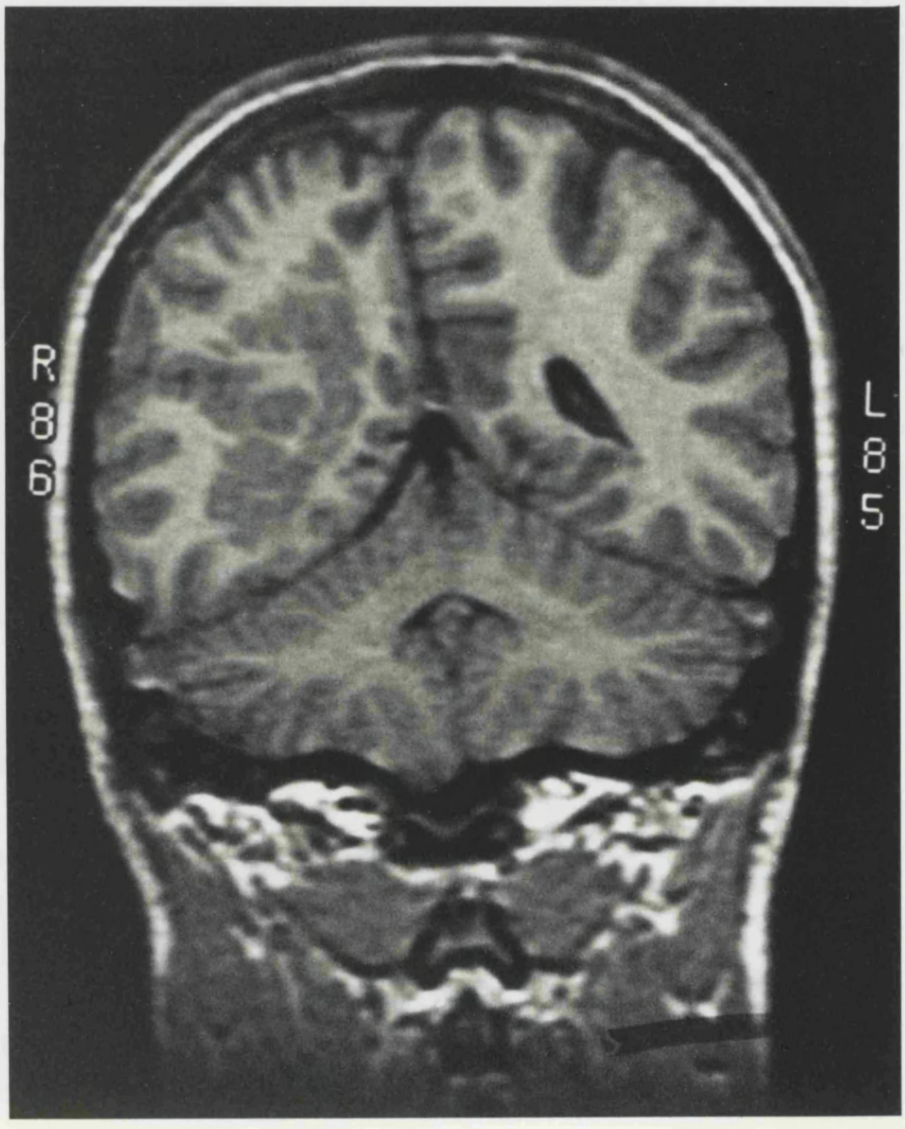

pathology in this case may well be polymicrogyria. Again, abnormality is found on quantitation in the visually normal left hemisphere, in further support of the extensive nature of dysgenesis.

Bilateral posterior macrogyria is seen in patient 7, with apparent cortical thickening in the affected area seen on routine inspection in multiple planes. Cortical thickening may be due to several different histopathologies (Friede, 1975; Raymond et al.,1995). A priori, truly thickened cortex implies either reduced projection to and from the cortex (if the surface density of neurons increases), supported by the low E_A bilaterally in this case, or increased mean neuronal neuropil (if the surface density of neurons does not increase). Increased neuropil/neuron and reduced projection are associated with increased ESM in 4/6 cases of probable polymicrogyria; the normality of ESM despite the extent of gyral abnormality in this case (see Figure 5.4), and the bilaterally low E_A and EGM argue against an increase in neuropil/neuron, instead suggesting that projection is reduced with either no change or a reduction in the amount of neuropil/neuron. A reduction in projection is supported by the abnormally low volume of SM in the left hemisphere. The bilaterally reduced ECC, with a normal absolute CCA, suggests that although total extracortical projection is reduced, interhemispheric projection seems to be maintained. This suggests lamina 3 neurons have maintained their projectional integrity (Jones, 1984), whether or not they are correctly positioned in the thickened cortex, and necessitates a reduction in intrahemispheric extracortical projection. This combination is therefore unlike polymicrogyria, but compatible with pachygyria, in which reduction in neuropil locally has been reported (Takada et al.,1994). Other histopathologies are possible; confirmation of the interpretation of the changes in surface area derivatives must await analysis of cases of known agyria (eg with familial lissencephaly). Possibly, however, ESM abnormality is seen only in polymicrogyria.

Figure 5.4. Vertex view of surface rendering of patient 7. Note that macrogyria occupies a large proportion of the posterior aspect of the hemispheres.

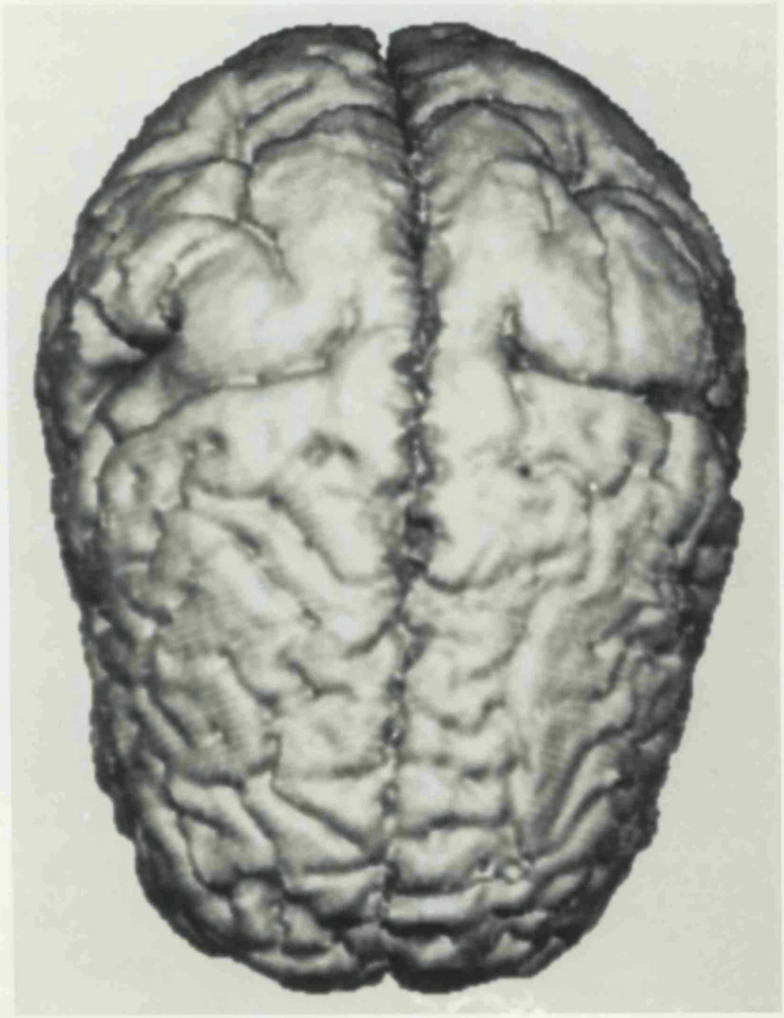

Alteration in the total number of neurons may complicate these analyses; the effect of changes in cell density has been discussed for patient 7 above. In all the other cases of dysgenesis, the effect of altered neuronal numbers can be similarly addressed; neurons must be connected to survive in the adult brain (Cowan et al.,1984), so that any change in neuron number must be accompanied by appropriate changes in neuropil and therefore in connections.

There remain patients with abnormal surface area derivatives in whom analysis is limited. Patient 3, for example, has a visually abnormal right hemisphere, with reduced distant connectivity suggested by the low SM volume, and reduced interhemispheric connectivity suggested by the low CCA. ECC is elevated in the contralateral hemisphere, detecting the extensive connectional disturbance that must affect the apparently normal hemisphere if interhemispheric connectivity is reduced. Patients 5, 10, and 75 all have subependymal heterotopia, with additional dysgenesis in patients 5 (subcortical heterotopia) and 10 (unilateral limited posterior macrogyria). All three of these patients appear to have connectional abnormalities as they all have abnormal ECC, two in visually normal hemispheres, including one patient who does not have any block abnormalities. Patient 14 also has bilaterally abnormal ECC, although the dysgenesis is limited, on inspection, to the right parietal region. However, further interpretation is not possible from the available results.

Amongst the patients with definite dysgenesis, there is no difference, in terms of age, duration of epilepsy or occurrence of secondary generalised seizures, between those who do and those who do not have abnormalities of the surface area derivatives. This finding, and the block volume and ratio findings in the patients with hippocampal sclerosis, argue against the surface area derivative findings being due to epilepsy, and for their association with its cause. That there

are surface area derivative abnormalities in two patients with proven hippocampal sclerosis who are seizure-free postoperatively means that such changes by themselves may not always be sufficient to cause epilepsy, even though they are likely to be related to the cause of the epilepsy.

Thus examination of the surface derivative variables allows a more detailed and quantitative description of the structural changes present in a given MRI study. The variables quantify changes in connectivity that may be associated with gross changes in gyral pattern, but that ECC and ESM may be abnormal without such changes argues that gross neuronal malpositioning and gyral abnormalities are not necessary for, whilst neuronal misconnection at least in some cases is associated with, epileptogenesis. The integration of block analysis may allow further exploration of connectional abnormalities revealed by surface area measures. Prediction and dissection of gross laminar pathology in vivo might become conceivable, as in patient 7, allowing also classification *in vivo* to be more precise.

5.4. Subependymal heterotopia: a special case

The block technique can provide information on more than just cerebral shape. It has been shown that male and female patients with SEH are different with respect to block analysis (see 4.4.2 and 4.7). Female patients with SEH in fact do not have block abnormalities of the cerebral hemispheres as seen in patients with other forms of CD, such as gyral abnormalities and subcortical heterotopia with or without associated SEH. Thus there is structural evidence in support of the hypothesis that SEH, in females at least, is a distinct dysgenesis (Raymond et al.,1994a), and quite different, for example, from subcortical heterotopia.

On the other hand, male patients with SEH do have more

extensive, quantitative abnormalities of cerebral structure. All four male patients have structurally abnormal brains in terms of the distribution of grey and subcortical matter. The male patients would therefore appear to be more like patients with other forms of CD. The hypothesis as initially postulated in the aims (see 1.7) that *all* patients with SEH differ from patients with other types of CD must therefore be modified. Male and female patients with symptomatic SEH seem to be structurally distinct, in support of the suggestion that there may be a different basis for the condition in the sexes (Huttenlocher et al.,1994). The possible mechanisms for the difference cannot be elucidated on the basis of the data. Sex differences in cortical development and dysgenesis have been documented in other conditions (Chevrie and Aicardi, 1986) and sex hormone influences on neurogenesis have been suggested (Murphy et al.,1993).

These findings illustrate the complexity of the relationship between structural abnormalities and malfunction in epilepsy. Female patients with SEH have epilepsy but do not appear to have structurally abnormal brains in terms of blocks. In fact, two patients with non-SEH CD also have no block abnormalities, the presence of which is therefore not necessary for epileptogenesis in all cases of CD.

5.5. The functional significance of extralesional structural changes in patients with dysgenesis

The postprocessing methods have demonstrated various changes in cerebral structural constitution. Such changes are present in some patients with apparently cryptogenic epilepsy. However, the functional significance of these changes has not been proven in this study, though their frequent association with epilepsy suggests that they are relevant in some way.

Gyral abnormalities were revealed only on reconstruction

in 17 patients with apparently normal scans. Whilst the location of gyral changes in 10/17 patients is compatible with the electroclinical seizure pattern (see 4.3.1), that the changes probably represent underlying dysgenesis (see 5.1.) means that still more extensive structural abnormality is likely to be present. Thus that electroclinical concordance is not present in the other 7 does not mean that the reconstruction findings are functionally unimportant. On the contrary, the implication is that these gyral changes are likely to be the tip of the iceberg of disordered cerebral structure, probably arising during development: extensive additional gyral abnormalities are also revealed in 27% of patients with definite dysgenesis. Such extensive structural disorder may be associated with extensive functional disorder.

Evidence for extensive functional changes in the brain in various forms of partial epilepsy does exist. Two lines of evidence will be discussed: the clinical study of patients with hypothalamic hamartomata and evidence from electrophysiological studies.

5.5.1. Hypothalalamic hamartoma

Epilepsy associated with hypothalamic hamartomata is characterised by the occurrence of gelastic seizures and is usually refractory to medical treatment (Cascino et al.,1993); its pathogenesis is unclear. Surgical removal of the abnormal area of the hypothalamus has been attempted for some of the manifestations of the abnormality. Precocious puberty may be successfully treated thus, but there are few reports of cessation of seizure activity (Nishio et al.,1994; Machado et al.,1991; Valdueza et al.,1994). Larger reviews (Breningstall, 1985; Cascino et al.,1993) suggest patients are unlikely to be rendered seizure-free (and that mortality and morbidity may be high). Intracranial electrographic recordings and stimulation (Arroyo et al.,1993) suggest that the pathways subserving gelastic seizures in general might be complex and involve the

anterior cingulate gyrus, the mesial frontal cortex and the basal temporal cortex. Cascino et al. (1993) also report results of intracranial electroencephalography in patients with hypothalamic hamartoma and gelastic seizures; seizure onset was felt to be anterior mesial temporal in 7 patients and inferior frontal in one. However, none of the electrographically-guided focal cortical resections performed for seizure relief was successful. These findings together indicate that whilst gelastic seizures are strongly associated with the presence of a hypothalamic hamartoma, the cortical mechanism of laughter and epileptogenesis in these cases may involve other regions of the brain, possibly wider areas of the neocortex. Prefrontal cortical input to the hypothalamus and reciprocal connections with the limbic system provide a possible anatomical substrate for this. In one case PET studies support the possibility of functional abnormality beyond the hypothalamic hamartoma itself (Cascino et al.,1993).

The association of cognitive impairment and decline with the presence of a hypothalamic hamartoma and epilepsy raises the possibility of extensive cortical dysfunction. The hypothesis that this is due to the presence of widespread associated dysgenetic abnormalities (Breningstall, 1985; Berkovic et al.,1988), is supported by the results presented: two patients with typical hypothalamic hamartomata have associated neocortical abnormalities demonstrated by the block technique. The block technique may prove useful in assessment of other patients with apparently potentially resectable lesions.

5.5.2. Electrophysiology

Functional abnormalities extending beyond the visualised lesion have also been demonstrated using electrophysiological techniques. In a recent report, Palmini et al. (1995) investigated electrical discharge patterns recorded

peroperatively on patients subsequently shown to have cerebral dysgenesis. They showed that discharge patterns they hold to be specific for dysgenetic lesions extended contiguously beyond the lesional margins as visualised at operation or on MRI in at least 5 of their patients, and that subsequent histological analysis of these areas showed them to be dysgenetic. When the area from which the specific electrical abnormalities were recorded could be completely resected, the outcome was better than when such areas could not be completely resected. Indeed, they suggest that incomplete excision of all dysgenetic tissue may have been responsible for the poor outcome of patients they had previously reported (Palmini et al.,1991). Curiously, complete removal of the area producing the specific electrical abnormalities did not lead to seizure freedom in 25% of cases (Palmini et al.,1995). It is not clear from their report why this should be, but even more extensive, noncontiguous, areas of functional abnormality might have been present beyond the field exposed at surgery and these areas may have been capable of supporting epileptogenesis. More complete structural study preoperatively of patients with suspected dysgenesis might identify remote areas of structural abnormality associated with the functional abnormalities, modifying therapeutic decisions.

That extensive areas of cortex, even that which looks normal and is noncontiguous with the area presumed responsible for the epilepsy, may support epileptogenesis is also compatible with the findings and ideas of Gloor (1990) and Fish et al. (1993). In the latter study, similar clinical responses - including epileptic auras - could be elicited in some patients undergoing depth electrode studies by stimulation of more than one noncontiguous anatomical site; this supported the hypothesis that at least some features of seizures, including the persistence of auras in patients rendered otherwise seizure-free by resective surgery, could be explained by "the activation of a widespread matrix of excitation in a widely distributed population of neurons not

necessarily located in contiguous areas..". Whether similar phenomena might operate in patients with epilepsy due to cerebral dysgenesis is not clear, but in some such patients, the findings presented here show that there are certainly anatomical abnormalities beyond the lesion: these may maintain unchanged seizure semiology by Gloor's hypothesis. However, the complexity of changes in functional circuitry associated with CD cannot be underestimated (Calabrese et al.,1994), and it would be simplistic to suggest that "distributed matrices" were the *direct* functional correlate of the extralesional abnormalities shown here.

Nevertheless, it is important to realise that the existence of abnormalities of connectivity have been shown in this thesis, albeit by surrogate measures (the use of histological methods over similar cerebral extents would be prohibitively tedious; Huttenlocher, 1974). The "distributed matrices" discussed above need not in themselves be qualitatively abnormal (eg polymicrogyria etc), but are connected, however obscurely, to pathogenic areas. Abnormalities of neuronal connections may be more important for abnormal function than are abnormalities of neuronal position (as seen in conditions generally accepted to be 'dysgenetic', eg pachygyria etc). Abnormalities of neuronal position are not necessarily associated with epilepsy, either in humans (eg Kuzniecky et al.,1994; Huttenlocher et al.,1994) or in animals, such as the mutant 'reeler' mouse, in which there is complete laminar inversion in the neocortex but normal connectivity as far as has been examined (Simmons et al.,1982; Caviness et al.,1984) and no epilepsy. The importance of neuronal connectivity, rather than neuronal positioning, for human epileptogenesis has been examined (Sisodiya, 1995) and is supported by the findings in this thesis that there may be extensive connectional abnormalities in visually apparently normal hemispheres.

5.6. Information extraction

There is a large amount of information in a high-resolution MRI. In a given study, there may be of the order of 1,000,000 separate voxels, each containing intensity information and each with spatial coordinates. Ignoring intensity information, the possible number of unique combinations of any number of voxels (up to 1,000,000) alone, irrespective of any patterns that they might form, is over 10^6 factorial - a huge number. Obviously, most of these would not form any recognisable pattern, and would not be of value in increasing our understanding of the brain. But in some cases, unique information would be made available by a combination of data not currently considered. Thus at the moment, typically 124 patterns (slices) are routinely examined. The pattern of spatial distribution of signal intensities is examined to detect the presence of abnormalities. Reformatting of the data increases the yield of abnormalities by increasing information extraction through the altered combination of voxels that are examined, but leaves much information still untapped.

In this study, reconstruction of the data into three-dimensional representations has increased the yield from the data. The grey-white interface has been extracted: this contour itself contains information and attempts have been made to extract some of the data present in this one combination of voxels. The amount of information that can be obtained from this interface is greater still - and depends on the tools used to extract information. Only its areal extent and fractal dimension have been measured; its texture and detailed intensity characteristics have, for example, not been considered. The total amount of information present is itself an area of much research interest: how much of this is useful to the biologist and doctor remains to be established.

It is important to emphasise that abnormalities have been

revealed by analysis where none were seen on inspection alone. In 58% of patients with apparently completely normal scans, new information was produced. The direct clinical utility of the information is as yet unclear, but the principle that analysis can reveal additional (or new) abnormalities is apparent.

5.7. Future directions

1. Automation of segmentation

For each case analysed using all the methods available in this study, approximately six hours of operator interaction was required. Of this time, the majority was spent in segmentation, and this is the most difficult part. If larger studies were to be performed, automation of the segmentation process would be important to speed the entire process. Methods of automated segmentation have been discussed (see methods section). In order to use cluster analysis, for example, on high-resolution volumetric data, new sequences would need to be devised allowing the collection of the required data in a reasonable time-frame, minimising costs and patient movement artefact. If non-biological ROI boundaries are used, however, some manual interaction will remain necessary.

2. Regionalisation of surface area derivatives

The surface area measures as currently derived are mean measures across the entire cerebral hemisphere. Regionalisation is likely to increase the utility of the data, as local areas of abnormality will not be averaged out by larger areas of normally-structured brain. This could be performed on the data already available by counting the number of voxels in the surface of each block, the volume of which is already known. The task would be intensive in terms of

operator time because of the way in which the data is acquired currently. There was insufficient time to perform these measurements in the course of this thesis.

The data as currently available are limited to regionalisation in the plane of the original slice data. If the data were available in other planes for similar analysis and regionalisation, its utility might again be increased. Thus, for example, if regionalisation were still performed in blocks, but three mutually-perpendicularly orientated block sets were available, then focal areas of abnormality might be established in the area of the intersection of abnormal blocks.

Perhaps the best regionalisation, however, would be operator-driven and selectable in each case, so that proportionalities in specific areas of interest could be studied. The major problem with this approach would be the determination of comparable areas in control subjects, given that regional cytoarchitectonic variations exist and may be related to cortical anatomy. If in fact general principles are applicable such that a given amount of surface area even when localised is related to a given volume of overlying grey matter (perhaps bearing in mind only whether the region is fundal, crown or wall), then comparison between regions within the same and different subjects may be simply achieved. On the other hand if such principles are not found, then the problem of intersubject comparability again raises its head. Novel methods of shape and gyral analysis would then be required.

3. Grey matter surface area

Currently, definition of the surface area of the grey matter is not possible on the T_1-weighted volume acquistion. On T_2-weighted images, however, sulcal depths can more easily be determined. If a rapid sequence with volumetric resolution and T_2-weighting could be devised (and acquired perhaps with

a proton-density or T_1-weighted data set, for automated segmentation), then the surface area of the grey matter could be more accurately determined. This would be of value for all the methods described in this thesis. In particular, it would allow better definition regionally of cortical thickness, and examination of cortical surfaces other than the dorsolateral fronto-parieto-temporal cortex, where gyral separation is enough to allow clear distinction of the pattern of gyration.

4. Corroborative studies

The direct study of connections in brains affected by dysgenesis would support the postulated hypotheses. This would be a mammoth task, the technology for which is now available. Injection of certain dyes (eg DiI) allows the tracing of axonal connections in the human cortex postmortem. To the author's knowledge, no such study has yet been performed on a brain with dysgenesis. Equally, detailed histological study of an entire brain affected apparently focally by dysgenesis has also not been performed using the Golgi stain that might demonstrate extensive and distributed alterations in neuronal morphology, in support of the suggestion that connectional abnormalities exist in distant parts of the brain.

5. Other cerebral conditions

Extensive connectional and dendritic abnormalities have also been shown and postulated in other diseases: this raises the possibility of using the methods developed in this thesis in other conditions associated with dysgenesis or misconnection from some other cause. Amongst these are dyslexia, mental retardation and schizophrenia.

Dyslexia has been associated with cortical dysgenesis. Galaburda and Kemper (1979) reported a case of a man with developmental dyslexia and easily controlled seizures who had focal polymicrogyria and several areas of focal cortical

dysplasia in the left hemisphere. It is of interest, in the context of the rest of the thesis, that the polymicrogyria was not apparent on macroscopic inspection and that the areas of cortical dysplasia were widespread and noncontiguous. Subtle callosal abnormalities have also been reported in patients with developmental dyslexia (Hynd et al.,1995). The use of the quantitative methods proposed here may help identify areas of neocortical abnormality in the brain in vivo in such patients.

Schizophrenia is one of a few psychiatric entities that is being increasingly studied using high-resolution MRI in an attempt to find underlying structural abnormalities. The hypothesis tested is often that prefrontal-basal ganglia connections are in some way altered, with changes in volume measures or relationships. On the whole these studies are inadequately performed (see Chapter 2). Using the techniques presented here, changes in brain shape, complexity and regional connectivity might be more rigorously examined.

6. Genes and development

Very little is known about the influence of genetic factors on cerebral development in humans. Most information has been derived from the study of the genetic constitution of patients with abnormal cerebral structure. The Miller-Dieker syndrome consists of microcephaly with peculiar facies, severe developmental delay and intractable seizures, amongst other features. The brain is agyric or pachygyric. A gene deletion associated with this familial lissencephaly syndrome has been identified (*LIS*-1; Reiner et al.,1993). An important feature is that a marked abnormality of cortical structure is produced by a single genetic defect. Identification of the structural defect by MRI has allowed cases to be identified and families to be studied. Similarly, an X chromosome locus has been suggested for a familial pachygyria and callosal agenesis syndrome (Berry-Kravis and Israel, 1994). In both cases, the identification of cases by MRI facilitated genetic study.

However, such gross cases are relatively rare. In addition, when MRI abnormalities are marked but there are no other features to suggest a syndromic diagnosis, identification of homologous cases may be difficult. It is possible that some of the methods described here may be of value in this regard.

Firstly, cerebral structural abnormalities may be detected where none are otherwise apparent: thus two patients with abnormalities shown only on three-dimensional reconstruction have a clinical diagnosis of familial frontal lobe epilepsy. Previously, no structural abnormalities were noted on neuroimaging of such patients (Scheffer et al.,1994). Unfortunately, no other members of the families of these patients have been scanned. If, however, it could be shown that the demonstrated gyral abnormalities segregated with the epilepsy, then the identification of genetic defects could be linked more directly to structural changes in the brains of the patients.

Secondly, the surface area derivatives might also be informative in this regard. Disorders of proportion can in some cases be related to laminar histopathology (see above). If either localised or generalised disorders of proportion of cerebral structures could be shown - perhaps even in patients with no apparent structural abnormalities on routine inspection - then genetic study of a larger number of patients might be possible, based on MRI-derived information rather than solely on clinical syndromic diagnosis. Regionalisation of the surface area derivative measures would be most useful for this. In this way, study of the genetic abnormalities associated with specific structural abnormalities might shed further light on normal developmental principles and processes. The importance of MRI - and postprocessing - as a screening tool in this context should not be overlooked.

Lastly, block analysis suggests that there may be a fundamental structural difference between males and females

with subependymal heterotopia (see Section 5.4). This suggests that genetic analysis of this condition should be separated for sex and shows how the techniques developed here may allow a purer culture for analysis using other methods.

7. Epileptogenesis in cerebral dysgenesis

The mechanism of epileptogenesis in cerebral dysgenesis is poorly understood. The concurrence of dysgenesis and epilepsy is too frequent to suppose that the two are unconnected. Palmini et al. (1995) suggest that dysgenetic lesions are intrinsically epileptogenic rather than merely irritative to the surrounding cortex, in the way that gliotic scars, for example, might be considered to be. They base this on peculiar electrical activity detected from dysgenetic lesions perioperatively, and from the finding that loss of this activity postexcision is associated with an increased chance of becoming seizure-free. They suggest that dysgenetic lesions may act as seizure pacemakers, entraining other normal cortex in seizure activity. The findings reported here may support this view. If there are other abnormalities of cortical structure, these may also be capable of supporting epileptogenesis and normally be entrained by the clearly abnormal area, but then released to act as pacemaker if the visible lesion is removed, so that seizures may continue with unchanged semiology, perhaps by the mechanism suggested by Gloor (1990). Abnormal connectivity within the cortex may support this pathological activity.

8. The still normal study

There are patients in this report who have focal epilepsy comparable to those in whom structural abnormalities have been demonstrated, yet who are normal on all measures. Equally, there are patients with dysgenesis (eg female patients with SEH) who have refractory epilepsy without extensive structural abnormalities as revealed by the techniques used here. This

may be because any such changes are swamped by an overwhelming majority of normal structure.

Further study is required to define dysgenesis yet more precisely. The use of postprocessing may help in the categorisation of cases more clearly, in the way that patient 2, with an undefined dysgenesis on inspection alone, is likely to have a polymicrogyric pathology on the basis of the surface area derivative findings. Classification including such findings may create a more pure culture for further analyses, whether these be structural, functional or genetic.

REFERENCES

Aboitiz F, Scheibel AB, Fisher RS, Zaidel E. Fiber composition of the human corpus callosum. Brain Research 1992;598:143-153.

Andermann F. Brain structure in epilepsy. In: Shorvon SD, Fish DR, Andermann F, Bydder GM, Stefan H, eds. Magnetic resonance Scanning and Epilepsy. New York: Plenum Press, 1994:21-27.

Andreasen NC, Flaum M, Swayze V, et al. Intelligence and brain structure in normal individuals. Am J Psychiatry 1993;150:130-134.

Andreasen NC, Harris G, Cizadlo T, et al. Techniques for measuring sulcal/gyral patterns in the brain as visualised through magnetic resonance scanning: BRAINPLOT and BRAINMAP. Proc Natl Acad Sci 1994;90:93-97.

Angevine JB, Sidman RL. Autoradiographic study of cell migration during histogenesis of cerebral cortex in the mouse. Nature 1961;192:766-768.

Armstrong E, Curtis M, Buxhoeveden DP, et al. Cortical gyrification in the rhesus monkey: a test of the mechanical folding hypothesis. Cereb Cortex 1991;1:426-432.

Armstrong E, Schleicher A, Omran H, Curtis M, Zilles K. The ontogeny of human gyrification. Cereb Cortex 1995;5:56-63.

Arroyo S, Lesser RP, Gordon B, et al. Mirth, laughter and gelastic seizures. Brain 1993;116:757-780.

Awad I, Rosenfeld J, Ahl J, Hahn J, Luders H. Intractable epilepsy and structural lesions of the brain: mapping, resection strategies, and seizure outcome. Epilepsia 1991;32:179-186.

Baddeley AJ, Gundersen HJG, Cruz-Orive LM. Estimation of surface area from vertical sections. J Microsc 1986;142:259-276.

Barkovich AJ, Chuang SH, Norman D. MR of neuronal migration anomalies. AJNR Am J Neuroradiol 1987;8:1009-1017.

Barkovich AJ, Norman D. Anomalies of the corpus callosum: correlation with further anomalies of the brain. AJNR Am J Neuroradiol 1988;9:493-501.

Barkovich AJ, Kjos BO. Nonlissencephalic cortical dysplasias: correlation of imaging findings with clinical deficits. AJNR Am J Neuroradiol 1992a;13:95-103.

Barkovich AJ, Kjos BO. Gray matter heterotopias: MR characteristics and correlation with developmental and neurologic manifestations. Radiology 1992b;1182:493-499.

Barkovich AJ, Rowley HA, Andermann F. MR in Epilepsy: value of high-resolution volumetric techniques. AJNR Am J Neuroradiol 1995;16:339-343.

Barron DH. An experimental analysis of some factors involved in the development of the fissure pattern of the cerebral cortex. J Exp Zool 1950;113:553-73.

Barth PG. Disorders of neuronal migration. Can J Neurol Sci 1987;14:1-16.

Becker LE. Synaptic dysgenesis. Can J Neurol Sci 1991;18:170-180.

Bergin PS, Raymond AA, Free SL, Sisodiya SM, Stevens JM. Magnetic resonance volumetry. Neurology 1994;44:1770-1771.

Berkovic SF, Andermann F, Melanson D, Ethier RE, Feindel W,

Gloor P. Hypothalamic hamartomas and ictal laughter: evolution of a characteristic epileptic syndrome and diagnostic value of magnetic resonance imaging. Ann Neurol 1988;23:429-439.

Berkovic SF, McIntosh AM, Kalnins RM, et al. Preoperative MRI predicts outcome of temporal lobectomy: an actuarial analysis. Neurology 1995;45:1358-1363.

Berry-Kravis E, Israel J. X-linked pachygyria and agenesis of the corpus callosum: evidence for an X chromosome lissencephaly locus. Ann Neurol 1994;36:229-233.

Billette de Villemeur T, Chiron C, Robain O. Unlayered polymicrogyria and agenesis of the corpus callosum: a relevant association?. Acta Neuropathol 1992;83:265-70.

Binnie CD, Chadwick D, Shorvon SD. Surgical treatment for epilepsy. ILAE Report. British Branch of the International League against Epilepsy. 1991.

Blatter DD, Bigler ED, Gale SD, et al. Quantitative volumetric analysis of brain MR: normative database spanning 5 decades of life. AJNR AM J Neuroradiol 1995;16:241-251.

Blinkov SM, Glezer II. The human brain in figures and tables. A quantitative handbook. New York: Plenum Press, 1968.

Bok ST. Histonomy of the Cerebral Cortex. Amsterdam: Elsevier Publishing Company, 1959.

Bookstein FL. Thin-plate splines and the atlas problem for biomedical images. In: Colchester A, Hawkes DJ eds. Information Processing in Medical Imaging, Proc IPMI 1991;326-342.

Bordarier C, Robain O, Rethore M, Dulac O, Dhellemes C. Inverted neurons in agyria. Hum Genet 1986;73:374-8.

Braendgaard H, Evans SM, Howard CV, Gundersen HJG. The total number of neurons in the human neocortex unbiasedly estimated using optical disectors. J Microsc 1990;157: 285-304.

Breier A, Buchanan RW, Elkashef A, Munson RC, Kirkpatrick B, Gellad F. Brain morphology and schizophrenia. Arch Gen Psychiatry 1992;49:921-926.

Breningstall GN. Gelastic seizures, precocious puberty and hypothalamic hamartoma. Neurology 1985;35:1180-1183.

Bruton CJ. Neuropathology of temporal lobe epilepsy. Oxford: Oxford University Press, 1988.

Calabrese P, Fink GR, Markowitsch HJ, et al. Left hemispheric neuronal heterotopia: a PET, MRI, EEG, and neuropsychological investigation of a university student. Neurology 1994;44:302-305.

Cascino GD, Andermann F, Berkovic SF, et al. Gelastic seizures and hypothalmic hamartomas: evaluation of patients undergoing chronic intracranial EEG monitoring and outcome of surgical treatment. Neurology 1993;43:747-750.

Caviness VS, Crandall JE, Edwards MA. The reeler malformation. In: Jones EG, Peters A, eds. Cerebral Cortex, Vol 7. New York: Plenum Press, 1984:59-89.

Cendes F, Andermann F, Gloor P, Lopes-Cendes I, Andermann E, Melanson D. Atrophy of mesial temporal structures in patients with temporal lobe seizures: cause or consequence of repeated seizures? Ann Neurol 1993:34:795-801.

Chevrie JJ, Aicardi J. The Aicardi syndrome. In: Pedley TM Meldrum B, eds. Recent Advances in Epilepsy. Edinburgh: Churchill Livingstone, 1986;3:189-210.

Cockerell OC, Johnson AL, Sander JWAS, Hart YM, Shorvon SD. The mortality of epilepsy: results from the National General Practice Survey of Epilepsy. Lancet 1994;344:918-921.

Cockerell OC, Eckle I, Goodridge DMG, Sander JWAS, Shorvon SD. Epilepsy in a population of 6000 reexamined: secular trends in first attendance rates, prevalence and prognosis. J Neurol Neurosurg Psychiatry 1995;58:570-576.

Collins DL, Neelin P, Peters TM, Evans AC. Automatic 3D intersubject registration of MR volumetric data in standardized Talairach space. J Comp Assis Tomog 1994;18:192-205.

Cook MJ, Fish DR, Shorvon SD, Straughan K, Stevens JM. Hippocampal volumetric and morphometric studies in frontal and temporal lobe epilepsy. Brain 1992;115:1001-1015.

Cook MJ, Free SL, Manford MRA, Fish DR, Shorvon SD, Stevens JM. Fractal description of cerebral cortical pattern in frontal lobe epilepsy. Eur Neurol 1995;35:327-335.

Cowan WM, Fawcett JW, O'Leary DDM, Stanfield BB. Regressive events in neurogenesis. Science 1984;225:1258-1265.

Daumas-Duport C, Scheithauer BW, Chodkiewicz JP, Laws ER, Vedrenne C. Dysembryoplastic neuroepithelial tumour. A surgically curable tumour of young patients with intractable partial seizures: a report of thirty-nine cases. Neurosurg 1988;23:545-556.

DeCarli C, Maisog J, Murphy DGM, Teichberg D, Rapoport SI, Horwitz B. Method for quantification of brain, ventricular and subarachnoid CSF volumes from MR images. J Comput Assis Tomog 1992;16:274-284.

Dekaban AS. Large defects in the cerebral hemispheres

associated with cortical dysgenesis. J Neuropathol Exp Neurol 1965;24:512-530.

Dekaban AS, Sakarugawa 1977. Megalencephaly. In: Vinken PJ, Bruyn GW, eds. Handbook of clinical neurology, Vol 30. Congenital malformations of the brain and skull, Part 1. Amsterdam: North Holland, 1977:647-660.

Duong T, DeRosa MJ, Poukens V, Vinters HV, Fisher RS. Neuronal cytoskeletal abnormalities in human cerebral cortical dysplasia. Acta Neuropathol 1994;87:493-503.

Duncan JS, Sagar H. Seizure characteristics, pathology, and outcome after temporal lobectomy. Neurology 1987;37:405-409.

Evans AC, Collins DL, Milner B. An MRI-based stereotactic atlas from 250 young normal subjects. Soc Neurosci Abstr 1992;18:408.

Falk D, Hildebolt C, Cheverud J, Kohn LA, Vannier M. Human cortical asymmetries determined with 3D MR technology. J Neuromethods 1991;39:185-191.

Ferrer I. A Golgi analysis of unlayered polymicrogyria. Acta Neuropathol 1984;65:69-76.

Ferrer I, Pineda M, Tallada M, et al. Abnormal local-circuit neurons in epilepsia partialis continua associated with focal cortical dysplasia. Acta Neuropathol 1992;83:647-652.

Filipek PA, Kennedy DN, Caviness VS et al. Magnetic resonance imaging-based brain morphometry: development and application to normal subjects. Ann Neurol 1989;25:61-67.

Filipek PA, Richelme C, Kennedy DN, Caviness VS. The young adult human brain, an MRI-based morphometric analysis. Cereb Cortex 1994;4:344-360.

Fish DR, Andermann F, Olivier A. Complex partial seizures and posterior temporal or extratemporal lesions: surgical strategies. Neurology 1991;41:1781-1784.

Fish DR, Gloor P, Quesney FL, Olivier A. Clinical responses to electrical brain stimulation of the temporal and frontal lobes in patients with epilepsy: pathophysiological implications. Brain 1993;116:397-414.

Fried I, Cascino GD. Lesional Surgery. In: Engel J, ed. Surgical treatment of the epilepsies. New York: Raven Press, 1993:501-509.

Friede R. Developmental neuropathology. New York: Springer-Verlag, 1975.

Galaburda AM, Kemper TL. Cytoarchitectonic abnormalities in developmental dyslexia: a case study. Ann Neurol 1979;6:94-100.

Ghosh A, Antonini A, McConnell SK, Shatz CJ. Requirement for subplate neurons in the formation of thalamocortical connections. Nature 1990;347:179-181.

Gloor P. Experiential phenomena of temporal lobe epilepsy. Facts and hypotheses. Brain 1990;113:1673-1694.

Goldman PS, Galkin TW. Prenatal removal of frontal association cortex in the fetal rhesus monkey: anatomical and functional consequences in postnatal life. Brain Res 1978;152:451-485.

Goldman-Rakic PS. Morphological consequences of prenatal injury to the primate brain. Progr Brain Res 1980;53:3-19.

Gould SJ. The mismeasure of man. New York: Norton, 1989.

Gundersen HJG. Stereology of arbitrary particles. A review of

unbiased number and size estimators and the presentation of some new ones, in memory of William R Thompson. J Microsc 1986;143:3-45.

Gundersen HJG, Jensen EB. The efficiency of systematic sampling in stereology and its prediction. J Microsc 1987;147:229-263.

Gur RC, Packer IK, Hungerbuhler JP, et al. Differences in the distribution of gray and white matter in human cerebral hemispheres. Science 1980;207:1226-1228.

Hajnal JV, Saeed N, Oatridge A, Williams EJ, Young IR, Bydder GM. Detection of subtle brain changes using subvoxel registration and subtraction of serial MR images. J Comput Ass Tomog 1995;19:677-691.

Harris GJ, Barta PE, Peng LW, Lee S, Brettschneider PD, Shah A. MR volume segmentation of gray matter and white matter using manual thresholding: dependence on image brightness. AJNR Am J Neuroradiol 1994;15:225-230.

Haug H. Remarks on the determination and significance of the gray cell coefficient J Comp Neurol 1956;104:473-492.

Haug H. Are neurons of the human cerebral cortex really lost during aging? A morphometric examination. In: Traber J, Gipsen WH, eds. Senile dementia of the Alzheimer type. Berlin: Springer, 1985:150-163.

Haug H. History of neuromorphometry. J Neurosci Methods 1986;18:1-17.

Haug H. Brain sizes, surfaces, and neuronal sizes of the cortex cerebri: a stereological investigation of man and his variability and a comparison with some mammals (Primates, Whales, Marsupials, Insectivores, and one Elephant). Am J Anat

1987;180:126-142.

Harding BN. Malformations of the nervous system. In: Adams JH, Duchen LW, eds. Greenfield's Neuropathology. 5th ed. London: Edward Arnold 1992:521-638.

Harris GJ, Barta PE, Peng LW, et al. MR volume segmentation of gray and white matter using manual thresholding: dependence on image brightness. AJNR Am J Neuroradiol 1994;15:225-230.

Henery CC, Mayhew TM. The cerebrum and cerebellum of the fixed human brain: efficient and unbiased estimates of volumes and cortical surface areas. J Anat 1989;167:167-180.

Hennig A. Fehler der Volumermittlung aus der Flächenrelation in dicken Schnitten (Holmes-Effekt). Mikroskopie 1969;25:154-174.

Huttenlocher PR. Dendritic development in neocortex of children with mental defect and infantile spasms. Neurology 1974;24:203-210.

Huttenlocher PR, Taravath S, Mojtahedi S. Periventricular heterotopia and epilepsy. Neurology 1994;44:51-54.

Hynd GW, Hall J, Novey ES, et al. Dyslexia and corpus callosum morphology. Arch Neurol 1995;52:32-38.

Innocenti GM. General organisation of callosal connections in the cerebral cortex. In: Jones EG, Peters A, eds. Cerebral Cortex, Vol 5. New York: Plenum Press, 1986:291-354.

Jack CR. MRI-based hippocampal volume measurements in epilepsy. Epilepsia 1994;35(suppl 6):S21-S29.

Jackson EF, Narayana PA, Falconer JC. Reproducibility of nonparametric feature map segmentation for determination of

normal human intracranial volumes with MR imaging data. J Mag Res Imaging 1994;4:692-700.

Jones EG. Laminar distribution of cortical efferent cells. In: Jones EG, Peters A, eds. Cerebral Cortex, Vol 1. New York: Plenum Press, 1984:521-554.

Jones EG, Valentino KL, Fleshman JWJ. Adjustment of connectivity in the rat neocortex after prenatal destruction of precursor cells of layers II-IV. Dev Brain Res 1982;2:425-431.

Kennedy DN, Filipek PA, Caviness VS. Anatomic segmentation and volumetric calculations in nuclear magnetic resonance imaging. IEEE Trans Med Imaging 1989;8:1-7.

Kertesz A, Polk M, Black SE, Howell J. Sex, handedness, and the morphometry of cerebral asymmetries on magnetic resonance imaging. Brain Res 1990;530:40-48.

Kikinis R, Shenton ME, Gerig G. Routine quantitative analysis of brain and cerebrospinal fluid spaces with MR imaging. J Mag Res Imaging 1992;2:619-629.

Klekamp J, Reidel A, Harper C, Kretschmann H-J. A quantitative study of Australian aboriginal and Caucasian brains. J Anat 1987;150:191-210.

Kohn MI, Tanna NK, Herman GT, et al. Analysis of brain and cerebrospinal fluid volumes with MR imaging. Radiology 1991;178:115-122.

Kuks JBM, Cook MJ, Fish DR, Stevens JM, Shorvon SD. Hippocampal sclerosis in epilepsy and childhood febrile seizures. Lancet 1993;342:1391-1394.

Kuzniecky R, Andermann F, and the CBPS Study Group. The

congenital bilateral perisylvian syndrome: imaging findings in a multicentre study AJNR 1994;15:139-144.

Levine DN, Fisher MA, Caviness VS. Porencephaly with microgyria: a pathologic study. Acta Neuropathol 1974;29:99-113.

Li LM, Fish DR, Sisodiya SM, Shorvon SD, Alsanjari N, Stevens JM. High resolution magnetic resonance imaging in adults with partial or secondary generalised epilepsy attending a tertiary referral unit. J Neurol Neurosurg Psychiatry 1995;59:384-387.

Loopuijt LD, Villablanca JR, Hovda DA. Morphological changes in the thalamus and neocortex of the cat brain after a restricted unilateral fetal neocortical lesion. Dev Brain Res 1995;85:259-272.

Machado HR, Hoffman HJ, Hwang PA. Gelastic seizures treated by resection of a hypothalamic hamartoma. Childs Nerv Syst 1991;7:462-465.

Mandlebrot BB. The fractal geometry of nature. New York: Freeman, 1982.

Manz HJ, Phillips TM, Rowden G, McCullough DC. Unilateral megalencephaly, cerebral cortical dysplasia, neuronal hypertrophy, and heterotopia: cytomorphometric, fluorometric cytochemical, and biochemical analyses. Acta Neuropathol 1979;45:97-103.

Mayhew TM. A review of recent advances in stereology for quantifying neural structure. J Neurocytol 1992;21:313-328.

Mayhew TM, Olsen DR. Magnetic resonance imaging (MRI) and model-free estimates of brain volume determined using the Cavalieri principle. J Anat 1991;178:133-144.

McKusick VA. Mendelian inheritance in man. Baltimore: Johns Hopkins University Press, 1979.

Meencke H, Veith G. Migration disturbances in epilepsy. In: Engel J. Wasterlain C, Cavalheiro EA, Heinemann U, Avanzini G, eds. Molecular Neurobiology of Epilepsy (Epilepsy Research Supplement 9). Amsterdam: Elsevier, 1992:31-40.

Miller AKH, Alston RL, Corsellis JAN. Variation with age in the volumes of grey and white matter in the cerebral hemispheres of man: measurements with an image analyser. Neuropathol Appl Neurobiol 1980;6:119-132.

Mitchison G. Neuronal branching patterns and the economy of cortical wiring. Proc R Soc Lond Ser B 1991;245:151-158.

Mountcastle VB. An organizing principle for cerebral function: the unit module and the distributed system. In: Edelman GM, Mountcastle VB, eds. The mindful brain: cortical organisation and the group-selective theory of higher brain function. Cambridge, Mass: MIT Press, 1978:7-50.

Murphy DGM, DeCarli C, Daly E, et al. X-chromosome effects on female brain: a magnetic resonance imaging study of Turner's syndrome. Lancet 1993;342:1197-1200.

Nishio S, Morioka T, Fukui M, Goto Y. Surgical treatment of intractable seizures due to hypothalamic hamartoma. Epilepsia 1994;35:514-519.

O'Leary DDM. Do cortical areas emerge from a protocortex? Trends Neurosci 1989;12:400-406.

Ono M, Kubik S, Abernathey CD. Atlas of the Cerebral Sulci. New York: Thieme Medical Publishers, 1990.

Palmini A, Andermann F, Olivier A, Tampieri D, Robitaille Y.

Focal neuronal migration disorders and intractable partial epilepsy: results of surgical treatment. Ann Neurol 1991;30:750-757.

Palmini A, Gambardella A, Andermann F, et al. Intrinsic epiletogenicity of human dysplastic cortex as suggested by corticography and surgical results. Ann Neurol 1995;37:476-487.

Parrish ML, Roessmann U, Levinsohn MW. Agenesis of the corpus callosum: a study of the frequency of associated malformations. Ann Neurol 1979;6:349-354.

Pfefferbaum A, Mathalon DH, Sullivan EV, Rawles JM, Zipursky RB, Lim KO. A quantitative magnetic resonance imaging study of changes in brain morphology from infancy to late adulthood. Arch Neurol 1994;51:874-887.

Pinto-Lord MC, Caviness VS Jr. Determinants of cell shape and orientation: A comparative Golgi analysis of cell-axon interrelationships in the developing neocortex of normal and reeler mice. J Comp Neurol 1979;187:49-70.

Placencia M, Shorvon SD, Paredes V, et al. Epileptic seizures in an Andean region of Ecuador. Brain 1992;115:771-782.

Prothero JW, Sundsten JW. Folding of the cerebral cortex in mammals: a scaling model. Brain Behav Evol 1984;24:152-167.

Purpura DP. Dendritic spine "dysgenesis" and mental retardation. Science 1974;186:1126-1128.

Purves D, Riddle DR, LaMantia A-S. Iterated patterns of brain circuitry (or how the cortex gets its spots) Trends Neurosci 1992;10:362-368.

Rademacher J, Caviness VS, Steinmetz H, Galaburda AM.

Topological variation of the human primary cortices: implications for neuroimaging, brain mapping and neurobiology. Cereb Cortex 1993;3:313-329.

Rakic P. Specification of cerebral cortical areas. Science 1988;241:170-176.

Rakic P. A small step for the cell, a giant leap for mankind: a hypothesis of neocortical expansion during evolution. Trends Neurosci 1995;18:383-388.

Rakic P, Cameron RS, Komuro H. Recognition, adhesion, transmembrane sinaling and cell motility in guided neuronal migration. Curr Opin Neurobiol 1994;4:63-69.

Raymond AA, Sisodiya SM, Fish DR, Stevens JM, Cook MJ, Shorvon SD. MRI features of adults with cortical dysgenesis and epilepsy. Epilepsia 1993;34(suppl 6):11.

Raymond AA, Fish DR, Stevens JM, Sisodiya SM, Alsanjari N, Shorvon SD. Subependymal heterotopia: a distinct neuronal migration disorder associated with epilepsy. J Neurol Neurosurg Psychiatry 1994a;57:1195-1202.

Raymond AA, Fish DR, Stevens JM, Cook MJ, Sisodiya SM, Shorvon SD. Association of hippocampal sclerosis with cortical dysgenesis in patients with epilepsy. Neurology 1994b;44:1841-1845.

Raymond AA, Fish DR, Sisodiya SM, Alsanjari N, Stevens JM, Shorvon SD. Abnormalities of gyration, heterotopias, tuberous sclerosis, focal cortical dysplasia, microdysgenesis, dysembryoplastic neuroepithelial tumours and dysgenesis of the archicortex in epilepsy. Clinical, electroencephalographic and neuroimaging features in 100 adult patients. Brain 1995;118:629-660.

Raz N, Torres IJ, Briggs SD, et al. Selective neuroanatomic abnormalities in Down's syndrome and their cognitive correlates: evidence from MRI morphometry. Neurology 1995;45:356-366.

Reid CB, Liang I, Walsh C. Systematic widespread clonal organisation in the cerebral cortex. Neuron 1995;15:299-310.

Reiner O, Carrozzo R, Shen Y, et al. Isolation of a Miller-Dieker lissencephaly gene containing G protein ß-subunit-like repeats. Nature 1993;364:717-21.

Reiss AL, Faruque F, Naidu S, et al. Neuroanatomy of Rett syndrome: a volumetric imaging study. Ann Neurol 1993;34:227-234.

Reutens DC, Stevens JM, Kingsley D, et al. Reliability of visual inspection for detection of volumetric hippocampal asymmetry. Neuroradiol (in press).

Richman DP, Stewart RM, Caviness VS Jr. Cerebral microgyria in a 27-week fetus: an architectonic and topographic analysis. J Neuropathol Exp Neurol 1974;33:374-384.

Richman DP, Stewart RM, Hutchinson JW, Caviness VS. Mechanical Model of brain convolutional development. Science 1975;189:18-21.

Rockel AJ, Hiorns RW, Powell TPS. The basic uniformity in structure of the neocortex. Brain 1980;103:221-244.

Rohlf FJ, Marcus LF. A revolution in morphometrics. TREE ? 1993;8:129-132.

Ruppin E, Schwartz EL, Yeshurun Y. Examining the volume efficiency of the cortical architecture in a multi-processor network model. Biol Cybern 1993;70:89-94.

Salanova V, Quesney LF, Rasmussen T, Andermann F, Olivier A. Reevaluation of surgical failures and the role of reoperation in 39 patients with frontal lobe epilepsy. Epilepsia 1994;35:70-80.

Sander JWAS. Some aspects of prognosis in the epilepsies: a review. Epilepsia 1993;34:1007-1016.

Sander JWAS, Hart YM, Johnson AL, Shorvon SD. National General Practice Study of Epilepsy: newly diagnosed epileptic seizures in a general population. Lancet 1990;336:1267-1271.

Sarnat HB. Cerebral Dysgenesis. New York: Oxford University Press, 1993.

Scheffer I, Bhatia KP, Lopes-Cendes I, et al. Autosomal dominant nocturnal frontal lobe epilepsy. A distinctive clinical disorder. Brain 1995;118:61-73.

Schlaepfer TE, Harris GJ, Yien AY, et al. Decreased regional cortical gray matter volume in schizophrenia. Am J Psychiatry 1994;151:842-848.

Schlaug G, Jäncke L, Huang Y, Steinmetz H. In vivo evidence of structural brain asymmetry in musicians. Science 1995;267:699-701.

Shorvon SD, Fish DR, Andermann F, Bydder GM, Stefan H, eds. Magnetic resonance Scanning and Epilepsy. New York: Plenum Press, 1994.

Sidman RL, Rakic P. Neuronal migration, with special reference to developing human brain: a review. Brain Res 1973;62:1-35.

Simmons PA, Lemmon V, Pearlman AL. Afferent and efferent connections of the striate and extrastriate visual cortex of the normal and reeler mouse. J Comp Neurol 1982;211:295-308.

Sisodiya SM. Wiring, dysmorphogenesis and epilepsy: a hypothesis. Seizure 1995;4:169-185.

Sisodiya SM, Free SL, Stevens JM, Fish DR, Shorvon SD. Widespread cerebral structural changes in patients with cortical dysgenesis and epilepsy. Brain 1995;118:1039-1050.

Sisodiya SM, Free SL, Fish DR, Shorvon SD. MRI-based surface area estimates in the normal adult human brain: evidence for structural organisation. J Anat 1996, in press.

Snedecor GW, Cochran WG. Statistical methods. Iowa State University Press, Sixth edition, 1967.

Spencer S. MRI and epilepsy surgery. Neurology 1995;45:1248-1250.

Steinmetz H, Herzog A, Huang Y, Hacklander T. Discordant brain-surface anatomy im monozygotic twins. N Engl J Med 1994;331:952-953.

Stevens JM. Imaging in epilepsy. Clinical MRI 1995, in press.

Stewart RM, Richman DP, Caviness VS Jr. Lissencephaly and pachygyria: an architectonic and topographical analysis. Acta Neuropathol 1975;31:1-12.

Takada K, Becker LE, Chan F. Aberrant dendritic development in the human agyric cortex: a quantitative and qualitative Golgi study of two cases. Clin Neuropathol 1994;7:111-119.

Talaraich J, Tourneux P. Referentially oriented cerebral MRI anatomy. Atlas of stereotaxic anatomical correlations for gray and white matter. New York: Thieme, 1993.

Tan S, Breen S. Radial mosaicism and tangential cell dispersion both contribute to mouse neocortical development.

Nature 1993;362:638-640.

Taylor DC, Falconer MA, Bruton CJ, Corsellis J, A. Focal dysplasia of the cerebral cortex in epilepsy. J Neurol Neurosurg Psychiatry 1971;34:369-87.

Tomasch J. Size, distribution, and number of fibres in the human corpus callosum. Anat Rec 1954;119,119-135.

Trenerry MR, Jack CR, Sharbrough FW, Cascino CD, Hirschorn KA, Marsh WR. Quantitative MRI hippocampal volumes: association with onset and duration of epilepsy and febrile convulsions in temporal lobectomy patients. Epil Res 1993;15:247-252.

Valdueza JM, Cristante L, Dammann O, et al. Hypothalamic hamartomas: with special reference to gelastic epilepsy and surgery. Neurosurgery 1994;34:949-95

Van Paesschen W, Sisodiya SM, Connelly A, et al. Quantitative hippocampal MRI and intractable temporal lobe epilepsy. Neurology 1995, in press.

Vannier MW, Butterfield RL, Jordan D, Murphy WA, Levitt RG, Gado M. Multispectral analysis of magnetic resonance images. Radiology 1985;154:221-224.

Von Economo C. The cytoarchitectonics of the human cerebral cortex. London: Oxford University Press 1929.

Walsh C, Cepko C. Clonal dispersion in proliferative layers of developing cerebral cortex. Nature 1993;362:632-635.

Welker W. Why does Cerebral Cortex Fissure and Fold? A Review of Determinants of Gyri and Sulci. In: Jones EG, Peters A. eds. Cerebral Cortex, Volume 8B. New York: Plenum Press, 1990:3-136.

Williams PL, Warwick R, Dyson M, Bannister LH, eds. Gray's Anatomy, 37th edition. Edinburgh: Churchill Livingston, 1989.

Williams RS, Ferrante RJ, Caviness VS. The cellular pathology of micogyria. A Golgi analysis. Acta Neuropathol 1976;36:269-283.

Winfield DA, Gatter KC, Powell TPS. An electron microscopic study of the types and proportions of neurons in the cortex of the motor and visual areas of the cat and rat. Brain 1980;103:245-258.

Wolf HK, Campos MG, Zentner J, et al. Surgical pathology of temporal lobe epilepsy. Experience with 216 cases. J Neuropathol and Exp Neurol 1993;52:499-506.

Yakovlev PI, Wadsworth RC. Schizencephalies: a study of the congenital clefts in the cerebral mantle. II. Clefts with hydrocephalus and lips separated. J Neuropathol Exp Neurol 1946;18:169-206.

AUTHOR'S BIBLIOGRAPHY

Papers

Bergin PS, Raymond AA, Free SL, Sisodiya SM, Stevens JM. Magnetic resonance volumetry. Neurology, 1994;44:1770-1771.

Raymond AA, Fish DR, Stevens JM, Sisodiya SM, Shorvon SD. Subependymal heterotopia: a distinct neuronal migration disorder associated with epilepsy. J Neurol Neurosurg Psychiatry, 1994;57:1195-1202.

Raymond AA, Fish DR, Stevens JM, Cook MJ, Sisodiya SM, Shorvon SD. Association of hippocampal sclerosis with cortical dysgenesis in patients with epilepsy. Neurology, 1994;44:1841-1845.

AA Raymond, DR Fish, SM Sisodiya, N Alsanjari, JM Stevens, SD Shorvon. Abnormalities of gyration, heterotopias, tuberous sclerosis, focal cortical dysplasia, microdysgenesis, dysembryoplastic neuroepithelial tumours and dysgenesisof the archicortex in epilepsy. Clinical, electroencephalographic and neuroimaging features in 100 adult patients. Brain, 1995;118:629-660.

Sisodiya SM. Wiring, dysmorphogenesis and epilepsy: a hypothesis. Seizure, 1995;4:169-185.

Sisodiya SM, Free SL, Stevens JM, Fish DR, Shorvon SD. Widespread cerebral structural changes in patients with cortical dysgenesis and epilepsy. Brain, 1995;118:1039-1050.

Sisodiya SM, Free SL, Fish DR, Shorvon SD. Increasing the yield from volumetric MRI in patients with epilepsy. Magnetic Resonance Imaging, 1995 (in press).

Sisodiya SM, Free SL, Fish DR, Shorvon SD. MRI-based surface

area estimates in the normal adult human brain. Journal of Anatomy, 1996 (in press).

Sisodiya SM, Stevens JM, Free SL, Fish DR, Shorvon SD. The demonstration of gyral abnormalities in patients with cryptogenic partial epilepsy using three-dimensional MRI. Archives of Neurology 1996 (in press).

Tofts PS, Sisodiya SM, Barker GJ, Webb S, MacManus D, Fish DR, Shorvon SD. MRI magnetisation transfer measurements in temporal lobe epilepsy. American Journal of Neuroradiology, 1995;16:1862-1863.

Li LM, Fish DR, Sisodiya SM, Shorvon SD, Alsanjari N, Stevens JM. High resolution magnetic resonance imaging in adults with partial or secondary generalised epilepsy attending a tertiary referral unit. J Neurol Neurosurg Psychiatry, 1995 (in press).

Van Paesschen W, Sisodiya SM, Connelly A, Duncan JS, Free SL, Raymond AA, Grunewald RA, Revesz T, Shorvon SD, Fish DR, Stevens JM, Johnson CL, Scaravilli F, Harkness WFJ, Jackson GD. Quantitative hippocampal MRI and intractable temporal lobe epilepsy. Neurology, 1995 (in press).

Walker M, Shorvon SD, Sisodiya SM, Smith SJM. A case of simple partial status epilepticus in occipital lobe epilepsy misdiagnosed as migraine: clinical, electrophysiological and MRI characteristics. Epilepsia, 1995 (in press).

Abstracts

Sisodiya SM, Free SL, Raymond AA, Fish DR, Shorvon SD. Morphometry of cortical dysgenetic lesions on magnetic resonance images of patients with epilepsy. Epilepsia, 1993;34 (suppl 6): 138.

AA Raymond, SM Sisodiya, DR Fish, JM Stevens, MJ Cook, SD Shorvon. MRI features of adults with cortical dysgenesis and epilepsy. Epilepsia, 1993;34(suppl 6):11.

Sisodiya SM, Free SL, Raymond AA, Stevens JM, Fish DR, Shorvon SD. Demonstration of unsuspected gyral abnormalities by three-dimensional reconstruction of magnetic resonance scans. Proceedings of the Fifth International Cleveland Clinic-Bethel Epilepsy Symposium, 1994.

Sisodiya SM, Free SL, Raymond AA, Stevens JM, Fish DR, Shorvon SD. Evidence from volumetric analysis of magnetic resonance images of abnormalities beyond those visualised in cortical dysgenesis. Proceedings of the Fifth International Cleveland Clinic-Bethel Epilepsy Symposium, 1994.

Sisodiya SM, Free SL, Raymond AA, Fish DR, Shorvon SD. Extralesional abnormalities on MR scanning are associated with gyral abnormalities and poor postoperative outcome in patients with cortical dysgenesis. Epilepsia, 1994:35(suppl 8):24.

Sisodiya SM, Raymond AA, Stevens JM, Fish DR, Shorvon SD. Demonstration of unsuspected gyral abnormalities by three-dimensional reconstruction of magnetic resonance images. Epilepsia, 1994;35(suppl 7):30.

Free SL, Sisodiya SM, Cook MJ, Fish DR, Shorvon SD. Three-dimensional fractal description of the white matter surface from MR images in epilepsy. Proceedings of the Fifth International Cleveland Clinic-Bethel Epilepsy Symposium, 1994.

Min LL, Sisodiya SM, Fish DR, Shorvon SD, Stevens JM. SMA seizure type: misleading term. Epilepsia, 1994;35(suppl 8):21.

Van Paesschen W, Sisodiya SM, Raymond AA, Grunewald RA, Duncan JS, Connelly A, Jackson GD, Shorvon SD, Fish DR, Stevens JM.

Combination of T2 relaxometry and volumetrics of the hippocampus identifies clinically useful subgroups of patients with intractable temporal lobe epilepsy. Epilepsia, 1994;35(suppl 7):30.

Van Paesschen W, Grunewald R, Duncan JS, Connelly A, Jackson GD, Sisodiya SM, Raymond AA, Shorvon SD, Fish DR, Stevens JM. Quantitative MRI in temporal lobe epilepsy and hippocampal sclerosis. Neurology, 1994;44(suppl 2):350.

Van Paesschen W, Grunewald R, Duncan JS, Connelly A, Jackson GD, Sisodiya SM, Raymond AA, Shorvon SD, Fish DR, Stevens JM. T2 relaxometry and volumetrics of hippocampus in the preoperative evaluation of intractable temporal lobe epilepsy. J Neurol, 1994;241(suppl 1):S87.

Van Paesschen W, Revesz T, Duncan JS, Connelly A, Harkness WFJ, Sisodiya SM, Raymond AA, Jackson GD, Alsanjari N, Shorvon SD, Fish DR. Quantitative neuropathology and quantitative MRI of hippocampal sclerosis. Epilepsia, 1994;35(suppl 8):

Koepp MJ, Richardson MP, Brooks DJ, Free S, Sisodiya SM, Duncan SJ. [^{11}C]Flumazenil PET and volumetric MRI in mesial temporal sclerosis. Epilepsia, 1995;36(suppl 3):S167.

Van Paesschen W, Revesz T, Sisodiya SM, Connelly A, Jackson GD, Duncan JS. Quantitaitve neuropathology and quantitative magnetic resonance imaging of the hippocampus of patients with intractable temporal lobe epilepsy. Epilepsia, 1995;36(suppl 3):S96.

Appendix 1. Region-of-interest boundary definitions

Cerebral hemisphere (CH) was isolated thus: dorsolaterally it was segmented along the natural boundary formed by its free surface; medially the hemispheres were separated along the interhemispheric fissure and the projection of this across the corpus callosum where this joined the hemispheres. If the corpus callosum was deformed, separation was performed along a perpendicular to the upper surface of the callosum dropped from the point of intersection of the interhemispheric fissure and the superior surface of the callosum. Inferomedially, the CH were separated from the cerebellum posteriorly; further anteriorly, the CH were dislocated from the superior colliculi; then from the cerebral peduncles along the shortest line from the base of the third ventricle in the midline to the ambient cistern along the bottom of the thalamus/pulvinar complex; further anteriorly in coronal images the suprapontine plane becomes apparent initially as an area of CSF in the middle of the brain stem: as soon as this became visible CH separation was achieved along the shortest line from the base of the third ventricle to this point and thence across along the shortest line segment to the ambient cistern again. Further anteriorly still, the CH were separated along the downward projection of the interhemispheric fissure, whilst making small deviations as required for medially-placed gyri of either hemisphere.

Subcortical matter (SM). The threshold for the SM was chosen in order to separate the cortex and white matter as closely as possible to the visually-judged boundary between these two tissue types. Except in the midline, the SM has its own natural boundary beneath the overlying cortical ribbon. Medially, the boundary, where not otherwise defined by the grey matter (for example in the corpus callosum), was drawn along the CH boundary. However in each CH inferomedially a special boundary protocol was defined to account for the difficulty in reliable delineation of the thalamus and

lentiform nucleus on the SPGR imaging sequence used for data acquisition. Thus, the thalamus was included entirely within the SM boundary, the medial aspect of this being identical to the CH boundary. Laterally, the subinsular lentiform nucleus was also included in the SM as its distinction from the surrounding SM was not reliable. The SM boundary was traced along the CH boundary inferomedially until the brain stem became separate from the CH. At this point, the medial border was defined along the interthalamic adhesion only, the automatic boundary allocated by the workstation software not being altered inferior to this along the midline. Once the post-chiasmal optic tracts became visible as separate entities from the CH, then the automatically-determined medial boundary of the SM was not altered manually. Inferiorly, however, the lentiform nucleus was included in the SM ROI: the boundary for this was chosen as the shortest line from the white matter overlying the posterior and medial orbital gyri to the infero-medial extremity of the internal capsule. In patients with ectopic grey matter, this grey matter was excluded from the SM ROI and considered to be part of the GM (except in the case of SEH; see section 4.4.2).

Inclusion of the thalamus and basal ganglia in the SM ROI should not bias the results, as the volume of these structures is small with respect to the volume of the SM, accounting for less than 5% of total cerebral white matter volume (Reiss et al.,1993). Interindividual variation in thalamic and lentiform nucleus volume is small in normal controls (Murphy et al.,1993; Reiss et al.,1993). The histopathological literature is remarkable for the absence of case reports documenting involvement of the thalamus or corpus striatum in dysgenetic processes, possibly because neurons destined for theses regions migrate along a separate pathway to their destinations (the corpus gangliothalamicus; Sarnat, 1992). That the overwhelming majority of changes in global or regional SM volumes (see Chapter 4) are reductions despite this fact suggests that if inclusion is confounding the results, it in

fact makes it less likely that such reductions would be detected: ie inclusion may increase false negative results, but not false positive ones.

Blurring of the grey-white interface on T_1-weighted images is a specific feature described in association with some forms of cerebral dysgenesis, particularly agyria/pachygyria, DNT, focal cortical dysplasia, and microdysgenesis (Raymond et al.,1995). In this thesis, blurring making choice of the interface position difficult was only found in one individual (patient 6). Repeat segmentation with the threshold level set so that the boundary was clearly either side of the blurred boundary did not alter the results of block volume analysis (Table X.1).

Table X.1.

Block (Fig 3.4)	Threshold ideal/repeat	Position with respect to normal range
RSM3	80/80	below
RSM3	80/82	below
RSM3	80/78	below
RGM3	80/80	above
RGM3	80/82	above
RGM3	80/78	above
RSM5	76/80	below
RSM6	76/80	below
RSM7	76/80	below
LSM4	76/80	below
LSM5	76/80	below
LSM6	76/80	below
LSM7	76/80	below
LSM8	76/80	below

For the SM volumes, setting a higher threshold would have reduced the volume of the block still further and kept it below the normal range: this alteration was therefore unnecessary.

The caudate nucleus was isolated according to its natural boundaries as are readily apparent on coronal SPGR sequences, with additional rules that the internal capsule was bisected along its length to achieve dislocation from the lentiform nucleus and that the nucleus accumbens was included.

The lateral ventricle was isolated along its natural boundaries throughout the entire extent of the hemispheres. The seed used to do this had its lower threshold set at 0 and its upper threshold set at the value chosen for the lower threshold for the SM ROI seed in the same study. The program counting the number of voxels in the SM surface counts all voxels in this surface including those in the SM-ventricle surface: this latter surface is obviously not relevant to considerations regarding the grey matter, and had to be eliminated before a meaningful surface voxel count could be determined for the SM. Thus, for computation of this latter value, the SM-ventricle surface was effectively eliminated by obliteration of the ventricle by inclusion of the ventricular ROI in the SM ROI only for surface voxel counting. This also ensured that falsely high SM_A or E_A did not arise from ventriculomegaly.

That the requirement for a separate seed (with a slightly lower threshold) for the left temporal lobe was due to scanner radiofrequency inhomogeneity was shown by scanning one subject (the author) prone and supine in the scanner. For the supine scan, a separate seed was required for accurate segmentation of the anatomical left temporal lobe; for the prone scan, a separate seed was required for accurate segmentation of the anatomical right temporal lobe, now in the region of the field previously occupied by the anatomical left temporal lobe.

Appendix 2. Angle of rotation about anterior-posterior axis required to alter slice position of IAM.

In section 3.10.2, it is stated that the angle about an anterior-posterior axis through which the brain has to be rotated to alter the slice position of the IAM by one slice is more than 60 degrees. This is shown by the following analysis:

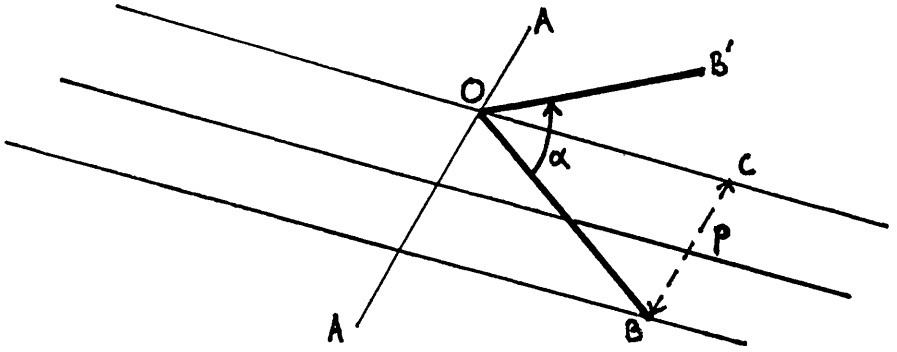

In the diagram above, line OB represents the distance from the the anterior-posterior axis of rotation (AOA) to the IAM on one side. Point O, on the axis of rotation, lies in a given (coronal) plane of imaging. These planes are represented by the three parallel lines. Point B, the point representing the IAM, lies initially in a coronal plane parallel to that containing Point O, but three millimetres anteriorly. Point C is the perpendicular projection from B to the plane containing O and the distance BC is initially 3mm. If the head rotates about the anterior-posterior axis passing through O, B describes a segment of a circle of radius OB. The angle of rotation is α. The perpendicular distance from the locus of B to the plane containing O is defined by **p** such that:

$$\mathbf{p} = 3\sin(90-\alpha)$$

If the position of the IAM is to change by one coronal slice, such that B' lies in the coronal plane between that containing O and that containing B, then **p** changes from 3mm to 1.5mm.

Thus,

$$\alpha = 90 - \sin^{-1}(1.5/3)$$
$$= 60$$

Therefore, the head has to rotate by 60 degrees or more in order that the position of the IAM change by one coronal slice. In practice, this degree of rotation is impossible to achieve.

Appendix 3.

Range of possible angles of rotation about vertical axis, γ, for given slice differences in position of internal auditory meati, calculated for IAM separation of 67.4mm, the mean IAM separation for 97 subjects (including all controls and all patients with definite dysgenesis on routine inspection). There was no significant difference for IAM separation between controls and patients with dysgenesis.

Slice difference in position of IAM's	Minimum rotation ,γ degrees	Maximum rotation,γ degrees
0	0	1.3
1	0	2.6
2	1.3	3.8
3	2.6	5.1
4	3.8	6.4
5	5.1	7.7

Appendix 4. Choice of block size

Blocks extending one-fifth and one-twentieth of the anterior-posterior extent were created in selected regions in the right hemisphere in controls (corresponding to those GM and SM blocks with the largest and smallest coefficients of variation) and means, standard deviations and coefficients of variation calculated. The latter were shown to be higher with smaller blocks than those for blocks one-tenth of hemispheric extent (Table X.2) in 75% of cases, reducing the volume sensitivity of the method. Whilst the coefficients of variation were lower in 75% for the larger blocks (one-fifth of the coronal extent), as might have been predicted from the total volume results, these larger blocks reduce the amount of spatial information extractable by 50%, reducing the spatial value of the technique.

Table X.2. Coefficients of variation [(S.D./mean) x 100%] for volumes of blocks of different anterior-posterior extents in 33 controls.

FIFTHS		TENTHS		TWENTIETHS		BLOCK
RSM	RCH	RSM	RCH	RSM	RCH	
21.25	14.95	38.19	23.36	62.17	38.96	1
				36.99	23.42	
		18.39	15.54	-	-	2
6.27	3.83	7.37	10.36	10.36	8.70	5
				13.08	10.88	
		6.55	11.89	11.56	12.87	6
				12.48	10.19	
17.82	12.23	14.28	11.75	-	-	9
		31.40	17.24	30.12	18.85	10
				99.15	56.73	

Abbreviations: SM = subcortical matter; CH = cerebral hemisphere; R = right. For block positions see Figure 3.4.

Appendix 5. Repeat SM surface voxel counts from 4 subjects scanned repeatedly and segmented by the author.

Subject	Scan Pair	Right SM_A voxel count		Ratio smaller /larger	Left SM_A voxel count		Ratio smaller/ larger	M/L first scan/ second scan
		Old	New		Old	New		
1	1-2	316586	310414	0.981	328745	313821	0.955	0.9766 0.9870
1	1-3 (prone)	316586	317591	0.997	328745	328107	0.998	0.9766 0.9103 (prone)
2	1-2	375775	383539	0.980	376634	382788	0.984	0.9631 1.0000
3	1-2	374206	373012	0.997	360939	370055	0.975	0.9697 0.9751
4	1-2	409306	401894	0.982	409429	387995	0.948	0.9583 0.9888
4	1-3	409306	387544	0.947	409429	392416	0.958	0.9583 0.9746

Results are presented for voxel count of SM for the original scan (scan 1; "old" results) in comparison to voxel counts from repeat scan (scan number 2 or 3; "new" results) for the right and left hemispheres. The values of M/L allow comparison of the degree of rotation for a *given* subject between separate scans.

Appendix 6. Patient clinical details

Appendix 6.1. Clinical details of patients with cortical dysgenesis

Patient number/sex age at scan/age at seizure onset	Seizures	MRI diagnosis
1/F/36/24y	L hemisensory SPS, SGS 1-2/m	R frontoparietal polymicrogyria
2/M/17/8y	CPS, tonic extension L leg. SGS once only	R occipital nodular heterotopia, overlying gyral abnormality
3/F/31/21y	L hemisensory SPS, no CPS for 10y. No SGS	Extensive R hemispheric gyral abnormality
4/M/18/1m	L arm aura then SGS, 1/m	R medial occipital and R lateral parietal full thickness clefts
5/F/36/6m	Head drops, both arems elevated and falls to ground. No SGS	L frontal lateral gyral abnormality, nodular subcortical and subependymal heterotopia
6/M/30/8y	Nocturnal SGS, 4/m. Mental retardation	Bilateral band heterotopia throughout both hemispheres and bilateral macrogyria
7/F/15/10y	SPS, drop attacks. Rare SGS	Bilateral posterior macrogyria
8/F/18/5y	CPS with visual aura. No SGS	L occipitotemporal macrogyria
9/F/34/23y	L arm focal motor, no SGS	Bilateral parietal full thickness clefts
10/F/29/2y	CPS with buzzing aura. Previously frequent SGS	Bilateral subependymal heterotopia and R posterior localised macrogyria

Patient number/sex age at scan/age at seizure onset	Seizures	MRI diagnosis
11/F/27/17y	L arm focal motor seizure then SGS	Bilateral small parietal subcortical heterotopic nodules
12/F/18/13m	CPS with jerking of all limbs. No SGS	Agenesis of corpus callosum and R temporal & anterior parietal dysgenesis, cleft & bilateral SEH
13/M/19/11y	Multiple seizure types: most are gelastic seizures	Hypothalamic hamartoma
14/F/28/12y	Nightly SGS	R parietal macrogyria
15/F/27/4y	SPS R hand. CPS 4/w. SGS aged 4-7 only	Bilateral extensive macrogyria with posterior subcortical band heterotopia
16/M/26/18m	Extension of head and arms, falls to the ground. No SGS	Bilateral parietal full thickness clefts with bilateral SEH
17/F/23/15y	CPS with hypothermia only (Shapiro syndrome)	Incomplete agenesis of corpus callosum
18/M/29/12y	R focal motor seizures and two SGS only	Bilateral frontal nodular subcortical heterotopia
19/M/33/18m	Absences. GS 2-3/y	Bilateral laminar subcortical heterotopia
20/M/27/26y	CPS only	R parieto-temporal cleft and R SEH
21/F/15/10m	R focal motor CPS. No SGS	L occipital, posterior parieto-temporal cleft
22/M/23/12y	Gelastic seizures Drop attacks.	Hypothalamic hamartoma

Appendix 6.2. Summary of abnormal results for patients with normal MRI scans on routine inspection.

Patient	Reconstruction	Whole hemispheric volumes	TRAT	No. abnormal blocks	No. abnormal pairs	Surface area derivatives	Fractal dimension
27	Abnormal		>			ESMR>	
28					2		
29	Abnormal						
30					2		
32	Abnormal			2			
33					2		
34	Abnormal		>	3			
35			>	2			
36	Abnormal			4	1		
37		RSM< & LSM<		2			
39				3			L>
41	Abnormal						
42	Abnormal			5	3		
43	Abnormal			n/a	n/a		
44	Abnormal			2			R&L>
46	Abnormal		<	4	2	ESML>	
47				3		ESMR> ESML>	

Patient	Reconstruction	Whole hemispheric volumes	TRAT	No. abnormal blocks	No. abnormal pairs	Surface area derivatives	Fractal dimension
49	Abnormal			5	1		
50				11		ECCR> ESMR>	L>
51		RSM & LSM<		15			
52				4			
53	Abnormal			1			L>
54	Abnormal					ESMR>	
55	Abnormal	RSM & LSM<		9		ESMR> ESML>	
56	Abnormal	nd	nd	nd	nd	nd	nd
57				5	1		
59	Abnormal	nd	nd	nd	nd	nd	nd
60	Abnormal	nd	nd	nd	nd	nd	nd
61	Abnormal	nd	nd	nd	nd	nd	nd
others	0/15	0/6	0/6	0/6	0/6	0/6	0/6

Abbreviations: see Table 4.4; nd = not done.

Appendix 6.3 Clinical details for patients with SEH only

Seizure onset was in the second decade or later in all the patients. Seizure semiology was suggestive of a generalised seizure disorder in 2/9 female and 2/4 male patients. The localisation of partial seizures suggested a temporal onset in 4/9 female patients and 2/4 male patients. In the other 3 female patients semiology suggested a parietal onset in one (76) and an occipital in another (75); localisation was not possible on clinical grounds in the remaining patient (77). Patient 76 had reduced two-point discrimination in the right hand. None of the other patients had any abnormal neurological findings. Two patients had a family history of epilepsy: patient 80 had an aunt with epilepsy with photosensitivity and patient 82 had a maternal uncle who had had absences in childhood. Only patient 80 had had febrile convulsions. Patient 72 was adopted and no details of family or early personal history were available.

Only 2 patients were seizure-free on medication alone. Patient 72, with clinical and electrical features of an idiopathic generalised seizure disorder, became free of attacks after the introduction of ethosuximide. Patient 77 was controlled on carbamazepine alone. Patient 80, with electroclinical features of an idiopathic generalised epilepsy was free of absences on sodium valproate, but has recently developed further tonic-clonic seizures. One patient (82) had only been treated with phenytoin at the time of reporting, and continued to have infrequent seizures. The volume of the subependymal tissue in a single hemisphere ranged from $0.15cm^3$ to $7.78cm^3$; this constituted at most 4% of the volume of grey matter in a hemisphere. For females, the volume of the SEH was not statistically significantly greater on the right than on the left in the 7 patients with bilateral SEH. However, the volume of SEH on the right was greater in females than in males (Mann-Whitney, $p<0.05$). There was no significant difference for the volume of SEH on the left. Further details are given in Tables X.3 and X.4.

Table X.3. Clinical details of patients with SEH

Patient	Age at scan/ seizure onset/sex	Seizure description
71	32/22/F	Altered awareness and staring for seconds to minutes.
72	34/19/F	(i) brief absences (ii) GTCS
73	26/15/F	Déjà vu; becomes unresponsive; oral/manual automatisms; ±SGS
74	48/27/F	(i) sudden falls with brief LOC (ii) previous absences
75	31/17/F	Objects become distorted or change colour; becomes unresponsive; ± motor automatisms; SGS thrice only
76	32/27/F	Tingling right side face and arm; ± becomes unresponsive and aphasic; postictal dysphasia; one SGS
77	26/19/F	Feels as if "on other side" looking through frosted glass; remains responsive; ± SGS
78	30/24/F	Becomes unresponsive, manual automatisms; ± SGS
79	24/21/F	Occasional aura; clonic movements both legs; no SGS
80	13/11/M	Matinal brief absences only
81	24/17/M	No aura; becomes pale and unresponsive; manual automatisms; ± SGS
82	21/20/M	(i) GTCS (ii) morning myoclonic jerks
83	30/20/M	Aura of visual fixation and uneasiness; becomes unresponsive; manual automatisms and bruxism; may shout "Hi!"

Table X.4. Details of MRI and MRI postprocessing in patients with SEH

Patient	MRI findings (UL = unilateral; BL = bilateral; LV = lateral ventricle)	Postprocessing results		
		RSEH volume	LSEH volume	Number of abnormal block values
71	UL; diffuse R trigone	2.21	-	0
72	BL; nodular in trigone and occipital horn R LV; L trigone	0.61	0.26	1
73	BL;large nodules; lateral margins body/trigone LV	7.06	7.35	1
74	BL; diffuse, lining trigones and occipital horns	3.10	2.49	0
75	BL; diffuse; lateral/inferolateral margins R trigone/temporal horns (R>L)	5.14	4.31	0
76	BL; diffuse, lining lateral margins both LV	6.67	6.37	0
77	UL; diffuse; lateral margin R trigone/posterior body LV	4.89	-	n/a
78	BL; diffuse; lateral margins body /trigone LV	7.78	7.01	0
79	BL; nodules; inferolateral margins trigones	2.61	0.15	1
80	UL; roof anterior horn R LV	1.47	-	8
81	UL; inferolateral margin trigone LV extending to temporal horn	-	2.27	8
82	UL; L trigone lateral margin	-	0.19	3
83	BL; trigones, extending to temporal horn on L	0.51	0.89	11

Appendix 6.4 Clinical and MRI details of patients with HS

Patient number/ sex/age at scan/ age at seizure onset	MRI diagnosis	Seizure types
100/F/26/9y	R HS	CPS. No SGS.
101/F/18/11y	L HS	CPS. Five SGS.
102/M/26/11m	L HS	CPS. SGS 1/m.
103/F/22/13y	L HS	CPS. No SGS.
104/F/24/3y	L HS	CPS. No SGS.
105/F/35/7y	R HS	CPS. SGS 4/y.
106/F/38/10	L HS	CPS. SGS 1/m.
107/M/31/9y	L HS	CPS. SGS 2/m.
108/M/36/19	R HS	CPS. 12 SGS.
109/F/25/1y	L HS	CPS No SGS.
110/M/39/18y	R HS	CPS. No SGS.
111/M/31/9y	R HS	CPS. Frequent SGS.
112/M/28/4y	L HS	CPS. Frequent SGS.
113/M/25/17y	L HS	CPS. No SGS.
114/M/16/18m	R HS	CPS. Frequent SGS.
115/F/30/9y	R HS	CPS. SGS 1/m.

ABBREVIATIONS
L=left R=right y=years m=month w=week S/CPS=simple/complex partial seizure SGS=secondary generalised seizures.

Appendix 7. Deduction of different neuron numbers in normal right and left hemispheres

For right-handed control subjects, left GM volume (LGMV) is significantly greater than right GMV, whilst right E_A is significantly greater than left E_A.
Assuming (after Haug, 1956 and Braendgaard et al.,1990; no cortical gliosis seen on T_2-weighted images in this study) grey matter volume is the product of the total number of neurons, N, in the hemisphere and the mean amount of neuropil/neuron, M,

$GMV = N \times M,$

and that E_A is directly the sum of the number of projectional neurons, P, and the neuropil extent in a hemisphere (see Discussion),

$E_A = (N \times M) + P,$

but it has been shown that P is a fixed proportion of N (Rockel et al.,1980; Winfield et al.,1980),

$\Rightarrow \quad RE_A > LE_A$

$\Rightarrow \quad (RN \times RM) + RP > (LN \times LM) + LP$

$\Rightarrow \quad (RN \times RM) + kRN > (LN \times LM) + kLN$ where $0<k<1$, k is constant,

$\Rightarrow \quad (RN \times RM) - (LN \times LM) > k(LN-RN)$

But,

$LGM > RGM$

$\Rightarrow \quad LN \times LM > RN \times RM$

Therefore,

$k(LN-RN) < 0$

$\Rightarrow \quad LN < RN$

and $LM > RM$

that is to say, there are more neurons in the normal right hemisphere than in the left in right handed controls, but there is more neuropil/neuron on average in the left hemisphere than in the right.

Brain (1995), **118**, 1039–1050

Widespread cerebral structural changes in patients with cortical dysgenesis and epilepsy

S. M. Sisodiya,[1] S. L. Free,[1] J. M. Stevens,[2] D. R. Fish[1] and S. D. Shorvon[1]

[1]*Epilepsy Research Group, Institute of Neurology and the* [2]*Department of Neuroradiology, National Hospital for Neurology and Neurosurgery, London, UK*

Correspondence to: Dr S. M. Sisodiya, Room 508, Institute of Neurology, Queen Square, London WC1N 3BG, UK

Summary

Cerebral cortical dysgenesis (CD), as revealed by MRI, is the second commonest cause of medically refractory chronic partial epilepsy. Surgical treatment is often disappointing in these cases. This has been attributed to the probable diffuse nature of the condition but proof of this in the human brain is lacking. We have quantitatively analysed MRI scans of 30 neurologically normal control subjects and 18 patients with CD, examining the regional distribution of grey and subcortical matter volumes. In 15 out of the 18 patients, we have demonstrated abnormalities of this distribution beyond the margins of the visualized lesion. Nine out of 10 patients with dysgenetic lesions visualized only in one hemisphere had volumetric abnormality in the apparently normal contralateral hemisphere. These abnormalities were not visible on reinspection of the MRI scans. Such abnormalities were not found in 10 patients with isolated hippocampal sclerosis (HS) although the history of generalized seizure activity and duration of epilepsy did not differ between the two groups of patients. Thus there is evidence for the existence of extensive structural disorganization outside visually identified focal lesions in the brains of patients with CD and chronic partial epilepsy. This disruption is not due to the effects of the epilepsy and must instead be associated with its cause. Possible mechanisms producing the abnormalities are discussed. The methodology described may be applied to other cortical diseases.

Keywords: cortical dysgenesis; epilepsy; MRI; quantitation

Abbreviations: CD = cerebral cortical dysgenesis; HS = hippocampal sclerosis; LG = left-sided grey matter block; LS = left-sided subcortical matter block; RG = right-sided grey matter block; RS = right-sided subcortical matter block; SPGR = spoiled gradient recalled; TR = the ratio volume of the entire left cerebral hemisphere:volume of the entire right cerebral hemisphere.

Introduction

Cerebral cortical dysgenesis is an important pathological condition often underlying neurological disorders including mental retardation, developmental delay, dyslexia and epilepsy (Galaburda and Kemper, 1979; Sarnat, 1992). It has been demonstrated by MRI scanning in a high proportion of patients with chronic partial epilepsy (Raymond *et al.*, 1994*a*). In such cases, the epilepsy is often refractory to medical therapy (Palmini *et al.*, 1991). Surgical resection of such lesions is sometimes performed in an attempt to improve seizure control. Experience has shown (Bruton, 1988; Guerrini *et al.*, 1992; Engel, 1993), however, that patients with dysgenesis, confirmed on histology of resected tissue, rarely become completely seizure-free, in contrast to the high likelihood that patients with other focal lesions, e.g. pure HS, have their seizure tendency reduced (Wieser *et al.*, 1993). It has been suggested (Palmini *et al.*, 1991; Andermann, 1994) that this is because the extent of structural abnormality in CD is greater than that seen by eye alone on MRI or at operation. In animal studies, it has been shown (Barron, 1950; Goldman and Galkin, 1978; Goldman-Rakic, 1980) that prenatal focal cortical lesioning produces noncontiguous, distant gyral abnormalities (including some in the contralateral hemisphere) that are thought to be due to distant connectivity changes. Local connectivity changes after prenatal lesions have also been demonstrated (Jones *et al.*, 1982). To date, however, structural changes distant to visible focal dysgenetic lesions have not been demonstrated in humans either by histology or structural imaging.

Most of the volume of grey matter of the cerebral cortex is composed of neuropil rather than neuronal cell bodies

(Haug, 1956). Neurons can only survive in the adult brain if they are connected to other neurons (Cowan *et al.*, 1984). There are known to be extensive reciprocal interconnections between disparate cortical regions (Goldman-Rakic, 1988). Thus, visually apparent lesions of the cerebral cortex on MRI scanning are connected to other parts of the cortex. The cortex is abnormal in the lesional area (Barth, 1987; Kuzniecky *et al.*, 1991; Barkovich and Kjos, 1992*a*) and dendritic abnormalities have been demonstrated in abnormal neurons in dysgenetic lesions (Ferrer, 1984; Bordarier *et al.*, 1986; Takada *et al.*, 1994). Therefore, regions connected to such lesional areas might also be abnormal and the neuropil here might be qualitatively or quantitatively abnormal. Thus, we postulate that there may be extralesional abnormalities, that are not necessarily visible, on MRI scans of patients with visually apparent focal dysgenesis. We further suggest that these abnormalities, reflecting neuropil connectional changes, may be manifest as abnormalities of the volume of grey or white matter in given regions of the brain.

To investigate this, visual inspection alone may not be adequate: in the less structurally convoluted shape of the hippocampus, for example, volumetric analysis has been shown to increase the yield of information above visual inspection alone (Reutens *et al.*, 1993). We have devised a system of volumetric analysis of MRI scans to define normal ranges of grey and white matter volume in specified regions of the brain and analysed the scans of patients with refractory partial epilepsy by comparison with these ranges. The method is not intended to identify lesions *de novo*, but rather to determine whether quantifiable abnormalities of grey or white matter exist in the rest of the brain, as well as in the lesion.

Methods

Subjects

Control subjects were neurologically normal volunteers drawn from staff at the National Hospital and their colleagues. Their age range was 23–52 years (median 30 years): 22 were male and eight female. All but one were caucasian. All gave informed consent for the scanning procedure; the study was approved by the ethics committee of the National Hospital for Neurology and Neurosurgery. Patients were scanned as part of a study investigating underlying cerebral abnormalities in patients with chronic epilepsy. All were drawn from the out-patient clinics at the National Hospital and the Chalfont Centre for Epilepsy. Thirty patients, all caucasian, with refractory partial epilepsy were selected: clinical details are presented in Table 1, along with an MRI diagnosis of the cortical abnormality present. Ten had HS demonstrated histologically following surgery; none of these 10 (age range 18–38 years) had any evidence on preoperative MRI of any other pathology (Raymond *et al.*, 1994*b*). All 10 had become seizure-free postoperatively (minimum follow-up 1 year). Eighteen patients (age range 15–36 years) had CD demonstrated on visual inspection of their scans. Inspection of the images by an experienced neuroradiologist (J.M.S.) did not reveal any other neocortical or white matter abnormality.

There was no significant statistical difference between the ages of the control or patient groups (Mann–Whitney, two-tailed, $P > 0.2$). In addition, age-related changes in head size and cortical grey and white matter volumes are not believed to be significant between the ages of 10 and 50 [Miller *et al.* (1980), DeCarli *et al.* (1992); Pfefferbaum *et al.* (1994) report a loss of cortical grey matter after the age of 21 years of 0.7 ml/year]. There were no variables of cerebral (global or local, absolute or ratio) volume that correlated with age in our own control group (maximum age 52 years).

Imaging

MRI was performed on a 1.5T GE Signa unit (GE, Milwaukee, USA). A coronal spoiled gradient recalled (SPGR) sequence was used for image analysis (TE 5 ms, TR 35 ms, flip angle 35°, acquisition matrix 256×128, 1 NEX, field of view 24 cm, producing 124 contiguous slices each 1.5 mm thick). Sagittal T_1-weighted (TR/TE/NEX 500/10/2) and axial proton density (2800/30/1) and T_2-weighted (2800/90/1) images were also routinely acquired. All these images were printed as hard copy for all subjects and reported by an experienced neuroradiologist (J.M.S.), who looked specifically at the pattern of gyration, sulcal depth and cortical thickness, and the pattern of the grey–white interface.

Image analysis

Studies were transferred to an independent imaging workstation (Allegro, ISG Technologies, Toronto, Canada). This allowed the semi-automated selection of defined regions of interest from the original images (segmentation). The procedure involved the selection of a threshold pixel intensity and the subsequent automatic growth of a region of interest, including all connected pixels within the threshold boundaries, from an initial seed placed by the operator. Manual interaction was required to edit the region of interest thus produced, e.g. to separate overlying meninges from the true region of interest. The regions of interest boundaries are defined below.

Regions of interest

The following areas were segmented on each image prior to the reconstruction of three-dimensional objects from regions of interest: (i) entire cerebral hemisphere removed from its contralateral homologue and from the brainstem; (ii) the caudate nucleus; and (iii) the remaining underlying hemispheric white matter and subcortical nuclei (primarily the thalamus and lentiform nucleus), together called the subcortical matter. The grey matter was obtained by subtracting the subcortical matter and caudate regions of interest from the entire cerebral hemispheric region of interest. Regions of interest were summed automatically to produce

Table 1 *Patient clinical and neuroimaging data*

Patient no./ sex/age at scan/ age at seizure onset	MRI diagnosis	Seizure types
1/F/36/24 years	R perisylvian polymicrogyria	L hemisensory, SGS 1–2/month
2/M/17/8 years	R occipital nodular heterotopia, overlying gyral abnormality	CPS, tonic extension L leg. SGS once only
3/F/35/21 years	Extensive R cerebral hemisphere gyral abnormality ?polymicrogyria	SPS, L hemisensory no CPS for 10 years No SGS
4/M/18/1 month	R medial occipital and R lateral parietal schizencephaly	L arm aura then SGS, 3/month
5/F/36/6 months	L frontal medial and lateral gyral abnormality and L frontal subependymal heterotopia	Dropping of head, raising of both arms and fall to ground. No SGS
6/M/30/8 years	Bilateral band heterotopia throughout hemispheres and bilateral macrogyria	Nocturnal SGS, 4/month Mental retardation
7/F/18/5 years	L occipitotemporal macrogyria	CPS with visual aura and automatism. No SGS
8/F/34/23 years	Bilateral closed-lip schizencephaly	Focal motor, L arm No SGS
9/F/28/12 years	R parietal macrogyria	Nightly SGS
10/F/27/4 years	Bilateral extensive macrogyria with posterior band heterotopia	SPS R hand, CPS 4/week. SGS 4–7 years only
11/F/15/10 months	L occipital, posterior parieto-temporal closed-lip schizencephaly	SPS (aura), CPS R focal motor. No SGS
12/M/27/26 years	R posterior parieto-temporal closed-lip schizencephaly	CPS. No SGS
13/F/23/15 years	Agenesis of corpus callosum and extensive gyral anomaly	CPS only with hypothermia
14/M/26/18 months	Bilateral subependymal heterotopia and parietal closed-lip schizencephaly	CPS, myoclonic jerks. 4 SGS only
15/M/22/17 years	L hippocampal enlargement, subependymal heterotopia	CPS with extension R arm
16/M/33/18 months	Bilateral subcortical band heterotopia	Absences. 2–3 GS/year
17/M/29/12 years	Bilateral subcortical band heterotopia, frontal	R focal motor and two SGS
18/F/15/10 years	Bilateral posterior macrogyria	SPS, drop attacks Rare SGS
19/F/18/11 years	L HS	CPS. 5 SGS
20/M/26/11 months	L HS	CPS. Monthly SGS
21/M/36/19 years	R HS	CPS. 12 SGS
22/F/24/3 years	L HS	CPS. No SGS
23/F/35/7 years	R HS	CPS. SGS 4/year
24/F/26/9 years	R HS	CPS. No SGS
25/F/38/10 years	L HS	CPS. SGS 1/month
26/M/31/9 years	L HS	CPS. SGS 2/month
27/F/22/13 years	L HS	CPS. No SGS
28/F/25/13 years	L HS	CPS only

L = left; R = right; S/CPS = simple/complex partial seizure (S)GS = (secondarily) generalized seizures.

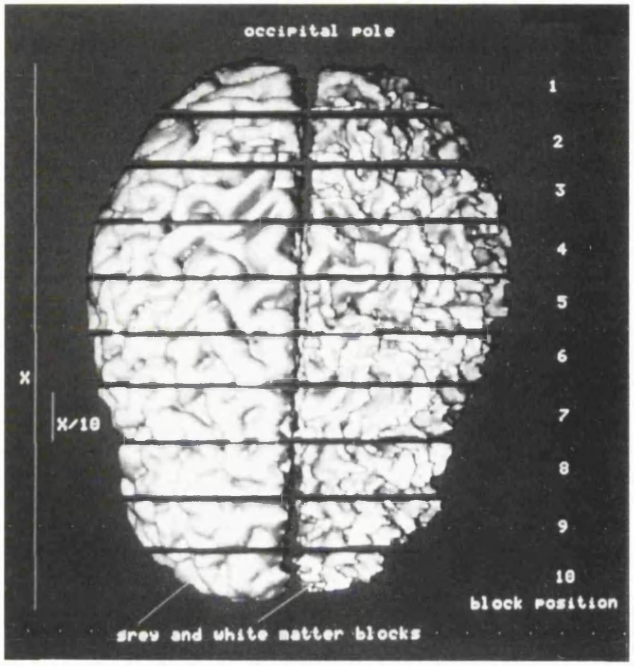

Fig. 1 Derivation of grey and subcortical matter blocks by division of coronal extent (X) of reconstructions into tenths (X/10). Block positions numbered. The blocks are called LG and LS, for left-sided grey matter and subcortical matter blocks, and RG and RS for the equivalent right-sided blocks.

three-dimensional volumes of interest that could be displayed, manipulated and measured. The protocols used for the definition of region of interest boundaries are given in detail in the Appendix.

Blocks

Hemispheric grey matter and subcortical matter volumes of interest were divided into smaller volumes (Fig. 1): these were defined independently in each hemisphere in each brain to span one-tenth of the total anterior–posterior extent of the hemisphere from which they were derived. The volume of each block for a given subject (40 in all per subject, 10 subcortical matter blocks and 10 grey matter blocks in each hemisphere) was then divided by the total segmented volume for that subject in order to normalize for brain volume and allow comparison of volume distribution measurements between subjects. In addition, to further investigate the symmetry noted in control subjects, the following ratios were also calculated: the volume of a given left-sided block of grey matter or subcortical matter compared with its right-sided homologue (*see* Fig. 2) and the volume of a given block of grey matter compared with its ipsilateral homologous subcortical matter block (Fig. 3). Thus in total, each brain yielded 80 volumetric (block or block ratio) variables.

Blocks one-tenth of the coronal extent of a hemisphere were chosen as they provide the maximum localizing information with the smallest coefficient of variation resulting from the caprice of gyral anatomy in the normal brain. The derivation of this methodology controls for differences in

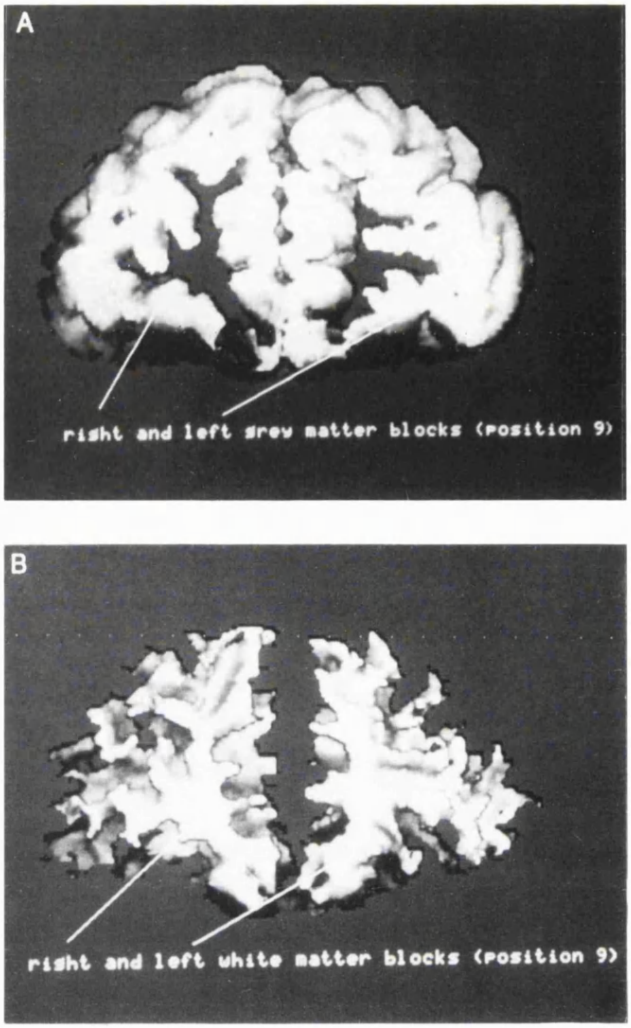

Fig. 2 Derivation of (**A**) LG/RG and (**B**) LS/RS ratios: **A**, left and right grey matter blocks; **B**, left and right subcortical matter blocks (in this case both from position 9 of a control subject's brain).

interhemispheric coronal extent and for axial rotation of the head in the scanner.

Patients' brains were analysed in the same manner and their 80 variables compared with the normal ranges. The maximum extent of dysgenetic lesions seen by eye was determined on the two-dimensional coronal images. Blocks were classified as 'intralesional' if they even partly overlapped the visualized lesion, or 'extralesional' if they did not.

Reliability

The stability of the choice of the threshold was determined by repeating the choice of the lower threshold limit for a given region of interest (the upper limit was fixed for all cases for the grey matter and subcortical matter) over a period of time. In three control subjects, the choice was repeated four times over a month. In 23 subjects (controls and patients), it was repeated once over an interval of 12 months for the cerebral hemisphere, and over a similar time period for 17 subjects for the subcortical matter. The

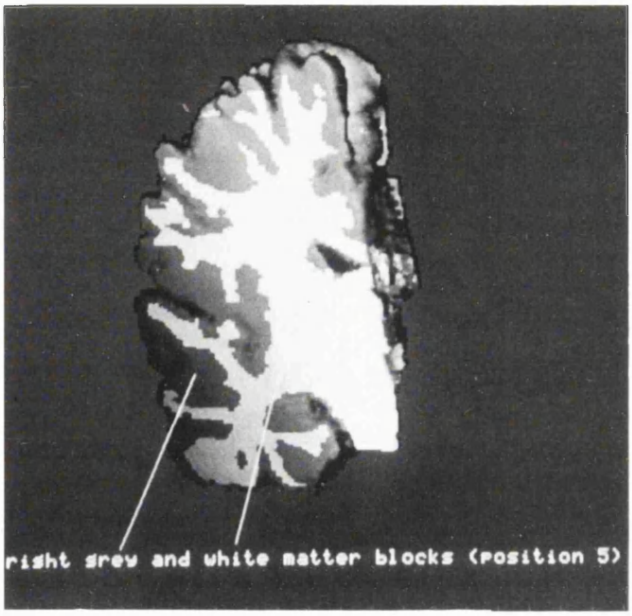

Fig. 3 Derivation of the grey matter: subcortical matter ratio. The figure shows the grey matter block and underlying subcortical matter block from position 5 in the right hemisphere, giving the ratio for RG/RS position 5.

correlation coefficient (Pearson) for the cerebral hemisphere threshold repetitions was greater than 0.98 for the two hemispheres considered separately. For the subcortical matter, the coefficient was greater than 0.99.

The determination of the regions of interest was repeated in five subjects four times each for the cerebral hemisphere, subcortical matter and caudate nucleus on each side at intervals throughout the study. This produced 40 cerebral hemispheres and 40 subcortical matter volumes. This was performed by one operator (S.M.S.). Inter-rater reliability was assessed by repeat segmentation of eight subjects by a second operator (S.L.F.), blinded to the segmentation generated by the first operator. The resulting volumes were compared in order to determine the overall reliability of the choice of the threshold and the boundary protocols.

It was found that the ratio of the volume of the smallest to the largest repeat hemispheric grey matter segmentation for a given subject was always greater than 98% for hemispheres segmented by one operator (mean for eight separate hemispheres, five copies of each = 98.7%). The corresponding figure for the subcortical matter was 95% (mean for eight separate hemispheres, five copies of each = 97%). For inter-rater reliability assessment, the mean ratio of the volume of the smallest to the largest cerebral hemisphere was 97.6%, and for the subcortical matter 94.3% (means for 16 separate hemispheres). This suggests that, in combination, the choice of threshold (as demonstrated already above), the boundary protocols and the manual editing are all highly reproducible both within and between operators.

Statistics

Analysis was performed in a statistics package, SPSS/PC+, Version 4.0.1 (SPSS Inc., Chicago, Ill., USA). Means and standard deviations were calculated for whole-object volumes and for the brain-size corrected blocks and ratios across the 30 controls. Normal ranges for all variables were taken as three standard deviations either side of the mean. Statistical significance was taken at the $P = 0.01$ level.

Results

Total hemispheric volume ratio (TR)

The mean value of TR for the 30 controls was 0.999 (SD = 0.013). The normal range for TR was 0.960–1.038. One control has a TR outside the normal range (TR value 1.042): in a sample of 30 controls, 0.081 would be expected to lie outside the normal range by chance alone.

Nine out of 18 patients with CD had a TR outside the normal range: only two of these nine were thought to have asymmetric hemispheres on visual inspection of the original images. The origin of the partial epilepsy in these nine cases lateralized to the smaller hemisphere in six.

Block volumes and ratios

Controls

The tightness of the distribution of either block volume or ratio varied along the coronal axis. This was quantified by calculation of the coefficient of variation for a variable (SD/mean). The coefficients of variation for each of the eight variable types in each of the 10 blocks is shown graphically in Fig. 4. It can be seen that the ranges were tightest in the central parts of the brain, covered by blocks 3–8.

Overall, if the 30 controls are considered together and all 80 variables in each subject considered to be independent, one would expect six out of 2400 abnormal variables: three out of 2400 (0.125%) were actually found. These abnormal variables were in three controls (one abnormal variable each) giving a mean number of abnormal variables per control of 0.1 (SD = 0.305; expected mean = 0.216).

On this basis, we took the presence of two or more variables (out of 80) more than three standard deviations from the mean for a given block or ratio in a single study to define a structurally abnormal brain in terms of the distribution of volume proportion. None of the controls were abnormal in these terms.

Patients with cortical dysgenesis

For the patients with CD as a group, 208 out of 1440 (14.4%) of the variables are abnormal. The number of abnormal values per subject is shown in Table 2. The range of the number of abnormalities per subject was 2–42. Each patient with CD had at least two abnormal variables. Of these 18 patients with CD, 15 have at least one extralesional abnormal variable. Ten out of 18 patients had CD visualized in only one hemisphere on MRI. Nine of them had block or ratio

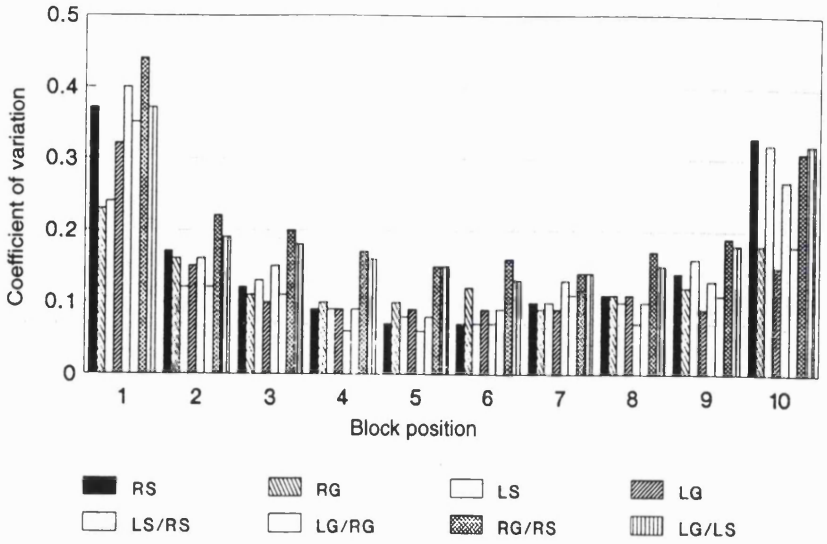

Fig. 4 Composite plot of coefficient of variation for value of each variable type (block or block ratio) against block position in 30 controls. For abbreviations *see* Fig. 1 legend.

Table 2 *Block and ratio data for patients with CD*

Patient no.	Total ratio	Abnormal values	
		Total	Extralesional
1	1.058↑	2	2
2	1.039↑	7	5
3	1.350↑	14	10
4	0.863↓	6	4
5	0.978	2	0
6	0.986	42	0
7	0.939↓	7	1
8	1.024	4	2
9	0.899↓	8	3
10	1.017	22	0
11	0.848↓	25	14
12	1.058↑	6	5
13	0.991	16	1
14	1.051↑	6	2
15	0.979	8	5
16	0.978	2	2
17	0.985	3	3
18	0.990	28	1

↑/↓ = above upper/below lower limit of normal range.

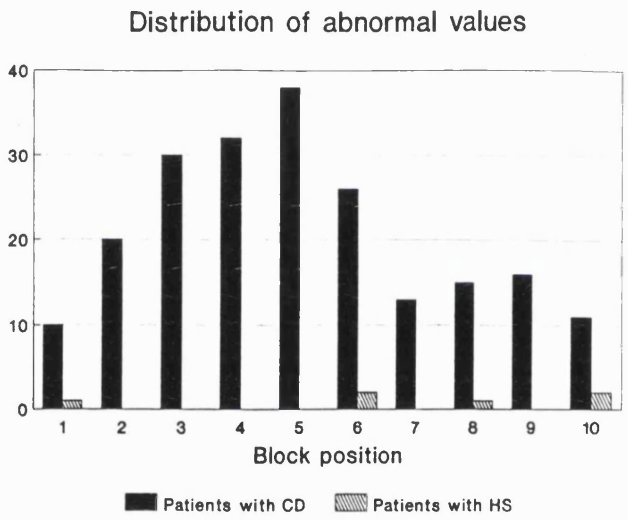

Fig. 5 Frequency histogram of number of abnormal values (blocks and block ratios) for patients with CD or HS, showing the distribution of the location of these abnormalities by block position.

abnormalities in the contralateral, apparently normal, hemisphere.

Visual reinspection of the original images did not reveal any abnormality of cortical structure or volume in the slices covered by the extralesionally abnormal blocks.

The location of the abnormal blocks and ratios is summarized in Fig. 5. The majority of the abnormalities in the patients with CD were found in the central blocks (e.g. 3–5). This is in contrast to the tightness of volume distribution in these blocks in the control group as shown in Fig. 4. In addition, for all the patients with CD considered together, only six out of 60 extralesional abnormal blocks were contiguous with blocks covering the lesion.

The nature of the abnormality within these blocks and ratios, whether they exceeded or fell below the control range, is summarized in Table 3. It should be noted that, for grey block volumes alone, the majority of the changes was due to an increase in the volume of the grey matter block (44 out of 45 abnormal values); conversely, for the subcortical matter, the majority of the changes were due to a decrease in the volume of the blocks concerned (50 out of 51 abnormal values). Correspondingly, but not always associated with either an increase in the value of the underlying homologous grey matter block or a decrease in the value of the homologous subcortical matter block, all the abnormalities of grey matter:subcortical matter ratios were increases over the normal range (83 values).

Table 3 *Summary of block or ratio changes*

Change in value	↑	↓		↑	↓
Patient group					
CD (n = 18)					
block or ratio			GM/GM or SM/SM ratio		
GM	44	1	GM/GM	4	3
SM	1	50	SM/SM	11	1
GM/SM	83	0			
HS (n = 10)					
block or ratio			GM/GM or SM/SM ratio		
GM	0	0	GM/GM	0	0
SM	0	1	SM/SM	0	0
GM/SM	4	0			

GM = grey matter; SM = subcortical matter; ↑ = values greater than upper limit of normal range; ↓ = values smaller than lower limit of normal range.

Patients with HS

There was no significant difference between the patients with isolated HS and those with CD in terms of history of secondarily generalized seizures or duration of epilepsy (Mann–Whitney, two-tailed, $P > 0.1$). As a group, however, the patients with HS had only six abnormal variables out of 800 in total. No patient had more than one abnormal value: thus none had a structurally abnormal brain as defined. The nature of the abnormality present is given in Table 3, and the location of the abnormalities shown in Fig. 5.

Discussion

Methodological issues

The basis of this work is segmentation of MRIs. Many of the issues concerning this process have been considered extensively elsewhere (Filipek *et al.*, 1989). Variation in signal intensity arising from the same tissue in different parts of the brain, especially the frontal and occipital poles, may affect the segmentation procedure. The choice of the threshold itself and the manual editing also affect segmentation. That the volumes of interest obtained are sensitive to the choice of the threshold emphasizes the importance of determining the reproducibility of the procedure and quantifying the variability obtained in practice. The high degree of repeatability of both the threshold choice and the overall volumes of interest produced by our protocol attests to the reliability of the techniques used.

One issue, however, is specific to the analysis of the images used here. Specific forms of CD (extensive cortical dysplasia and polymicrogyria) are occasionally reported to be associated with blurring of the grey–white interface either on MRI (Marchal *et al.*, 1989) or histologically (Farrell *et al.*, 1992): as this is a boundary used in this work, such blurring might be considered to make segmentation more difficult. Blurring was noted in the images of patient 6. However, alteration of the threshold for region of interest growing in the segmentation procedure over a range of values that included the entire blurred boundary did not alter the results: abnormal blocks and ratios remained so. This presumably reflects the high degree of structural and volumetric abnormality present in this brain. No other patients, however, were found to have visible blurring of the grey–white interface and therefore this is unlikely to account for the results.

Ideally, the thalamus and lentiform nucleus would be segmented as separate regions of interest and analysed independently of either the grey matter or the white matter; however, the MRI acquisition sequence used precluded this. The volume of thalamus and lentiform nucleus together account for <2.5% of total intracranial (cerebral and cerebrospinal fluid) volume (Murphy *et al.*, 1993) and <5% of the total cerebral white matter volume (Reiss *et al.*, 1993). In addition, the inter-individual variation in thalamic and lentiform nucleus volume is small in normal controls (Murphy *et al.*, 1993; Reiss *et al.*, 1993). There is no evidence to suggest specific loss of thalamic or lentiform volume in association with chronic partial epilepsy: indeed, the histopatholgical literature on CD is remarkable for stating that the basal nuclei are rarely involved in the dysgenetic process (Volpe and Adams, 1972; Richman *et al.*, 1974; Stewart *et al.*, 1975; Choi and Matthias, 1987). For these reasons, we included the deep nuclei in the subcortical matter volume of interest and do not think that changes in the volume of these nuclei were responsible for our findings.

The choice of blocks for the analysis of the data, though not arbitrary, is artificial. However, the blocks are intended to constitute a (quantitative) analytical methodology and in this sense they are no different to, say, the scalp positioning of EEG electrodes. Other workers have used different ways of subdividing the cortex regionally for the investigation of focal loss of grey matter (Rusinek *et al.*, 1991; Schlaepfer *et al.*, 1994). In this study, coronal blocks were chosen because of machine limitations; ideally, gyrus-specific volumes should be measured, but these are difficult to define across a range of subjects in three dimensions, morphological variability and the objective choice of gyral landmarks being major difficulties. It should also be stated that the blocks and block ratios are measures not of absolute tissue volumes but rather of the distribution of volume proportions and symmetries in the brain.

The last methodological issue leads us into a discussion of the reported findings. This is the determination of the coronal extent of lesions. The choice was over-inclusive where any doubt existed about the 'boundaries' of the lesion. In addition, for patients with CD, only six out of 60 extralesional abnormal values are contiguous with blocks including the lesional areas. Thus extralesionally abnormal blocks are unlikely to contain subtle continuations of focal lesions.

Cerebral structure

In controls, the cerebral hemispheres are highly symmetrical in volume terms. Only one control out of 30 falls outside

the normal range for this ratio (TR). When volumetric analysis is performed regionally, using block volumes or block ratios, the tight distribution of volumes of grey and subcortical matter is maintained, with only three out of a total of 2400 values falling outside normal ranges as defined.

In previous MRI-based quantitation (Murphy *et al.*, 1992; Reiss *et al.*, 1993; Filipek *et al.*, 1994), a similar degree of symmetry has been reported. Other workers (Jack *et al.*, 1989; Kertesz *et al.*, 1992) have reported regional asymmetries on MRI data. Morphometry based on post-mortem specimens has produced conflicting results on the symmetry of hemispheric volumes (Habib, 1989; Weis *et al.*, 1989). Our results confirm the volumetric symmetry of the cerebral hemispheres *in vivo* in normal subjects when the hemispheres are accurately and reproducibly defined. Asymmetry beyond the normal range as defined here is not sufficient to cause overt neurological disease as one of the controls has an abnormal degree of asymmetry without accompanying clinical disease.

Quantitative analysis of cerebral hemisphere asymmetry of patients with chronic partial epilepsy has not previously been reported from MRI-based work. The fact that nine out of 18 patients with CD have volumetrically symmetrical hemispheres, despite the presence of dysgenesis, supports the hypothesis (Filipek *et al.*, 1994) that the achievement of this symmetry may represent a fundamental developmental aim (whatever its mechanism). However, nine out of 18 patients with CD do have a significant asymmetry. The fact that other patients with CD and similar electroclinical histories do not have such asymmetry argues against this finding being due to epilepsy itself and suggests instead that it is associated with the cause of the epilepsy. These patients may have a diffuse abnormality of the structure of the brain despite the focal nature of the visualized dysgenetic lesion.

This suggestion is confirmed, in the first quantitative MRI demonstration of the existence of extralesional structural change in the brains of patients with apparently focal cerebral dysgenesis, by the analysis of the regional distribution of grey and subcortical matter volumes. Whilst the patients with CD have many more abnormal values in total as a group when compared with either the controls or the patients with HS, the measure of chief interest is the number of abnormal values per subject, the threshold for normality of structural organization being taken as fewer than two abnormal values out of 80 in a given subject. No control subject has more than one abnormal value. On the other hand, all the patients with CD have two or more abnormalities. All of these patients therefore have structurally abnormal brains as defined. Fifteen of 18 patients with visually focal lesions have extralesional volumetric abnormalities. In particular, for example, 10 of the patients with CD have unilateral lesions only on MRI: nine of them have block or ratio abnormalities in the contralateral hemisphere which was reportedly normal on visual inspection. The visible lesion may thus simply be the most obvious manifestation of abnormal structure in an extensively disorganized brain. It is well known that epileptogenic regions may be distant from discrete MRI-detected lesions (Awad *et al.*, 1991; Fish *et al.*, 1991), and this is especially evident in patients with CD (Guerrini *et al.*, 1992; Raymond *et al.*, 1995). Presumably, distributed functional disruption may accompany distributed structural disorganization. The implication is that if the visualized abnormality in these 15 patients were excised, then it is unlikely that the patients would become seizure-free, as some (volumetrically) abnormal tissue would remain.

It is unlikely, however, that these patients will undergo surgery precisely because experience shows that they are unlikely to do well (Bruton, 1988; Engel, 1993). The prediction could, however, be tested either in those patients who will undergo surgery or in patients with other dysgenetic pathologies. We are currently analysing the preoperative scans of patients with histologically proven dysembryoplastic neuroepithelial tumours to test the equivalent hypothesis that patients with dysgenesis and extralesional volumetric abnormalities will fail to become seizure-free despite complete resection of the visible lesion.

It might be argued that the volumetric abnormalities in the brains of patients with CD are due to epilepsy, head injury or drug effects. It was for this reason that patients with isolated HS were analysed. In these patients, the HS alone was held responsible for the epilepsy: there was no evidence of any other associated lesion (Raymond *et al.*, 1994*b*). The clinical seizure histories, in terms of the occurrence of secondarily generalized seizures and duration of epilepsy, were not significantly different from the patients with CD, yet none of those with HS had a structurally abnormal brain as defined. Thus our findings in patients with CD cannot be ascribed to the effects of epilepsy, and are more likely to be associated with its cause.

The results also provide a tentative mechanism for the development of these abnormalities in terms of altered connectivity as proposed in the introduction. Thus, there are many abnormal grey matter:subcortical matter ratio values: all, notably, are increases above the upper limit of the normal range. This may be explained in a number of ways. First, it may be due to a pure increase in the non-neuronal component of the grey matter, i.e. the glia and blood vessels. However, there is very limited histopathological support for this idea, it being reported with any frequency only in focal cortical dysplasia and polymicrogyria with focal scarring (Barth, 1987). In some of these cases, Barkovich *et al.* (1992*b*) report increased MRI signal in the lesional areas. This was not seen in our cases and certainly not in the extralesional sites. Secondly, it may be due to a pure increase in the number of neurons in lesional and extralesional abnormal areas: however, the increase in grey matter is associated with a relative decrease in the accompanying white matter and thus it would be necessary to postulate that the increased number of neurons projected thinner axons. Such axons might have altered terminal arborization as compared with unthinned, normal axons (Mitchison, 1991) and thus connectivity would have to be altered. Thus a pure change in the number of neurons alone without altered connectivity

is also unlikely to explain the results. However, if the neuropil is considered altered in the first place, with increased local connectivity by axons not entering the white matter [as found by Ferrer *et al.* (1992) in one case], then the results can be more readily explained, whether the number of neurons is altered or not. Thus we believe that interneuronal connectivity changes may underlie our findings of regionally altered grey matter and subcortical matter block volumes and ratios. We emphasize that we have shown volumetric changes, and that our interpretation of these changes is in terms of altered connectivity: we do not suggest that these block and volume abnormalities necessarily represent further areas of CD in the currently accepted pathological sense (e.g. recognizable polymicrogyria, etc.). Thus, these extralesional areas may not become visible using other MRI sequences, even those that may detect dysgenetic lesions possibly not revealed by the SPGR sequence we have used (Bergin *et al.*, 1995). Local (Jones *et al.*, 1982) and widespread (Goldman-Rakic, 1980) alteration of connectivity is seen in animal experiments involving the disruption of corticogenesis. These animals, however, were not epileptic. Altered connectivity as inferred from dendritic changes is seen in humans with epilepsy and, for example, mental retardation (Huttenlocher, 1974; Purpura, 1974). Volumetric analysis of scans of such patients would be of considerable interest, especially as the scans themselves are often visually normal.

The results also demonstrate the importance of quantitative analysis of MRI data. This has already been shown, for example, in volumetric analysis of the hippocampi (Reutens *et al.*, 1993). We have shown that significant asymmetry of the cerebral hemispheres was found in nine of 18 patients with CD, though it had been reported on initial visual inspection in only two. These were patients 3 and 11, in whom hemispheres differ by over 10% in volume, whilst an asymmetry of over 4% is significant by our results. It is apparent, therefore, that significant quantitative changes in regions of interest in MRIs may not always be visible if these changes are small. In this study, reinspection of the original images did not reveal additional abnormalities in the extralesional abnormal blocks. Thus quantitation allows the extraction of more of the information present in a volumetric data set. In clinical use, the application of this technique to scans of patients with focal epilepsy and no visible abnormality ('cryptogenic epilepsy') may reveal the presence of volumetric abnormality that increases the vigour with which visualizable dysgenetic pathology is sought, and may lead to a revision of the proferred likelihood of rendering the patient seizure-free after therapeutic surgery.

In broader terms, the exploration of human disease has often increased understanding of normal structure and function. The extensive disruption demonstrated here highlights the presence, albeit at a gross macroscopic level, of extensive regional connectivity in the human brain. We are currently analysing further interrelationships between blocks within a given individual and the strength of these correlations across individuals to better understand structural organization in the human brain.

In conclusion, we have demonstrated the existence of extralesional volumetric abnormality of grey and subcortical matter in patients with CD and proposed a possible developmental mechanism for this, using a novel and quantitative method of analysis of volumetric MRI data. The methodology could be used for the investigation of other cerebral cortical diseases, such as other forms of epilepsy, mental retardation, dementia and schizophrenia.

Acknowledgements

We wish to thank the patients and the staff of the MRI unit at St Mary's Hospital, London and Dr J. S. Duncan for permission to study his patients. S.M.S. and S.L.F. are supported by the Wellcome Trust.

References

Andermann F. Brain structure in epilepsy. In: Shorvon SD, Fish DR, Andermann F, Bydder GM, Stefan H, editors. Magnetic resonance scanning and epilepsy. New York: Plenum Press, 1994: 21–7.

Awad IA, Rosenfeld J, Ahl J, Hahn JF, Luders H. Intractable epilepsy and structural lesions of the brain: mapping, resection strategies, and seizure outcome. Epilepsia 1991; 32: 179–86.

Barkovich AJ, Kjos BO. Gray matter heterotopias: MR characteristics and correlation with developmental and neurologic manifestations. Radiology 1992a; 182: 493–9.

Barkovich AJ, Kjos BO. Nonlissencephalic cortical dysplasias: correlation of imaging findings with clinical deficits [see comments]. AJNR AM J Neuroradiol 1992b; 13: 95–103. Comment in: AJNR Am J Neuroradiol 1992b; 13: 104–6.

Barron DH. An experimental analysis of some factors involved in the development of the fissure pattern of the cerebral cortex. J Exp Zool 1950; 113: 553–73.

Barth PG. Disorders of neuronal migration. [Review]. Can J Neurol Sci 1987; 14: 1–16.

Bergin PS, Fish DR, Shorvon SD, Oatridge A, deSouza NM, Bydder GM. Magnetic resonance imaging in partial epilepsy: additional abnormalities shown with fluid attenuated inversion recovery (FLAIR) pulse sequence. J Neurol Neurosurg Psychiatry 1995; 58: 439–43.

Bordarier C, Robain O, Rethore MO, Dulac O, Dhellemes C. Inverted neurons in agyria. A Golgi study of a case with abnormal chrosmosome 17. Hum Genet 1986; 73: 374–8.

Bruton CJ. The neuropathology of temporal lobe epilepsy. Oxford: Oxford University Press, 1988.

Choi BH, Matthias SC. Cortical dysplasia associated with massive ectopia of neurons and glial cells within the subarachnoid space. Acta Neuropathol (Berl) 1987; 73: 105–9.

Cowan WM, Fawcett JW, O'Leary DDM, Stanfield BB. Regressive events in neurogenesis. Science 1984; 225: 1258–65.

DeCarli C, Maisog J, Murphy DGM, Teichberg D, Rapoport SI, Horwitz B. Method for quantification of brain, ventricular and subarachnoid CSF volumes from MR images. J Comput Assist Tomogr 1992; 16: 274–84.

Engel J. Update on surgical treatment of the epilepsies: summary of The Second International Palm Desert Conference on the Surgical Treatment of the Epilepsies (1992). Neurology 1993; 43: 1612–17.

Farrell MA, DeRosa MJ, Curran JG, Lenard Secor D, Cornford ME, Comair YG, et al. Neuropathologic findings in cortical resections (including hemispherectomies) performed for the treatment of intractable childhood epilepsy. Acta Neuropathol (Berl) 1992; 83: 246–59.

Ferrer I. A Golgi analysis of unlayered polymicrogyria. Acta Neuropathol (Berl) 1984; 65: 69–76.

Ferrer I, Pineda M, Tallada M, Oliver B, Russi A, Oller L, et al. Abnormal local-circuit neurons in epilepsia partialis continua associated with focal cortical dysplasia. Acta Neuropathol (Berl) 1992; 83: 647–52.

Filipek PA, Kennedy DN, Caviness VS Jr, Rossnick SL, Spraggins TA, Starewicz PM. Magnetic resonance imaging-based morphometry: development and application to normal subjects. Ann Neurol 1989; 25: 61–7.

Filipek PA, Richelme C, Kennedy DN, Caviness VS Jr. The young adult human brain: an MRI-based morphometric analysis. Cereb Cortex 1994; 4: 344–60.

Fish D, Andermann F, Olivier A. Complex partial seizures and small posterior temporal or extratemporal structural lesions: surgical management. Neurology 1991; 41: 1781–4.

Galaburda AM, Kemper TL. Cytoarchitectonic abnormalities in developmental dyslexia: a case study. Ann Neurol 1979; 6: 94–100.

Goldman PS, Galkin TW. Prenatal removal of frontal association cortex in the fetal rhesus monkey: anatomical and functional consequences in postnatal life. Brain Res 1978; 152: 451–85.

Goldman-Rakic PS. Morphological consequences of prenatal injury to the primate brain. [Review]. Prog Brain Res 1980; 53: 3–19.

Goldman-Rakic PS. Topography of cognition: parallel distributed networks in primate association cortex. [Review]. Annu Rev Neurosci 1988; 11: 137–56.

Guerrini R, Dravet C, Raybaud C, Roger J, Bureau M, Battaglia A, et al. Epilepsy and focal gyral anomalies detected by MRI: electroclinico-morphological correlations and follow-up. Dev Med Child Neurol 1992; 34: 706–18.

Habib M. Anatomical asymmetries of the human cerebral cortex. [Review]. Int J Neurosci 1989; 47: 67–80.

Haug H. Remarks on the determination and significance of the gray cell coefficient. J Comp Neurol 1956; 104: 473–92.

Huttenlocher PR. Dendritic development in neocortex of children with mental defect and infantile spasms. Neurology 1974; 24: 203–10.

Jack CR Jr, Twomey CK, Zinsmeister AR, Sharbrough FW, Petersen RC, Cascino GD. Anterior temporal lobes and hippocampal formations: normative volumetric measurements from MR images in young adults. Radiology 1989; 172: 549–54.

Jones EG, Valentino KL, Fleshman JW Jr. Adjustment of connectivity in rat neocortex after prenatal destruction of precursor cells of layers II-IV. Brain Res 1982; 254: 425–31.

Kertesz A, Polk M, Black SE, Howell J. Anatomical asymmetries and functional laterality. Brain 1992; 115: 589–605.

Kuzniecky R, Garcia JH, Faught E, Morawetz RB. Cortical dysplasia in temporal lobe epilepsy: magnetic resonance imaging correlations. Ann Neurol 1991; 29: 293–8.

Marchal G, Andermann F, Tampieri D, Robitaille Y, Melanson D, Sinclair B, et al. Generalized cortical dysplasia manifested by diffusely thick cerebral cortex. Arch Neurol 1989; 46: 430–4.

Miller AKH, Alston RL, Corsellis JAN. Variation with age in the volumes of grey and white matter in the cerebral hemispheres of man: measurements with an image analyser. Neuropathol Appl Neurobiol 1980; 6: 119–32.

Mitchison G. Neuronal branching patterns and the economy of cortical wiring. Proc R Soc Lond B Biol Sci 1991; 245: 151–8.

Murphy DGM, DeCarli C, Schapiro MB, Rapoport SI, Horwitz B. Age-related differences in volumes of subcortical nuclei, brain matter, and cerebrospinal fluid in healthy men as measured with magnetic resonance imaging [published erratum appears in Arch Neurol 1994; 51: 60]. Arch Neurol 1992; 49: 839–45.

Murphy DGM, DeCarli C, Daly E, Haxby JV, Allen G, White BJ, et al. X-chromosome effects on female brain: a magnetic resonance imaging study of Turner's syndrome [see comments]. Lancet 1993; 342: 1197–200. Comment in: Lancet 1993; 342: 1188–9.

Palmini A, Andermann F, Olivier A, Tampieri D, Robitaille Y, Andermann E, et al. Focal neuronal migration disorders and intractable partial epilepsy: a study of 30 patients. [Review]. Ann Neurol 1991; 30: 741–9.

Pfefferbaum A, Mathalon DH, Sullivan EV, Rawles JM, Zipursky RB, Lim KO. A quantitative magnetic resonance imaging study of changes in brain morphology from infancy to late adulthood. Arch Neurol 1994; 51: 874–87.

Purpura DP. Dendritic spine 'dysgenesis' and mental retardation. Science 1974; 186: 1126–8.

Raymond AA, Cook MJC, Fish DR, Shorvon SD. Cortical dysgenesis in adults with epilepsy. In: Shorvon SD, Fish DR, Andermann F, Bydder GM, Stefan H, editors. Magnetic resonance scanning and epilepsy. New York: Plenum Press, 1994a: 89–94.

Raymond AA, Fish DR, Stevens JM, Cook MJ, Sisodiya SM, Shorvon SD. Association of hippocampal sclerosis with cortical dysgenesis in patients with epilepsy. Neurology 1994b; 44: 1841–5.

Raymond AA, Fish DR, Sisodiya SM, Alsanjari N, Stevens JM, Shorvon SD. Abnormalities of gyration, heterotopias, tuberous sclerosis, focal cortical dysplasia, microdysgenesis, dysembryoplastic neuroepithelial tumours and dysgenesis of the archicortex in epilepsy. Clinical, electroencephalographic and neuroimaging features in 100 adult patients. Brain. 1995. In press.

Reiss AL, Faruque F, Naidu S, Abrams M, Beaty T, Bryan RN, et al. Neuroanatomy of Rett syndrome: a volumetric imaging study. Ann Neurol 1993; 34: 227–34.

Reutens D, Cook M, Kingsley D, Kendall B, Moseley I, Free S, et al.

Volumetric MRI is essential for reliable detection of hippocampal asymmetry [abstract]. Epilepsia 1993; 34 Suppl 6: 138.

Richman DP, Stewart RM, Caviness VS Jr. Cerebral microgyria in a 27-week fetus: an architectonic and topographic analysis. J Neuropathol Exp Neurol 1974; 33: 374–84.

Rusinek H, de Leon MJ, George AE, Stylopoulos LA, Chandra R, Smith G, et al. Alzheimer disease: measuring loss of cerebral grey matter with MR imaging [see comments]. Radiology 1991; 178: 109–14. Comment in: Radiology 1991; 178: 22–4.

Sarnat HB. Cerebral Dysgenesis. New York: Oxford University Press, 1992.

Schlaepfer TE, Harris GJ, Yien AY, Peng LW, Lee S, Federman EB, et al. Decreased regional cortical gray matter volume in schizophrenia. Am J Psychiatry 1994; 151: 842–8.

Stewart RM, Richman DP, Caviness VS Jr. Lissencephaly and Pachygyria: an architectonic and topographical analysis. Acta Neuropathol (Berl) 1975; 31: 1–12.

Takada K, Becker LE, Chan F. Aberrant dendritic development in the human agyric cortex: a quantitative and qualitative Golgi study of two cases. Clin Neuropathol 1994; 7: 111–19.

Volpe JJ, Adams RD. Cerebro-hepato-renal syndrome of Zellweger: an inherited disorder of neuronal migration. Acta Neuropathol (Berl) 1972; 20: 175–98.

Weis S, Haug H, Holoubek B, Orun H. The cerebral dominances: quantitative morphology of the human cerebral cortex. Intern J Neurosci 1989; 47: 165–8.

Wieser HG, Engel J Jr, Williamson PD, Babb TL, Gloor P. Surgically remediable temporal lobe syndromes. In: Engel J Jr, editor. Surgical treatment of the epilepsies. 2nd ed. New York: Raven Press, 1993: 49–63.

Received November 22, 1994. Revised February 21, 1995. Accepted April 3, 1995

Appendix: protocols used for the definition of region of interest boundaries from MRIs

Cerebral hemispheres

Each cerebral hemisphere was isolated according to the following boundaries: dorsolaterally it was segmented along the natural boundary formed by its free surface; medially the hemispheres were separated along the interhemispheric fissure and the projection of this across the corpus callosum where this joined the hemispheres. If the corpus callosum was deformed, separation was performed along a perpendicular to the upper surface of the callosum dropped from the point of intersection of the interhemispheric fissure and the superior surface of the callosum. Inferomedially, the cerebral hemispheres were separated from the cerebellum posteriorly; further anteriorly, the cerebral hemispheres were dislocated from the superior colliculi; then from the cerebral peduncles along the shortest line from the base of the third ventricle in the midline to the ambient cistern along the bottom of the thalamus/pulvinar complex; further anteriorly, in coronal images, the suprapontine plane becomes apparent initially as an area of CSF in the middle of the brainstem: as soon as this became visible cerebral hemisphere separation was achieved along the shortest line from the base of the third ventricle to this point and thence across along the shortest line segment to the ambient cistern again. Further anteriorly still, the cerebral hemispheres were separated along the downward projection of the interhemispheric fissure, whilst making small deviations as required for medially placed gyri of either hemisphere.

Subcortical matter

The threshold for the subcortical matter was chosen in order to separate the cortex and white matter as closely as possible to the visually judged boundary between these two tissue types. Ultimately, this boundary can only be determined at a subcellular level, being the sum of all the points marking the emergence of the axon from the axon hillock. As this is clearly an impossible task currently, all determinations of this boundary, whether histological or on imaging must to some extent be approximate. In this case, the critical issue becomes less one of microscopic precision, provided the choice is anatomically sensible, and instead one of reproducibility. This is addressed in the reliability analysis. Except in the midline, the subcortical matter thus defined has its own natural boundary beneath the overlying cortical ribbon. Medially, the boundary, where not otherwise defined by the grey matter (e.g. in the corpus callosum), was drawn along the cerebral hemisphere boundary. However, in each cerebral hemisphere inferomedially a special boundary protocol was defined to account for the difficulty in reliable delineation of the thalamus and lentiform nucleus on the SPGR imaging sequence used for data acquisition. Thus, the thalamus was included entirely within the subcortical matter boundary, the medial aspect of this being identical to the cerebral hemisphere boundary. Laterally, the subinsular lentiform nucleus was also included in the subcortical matter as its distinction from the surrounding subcortical matter was not reliable. The subcortical matter boundary was traced along the cerebral hemisphere boundary inferomedially until the brainstem became separate from the cerebral hemisphere. At this point, the medial border was defined along the interthalamic adhesion only, the automatic boundary allocated by the workstation software not being altered inferior to this along the midline. Once the post-chiasmal optic tracts became visible as separate entities from the cerebral hemisphere, then the automatically determined medial boundary of the subcortical matter was not altered manually. Inferiorly, however, the lentiform nucleus was included in the subcortical matter region of interest: the boundary for this was chosen as the shortest line from the white matter overlying the posterior and medial orbital gyri to the infero-medial extremity of the internal capsule. In patients with ectopic grey matter (e.g. subcortical heterotopia or schizencephaly), this grey matter was

excluded from the subcortical matter region of interest and considered to be part of the grey matter.

The caudate nucleus

The caudate nucleus was isolated according to its natural boundaries as are readily apparent on coronal SPGR sequences, except that the internal capsule was bisected along its length to achieve dislocation from the lentiform nucleus and that the nucleus accumbens was included. Results of analysis of caudate volumes will be considered elsewhere.

These boundaries form easily determined regions of interest when used on coronal SPGR images: this is demonstrated by the reproducibility of the volumes obtained by summing the regions of interest produced according to the protocols.

J. Anat. (1996) 188, pp. 000–000, with 3 figures Printed in Great Britain

MRI-based surface area estimates in the normal adult human brain: evidence for structural organisation

SANJAY SISODIYA, SAMANTHA FREE, DAVID FISH AND SIMON SHORVON

Epilepsy Research Group, Institute of Neurology, London, UK

(*Accepted 26 September 1995*)

ABSTRACT

There are a number of quantitative relationships between geometric parameters describing the structure of the normal human cerebral cortex examined in vivo using volumetric magnetic resonance imaging. A voxel-counting method is used to estimate grey–white interface surface area. The effects of bias associated with the method are considered. In 33 normal controls, the cerebral hemispheres were symmetric in terms of total volume, irrespective of handedness, but not in terms of surface areas for right-handers. The surface area of the grey matter–white matter interface was directly proportional to the cortical grey matter volume, suggesting that growth of the neocortex is primarily tangential, with repetition of a basic structural element rather than gross alterations in the thickness of the cortex. The majority of the surface area of the grey–white interface lies within gyral white matter cores. The mean thickness of the cortex of the right cerebral hemisphere in vivo was 3.0 mm and that of the left 3.3 mm. There was a relationship between the cross-sectional area of the corpus callosum and grey–white interface surface area, suggesting that a fixed proportion of cortical neurons extend interhemispheric axons. These findings suggest that there are general architectural principles governing the organisation of the complex, but ordered, human cerebral cortex.

Key words: Cerebral cortex; volumetric imaging; brain measurement; cortical dysgenesis.

INTRODUCTION

The human brain is both extraordinarily complex and highly ordered. Stereological estimation of the total number of neurons from aged postmortem brains suggests that there are at least 14 billion neurons present in human neocortex in one hemisphere (Braendgaard et al. 1990); there may be up to 4000 synapses on a given neuron (Cherniak, 1990). However, the entire human genome is thought to contain fewer than 100000 genes (McKusick, 1979). Given this limitation in the total amount of genetic information available for specifying structure and connectivity, general principles determining the structure and development of the cortex must exist.

Evidence of cortical organisation and the ordered nature of development can be found in the adult brain at many levels of analysis, from the cellular to the macroscopic. One recently postulated regulation is that the 2 cerebral hemispheres should be of very similar total volume (Filipek et al. 1994). Whilst the mechanism of the generation of symmetry remains unknown, it seems clear that volumetric asymmetry of the hemispheres is associated with abnormal structure and function, for example in dysgenetic brains that support epileptogenesis (Sisodiya et al. 1995). Ordered structures supporting normal function are likely to arise from ordered development.

The folding of the cerebral cortex has also attracted much interest. Current thinking attributes folding to the growth of the neocortex due to expansion of the neuropil (Armstrong et al. 1991, 1995). This is postulated to be limited very largely to a tangential direction (Richman et al. 1975) with hardly any significant increase in cortical thickness even across species (Welker, 1990). Through evolution and in fetal development, the neocortex is thought to enlarge by replication of a basic columnar multicellular element, which is repeated and locally elaborated rather than fundamentally changed (Rockel et al. 1980). Bok

Correspondence to Dr S. M. Sisodiya, Epilepsy Research Group, Institute of Neurology, Queen Square, London WC1N 3BG, UK.

(1959) and Rockel et al. (1980) estimated the surface density of neurons and determined that this value is constant over a limited range of sample areas and subject numbers in dead human and mammalian brains. They also suggested that the proportion of neurons in each functional category for a given surface area was fixed. Thus reliable determination of cortical surface area might provide a means of estimating total, regional and function-specific neuronal numbers. A knowledge of the number of neurons, and the proportion allocated to a certain functional group, would be of importance in the further investigation of normal cortical organisation and its disruption.

Magnetic resonance imaging (MRI) has revolutionised the examination of the human cerebral cortex in vivo (Shorvon et al. 1994), providing unrivalled access to detailed quantitative information about the living brain. MRI data can furnish unbiased structural information, for example about object volumes by use of the Cavalieri principle (Mayhew & Olsen, 1991). Stereological methods also exist for the unbiased estimation of surface area of an arbitrary object from parallel slices through that object (Baddeley et al. 1986) and depend on satisfying certain conditions about the randomness of sampling. Unfortunately, these criteria cannot be met by data acquired for clinical purposes. We have used a model-based method of estimation of surface areas from volumetric MRI data. It is biased; we have, however, attempted to explore this bias and discuss its effects on our results.

The cortical grey matter (GM) is essentially a folded sheet with external (free) and internal (grey–white interface) surface areas. Ruppin et al. (1993) on theoretical grounds showed that a folded cortex increases processing efficiency in terms of usage of volume. Whilst all published data on cortical GM surface area measurements concern the free surface, the inner surface can be defined with greater precision globally on MR images. We have measured this surface and refer to it as the surface area of the subcortical matter (SM, defined here as the cerebral hemispheric white matter and subcortical nuclei). The SM surface area is a boundary created on MRI by intergyral arcuate (or 'U' fibres; Welker, 1990) and aggregating projectional fibres passing through this interface. Such projectional fibres are most plentiful in the walls and at the crowns of gyri and least numerous in the depths of the sulci (Welker, 1990).

We have sought to test the following hypotheses about the structure of the normal brain with our MRI data. (1) Cortical surface area (SM area in particular) should be symmetric between the 2 hemispheres. (2) Geometrically, *if* cortical thickness is indeed limited in its absolute range and variability, then SM surface area should correlate with cortical grey matter volume. (3) That the SM area should be highly folded so that the majority of its area should be in gyral cores, increasing area without greatly increasing volume. (4) If the finding by Rockel et al. (1980) of a fixed proportion of neurons under a given amount of cortical surface being functionally dedicated is generally applicable to the cortex as a whole, then a fixed proportion of cortical neurons should extend interhemispheric axons. There should be a linear correlation between the SM surface area and the cross-sectional area of the corpus callosum.

MATERIALS AND METHODS

Subjects

Thirty-three neurologically normal volunteer subjects, 11 female and 22 male, were scanned as part of a larger survey of structural abnormalities underlying chronic partial epilepsy. Their age range was 19–52 (median 29). All gave informed consent for the scanning procedure; scanning was approved by the ethics committee of the National Hospital for Neurology and Neurosurgery. 27 subjects were right-handed and 5 left-handed; handedness could not be ascertained for 1 subject. Inclusion of this subject in either the right or left-handed groups, or exclusion from the handedness analysis, did not alter the nature of the results.

Scanning

Images were acquired on a 1.5 T GE Sigma unit (GE, Milwaukee, USA). A coronal SPGR sequence was used for image analysis (TR 35 ms, TE 5 ms, 1 NEX, flip angle 35°, acquisition matrix 256 × 128, field of view 24 cm, producing 124 contiguous slices each 1.5 mm thick). Voxel dimensions in the plane of image segmentation were 0.9375 mm by 0.9375 mm. The position of the head in the head coil was central but random within limits dictated by the need to produce images that were suitable for a clinical study. No neocortical abnormalities were detected on inspection of the scans by an experienced neuroradiologist.

Image processing

Studies were transferred to an independent imaging workstation (Allegro, ISG Technologies, Canada).

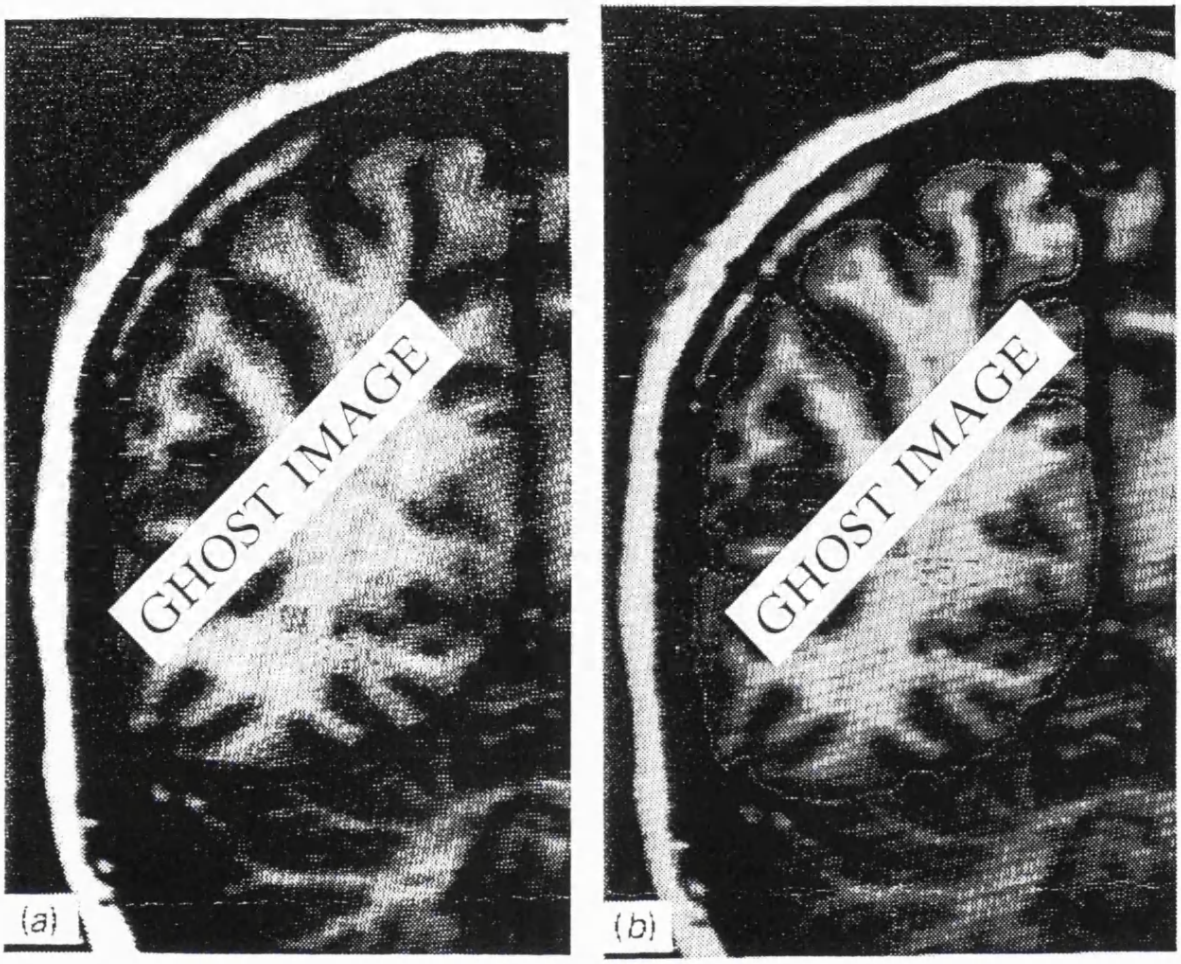

Fig. 1. Coronal MR images from normal subject illustrating segmentation boundaries. Image contrast was changed to enable the segmentation of the regions to be more easily visualised in the illustrations. (*a*) SM segmentation; (*b*) GM segmentation.

All images are automatically converted into an isotropic voxel format (voxel edge length 0.468 75 mm). Defined regions of interest were selected semiautomatically from the original images (segmentation). The procedure involved the selection of a threshold pixel intensity and the subsequent automatic growth of a region of interest (ROI), including all connected pixels within the threshold boundaries, from an initial seed placed by the operator. Manual interaction was required to edit the ROIs thus produced, for example, to separate overlying meninges from the true ROI. Cortical grey matter and subcortical matter boundaries (hemisphere white matter and subcortical nuclei) were isolated as detailed elsewhere (Sisodiya et al. 1995). The archicortex was included in the cortical grey matter ROI. Examples of the boundaries considered to enclose GM and, for the purposes of measurement of surface area and volume, SM, are shown in Figure 1. The coronally-acquired volumetric data set was reformatted in 3 mutually-perpendicular planes using the proprietary software and on these data an optimal interhemispheric plane of section was chosen to produce an approximately sagittal image through the smallest cross-sectional area of the corpus callosum, from which the cross-sectional area of this structure could be measured. The maximum length, L, of the corpus callosum was measured on each of these reformats. The maximum anterior–posterior extent of the corpus callosum, M, in the original data was determined from the number of coronal slices in which it was visible, knowing the thickness of each slice. Comparison of this length with that determined from the reformat gives a measure of the degree of rotation of the head in the scanner around axial and coronal axes such that:

$$M/L = \text{cosine (angle of rotation of head around axial axis)} \times \text{cosine (angle of rotation of head around coronal axis).}$$

Rotation around a sagittal axis will not affect this result. This ratio provides an internal measure of

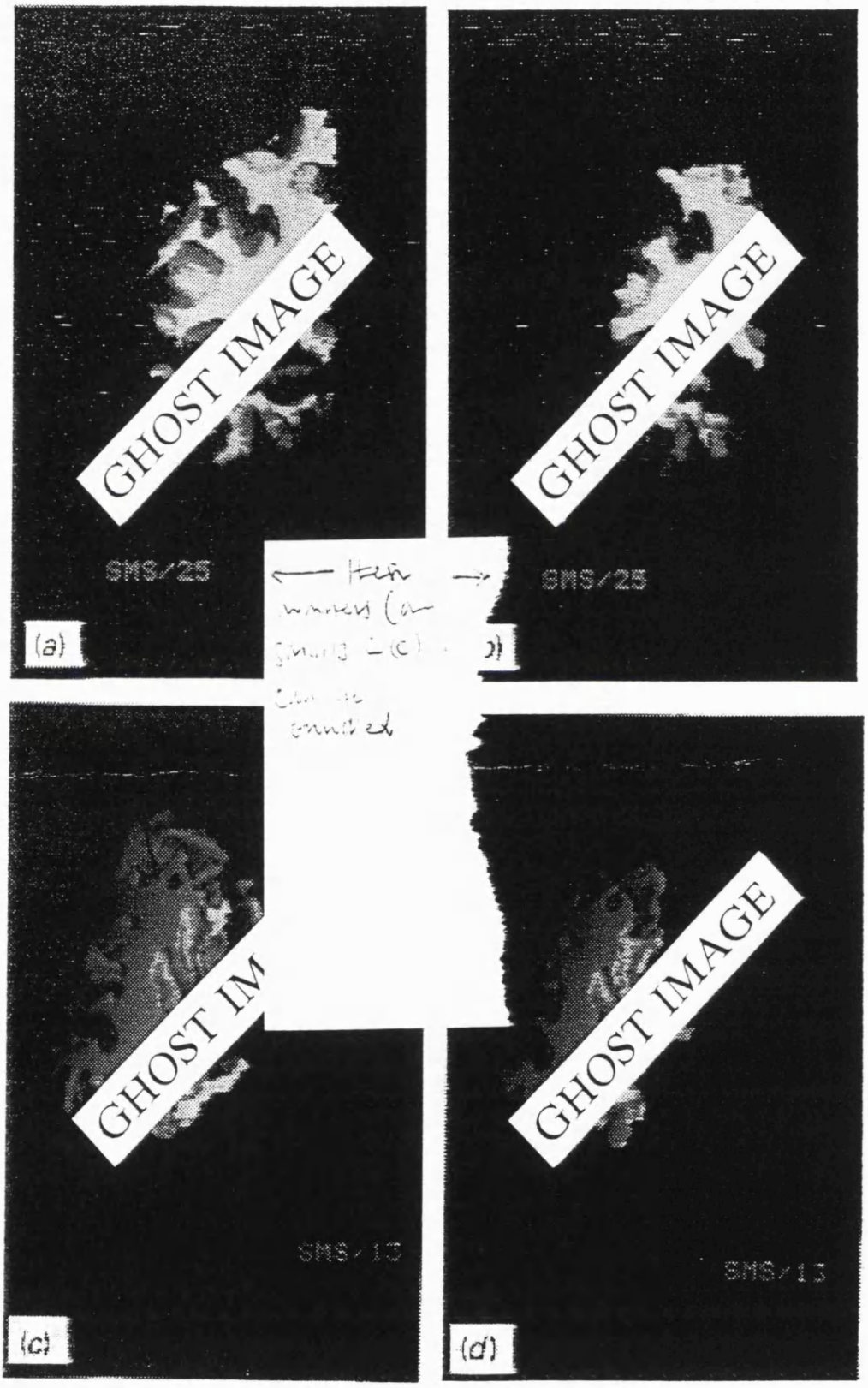

Fig. 2. Portion of SM (*a*, *c*, 1.5 cm thick) showing effect of pruning of an arbitrary 3 mm gyral cores from the surface. Note the smoother outline of the edited objects (*b*, *d*). (*a*) and (*b*) are viewed from the frontal pole; (*c*) and (*d*) are viewed from an inferolateral oblique projection.

relative head rotation between separate scans for a given individual.

Once ROIs were isolated in every relevant slice in a given study, they were reconstructed into 3-dimensional objects whose volume was automatically calculated by the workstation. In addition, using both

proprietary and in-house software, the number of voxels in the surface contour of each SM object was counted.

Estimation of bias: effect of head rotation and position in the scanner

The grey–white interface is a convoluted 3-dimensional contour, with a finite thickness. Its appearance on the coronal MRI slices depends partly on the orientation of the head with respect to the slices that scan it. This was not precisely fixed, although the range of variation of slice orientation with respect to major landmarks (e.g. the long axis of the corpus callosum) was limited by (1) the nature of scanning brains in vivo in the long tunnels of MRI machines, as subjects are required to lie supine and comfortably within the scanner and (2) the need to produce images that are readily comparable between subjects by visual inspection by a neuroradiologist. Coronal images of the hemispheres are the most commonly produced to allow detailed inspection of the pattern of gyration, sulcal depth, grey–white interface anatomy and white matter in order that abnormalities of these regions might be detected. Acquisition of data was therefore not isotropic about an arbitrary horizontal plane (e.g. the midsagittal plane).

The grey–white interface occupies voxels within these oriented slices according to its intensity characteristics and to its anatomy. Even slightly different positions of the head might alter the number of voxels occupied and thus the voxel count-based estimate of surface area. Determination of the effect of different mutual orientations of the head and the imaging slices was possible for 4 individuals who were rescanned (2 subjects twice each, 2 subjects 3 times) without attempting to align the brain to previous scanning positions. One of these subjects was scanned lying in a tilted prone and 2 different supine positions, effecting a radical alteration in imaging slice angle with respect to major brain axes. These scans were then segmented as usual and the relative intraindividual rotation in each case was estimated using the ratio M/L.

Geometric analyses

From the measured values of right and left subcortical matter volumes (SM_V, in cm^3), SM surface area (SM_A, in number of voxels) and corpus callosum cross-sectional area (CCA, in mm^2), various further parameters were derived.

1. *Predicted and extra-SM surface area derivatives.* For each hemisphere individually, the volume of the SM (SM_V) was considered to be spherical. From simple geometric considerations, it can be shown that the surface area of a sphere of volume SM_V is P_S such that:

$$P_S = 4\pi\left(\frac{3\sqrt{SM_V}}{4\pi}\right)^{\frac{2}{3}}$$

P_S was converted into a voxel count (P_A) enabling its manipulation and comparison with the voxel-counted surface area measured directly ($P_A = P_S/0.2197$, this constant factor being calculated from the surface area (0.468 75 mm^2) of one face of the cubic voxels constituting the SM surface contour in the proprietary imaging software). The extra-SM surface area, E_A, is the additional surface area of the SM produced by the folding (invagination and drawing out) of its surface and was defined as:

E_A = (measured surface area) − (predicted surface area)
$= SM_A - P_A$.

Thus predicted, P_A, and extra, E_A, surface area values were derived for the SM of each hemisphere.

An estimation of the contribution to the surface voxel count made by the white matter core of the gyri was assessed in 10 subjects. This was performed by manual editing of the initial segmentation in each of 10 continguous slices from a posterior portion of 1 hemisphere, in a position in which gyral white matter cores had been imaged such that they lay parallel to the coronal slices, minimising overprojection and maximising their distinction. The 10 slices constituted an approximately cylindrical portion of the hemisphere. The segmentation was completely edited so that all white matter protrusions less than an arbitrary 3 mm in diameter were removed (Fig. 2). The aim was to create a smooth, unfolded SM surface and determine what effect this had on the area and volume measures. The figure of 3 mm chosen as a preliminary investigation suggested that most gyral white matter cores were of a smaller diameter. The surface voxel number and volume of SM objects derived from these 10 slices before and after this editing were measured. In addition, the surface area of a cylinder of the same volume as the original unedited cylindrical portion of the SM was calculated. The extra surface area present on the real object as a result of folding of the SM within this region was determined by subtraction of the predicted surface area of this isovolumic object from the measured surface area of the original object.

2. *Calculation of mean cortical grey matter thickness.* Across the control group, mean cortical thick-

ness for each entire hemisphere was calculated according to:

$$\text{Thickness (mm)} = \frac{\text{GM volume}}{\text{SM surface area}}$$

where the GM volume is in mm^3 and the area is SM_A voxels × 0.2197 mm^2/voxel.

Reliability

The reliability of the segmentation procedure, for GM and SM volumes-of-interest, has been documented elsewhere (Sisodiya et al. 1995). The segmentation has been shown to be highly reproducible. The ratio of the volume of the smallest to the largest repeat GM segmentation for a given subject was always greater than 98% for hemispheres segmented by a given operator (mean for 8 separate hemispheres, 5 copies of each: 98.7%). The corresponding figure for the SM was 95% (mean for 8 separate hemispheres, 5 copies of each: 97%). For interrater reliability assessment, the mean ratio of the volume of the smallest to the largest cerebral hemisphere was 97.6%, and for the SM 94.3% (for 16 separate hemispheres segmented by 2 independent raters).

The surface voxel counts for repeat segmentations of the SM were noted, to determine the variation introduced by segmentation alone. For 8 hemispheres segmented 5 times each by a single observer, the mean ratio of minimum to maximum voxel count was 0.97 (S.D. 0.011, range 0.938–0.994). For 8 separate hemispheres segmented by 2 operators, the mean minimum to maximum ratio was 0.98 (range 0.95–1.00).

Statistics

Analysis was performed using SPSS for Windows, Version 6.1 (SPSS Inc., Chicago). Spearman rank correlation coefficients were used for the pruning experiment results, whilst elsewhere Pearson correlation coefficients were used. Grouped results were compared using specified tests for paired or independent samples. Significance was taken at the 0.05 level. Standard deviation values of mean results are presented in brackets after mean results. Statistics for the group of left-handers are also presented, though the number in this group is small: exclusion of left-handers from the whole group did not alter the nature of the findings in the remaining right-handers.

Throughout the rest of the paper, abbreviations prefixed R apply to parameters referring to the right cerebral hemisphere, and those prefixed L, to the left hemisphere.

RESULTS

Effects of head orientation

For the 6 pairs of repeat segmentations of 4 individuals scanned in different positions, the minimum value of the ratio of the surface voxel counts for a given hemisphere was 0.947 for the right hemisphere and 0.948 for the left hemisphere. The full results, including the estimate of head rotation, M/L, are given in Table 1. The repeat segmentations were not included in the following results.

Measured hemisphere surface areas and volumes

Mean values for these parameters are presented in Table 2. The ratio of the volume of the entire L hemisphere (GM + SM) to the volume of the entire R hemisphere is 0.999 (0.013). There is no significant difference between right and left-handers or between the sexes for this measure. Only 1 subject had a volume ratio more than 3 S.D.s from the mean (actual value, 1.042).

There was no significant difference between right and left-handers as separate groups for the following variables in isolation: right SM_A, E_A, P_A; right SM, GM, total hemisphere volume; left SM_A, E_A, P_A; left SM, GM, total hemisphere volume.

For right-handers, SM_A, E_A, and P_A were bigger on the right than on the left (t test $P < 0.0005$). There was no significant difference for the left-handers for SM_A ($P = 0.225$), or E_A; P_A was significantly larger on the right than the left ($P = 0.016$). For right-handers, grey matter volume was significantly higher, and subcortical matter volume significantly lower, on the left compared with the right (t test, $P < 0.0005$). The same holds true for the left-handers separately (P values 0.023 and 0.017, respectively).

Values of total cerebral volume, right and left hemisphere volume, right and left GM volume, and right and left SM surface voxel counts are significantly higher for male subjects than for female subjects (t test, $P < 0.002$ for all variables). However, hemisphere SM areas corrected (by division) for total cerebral volume or for hemisphere GM volume are not significantly different between the sexes.

Predicted and extra surface areas

Based on the formulae presented in the Methods section, the mean values for males and females for the

Table 1. *Effect of head orientation on voxel counts: repeat scan results**

Subject	Scan pair	Right SM_A voxel count: Old	Right SM_A voxel count: New	Ratio smaller/larger	Left SM_A voxel count: Old	Left SM_A voxel count: New	Ratio smaller/larger	M/L 1st scan/2nd scan
1	1–2	316586	310414	0.981	328745	313821	0.955	0.9766 0.9870
1	1–3 (prone)	316586	317591	0.997	328745	328107	0.998	0.9766 0.9103 (prone)
2	1–2	375775	383539	0.980	376634	382788	0.984	0.9631 1.0000
3	1–2	374206	373012	0.997	360939	370055	0.975	0.9697 0.9751
4	1–2	409306	401894	0.982	409429	387995	0.948	0.9583 0.9888
4	1–3	409306	387544	0.947	409429	392416	0.958	0.9583 0.9746

* Results are presented for voxel count of SM for the original scan (scan 1; 'old' results) in comparison with voxel counts from repeat scan (scan number 2 or 3; 'new' results) for the right and left hemispheres. The values of M/L allow comparison of the degree of rotation for a *given* subject between separate scans.

Table 2. *Mean (S.D.) measured hemisphere surface areas and volumes for males and females*

	R	L
Males		
Surface area (SM_A, number of voxels)	390900 (24300)	378300 (23400)
GM volume (cm^3)	263 (28)	272 (28)
SM volume (cm^3)	261 (25)	245 (21)
Females		
SM_A	342500 (37500)	336700 (32300)
GM volume	225 (21)	235 (24)
SM volume	229 (36)	222 (31)

GM, cortical grey matter; SM, subcortical matter (hemisphere white matter and subcortical nuclei).

Table 3. *Mean predicted and extra-SM surface area values for each hemisphere*

Voxel count	R	L
Predicted area (P_A)	75900 (6640)	73300 (5570)
Extra area (E_A)	298900 (31040)	291100 (28200)

predicted (P_A) surface area of the RSM and LSM, and the extra right and left SM surface area (E_A), are presented in Table 3. There was no significant sex difference for these measures when they were corrected either for total segmented volume or ipsilateral hemisphere grey matter volume. Hence male and female subjects were grouped, as there was no effect of sex independent of brain size and future analyses will compare surface areas measured with those expected given brain size.

The proportion of the measured SM surface area (SM_A) that is extra surface area (E_A) is high and significantly different (*t* test, $P = 0.002$) for the sexes. For males, the mean value of E_A/SM_A was 80.0% (0.8%) for the RSM and 80.2% (0.9%) for the LSM; for females, the values for RSM and LSM were 79.1% (0.4%) and 79.2% (0.5%) respectively. There was no significant difference between the 2 hemispheres either for right or left-handers.

For the blocks of SM edited arbitrarily such that all white matter protrusions less than 3 mm in diameter were removed, the mean percentage loss in volume produced for the 9 subjects was 22%, and the mean percentage loss in surface area significantly greater at 41% (Mann–Whitney, $P < 0.0005$). The measured loss of surface voxel count produced by the editing correlated highly with the calculated extra surface area of each subject due to folding of the surface of the object (Spearman correlation coefficient 0.95, $P < 0.0005$).

Correlation between GM volumes and SM surface area measures

For the group as a whole, the coefficients for the correlations (Pearson) between GM volume, log GM volumes, and the actual and extra-SM surface area measures and their logarithmic values within a given

Table 4. *Volume-area correlation coefficients*

	R				L			
	SM_A	E	log SM_A	log E	SM_A	E	log SM_A	log E
GM	0.51*	0.54†	0.49*	0.52*	0.66‡	0.69‡	0.65‡	0.62‡
log GM	0.51*	0.54†	0.49*	0.52*	0.66‡	0.69‡	0.66‡	0.63‡

Significance of Pearson correlation coefficients: * at $P < 0.005$; † at $P = 0.001$; ‡ $P < 0.0005$. SM_A, total subcortical matter area; E_A, extra-SM matter area; all logs to base 10.

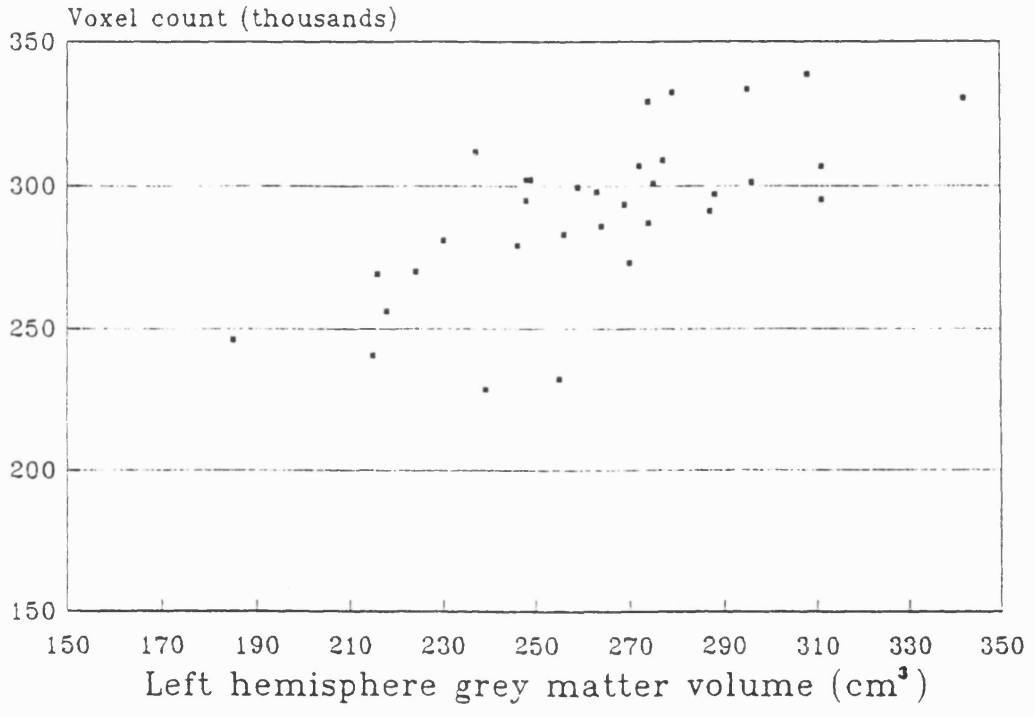

Fig. 3. Plot of E_A (extra-SM area) against GM volume for the left hemisphere for 33 controls. The correlation coefficient is 0.69 ($P < 0.0005$).

hemisphere are presented in Table 4. Both for R and L hemispheres, there was a significant correlation between the measured SM surface area and the volume of the GM. The correlation was increased when the extra-SM surface area was considered. Neither log–linear nor log–log correlations were higher than the linear correlation coefficients. A plot of extra-SM area against GM volume for the left hemisphere is shown in Figure 3.

Mean cortical grey matter thickness

The mean values for cortical thickness of the R hemisphere was 3.0 mm (0.37) and for the L, 3.3 mm (0.32). Left cortical thickness was greater than right cortical thickness in all groups. There was no significant sex or handedness difference for hemispheric cortical thickness.

Corpus callosum cross-sectional area and correlations

The mean area of the corpus callosum (CCA) was 696 mm^2 (S.D. 73), with no significant sex or handedness difference. Across the group, CCA correlated highly with the R extra-SM surface (E_A) area ($r = 0.5404$, $P = 0.002$) and with the L extra-SM area (E_A) ($r = 0.4844$, $P = 0.004$).

DISCUSSION

Methodology

The recognition of the grey–white interface is important both for the understanding of normal brain structure and its disruption in pathological conditions, such as cortical dysgenesis (Raymond et al. 1995). It defines the extent and volume of both the grey matter

and the white matter. Ultimately this interface can only be determined at a subcellular microscopic level, being the sum of the junctions of the axon hillock and axon. Currently this is an impossible task and surrogates for this measure must be employed. The method used to define a contour will determine its observed characteristics: the method may be the position of a colour change if histological stains are used, or it may be the position where signal of white matter intensity begins to predominate on MR images. These images are composed of voxels which have both an intensity value and a position that can be determined. The 'biological' grey–white interface will occupy a certain configuration of voxels in the volumetric data set. This configuration will depend on both the biology of the real interface (its 'thickness' and anatomy) and the position of this interface in voxel space within the scanner. One might imagine that more voxels will be occupied by the same interface in certain positions than in other positions.

Consider a contour placed in a space composed of identical voxels, the surface area of the contour being determined, as above, by the number of voxels (of the containing space) even partly intruded upon by the surface. If the surface contour is the size and shape of a single voxel (edge length 1 unit), minimally, this surface could be oriented to occupy a single voxel of its containing space producing a surface area figure of 1. On the other hand, it could be ~~rotated~~ in 3 dimensions to intrude on 12 voxels. Thus orientation alone could make a difference of 12-fold to the observed voxel count that would represent this surface. Consider extending the surface contour so that whilst it remains cubical, its edge is now 1.1 units long. Minimally, this surface occupies 8 voxels in the original voxel space, whilst maximally it can still only intrude upon 12. Thus the impact of orientation in voxel space on this slightly less regular or more 'complex' (with regard to its embedding space) surface is reduced. If the surface in question is now made a rectangular cuboid composed of 2 unit voxels with 1 common face, the ratio of maximum to minimum voxel occupation produced by orientation changes will be less than 12-fold, as all voxels even partly intruded upon by the common face of 1 voxel will already have been intruded upon by the other voxel through this common face. Thus increasing complexity of the surface contour will reduce the effect of orientation of the contour in voxel space.

For surfaces which are any more complex, such thought experiments become very difficult, and the bias introduced by orientation can only be estimated empirically. For this reason, 4 brains scanned in different orientations were studied. The results show that for even radical changes in orientation (in the subject who was scanned supine and tilted prone), the change in the voxel count produced is equal to or less than the variation produced by repeat segmentation of a single study alone. Empirically, therefore, for these 4 brains, it would appear that whilst orientation does have an effect on the voxel count, the complex nature of the SM surface with respect to the imaging slices is such that this effect is small, and much smaller than the range of measured surface voxel counts across the entire subject group.

To extrapolate the finding that orientation has a small effect on voxel count to all the brains in the study would presuppose that all the brains are of equal complexity: such assumptions may be the downfall of model-based derivations of structural parameters (Gundersen, 1986). However, we have in fact estimated the complexity of all the SM surfaces in this report using 3-dimensional fractal analysis of the SM surface, based on a dilation technique (S. Free, unpublished observations). This analysis shows that the complexity of the SM surfaces—in an orientation, size and shape-independent analysis—of our normal subjects is in fact remarkably similar across the subjects (range for right SM surface: 2.27–2.31; range for left SM surface 2.28–2.31). Therefore we feel that the assumption that all the SM surfaces are approximately of equal complexity is not unfounded or unsustainable. Thus although bias is introduced by the nonstereological methodology employed, it is calculable and very limited for this group of subjects; the results are robust to the impact of brain orientation in the scanner.

Stereological quantitation of surface areas is possible from vertical slices as revealed by Baddeley et al. (1989). Ideally, we would have used the elegant methodology propounded by these workers and employed already in the estimation of surface areas from postmortem data (Henery & Mayhew, 1989). However, there are a number of clinical restraints on data acquisition that prevent this methodology being used. Most importantly, the data were not collected with random (isotropic) orientation of imaging planes with respect to the horizontal plane. Isotropic orientation is possible with current MRI technology; the plane of acquisition may be made isotropic random with respect to an arbitrary horizontal plane without the subject needing to be moved, and is indeed one of the great advantages of MRI. However, each image series in all subjects needs, as far as possible, to be visually comparable, particularly with respect to neocortical structure and the hippocampus (by

orienting the imaging plane approximately perpendicular to the axis of the hippocampus, partial volume effects on this structure are minimised and this is important for the clinical context of the scans (Cook et al. 1992)). Isotropic sectioning would impair intersubject visual comparison and greatly reduce the clinical value of scans that are analysed, almost invariably, by eye. Large series of brains are likely to be acquired in a clinical setting, and visual analysis is likely to remain the favoured methodology. We should make clear that reformatting of the data is possible, but this will not create a new isotropic data set: the grey–white interface has already been converted into voxels at the moment of imaging and reformatting cannot now make it randomly *acquired*.

Gundersen (1986) stated that biased, nonstereological analyses are hampered because experimenters need to deal with 'only a vague idea about the significance of the bias which cannot be estimated in any non-trivial case'. Whilst we acknowledge the 'scientific effectiveness' and simplicity of stereological analyses, in practice it may not be possible to apply such methods to all data sets. We have attempted to quantify the order of the bias arising from the nonstereological analysis. We have shown that it is small with respect to biological variability, presumably a result of the complexity of the grey–white interface.

As discussed above, the exact numerical characteristics of the 'real' grey–white interface cannot currently be analysed. All estimates will depend on part at least on the method used to derive those estimates—including visual assessment on macroscopic slices. The grey–white interface in our data is composed of a number of voxels: how these relate to the 'real' interface cannot be determined, and will depend on the variables of biological interest—the anatomy of the interface and its thickness—and head orientation. We have already addressed the error that orientation may generate. In none of our cases was there a history of neurological disease or of blurring of the grey–white interface on the images when inspected by an experienced neuroradiologist. Thus we feel that the voxel count that we derive is a measure of the anatomy of the 'real' interface, and given the absence of blurring in any of our cases, more particularly a measure of the surface extent of the grey–white interface.

Volume and area measures and correlations

To our knowledge this is the first report of white matter surface area measures in living brains, although Henery & Mayhew raised the possibility of making cortical surface area measurements in vivo from MR images in 1989.

Area and volume measures. The total range of variation of surface voxel counts of the SM is large (from 287070 to 448335 voxels). The range of variation for GM and total hemisphere volumes is also large. Male brains are larger than female brains for all these parameters. However, when corrected for total brain size, there is no significant difference between male and female SM areas or grey volumes. We can estimate what the surface area might be in real square centimetre terms using the fact that the interface contour is designed to be single voxel thickness and 8-connected within the computer, and that the calculated length of the edge of the isotropic voxels that compose the surface is 0.46875 mm. As each voxel contributes at least a single face to the surface of the contour, the minimum calculated mean surface area of the SM surface of the right hemisphere is 82450 mm^2, and of the left hemisphere, 80200 mm^2. The only reason for doing this is to compare these figures with the areas derived by other workers using other methods. Henery & Mayhew (1989) estimated the outer surface area of the grey matter using stereological methodology on postmortem specimens, and derived values of 63800–80700 mm^2 for the right hemisphere and 72000–83700 mm^2 for the left. Postmortem aged (mean age 80 yr) brains from diseased subjects were used. Shrinkage of the human brain is known to occur after the age of 50 yr (Miller et al. 1980; Haug, 1987), so that these values are probably lower than might be found for younger brains as in our sample. Nevertheless, our MRI values for the surface area of the SM are in approximately the same range as histologically-derived surface area values for the free cortical surface. Absolute validation for the value of the SM surface areas produced by our methodology will never be possible because the area will always depend on the method used to investigate it (even if its position is determined by visual inspection); we have shown that it is a fractal surface, so that there may be no 'absolute' value for its surface area, only methodology and scale-specific ones (~~Free et al. 1995~~). Provided comparisons between subjects are kept within a given analytic framework, however, the data will still be useful.

Our contention that the white matter cores within gyri contribute little volume to the SM, but increase its surface area greatly is supported by the finding that the ratio of extra-SM area to the total SM area (the ratio E_A/SM_A) is high. This is the impression gained from Figure 2, the gyral cores being fat 'spikes' on the

surface of the white matter core (like the spines on a porcupine, contributing little volume but much surface area in comparison to the body). Measurement of the surface area of a block of SM before and after arbitrary but defined pruning supports this proposition: the removal of all protruding white matter cores 3 mm or less in diameter leads to a mean loss of 41.2% of the surface area, but significantly less volume loss (21.7%). The observed loss of surface area correlates significantly with the calculated extra surface area obtained by considering the volume of the block to be in the form of a cylinder and subtracting the predicted surface area for this from the observed original surface area. That the observed loss and calculated extra surface area are not identical may simply be because an arbitrary (though defined) white matter core size of 3 mm was specified; real gyral cores have various diameters and shapes, and a more sophisticated method might have been to remove cores depending on individual brain size. The aim, however, was to demonstrate a principle. The experiment shows that the extra-SM area, E_A, may be taken as an estimate of the surface area of the gyral cores, that is the area directly overlain by cortical grey matter in gyral crowns and walls rather than in sulcal depths. It is known that the (nonuniform) density of projectional fibres is much lower in sulcal depths than in gyral crowns and walls (Welker, 1990): thus E_A is a better average measure of projectional axon numbers (and hence total neuronal numbers as proposed by Rockel et al. 1980) than the total SM area, SM_A, and may be considered to be more biologically relevant. In brains where grey matter is pathologically thickened (for example as a result of lissencephaly), E_A may be a better measure of projectional neuronal numbers than either SM_A or grey matter volume itself.

Our volume results support the contention of Filipek et al. (1994) that symmetry between the hemispheres may be 'rigorously developmentally regulated': the mean ratio of the volume of the entire left hemisphere to that of the entire right hemisphere is 0.999, irrespective of handedness. The importance of such findings is highlighted by the demonstration that loss of this normal symmetry is associated with abnormal cortical function in some cases (Sisodiya et al. 1995). The extra-SM surface area, E_A, however, is not symmetrical for right-handers, being larger on the right than on the left. For right-handers, that total cortical volume is symmetric whilst extra-SM surface area is not may permit the reconciliation of volume symmetry and cytoarchitectural and gyral anatomical asymmetries in the normal brain (Bear et al. 1986; Rademacher et al. 1993). We have found that grey matter volume is significantly higher and subcortical matter volume significantly lower on the left than on the right for right-handers, with similar findings for left-handers. One interpretation of the data is that, for right-handers, there are fewer projectional neurons on the left than on the right (E_A difference), but more neuropil per neuron (grey matter volume difference). It has been suggested that the right and left hemispheres may have differing processing roles and this has been supported by the demonstration of differences in the proportions of grey and white matter between the hemispheres using other techniques (Gur et al. 1979). We have too few left-handers in the sample overall to determine whether these differences apply to them also, though it remains important to separate the lacterality analyses for right and left-handers in case there is a difference.

Volume-area correlations: mean cortical thickness. We have shown that the measured SM surface area correlates linearly with the volume of the overlying GM in vivo. Log–log and log–linear correlations do not improve on the linear correlation. Haug (1987) showed a linear correlation for humans between cortical surface area and brain volume, but this was determined from a study of dead brains and brain volume was not clearly defined. It is not intuitively obvious that a surface area of a complex object and its volume should be linearly related: for spheres, for example, the surface area is related to the two-thirds power of the volume; for an infinitely prickly hedgehog with infinitesimal volume, the surface area would be an infinite power of the volume. For real folded objects, a power relationship of surface area to volume somewhere between indicates that the object surface is folded, and the magnitude of the power is a measure of the degree of folding. For the SM as a real object, the degree of folding is characterised by a power relationship of surface area to volume of 1.

Thus, as cortical grey matter volume increases, as a consequence so too does SM surface area *in direct proportion*. This implies that, although GM thickness in a single individual does vary ~~across~~ the extent of the cortex (Welker, 1990) and even over a single gyrus (von Economo, 1929), this variation is not significantly different across our range of normal subjects: increase in GM volume would not seem to be achieved from one brain to another by an alteration in the range of thicknesses of the cortex between normal brains. Indeed, there are theoretical grounds for believing that there is a limit to cortical thickness (Prothero & Sundsten, 1984). Our results are compatible with the hypothesis that cortical growth is associated with an increase in the number of basic

modules that are functionally organised in parallel vertical columns, or with expansion of their associated neuropil (Mountcastle, 1978; Rockel et al. 1980; Hofman, 1985), rather than with an alteration in the basic constitution of such columns. It might be speculated that in this way less genetic information would be required to specify the entire entity of the cortex, some general principles applied to basic building blocks being sufficient.

That cortical thickness in the normal human brain only varies over a limited range in absolute terms (both across species and within a single species; Welker, 1990) allows the meaningful calculation of a mean value for cortical thickness. Over our entire control group (66 hemispheres), we derive a value of 3.2 mm. This compares with a value of 2.5 mm (range 4.5 to 1.3 mm) calculated by von Economo (1929), about 1.9 to 3.1 mm given by Rockel et al. (1980) and 2.1 to 2.5 mm reported by Henery & Mayhew (1989): all these values were derived from dead human brains. Whilst the thickness of the GM can be measured in certain areas of the cortex directly from volumetric MRI data, it is impossible currently to do this over the entire extent of the GM as in the depths of sulci, on MRI, GM from adjacent gyri may abut and thus the free cortical surface cannot be defined precisely. In addition, the definition of a line measuring cortical thickness at any particular point is complicated by the 3-dimensional, anisotropic nature of the cortical ribbon. We are not aware of any other MRI-based report of the mean thickness of the GM in vivo.

Rockel et al. (1980), using a number of mammalian brains and 2 human brains, found that across species, in a limited number of regions in each brain, the surface density of neurons was relatively constant (except in visual cortex). Given that cortical thickness varies in a limited and uniform way across individuals, the cortical free surface is likely to relate linearly to the extra-SM surface. Thus the extra-SM area should correlate with the total number of neurons and provide an estimate of this in the normally developed brain. The extra-SM area also correlates with the total GM volume in the normal brain. GM is composed of neurons and, mostly, of neuropil (Haug, 1956): thus extra-SM area should predict the amount of neuropil. On the basis of this MRI evidence, the amount of neuropil in the normal brain would appear to be a constant proportion of the total GM volume, as suggested on histological grounds by Haug (1987). Measured deviations on MR images from these proportionalities in an area of interest should therefore suggest that either the number of neurons or their associated neuropil is abnormal within that region. Regionalisation of the measures may increase their utility and power: Haug (1987) used stereological techniques and reported relatively constant local surface densities for neurons in specified regions of the brain.

Whilst confirmation of these suggested principles across the entire cerebrum requires experimental determination of neuron density in a much more widespread (but not necessarily more intensive) fashion than has yet been performed, predictions may be tested in surgically resected areas of abnormal (for example, epileptogenic dysgenetic) cortex.

Corpus callosum area and cerebral connectivity. Our results for the area of the corpus callosum are in accord with those of other workers who have estimated the cross-sectional area of the corpus callosum (CCA) from MRI data (Kertesz et al. 1987; Laissy et al. 1993) and postmortem material (Blinkov & Glezer, 1968). We have examined the relationship between the CCA and various surface and volume measures. Histopathological studies of the human corpus callosum (Tomasch, 1954; Aboitiz et al. 1992) suggest that in the normal brain, CCA correlates with the number of fibres of passage. Kertesz et al. (1987) did not find any correlation between CCA and a biased estimate of brain size (from a single nonrandom axial slice): we were not able to demonstrate significant correlation between CCA and GM or SM volumes. However, we have shown that CCA does correlate with the extra-SM surface area of both hemispheres separately. We suggest that this is because the extra-SM area value is a surrogate for the total number of projectional neurons in each hemisphere, the proportion of this number extending interhemispheric axons being fixed in a normal brain (Rockel et al. 1980). An abnormal ratio of CCA to extra-SM area with normal grey matter volume should indicate an extensive abnormality of interhemispheric connectivity. Although some studies suggest that handedness has an effect on callosal area (Witelson, 1985), a large study of 52 right and left-handers showed that handedness and sex had no effect on callosal area measured on MRI (Kertesz et al. 1987).

CONCLUSION

Our approach makes use of the large amount of data available in volumetric MRI scans, much of which may be inaccessible to visual analysis alone. There would indeed appear to be general relationships describing the structure of the brain and suggesting that there may be general structural principles guiding its construction. The correlation of surface area with

tissue volumes and other area measurements, such as those of the corpus callosum, may provide a way in which cortical organisation and its disruption may be investigated in vivo. Thus it might be predicted, for example, that in an area of lissencephaly (Barth, 1987) the absolute amount of extra-SM area would be reduced, the relationship between a local volume of GM and the underlying extra-SM area would be altered, producing a calculable thickening of the cortex, and the actual CCA reduced compared with that predicted, suggesting that interhemispheric connectivity was reduced and that the reduced contribution to the extra-SM area made by thickened cortex was due to reduced projection from lamina III neurons. This may also allow the detection of small areas of abnormal cortical organisation. Analysis of the maldeveloped brain may be of clinical value (Shorvon et al. 1994) and might cast further light on developmental principles guiding the formation of the human cerebral cortex.

ACKNOWLEDGEMENTS

We would like to thank the anonymous reviewers for their comments. The project was supported by the Wellcome Trust.

REFERENCES

ABOITIZ F, SCHEIBEL AB, FISHER RS, ZAIDEL E (1992) Fiber composition of the human corpus callosum. *Brain Research* **598**, 143–153.

ARMSTRONG E, CURTIS M, BUXHOEVEDEN DP, FREGOE C, ZILLES K, CASANOVA M et al. (1991) Cortical gyrification in the Rhesus monkey: a test of the mechanical folding hypothesis. *Cerebral Cortex* **1**, 426–432.

ARMSTRONG E, SCHLEICHER A, OMRAN H, CURTIS M, ZILLES K (1995) The ontogeny of human gyrification. *Cerebral Cortex* **5**, 56–63.

BADDELEY AJ, GUNDERSEN HJG, CRUZ-ORIVE LM (1986) Estimation of surface area from vertical sections. *Journal of Microscopy* **142**, 259–276.

BARTH PG (1987) Disorders of neuronal migration. *Canadian Journal of Neurological Sciences* **14**, 1–16.

BEAR D, SCHIFF D, SAVER J, GREENBERG M, FREEMAN R (1986) Quantitative analysis of cerebral asymmetries. Fronto-occipital correlation, sexual dimorphism and association with handedness. *Archives of Neurology* **43**, 598–603.

BLINKOV SM, GLEZER II (1968) *The Human Brain in Figures and Tables. A Quantitative Handbook*. New York: Plenum Press.

BOK ST (1959) *Histonomy of the Cerebral Cortex*. Amsterdam: Elsevier.

BRAENDGAARD H, EVANS SM, HOWARD CV, GUNDERSEN HJG (1990) The total number of neurons in the human neocortex unbiasedly estimated using optical disectors. *Journal of Microscopy* **157**, 285–304.

CHERNIAK C (1990) The bounded brain: toward quantitative neuroanatomy. *Journal of Cognitive Neuroscience* **2**, 58–68.

COOK MJ, FISH DR, SHORVON SD, STRAUGHAN K, STEVENS JM (1992) Hippocampal volumetric and morphometric studies in frontal and temporal lobe epilepsy. *Brain* **115**, 1001–1015.

FILIPEK PA, RICHELME C, KENNEDY DN, CAVINESS VS JR (1994) The young adult human brain, an MRI-based morphometric analysis. *Cerebral Cortex* **4**, 344–360.

GUNDERSEN HJG (1986) Stereology of arbitrary particles. A review of unbiased number and size estimators and the presentation of some new ones, in memory of William R. Thompson. *Journal of Microscopy* **143**, 3–45.

GUR RC, PACKER IK, HUNGERBUHLER JP, REIVICH M, OBRIST WD, AMARNEK WS et al. (1979) Differences in the distribution of gray and white matter in human cerebral hemispheres. *Science* **207**, 1226–1228.

HAUG H (1956) Remarks on the determination and significance of the gray cell coefficient. *Journal of Comparative Neurology* **104**, 473–492.

HAUG H (1987) Brain sizes, surfaces, and neuronal sizes of the cortex cerebri: a stereological investigation of man and his variability and a comparison with some mammals (primates, whales, marsupials, insectivores, and one elephant). *American Journal of Anatomy* **180**, 126–142.

HENERY CC, MAYHEW TM (1989) The cerebrum and cerebellum of the fixed human brain: efficient and unbiased estimates of volumes and cortical surface areas. *Journal of Anatomy* **167**, 167–180.

HOFMAN MA (1985) Size and shape of the cerebral cortex in mammals. *Brain Behaviour and Evolution* **27**, 28–40.

KERTESZ A, POLK M, HOWELL J, BLACK SE (1987) Cerebral dominance, sex, and callosal size in MRI. *Neurology* **37**, 1385–1387.

LAISSY JP, PATRUX B, DUCHATEAU C, HANNEQUIN D, HUGONET P, AIT-YAHIA H et al. (1993) Midsagittal MR measurements of the corpus callosum in healthy subjects and diseased patients: a prospective survey. *American Journal of Neuroradiology* **14**, 145–154.

MAYHEW TM, OLSEN DR (1991) Magnetic resonance imaging (MRI) and model-free estimates of brain volume determined using the Cavalieri principle. *Journal of Anatomy* **178**, 133–144.

MCKUSICK VA (1979) *Mendelian Inheritance in Man*. Baltimore: Johns Hopkins University Press.

MILLER AKH, ALSTON RL, CORSELLIS JAN (1980) Variation with age in the volumes of grey and white matter in the cerebral hemispheres of man: measurements with an image analyser. *Neuropathology and Applied Neurobiology* **6**, 119–132.

MOUNTCASTLE VB (1978) An organizing principle for cerebral function: the unit module and the distributed system. In *The Mindful Brain: Cortical Organisation and the Group-selective Theory of Higher Brain Function* (ed. G. M. Edelman & V. B. Mountcastle), pp. 7–50. Cambridge, Mass.: MIT Press.

PROTHERO JW, SUNDSTEN JW (1984) Folding of the cerebral in mammals: a scaling model. *Brain, Behaviour and Evolution* **24**, 152–167.

RADEMACHER J, CAVINESS VS, STEINMETZ H, GALABURDA AM (1993) Topological variation of the human primary cortices: implications for neuroimaging, brain mapping and neurobiology. *Cerebral Cortex* **3**, 313–329.

RAYMOND AA, FISH DR, SISODIYA SM, ALSANJARI N, STEVENS JM, SHORVON SD (1995) Abnormalities of gyration, heterotopias, tuberous sclerosis, focal cortical dysplasia, microdysgenesis, dysembryoplastic neuroepithelial tumours and dysgenesis of the archicortex in epilepsy. Clinical, electroencephalographic and neuroimaging features in 100 adult patients. *Brain* **118**, 629–660.

RICHMAN DP, STEWART RM, HUTCHINSON JW, CAVINESS VS (1975) Mechanical model of brain convolutional development. Pathologic and experimental data suggest a model based on differential growth within the cerebral cortex. *Science* **189**, 18–21.

ROCKEL AJ, HIORNS RW, POWELL TPS (1980) The basic uniformity in structure of the neocortex. *Brain* **103**, 221–244.

RUPPIN E, SCHWARTZ EL, YESHURUN Y (1993) Examining the volume efficiency of the cortical architecture in a multi-processor network model. *Biological Cybernetics* **70**, 89–94.

SHORVON SD, FISH DR, ANDERMANN F, BYDDER GM, STEFAN H (ed.) (1994) *Magnetic Resonance Scanning and Epilepsy*. New York: Plenum Press.

SISODIYA SM, FREE SL, STEVENS JM, FISH DR, SHORVON SD (1995) Widespread cerebral structural changes in patients with cortical dysgenesis and epilepsy. *Brain* in press

TOMASCH J (1954) Size, distribution, and number of fibres in the human corpus callosum. *Anatomical Record* **119**, 119–135.

published
Brain 118, 1039 – 1050

VON ECONOMO C (1929) The cytoarchitectonics of the human cerebral cortex. London: Oxford University Press.

WELKER W (1990) Why does cerebral cortex fissure and fold? A review of determinants of gyri and sulci. In *Cerebral Cortex* **8B** (ed. E. G. Jones & A. Peters), pp. 3–136. New York: Plenum Press.

WITELSON S (1985) The brain connection: the corpus callosum is larger in left-handers. *Science* **229**, 665–668.

ORIGINAL CONTRIBUTION

The Demonstration of Gyral Abnormalities in Patients With Cryptogenic Partial Epilepsy Using Three-Dimensional MRI

Sanjay M. Sisodiya, MA, MRCP; John M. Stevens, DRACR, FRCR; David R. Fish, MD, FRCP; Samantha L. Free, PhD; Simon D. Shorvon, MD, FRCP

Background: Despite the use of high-resolution magnetic resonance imaging (MRI) in the demonstration of structural abnormalities underlying chronic partial epilepsy, a significant proportion of MRI scans in such cases still appear normal when viewed conventionally as two-dimensional images, especially in extratemporal epilepsies.

Objectives: To increase the yield of MRI in patients with extratemporal epilepsies. To examine specific regions of three-dimensional surface renderings of the cerebral hemispheres.

Design: Postprocessing of volumetric MRI data was used to detect abnormalities of gyration that may not be seen otherwise.

Setting: Scans were obtained at a hospital clinical imaging facility.

Participants: Sixty-four subjects were studied: 33 controls, 15 patients with hippocampal sclerosis (as disease controls), and 16 patients with cryptogenic partial epilepsy that on clinical grounds was extratemporal.

Main Outcome Measures: Gyral patterns were evaluated for abnormality by visual comparison between subjects.

Results: Inspection of the routine two-dimensional images had failed to demonstrate relevant underlying neocortical abnormality in any of the patients' scans. Three-dimensional reconstruction revealed abnormal gyral patterns in the frontal lobe convexity in seven of the 16 cryptogenic clinically extratemporal cases. Macrogyria was revealed in one case and increased gyral complexity with altered disposition was seen in six cases. Similar gyral patterns were not seen in any subjects from the other groups.

Conclusion: Three-dimensional analysis of volumetric MRI data can reveal structural abnormality that is not visible when the data are viewed as two-dimensional images only.

(Arch Neurol. 1996;53:28-34)

From the Epilepsy Research Group, Institute of Neurology (Drs Sisodiya, Stevens, Fish, Free, and Shorvon), and Department of Neuroradiology, The National Hospital for Neurology and Neurosurgery (Dr Stevens), London, England; and the National Society for Epilepsy, Chalfont Centre for Epilepsy, Bucks, England (Drs Sisodiya, Stevens, Fish, Free, and Shorvon).

THE DETECTION of underlying structural abnormality in the cerebral cortex plays an important role in the management of patients with chronic partial epilepsy,[1] and this detection may in some cases encourage consideration of a possible surgical approach to therapy.[2] Magnetic resonance imaging (MRI) has revolutionized the examination of the cerebral hemispheres in vivo[3]; lesions have been demonstrated in a high proportion of patients previously believed to have cryptogenic partial epilepsy.[4] While the majority of patients with refractory partial epilepsy have mesial temporal seizure onset due to hippocampal sclerosis, extratemporal seizures occur in approximately one fifth of patients with partial epilepsy, with frontal lobe seizures most common in this group.[5,6]

In 1989, Swartz et al[7] presented a series of patients with frontal lobe epilepsy who were studied using 0.5-T MRI and positron emission tomography. On MRI, abnormalities were noted in 46% of their cases. Despite the use of higher-resolution machines, volumetric scanning, and reformatting, this figure has not been improved on; thus, even today up to 50% of cases with frontal lobe epilepsy may have normal scans.[8,9] This perhaps should not be surprising. The cerebral cortex is a convoluted three-dimensional structure and abnormalities in its surface gyration that represent underlying pathologic cortical architecture[10] may not be appreciated when it is viewed in two-dimensional slices. Such gyral abnormalities may only be seen when the cerebral hemispheres are viewed as uncut three-dimensional structures. Three-dimensional reconstruction of MRI data has

See Subjects and Methods on next page

SUBJECTS AND METHODS

SUBJECTS

Control subjects were neurologically normal volunteers drawn from staff at our institution and their colleagues. Their ages ranged from 19 to 52 years (median age, 30 years), 22 were men and 11 were women. All gave informed consent for the scanning procedure; scanning was approved by the ethics committee of the National Hospital for Neurology and Neurosurgery. Patients were drawn from the outpatient clinics at the National Hospital and the Chalfont Centre for Epilepsy. Thirty-one patients with partial epilepsy were studied. Fifteen patients (age range, 18 to 38 years) had isolated hippocampal sclerosis identified on MRI and confirmed histologically in 10; no other lesions were seen on routine inspection of the MRI. The 10 patients who underwent surgery were free of seizures postoperatively (minimum follow-up period, 12 months). Sixteen patients (age range, 18 to 60 years) had extratemporal seizures, most probably frontal, on clinical grounds (historical and interictal electroencephalographic [EEG] evidence only in three, additional videotelemetric data in 13). These patients were selected because no lesion had been seen on routine MRI (see below). One patient (patient 7) had had a temporal lobectomy at another medical center, but seizures returned with unchanged ictal semiology and increased frequency and he was referred to our center for further evaluation.

METHODS

Magnetic resonance imaging was performed on a 1.5-T scanner (GE Signa, General Electric, Milwaukee, Wis). A coronal SPGR sequence was used for image analysis (repetition time [TR], 35 milliseconds; echo time [TE], 5 milliseconds; number of excitations [NEX], 1; flip angle, 35°; acquisition matrix, 256×128; and field of view, 24 cm, producing 124 contiguous slices each 1.5 mm thick). Sagittal T_1-weighted (TR, 500 milliseconds; TE, 10 milliseconds; and NEX, 2) and axial proton density (TR, 2800 milliseconds; TE, 30 milliseconds; and NEX, 1) and T_2-weighted images (TR, 2800 milliseconds; TE, 90 milliseconds; and NEX, 1) were also routinely acquired. The scans were inspected by one of us (J.M.S., an experienced neuroradiologist) specifically looking for abnormalities of the pattern of gyration, sulcal depth, and cortical thickness and the pattern of the gray-white interface.

THREE-DIMENSIONAL RECONSTRUCTION AND COMPARISON

Studies were transferred to an independent imaging workstation (Allegro, ISG Technologies, Toronto, Ontario). This allowed the semiautomated selection of defined regions of interest (ROIs) from the original (coronal) images (segmentation). The procedure involved the selection of a threshold pixel intensity and the subsequent automatic growth of an ROI, including all connected pixels within the threshold boundaries, from an initial seed placed by the operator. Manual interaction was required to edit the ROIs, for example, to separate overlying meninges from the true ROIs. The ROI boundaries were the free cortical surfaces of the cerebral hemispheres. The ROIs were stacked by the workstation to produce three-dimensional images; approximately 20 minutes of operator interaction were required for the entire process in a single subject. Three-dimensional reconstructions were displayed on a high-resolution 54-cm monitor. The reconstructions could be magnified and rotated. They were lit by on-screen computer-generated light sources that could be moved with respect to the reconstructed objects.

The dorsolateral aspects of the frontal lobes in the three-dimensional reconstructions of each patient were compared with those from each control subject, each patient, and with normal subjects' sulcal patterns from a published atlas.[13] Each surface rendering could therefore be compared with 88 others. Abnormalities of the gyral pattern were determined by this comparison, performed by two operators (S.M.S. and J.M.S.), both blinded to each individual patient's clinical details. The following specific features were examined: (1) gyral width—gyri broader or narrower than neighboring gyri or those in the contralateral hemisphere or any disproportionate with the size of the brain in comparison with other subjects; (2) gyral disposition—gyri could be of normal dimensions but abnormally positioned or terminated with respect to other neighboring gyri so that unique patterns were formed; and (3) gyral complexity—regions where additional gyri were present, possibly associated with either abnormal gyral width or abnormal gyral disposition. Abnormalities of the gyral pattern were defined as configurations, identified by these criteria, not seen in controls or in more than one other patient.

After reconstruction and comparison, the original two-dimensional images were reinspected by the neuroradiologist (J.M.S.) to see if the abnormalities detected in three-dimensional images could be picked up with hindsight; however, in no case was this possible.

RELIABILITY

The use of reconstructive techniques in the generation of three-dimensional renderings is well established; the appearance of rendered images is robust to the most important step in the generation of the images, that of the choice of threshold values.[14] The stability of the choice of the threshold was determined by repeating the choice of the lower threshold limit for a given ROI (the upper limit was fixed for all cases) over a period of time. In three control subjects, the choice was repeated four times over 1 month. In 53 subjects (controls and patients), it was repeated twice over an interval of 18 months. The Pearson correlation coefficient for the threshold repetitions was .988 ($P<.005$).

The segmentation of the ROIs was repeated in five subjects four times each at intervals throughout the study. This was performed by one operator (S.M.S.). In addition, the entire segmentation process was repeated for eight subjects by another operator (S.L.F.) blinded to the segmentation produced by the first operator. The resulting images and volumes were compared to determine the overall intrarater and interrater reliability of the choice of the threshold, boundaries, and editing. The repeated renderings did not appear different on inspection. Reliability as determined by volume measures has been previously reported and was high.[15] Thus, the choice of threshold, the choice of boundary, and the manual editing are all highly reproducible, both on qualitative and quantitative grounds.

Clinical, EEG, and Two- and Three-Dimensional MRI Data on Patients*

Patient No./ Age at Scan, y/ Sex/Age at Onset, y	Clinical Details and Seizure Semiology	EEG Interictal; Ictal	MRI, Two/Three Dimensional
1/33/F/7 (Figure 1)	Mild L hemiparesis; nocturnal CPS (>40/night), L thigh tingling, UL posturing (L>R), LL stiffening, clonic movements of L limbs, for 20 to 30 s	Excess slow waves, higher voltage on R; generalized attentuation before attack, arising from non-REM sleep	Normal/area of focal broadening R middle frontal gyrus
2/22/M/7 (Figure 2)	Tingling aura L shin, grimacing, stiffening L. hip and knee flexion, ankle eversion, then clonic movements of L leg and SGS most nights	Vertex epileptic activity, field suggestive of horizontal dipole, often seen with small lesions; first ictal changes in R central region, where postictal slow activity also predominant	Normal/increased complexity of R middle frontal gyrus (arrows)
3/36/F/8 (Figure 3)	Familial (onset in daughter at 6 y); brief attacks (six per night) from sleep with grimacing, dystonic posturing UL. then LL; clonic movements at end of seizure; immediate recovery of consciousness	Rare sharp transient over L temporal region; no changes before attack when muscle artifact obscures record	Normal/increased complexity L middle frontal gyrus (arrows)
4/60/M/40 (Figure 4)	CPS with head turning to L and abnormal movements of R arm; brief attacks, up to 200/d	Frequent sharp waves, or sharp–slow wave complexes maximal at F_3, also bilateral sharp–slow wave complexes; no ictal changes	Only generalized cortical atrophy/generalized atrophy apparent, abnormal gyral configuration in L frontal lobe with stellate appearance of superior and middle frontal gyri
5/43/F/12 (Figure 5)	Brief nocturnal CPS (20/night), bilateral tonic posturing UL, then LL; immediate recovery; rare SGS	Bilateral independent frontal temporal epileptiform discharges; ictal nonlocalizing	Normal/increased gyral complexity over middle frontal gyrus (arrows)
6/27/F/7 (Figure 6)	CPS (seven per d), brief; early cessation of respiration, then R limb dystonic posturing and occasional rhythmic jerking of whole body	Occasional sharp waves over F_3; ictal EEG unchanged initially, then obscured by artifact	Normal/stellate appearance, L frontal gyri (arrows), as in patient 4
7/27/M/9 (Figure 7)	Previous R temporal lobectomy, but seizures recurred after 4 y with unchanged semiology: fidgeting all four limbs, complex automatisms; frequent, brief attacks	Depth studies showed interictal spiking activity on R frontal electrode; rhythmic slow activity on same electrode, first ictal change noted suggesting onset in R frontal convexity; no evidence for onset in R temporal stump	R temporal lobectomy noted/abnormal gyral pattern, anteriorly R frontal lobe involving middle and inferior frontal gyri (arrows)

**EEG indicates electroencephalogram; MRI, magnetic resonance imaging; CPS, complex partial seizures; UL, upper limbs; LL, lower limbs; REM, rapid eye movement; and SGS, secondarily generalized seizures. For the two-dimensional MRI, the results are given of visual inspection by the neuroradiologist of the routinely printed two-dimensional images; for the three-dimensional MRI, the results are given of inspection of the three-dimensional reconstructed images.*

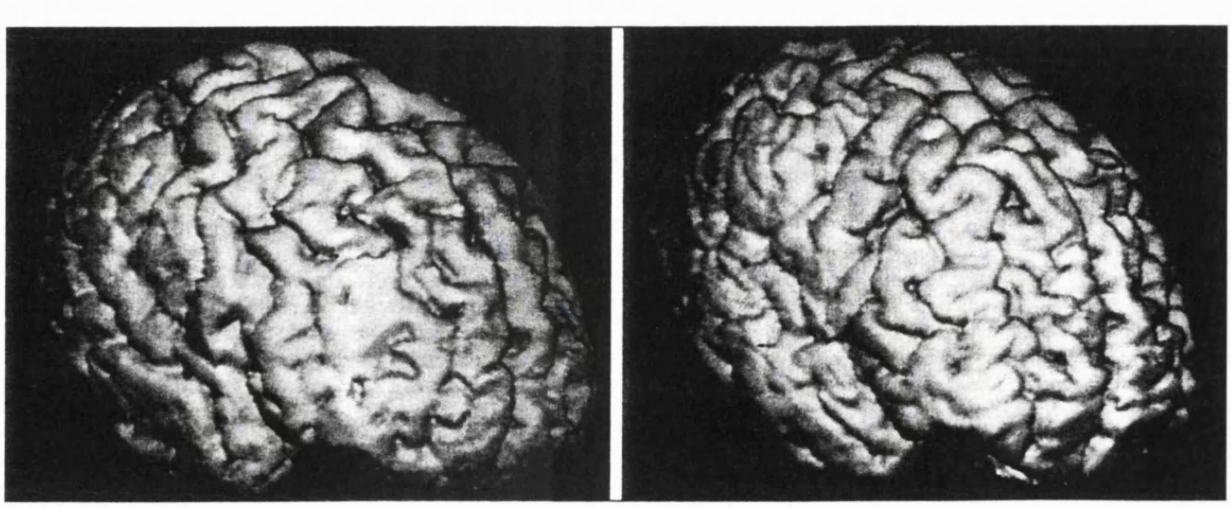

Figure 1. *Brain of patient 1 (left) and normal subject (right). See Table for details.*

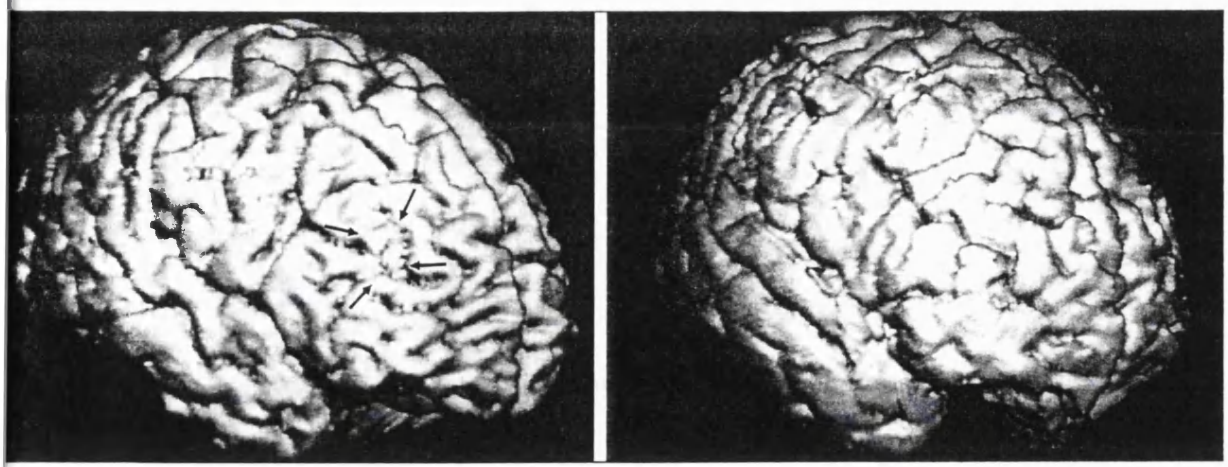

re 2. *Brain of patient 2 (left) and normal subject (right). See Table for details.*

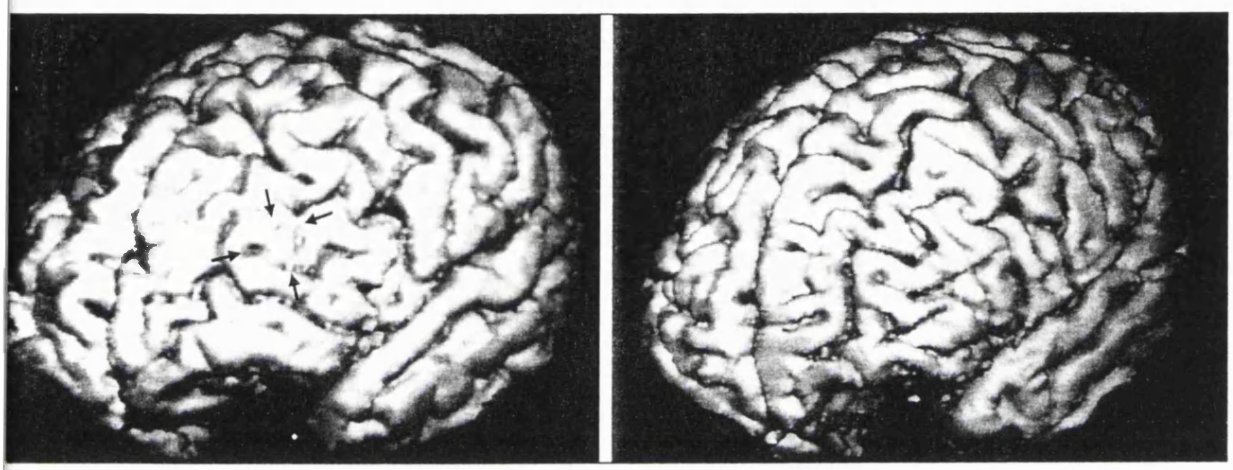

re 3. *Brain of patient 3 (left) and normal subject (right). See Table for details.*

n applied to neurosurgical planning[11] and to the more cise location and delineation of *known* lesions,[12] but not, our knowledge, to the revelation of possible lesions in any ies in which routine inspection of the two-dimensional ages was normal.

In this report, we describe a postprocessing study 16 patients with electroclinical histories suggesting an ratemporal (probably frontal lobe) seizure disorder in om routine visual inspection of two-dimensional im- s from a volumetric MRI scan did not reveal any ab- rmalities. We reconstructed their scan data into com- ter-resident three-dimensional images and examined dorsolateral convexity of the frontal lobe. By com- ring the gyral anatomy of these subjects with the pat- n seen in control subjects and patients with epilepsy e to mesial temporal sclerosis, we sought to identify ruption of the normal pattern of gyration in the fron- lobe. We have correlated our structural findings with zure types. We discuss the possible significance of the monstrated abnormalities with respect to epileptogen- s in these individuals and the use of the technique in neral.

RESULTS

n visual inspection of the two-dimensional images, none the controls' scans were thought to have any neocortical abnormality. Only one of the 31 patients with partial epilepsy had any neocortical abnormality identified on inspection of the two-dimensional images: this was a previous right temporal lobectomy in patient 7. This patient, however, had a frontal seizure disorder.

Of the 16 patients with extratemporal epilepsy, seven had an abnormality of the gyral pattern in the frontal lobe convexity on the reconstructed three-dimensional images. The clinical details, seizure semiology, and interictal and ictal EEG data for these eight patients are given in the **Table**. For each patient the result of the initial MRI, routinely inspected in two-dimensional slices, is also provided; in addition, a description is given of the appearance of the three-dimensional reconstructions. For each patient, the three-dimensional reconstruction illustrated in each Figure, left, is shown alongside a reconstruction in approximately the same projection of a normal subject in each Figure, right (**Figure 1** through **Figure 7** as referenced in the Table).

The observed frontal lobe gyral abnormalities in five of the reported cases were seen only in one patient each; none of the other 88 cases (controls, other patients, and those reported in the published atlas) had a similar pattern. Only patients 4 and 6 had similar abnormalities on reconstruction, but these changes were not seen in any of the other 87 cases compared.

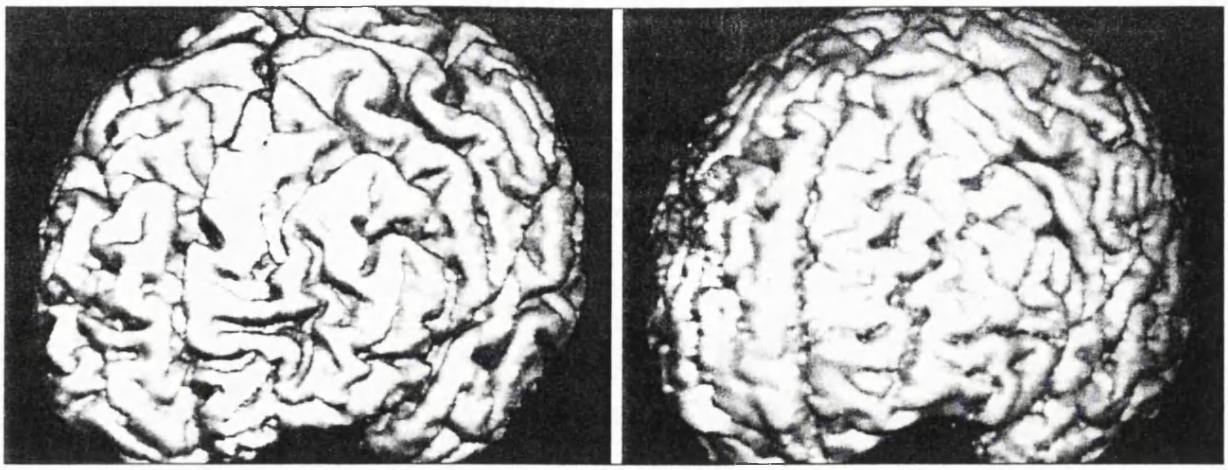

Figure 4. *Brain of patient 4 (left) and normal subject (right). See Table for details.*

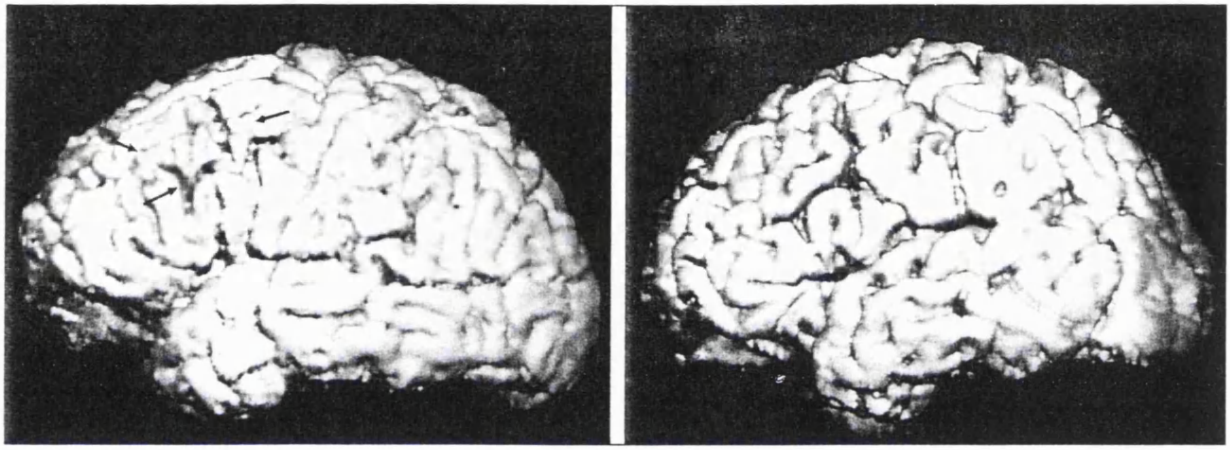

Figure 5. *Brain of patient 5 (left) and normal subject (right). See Table for details.*

COMMENT

Human gyral variability may be considerable; even monozygotic twins may have discordant gyral patterns.[16] This has been determined by analysis of two-dimensional images. Three-dimensional models of a "normal" brain have been synthesized to account for variability in gyral patterns for surgical and coregistration purposes.[17] These models deform brains anisotropically and produce an "average" brain by sophisticated superimposition of the modified images. While such techniques allow objective comparisons to be made, individual detail is modified or lost by deformation and averaging of data from numerous individuals. Such individual detail relates closely to cytoarchitectonic fields and may provide a better guide to functional localization than does reference to an idealized brain.[18] We have chosen to visually examine individual brains in the hope of identifying subtle alterations in the gyral pattern that may relate to underlying cytoarchitectonic changes. This method is more time consuming; its subjectivity was minimized by blinding the raters to the nature of an individual subject's seizure localization based on electroclinical information. In this group, the individual gyral patterns seen in each of five subjects were not seen in the other 88 subjects. In two cases, similar changes were seen that were not present in the other 87. We therefore believe that the changes in these eight subjects are abnormal and represent intrinsic lesions.

The detection of a structural abnormality is important for extratemporal epilepsy surgery.[19-21] For frontal lobe epilepsy, the most common extratemporal seizure disorder, clinical features of the seizure remain important in localization of seizure onset[9,22]; surface EEG data may be unhelpful and even misleading.[9,23] Depth electrode studies are often performed for further localization, but occasionally these too are unhelpful[9] and are not free of risk. Magnetic resonance imaging has been shown to be of value, though even high-quality MRI may be normal when a lesion is present.[9] Approximately 50% of high-resolution MRI scans in patients with frontal lobe epilepsy are reportedly normal on inspection of two-dimensional images alone.[8,9] We have shown that reconstructive techniques may reveal gyral abnormalities in seven (44%) of 16 such cases.

In these seven patients, there is electroclinical correlation with the demonstrated abnormalities. Based on intracranial EEG and surgical evidence, Bancaud and Talairach[23] have listed clinical and EEG features suggestive of dorsolateral frontal lobe seizures. Thus, patients 1 through 3, 5, and 6 have clinical seizure patterns typically manifest from abnormalities in the intermediate dorsolateral frontal lobe cortex (ie, superior and middle frontal

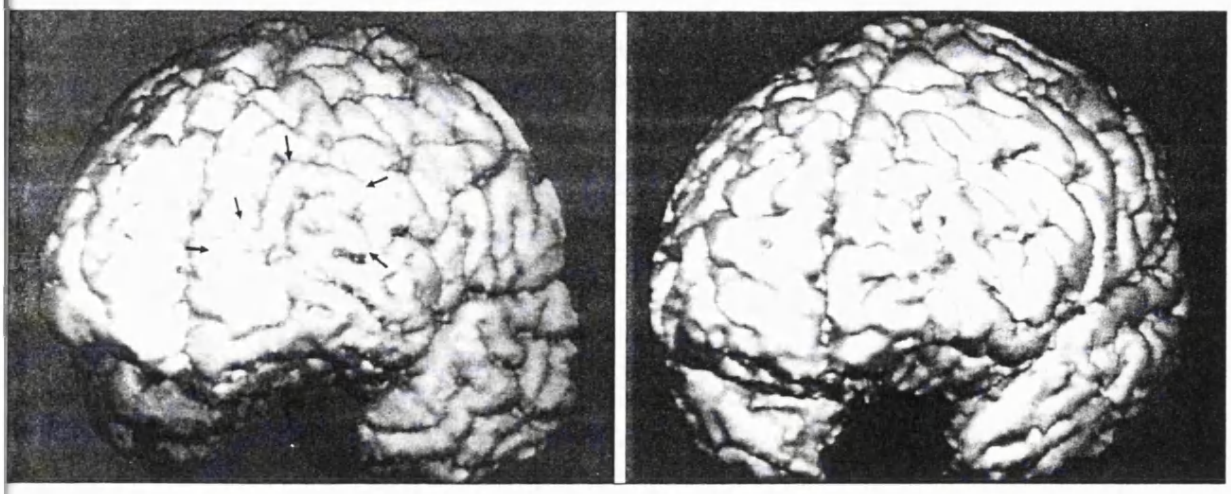

Figure 6. *Brain of patient 6 (left) and normal subject (right). See Table for details.*

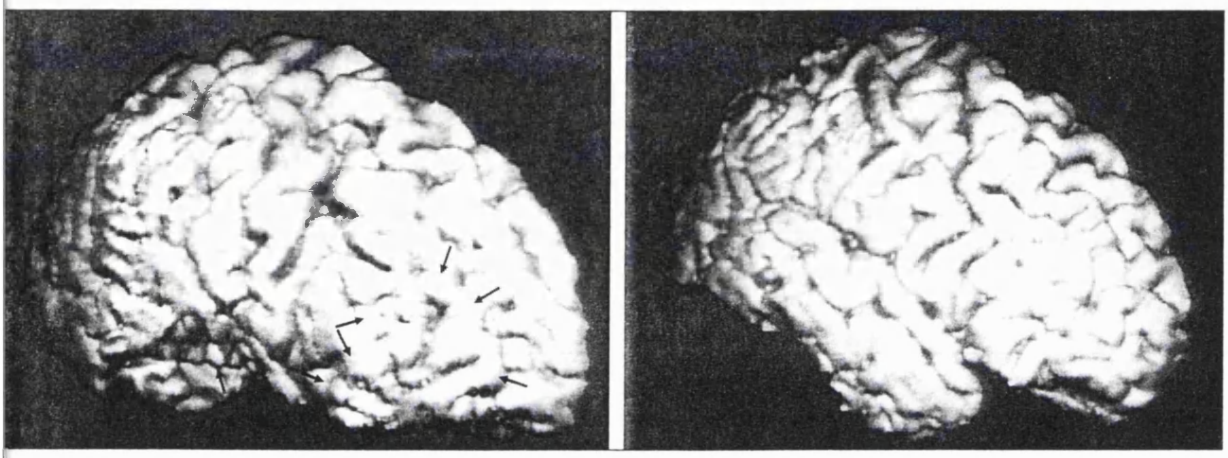

Figure 7. *Brain of patient 7 (left) and normal subject (right). See Table for details.*

gyri).[24] The laterality of clonic movements and the sensory auras, as well as the complex limb posturing of patient 2, for example, strongly suggest seizure onset in the right superior or middle frontal gyri. The demonstrated lesion is in the right middle frontal gyrus. Bilateral EEG changes are not infrequently seen with proven frontal lobe lesions[3] and may occasionally indicate the presence of bilateral lesions, though in none of our cases was there an unambiguous gyral abnormality in the contralateral hemisphere. Thus, in all cases the disruptions of the pattern of gyration demonstrated are compatible with the observed electroclinical findings and their involvement in epileptogenesis is feasible.

In the absence of surgical resection of these postulated lesions, absolute proof of their relevance to the epileptogenic process cannot be provided in the majority of these patients. However, confirmation of the relevance of the abnormality demonstrated in the three-dimensional image is available for patient 7 who had had a right temporal lobectomy without relief from his seizures. Depth electrode studies confirmed that his seizures arose from the dorsolateral right frontal convexity. In this case, the importance of the demonstration of a structural abnormality is clearly apparent. The patient declined further surgery after depth studies.

Gyral abnormalities are the macroscopic manifestation of disordered cytoarchitecture.[10] This was initially observed on postmortem specimens.[25-27] Abnormal two-dimensional MRI findings have sometimes been correlated with histologically demonstrated disruption of cortical architecture.[28-30] We presume that the abnormalities demonstrated herein in three-dimensional images also reflect deranged cortical structure at a histological level. In our own MRI series,[31] tumors and vascular malformations are the most common diagnoses of frontal lobe lesions, followed by cerebral dysgeneses. For our study, we specifically excluded patients with tumors and vascular malformations; thus, we believe that some form of cerebral dysgenesis is the most likely histological diagnosis in our cases. By quantitative analysis of volumetric MRI data, we have recently shown that cerebral dysgenesis is a widespread disorder of cerebral structure, usually extending beyond the visualized abnormality alone.[15] This may account for the poor outcome of lesional surgery when the underlying pathologic condition is cerebral dysgenesis.[19,32] Suspicion of an underlying diagnosis of cerebral dysgenesis may discourage intervention, such as intracranial electrographic studies, particularly as the epileptogenic zone associated with frontal seizures may be extensive.[33] The demonstration of a lesion, however, is important because it should stimulate further inquiry into the bounds of the abnormality guided by our findings. In the future,

this may encourage directed depth electrode placement and lead to improved surgical outcome in this group of patients. The prognosis for control of epilepsy following surgery is better, in general terms, in those patients in whom a lesion is visualized and maximally resected than in those in whom no etiology is apparent,[19,20] or in whom the seizure focus rather than the lesion is resected.[21]

Patients 3 and 5 have a familial frontal lobe seizure disorder. In a recent report on this condition,[34] no neuroimaging abnormalities were identified on routine inspection. If gyral anomalies can be demonstrated to segregate with epilepsy in such families, this offers not only proof of the significance of these gyral anomalies but also raises the possibility of uncovering a genetic basis for gyral (mal)development, as is known to exist, for example, in the Miller-Dieker syndrome.[35]

This was a highly selected series of medically refractory patients in whom the demonstration of a lesion becomes more important. Nine of our 16 patients with probable frontal epilepsy still had no focal abnormality demonstrated. It may be that they have anomalies in areas that we have not examined, such as the mesial and orbital frontal cortex, because anatomical distinction by segmentation in these areas is difficult; our results are, therefore, likely to be a conservative estimate. Lesions might also be revealed using other MRI techniques (eg, fluid attenuated inversion recovery scanning[36]). We are currently analyzing all the reconstructions to determine what proportion may harbor a gyral abnormality of other regions. We are also investigating preoperative and postoperative cases as the revelation of structural abnormality might not only guide surgical policy, including the placement of depth electrodes, but also prevent inappropriate surgical intervention.

We conclude that further postprocessing of the data present in volumetric MRI scans is of value in cases where the subject has refractory chronic partial epilepsy and the two-dimensional MRI is noncontributory. The technique may also be useful in other conditions associated with cerebral dysgenesis, such as cryptogenic mental retardation and developmental dyslexia, in which routine two-dimensional imaging has failed to demonstrate abnormality. We suggest that more complete and comprehensible use of the spatial information present in volumetric data sets may be made by reconstitution of the three dimensionality of the structures being investigated.

Accepted for publication September 8, 1995.

The project was supported by the Wellcome Trust, London.

We thank the patients and the staff of the MRI Unit of St Mary's Hospital, London.

Correspondence to the Epilepsy Research Group, Institute of Neurology, Queen Sq, London, England WC1N 3BG (Dr Sisodiya).

REFERENCES

1. Andermann F. Brain structure in epilepsy. In: Shorvon SD, Fish DR, Andermann F, Bydder GM, Stefan H, eds. *Magnetic Resonance Scanning and Epilepsy.* Orlando, Fla: Plenum Press; 1994:21-27.
2. Cascino GD, Boon PAJM, Fish DR. Surgically remediable lesional syndromes. In: Engel J Jr, ed. *Surgical Treatment of the Epilepsies.* 2nd ed. New York, NY: Raven Press; 1993:77-87.
3. Shorvon SD. Magnetic resonance imaging in epilepsy: the central clinical research questions. In: Shorvon SD, Fish DR, Andermann F, Bydder GM, Stefan H, eds. *Magnetic Resonance Scanning and Epilepsy.* Orlando, Fla: Plenum Press; 1994:3-13.
4. Raymond AA, Cook MJC, Fish DR, Shorvon SD. Cortical dysgenesis in adults with epilepsy. In: Shorvon SD, Fish DR, Andermann F, Bydder GM, Stefan H, eds. *Magnetic Resonance Scanning and Epilepsy.* Orlando, Fla: Plenum Press; 1994:89-94.
5. Williamson PD. Frontal lobe seizures: problems of diagnosis and classification. In: Chauvel P, Delgado-Escueta AV, Halgren E, Bancaud J, eds. *Advances in Neurology.* New York, NY: Raven Press; 1992;57:289-310.
6. Williamson PD, Spencer SS. Clinical and EEG features of complex partial seizures of extratemporal origin. *Epilepsia.* 1986;27(suppl 2):S46-S63.
7. Swartz BE, Halgren E, Delgado-Escueta A, et al. Neuroimaging in patients with seizures of probable frontal lobe origin. *Epilepsia.* 1989;30:547-558.
8. Min LL, Sisodiya SM, Fish DR, Shorvon SD, Stevens JM. SMA type seizure: misleading term. *Epilepsia.* 1994;35(suppl 8):21. Abstract.
9. Laskowitz DT, Sperling MR, French JA, O'Connor MJ. The syndrome of frontal lobe epilepsy. *Neurology.* 1995;45:780-787.
10. Barth PG. Disorders of neuronal migration. *Can J Neurol Sci.* 1987;14:1-16.
11. Jack CR Jr, Marsh WR, Hirschorn KA, et al. EEG scalp electrode projection onto three-dimensional surface rendered images of the brain. *Radiology.* 1990; 176:413-418.
12. Damasio H, Frank R. Three-dimensional in vivo mapping of brain lesions in humans. *Arch Neurol.* 1992;49:137-144.
13. Ono M, Kubik S, Abernathey CD. *Atlas of the Cerebral Sulci.* New York, NY: Springer-Verlag NY Inc; 1990.
14. Kohn MI, Tanna NK, Herman GT, et al. Analysis of brain and cerebrospinal fluid volumes with MR imaging. *Radiology.* 1991;178:115-122.
15. Sisodiya SM, Free SL, Stevens JM, Fish DR, Shorvon SD. Widespread cerebral structural changes in patients with cortical dysgenesis and epilepsy. *Brain.* 1995;118:1039-1050.
16. Steinmetz H, Herzog A, Huang Y, Hacklander T. Discordant brain-surface anatomy im monozygotic twins. *N Engl J Med.* 1994;331:952-953.
17. MacDonald D, Avis D, Evans AC. Multiple surface identification and matching in MR images. *Proc SPIE.* 1994;2359:160-169.
18. Rademacher J, Caviness VS Jr, Steinmetz H, Galaburda AM. Topographical variation of the human primary cortices. *Cereb Cortex.* 1993;3:313-329.
19. Fish DR, Smith SJ, Quesney LF, Andermann F, Rasmussen T. Surgical treatment of children wirh medically refractory epilepsy: results and highlights of 40 years' experience. *Epilepsia.* 1993;34:244-247.
20. Cascino GD, Jack CR, Parisi JE, et al. MRI in the presurgical evaluation of patients with frontal lobe epilepsy and children with temporal lobe epilepsy. *Epilepsy Res.* 1991;11:51-59.
21. Awad I, Rosenfeld J, Ahl J, Hahn J, Luders H. Intractable epilepsy and structural lesions of the brain. *Epilepsia.* 1991;32:179-186.
22. Salanova V, Morris HH, Van Ness P, Kotagal P, Wyllie E, Luders H. Frontal lobe seizures. *Epilepsia.* 1995;36:16-24.
23. Bancaud J, Talairach J. Clinical semiology of frontal lobe seizures. In: Chauvel P, Delgado-Escueta AV, Halgren E, Bancaud J, eds. *Advances in Neurology.* New York, NY: Raven Press; 1992;57:3-58.
24. Quesney LF, Constain M, Rasmussen T. Seizures from the dorsolateral frontal lobe. In: Chauvel P, Delgado-Escueta AV, Halgren E, Bancaud J, eds. *Advances in Neurology.* New York, NY: Raven Press; 1992;57:233-244.
25. Rakic P. Defects of neuronal migration and the pathogenesis of cortical malformations. *Prog Brain Res.* 1988;73:15-37.
26. Sarnat HB. Cerebral dysplasias as expressions of altered maturational processes. *Can J Neurol Sci.* 1991;18:196-204.
27. Williams RS. The cellular pathology of microgyria. *Acta Neuropathol (Berl).* 1976;36:269-283.
28. Kuzniecky R, Garcia JH, Faught E, Morawetz RB. Cortical dysplasia in temporal lobe epilepsy. *Ann Neurol.* 1991;29:293-298.
29. Barkovich AJ, Kjos BO. Gray matter heterotopias. *Radiology.* 1992;182:493-499.
30. Marchal G, Andermann F, Tampieri D, et al. Generalized cortical dysplasia manifested by diffusely thick cerebral cortex. *Arch Neurol.* 1989;46:430-434.
31. Li LM, Fish DR, Sisodiya SM, Shorvon SD, Alsanjari N, Stevens JM. High resolution magnetic resonance imaging in adults with partial or secondary generalised epilepsy attending a tertiary referral unit. *J Neurol Neurosurg Psychiatry.* In press.
32. Bruton CJ. *Neuropathology of Temporal Lobe Epilepsy.* New York, NY: Oxford University Press Inc; 1988.
33. Salanova V, Quesney LF, Rasmussen T, Andermann F, Olivier A. Reevaluation of surgical failures and the role of reoperation in 39 patients with frontal lobe epilepsy. *Epilepsia.* 1994;35:70-80.
34. Scheffer I, Bhatia K, Lopes-Cendes I, et al. Autosomal dominant nocturnal frontal lobe epilepsy. *Brain.* 1995;118:61-73.
35. Reiner O, Carrozzo R, Shen Y, et al. Isolation of a Miller-Dieker lissencephaly gene containing G protein β-subunit-like repeats. *Nature.* 1993;364:717-721.
36. Bergin PS, Fish DR, Shorvon SD, Oatridge A, deSouza NM, Bydder G. Magnetic resonance imaging in partial epilepsy. *J Neurol Neurosurg Psychiatry.* 1995;58:439-443.

Seizure 1995; **4**: 169–185

REVIEW ARTICLE

Wiring, dysmorphogenesis and epilepsy: a hypothesis*

S.M. SISODIYA

Epilepsy Research Group, Institute of Neurology, Queen Square, London WC1N 3BG, UK

Cerebral cortical dysgenesis has been found by magnetic resonance imaging to be the second most common pathology underlying medically refractory chronic partial epilepsy. Patients with the latter condition form the largest group in specialist epilepsy clinics. The pathogenesis of the epilepsy in cortical dysgenesis remains largely obscure. The most popular current hypothesis holds neuronal misconnection secondary to neuronal malpositioning culpable for seizure activity. However, a review of the published literature of cortical dysgenesis and an analysis of newer magnetic resonance and histopathological data, suggests that this view is no longer tenable. A modified hypothesis is proposed in which neuronal connectivity itself is postulated to be the primary motive force in both cerebral morphogenesis and epileptogenesis in cases of cortical dysgenesis. This hypothesis leads to the generation of a model for cortical development and directly testable predictions of intercellular connectivity, as well as a potential tool for the prediction of the possibility of freedom from seizure activity after surgical resection of dysgenetic lesions in individual cases.

Key words: cerebral development; cortical dysgenesis; epilepsy; connectivity.

INTRODUCTION

The relationship between structure and function has been an area of consistently fruitful investigation in the world of biology. Technical advances have led to more detailed structural analysis and this in turn has led to deeper functional understanding. In the study of the aetiopathogenesis of epilepsy the situation is no different. Investigation of the pathological substrate underlying certain forms of chronic partial epilepsy led to a hypothesis for the morphogenesis of the normal brain by Richman *et al.* in 1975[1]. Here the support for this hypothesis is critically reviewed in the light of both older studies and new data obtained from magnetic resonance imaging that allow ante-mortem in vivo analysis of certain cerebral abnormalities underlying epilepsy. The hypothesis is found wanting; a modified form is proposed that identifies neuronal connectivity as the primary generative force behind both morphogenesis and epileptogenesis in partial epilepsy.

Abnormal development of the structure of the cortex, both at a macroscopic and histological level, has been recognized for more than a century as a possible cause of abortion, abnormal infantile neurological development, mental retardation and epilepsy, often in combination[2]. The earliest abnormalities to be discovered were those of cerebral gyration: polymicrogyria, lissencephaly and schizencephaly. These gyral anomalies (GA) are thought to be developmental as they have been found in aborted foetuses as early as 18 weeks of gestation[3]. Subsequently each of these groups has been recognized to be heterogeneous in composition, both aetiologically and structurally (for a review see Barth, 1987)[4]. In addition, other forms of cortical maldevelopment have been recognized, such as dysembryoplastic neuroepithelial tumours[5,6], focal cortical dysplasia[7] and microdysgenesis[8]. Collectively, these anomalies may be called cortical dysgeneses (CD)[9].

Magnetic resonance imaging has revealed that CD is found in a large proportion of brains of patients with chronic partial epilepsy[10]. In some

* Entry for the 1994 Gowers Young Physician Prize.

1059–1311/95/030169 + 17 $08.00/0

cases, surgical resection of CD has been performed for the treatment of medically intractable seizures in this patient group[11]; the occasional success of such treatment bears witness to the aetiological significance of CD. The identification of underlying structural abnormalities, including CD and GA, has thus become an area of intense interest in epilepsy research and the management of patients with chronic partial epilepsy. Unfortunately, experience has shown that, apart from those patients with dysembryoplastic neuroepithelial tumours (DNT), resection of CD lesions rarely leads to the complete cessation of clinical seizure activity. An explanation of this is not yet forthcoming.

Why CD lesions should in the first instance be epileptogenic is a question that has itself yet to be answered. The weight of opinion currently is that in the case of GA, the disordered distribution of neurons leads to errors in connectivity that in turn are responsible for epileptogenesis. In this essay, the opposite point of view will be explored and the hypothesis postulated that primary neuronal and connectional abnormalities lead to the development of epilepsy and that when extensive enough, such changes lead to visible abnormalities of cortical structure. This approach provides a robust explanation of normal and abnormal gyral morphogenesis, epileptogenesis in CD, and the failure of current surgical therapy for resective cure of chronic partial epilepsy due to CD.

THE SUBSTRATE: CORTICAL ANATOMY AND DEVELOPMENT

The adult human neocortex is histologically composed of six layers[12]. The outermost, subpial layer is composed mainly of tangentially-oriented fibres and is called the molecular layer, or layer I. Passing progressively further inwards, five major cellular layers are discernible on the grounds of cellular morphology and disposition: they are labelled layers II–VI, respectively.

The convoluted adult form of the human cerebral hemispheres develops from the telencephalic vesicles—paired spherical structures at the rostral end of the neural tube[13]. The archicortical hippocampal structures develop from the medial walls of these primordia, the corpus striatum from the ganglionic eminences in the ventral walls and the neocortex (the cortical ribbon) from the dorsolateral walls.

Neocortical development, with which we are concerned, occurs in a number of overlapping phases, reviewed by Caviness[14]. Initially, the dorsolateral aspect of the telencephalic vesicle is a pseudostratified epithelium. Mitotic activity within this germinative zone eventually gives rise to successive waves of daughter cells, which migrate centrifugally and establish a number of cell layers between the ventricular epithelium and the overlying primitive meninges. The layers are formed in two groups: an early scaffolding structure, the preplate, is subsequently invaded by the migrating cells of the developing cortical plate which splits the preplate into the presumptive molecular layer and a subcortical collection of cells in the subplate.

Before these complex cellular movements occur, however, the early pseudostratified epithelium acquires an investment of corticopetal neuronal fibres, thought to arise from the presumptive dorsal thalamus and mesencephalic tegmentum[15]. These fibres pass from the diencephalon to the telencephalon through the attachment of the telencephalic vesicle to the dorsum of the diencephalon, in a region which will become the internal capsule within the corpus striatum. These fibres pass subpially to the dorsolateral aspect of the telencephalon by day 44 of gestation.

At this stage, mitotic activity in the periventricular germinative zone gives rise to preplate cells, which form, for example, bipolar Cajal–Retzius cells horizontally disposed within the primitive plexiform layer formed by the corticopetal fibres. It should be noted that even at this stage axodendritic synapses can be seen between these entities[16], arguing for an early role for intercellular connectivity.

By day 54, the cortical plate is beginning to form[17]. Neurons generated in the periventricular zone migrate centrifugally along radially-disposed processes of glial cells. Successive waves of cells pass into the preplate, splitting this tangentially into the presumptive molecular layer, which retains within it a few cells, and the deeper subcortical remnant, the subplate, which gives rise to the few neurons found in the mature brain at the boundary between layer VI and the white matter. Successive generations of mitotic progeny pass through earlier generations in their migration and thus establish an 'inside out' gradient of formation of the layers of the cortical plate[18].

Importantly, synapses can be seen in the split layers of the preplate before any become apparent in the developing cortical plate. The early invading corticopetal afferents connect as detailed above, whilst thalamic afferents destined to synapse within the cortical plate arrive at an early stage and synapse on cells in the subplate[19]. These early connections seem to be very important in the subsequent organization of the cortex,

as selective ablation of cells regionally in the subplate leads to the failure of the local thalamic afferents to pass eventually into the overlying cortical plate, even though their predestined targets are in their correct positions[20]. Instead the afferents take a tangential course through the white matter and come to underlie the cingulate cortex. This argues strongly for a precocious role for early interneuronal connectivity in the formation of later definitive connectivity.

There is rapid growth of the cortical plate (CP). Neurons migrate mainly between the seventh and 16th week of gestation, through the timing of the cessation of migration in the human is not clear, and in far fewer numbers may continue even postnatally[21]. Cells of layer VI are in place first, followed by those of more superficial layers until those of layer II are in position.

Neurons in the various laminae differentiate into one of a group of shapes typical for that layer[22]. They have layer-specific afferent and efferent connections. All laminae possess interneurons, forming so-called local circuits, and projectional neurons, almost invariably of pyramidal morphology, whose axons pass out of the immediate cortical organization to more distant areas. Projectional cells of layer II tend to be associative, producing and receiving intrahemispheric, corticocortical fibres; layer III projectional cells give rise to and accept transcallosal, interhemispheric fibres. Cells of layer IV tend to have reciprocal connections with the thalamus. The infragranular layers V and VI project subcortically, layer V cells to the spinal cord, tectum, striatum, pons and medulla and layer VI cells to the thalamus and claustrum[23].

The timing of synaptic development across the cortex remains a somewhat ill-defined and disputed topic. It is not clear whether synapses develop concurrently throughout the cortex as Rakic and his colleagues maintain[24], or whether there are laminar and regional ontogenetic gradients[25]. Nevertheless, there is agreement that synaptogenesis within the CP occurs most markedly after 23 weeks of gestation (e.g. Molliver *et al*[16]).

Macroscopic morphogenesis, with the formation of gyri and sulci and the larger movements that change the originally spherical vesicle into the adult form of the cerebrum, proceed throughout gestation. The earliest fissures visible are the sylvian and callosal (10–15 weeks)[26]. As gestation progresses, more and more gyri and sulci are formed—the exact position and extent becoming more variable the later gyri form[26,27].

As growth proceeds in the cortical plate, which becomes the mature neocortex, radial expansion is limited such that the human cortex extends for only 2–5 mm perpendicularly to the pial surface. Conversely, growth parallel to the pial surface (tangential growth), is much greater, contributing the major component to the overall 400-fold growth in the volume of the neocortex from the 13th week to term[28]. This ontogeny recapitulates the phylogenetic progression in the morphogenesis and functional diversity of the cortex as will be discussed further.

This account is a gross simplification of the subtleties of human neocortical maturation, much of which remains incompletely understood. It has been shown recently, for example, that the long-held belief that only radial movement of neurons occurs in embryogenesis is false: tangential migration of clonal populations does occur[29,30]. Thus the radial unit hypothesis[31] in its pure form is no longer tenable[32]. The periventricular germinative epithelium cannot be regarded as a 'protomap' of the adult configuration of the cortex[33], with cells in different laminae arising essentially from the same progenitor cells and thus committed at an early stage to function in a coherent 'radial unit' (or vertical column) in the mature cortex. This in addition invalidates a view that dysgenesis of the cortex can be regarded in terms of a reduction in either the number of radial units or the number of cells within a unit[31].

ABNORMAL CORTICAL DEVELOPMENT: THE CORTICAL DYSGENESES

Cortical development as summarized above may be disrupted at any stage. Attention in this essay will be focused on abnormalities that are associated with changes in the disposition of the grey and white matter in the cerebral hemispheres and with other lesions of a more focal nature, believed to be developmental in origin, all of which are associated with epilepsy. Thus, pachygyria, agyria (or lissencephaly), schizencephaly, subependymal heterotopia and subcortical heterotopia will be discussed. In all of these conditions, there is abnormal positioning of neurons in the adult brain, associated in some with a disruption of the normal six-layered configuration of the cortical ribbon. Although these conditions are sometimes referred to as neuronal migration disorders[4], this may not be appropriate as there is evidence that some are post-migrational.

Abnormal neuronal positioning may be much more subtle and involve fewer neurons, resulting in microdysgenesis[34], with the finding of excessive numbers of neurons in the subcortical white matter. Abnormal neurons may be found in any

of these conditions, although there has been relatively little investigation at the cellular level in these diseases. The occurrence of abnormal neurons throughout a possibly normally-laminated cortex is the hallmark, however, of the condition known as focal cortical dysplasia[7].

Aberrant cellular development may include non-neuronal elements and produce a focal lesion with abnormal structure called a dysembryoplastic neuroepithelial tumour (DNT)[5,6], a recently-described anomaly held responsible for a number of cases of chronic partial epilepsy.

Together, these conditions may be grouped under the heading of cortical dysgenesis[9]. The conditions have been extensively documented and reviewed[4,35,36]; they will be briefly described below.

1. *Agyria* or *Lissencephaly* describe a brain in which gyration is absent. There are at least two distinct histopathologies. In type I the affected cortex is four-layered: there is a superficial, subpial molecular layer, then a disorganized outer cellular layer, a cell-sparse zone and finally an inner cellular layer with numerous cells whose migration is believed to have been arrested and which would normally have constituted mainly layers II and III. The migratory defect in type I lissencephaly is thought to have occurred between 12 and 16 weeks of gestation. Type II lissencephaly is characterized by a smooth cerebral surface and a thickened cortex in which there is little discernible layering of any sort—neurons instead being grouped in clusters and columns. In the white matter underlying the superficially-placed neurons are heterotopic neurons forming nodules. Other, as yet unclassified, varieties of lissencephaly also exist[4].
2. *Pachygyria* is the presence of broader and fewer gyri than normal. Histologically, the picture is identical to that seen in agyria, and the two often occur together in the same brain. It is believed that pachygyria is simply a less severe form of agyria. Macrogyria is a purely descriptive term, applied to gyri that appear broadened, either on inspection or on imaging. It carries no histopathological implications, and indeed may be due to at least six different pathologies, including pachygyria, polymicrogyria and forme fruste of tuberous sclerosis.
3. *Polymicrogyria* is the macroscopic finding of a large number of narrowed, thinned gyri. On inspection, whilst this may be visible, fusion of adjacent molecular layers may give the impression of macrogyria. Histologically, there are layered and unlayered varieties. In the layered form, there is believed to be post-migrational destruction of cells, mainly in lamina V, probably due to transient vascular insufficiency. This is associated with an increased convolutedness of the overlying laminae, with the generation of small gyri of reduced thickness and width. The insult causing layered polymicrogyria is believed to act between 18 and 24 weeks of gestation. Unlayered polymicrogyria is macroscopically indistinguishable, but a cell-sparse layer suggestive of laminar destruction is not present. The cause is believed to act between 12 and 17 weeks of gestation.
4. *Schizencephaly* is the presence of clefts extending across the wall of the hemisphere, from the pia to the ependyma. The walls of the cleft are lined by grey matter, which may be polymicrogyric. The walls may be apposed or separated. It is believed to result from a destructive influence that in less dramatic cases produces polymicrogyria.
5. *Subependymal heterotopia* is the presence in either nodular or band form of ectopic grey matter in the post-developmental brain lying underneath the ventricular ependyma. It is found most commonly around the trigones and is usually associated with normal gyration of the overlying cortex. It may be due to a failure of migration or of apoptosis.
6. *Subcortical heterotopia* is the presence of aggregations, in either laminar, band or nodular form, of neurons in the subcortical grey matter, commonly in the centrum semiovale. It may be associated, especially if extensive, with abnormal gyration of the overlying cortical ribbon. It is believed to be due to a premature arrest of neuronal migration.
7. *Microdysgenesis* is the presence of small numbers of neurons in the subcortical white matter. Such neurons are present normally, but it is believed that in some subjects with epilepsy the quantity of such neurons is excessive[34].
8. *Focal cortical dysplasia* is the presence of abnormally large and dysmorphic neurons in many layers of an otherwise normally layered and convoluted cortex and is found in the brains of a number of cases of patients with partial epilepsy. There may also be abnormal glial cells in these areas.
9. *Dysembryoplastic neuroepithelial tumour* is the most recently recognized variety of cortical dysgenesis. Histologically, it is characterized by the presence of multinodular archi-

tecture, cellular polymorphism and associated intralesional neuronal dysplasia.

The ante-mortem revelation of these conditions became possible with the advent of computerized tomography (CT) scanning. Magnetic resonance (MR) scanning, affording a far greater ability to delineate soft tissues, has revealed that these anomalies occur much more frequently than previously supposed[10], accounting for up to 24% of structural abnormalities presumed to underlie chronic partial epilepsy in some series.

Having described normal and abnormal brain development and shape, we can now return to the theme here: how can these structural abnormalities of development (dysmorphogeneses) be linked to neuronal malpositioning and how can they be related to abnormal function in epileptogenesis?

RICHMAN'S MECHANICAL HYPOTHESIS OF CEREBRAL GYRATION

In 1975, based on their histological analysis of a case of polymicrogyria and one of lissencephaly, Richman *et al*[1] proposed a model of cerebral gyral formation. In their case of polymicrogyria, cells in layers II and III were considered to be normal, whilst those in layer V were decimated in number, with fewer cells variably also in layer IV and a normal complement in layer VI. In their case of lissencephaly, there was a deficiency of cells in the more superficial layers, with a more normal complement in layers V and VI, under which was a cell-sparse zone. Under this was a large number of heterotopic neurons presumed to have been destined for layers II–IV, but whose migration had been arrested. In the polymicrogyria, the cells in layer IV were thought to have migrated and then been destroyed, this being therefore a post-migrational anomaly. The lissencephalic cortex was thicker than normal and the polymicrogyric cortex thinner.

To explain this association of cytoarchitectonic abnormalities with the observed gyral changes, they postulated a model of cortical gyration as follows. They considered the cortex divided into two strata, the more superficial comprizing layers I–III, and the deeper, layers IV–VI. Initially, these strata were thought of as homogeneous, incompressible flat layers bonded to each other and to an infinitely deep core. The layers had given uniform thickness and elasticity. They proposed that in the normal brain, the superficial stratum grew more than the deeper one and demonstrated that, under certain conditions—including the maintenance of a uniform radial thickness—this would lead to a buckling of the surface of this structure, with a sinusoidal displacement of points perpendicular to the surface. Thus, gyri and sulci would form. The distance between homologous points on the gyri or sulci (the wavelength of the surface undulations) was calculable and they predicted that it would be eight times the summed thickness of their two strata.

In the case of the polymicrogyria, they suggested, based on estimated measurements of the surface areas of the various laminae in their case, that there had been deficient growth of the deeper layer due to absence of lamina V (mainly), with the calculable effect of an increased buckling of the cortical surface—polymicrogyria. In the lissencephalic case, they presumed that the growth of the more superficial layers was less than that of the core (with its malmigrated complement of neurons), with the calculable effect that buckling would not occur. Thus, based on observed abnormalities of cell position, they were able to predict the observed morphology of the cortical surface. They postulated that differential growth between the two strata was responsible for dysmorphogenesis. Richman *et al*[1] thus considered that intracortical factors determined morphogenesis.

Subsequently, Armstrong *et al*[37], in a test of Richman's hypothesis, quantified the volume ratio of supragranular to infragranular layers (equivalent to Richman's stratum 1 and 2, respectively) and found a significant correlation between this parameter and an index of convolutedness in the brain of the rhesus monkey. They explicitly considered differential growth not only to be morphogenetic but also to be due to changes in the neuropil extent in the supragranular and infragranular layers. Others have also explicitly attributed this intracortical determination to interneuronal connectivity, that is, the development of the neuropil. Other workers (e.g. Barth[4]) have ascribed epileptogenesis in CD to the malpositioning of neurons, which they have accepted leads to dysmorphogenesis as modelled by Richman *et al*[1].

Since then, other models have been proposed for gyrogenesis, and though many other useful concepts have arisen (e.g. Prothero[38]), no one model has been as widely accepted as theirs. Abnormal gyral patterns are interpreted in the context of this model, and histology, where available, considered in the same light. Indeed in

its fundamental principles, it is an intuitively agreeable hypothesis.

Thus overall, current thinking would suggest that cortical neuronal positioning determines interneuronal connectivity, which is the implicit expansionist force in Richman's model. Conversely, malpositioning of neurons is believed to lead to miswiring between them, leading to abnormal growth and dysmorphogenesis as seen in CD. Both dysmorphogenesis and misconnection secondary to neuronal malpositioning are then held to cause epilepsy.

However, evidence will now be considered that shows firstly that in its original form the mechanical model of cerebral gyration cannot be maintained. Then the causal linkages between malpositioning and misconnection, dysmorphogenesis and epileptogenesis will be challenged. Finally, a revised hypothesis will be proposed linking these aspects of cerebral structure and function.

ASSUMPTIONS INVALIDATED: PREDICTIONS NOT UPHELD

With the use of certain assumptions, Richman *et al*[1] make a number of predictions from their model. The most important of these is that the ratio of the intergyral separation (the wavelength of gyration) to the cortical thickness in the normal foetal brain should be eight and the ratio in polymicrogyric brain, one. However, the evidence available does not bear this out:

1. As reviewed and emphasized by Welker[39], the human cortical ribbon is not of uniform thickness, either during embryogenesis or in the adult: gyral crown cortex is thicker than gyral fundal cortex and both vary according to the area of the brain being examined. Whilst the difference in absolute terms is never great (e.g. 2–5 mm), it is significant enough to invalidate the simple model originally proposed, which assumes a uniform total thickness across the cerebral surface. The picture published by Richman *et al* themselves in their original paper shows a polymicrogyric cortex which is clearly not of uniform thickness: gyral crown cortex may be three times as thick as fundal cortex. It is possible that the plane of section may confound the issue, though we must assume that the authors would have addressed this possibility in their choice of illustration.
2. In addition, for gyrogenesis in the normal brain, Richman *et al* assume that the thicknesses of their two composite layers are the same across the cerebrum. The extensive histological analyses of Bok[40] give the lie to this assumption. In elegant work, Bok demonstrates that the thickness of the more superficial layers is greater in the fundus than at the crown of a gyrus, and that the reverse is true for the deeper layers. Bok's own interpretation of this is that neuronal architecture has to alter in response to these morphological facts. This view is counter to the thesis of this essay, in which neuronal changes are held to be morphogenetic, but this does not detract from the conclusion that another of the model's assumptions cannot be maintained.
3. The ratio of gyral wavelength to cortical thickness in the normal brain should be eight according to the model. It has already been shown above that the cortical thickness is not uniform (even when the perpendicularity of the plane of section to the gyral surface is assured). Nevertheless, if for the moment this problem is ignored and a mean value for the thickness of the cortical ribbon produced, for the normal brain, this ratio is not always eight. Measurements have shown that in the normal brain, the gyral wavelength may be as small as 8 mm: the corresponding mean cortical thickness is more than 3 mm. That this prediction is not upheld must reflect either the invalidity of the assumptions or an inadequacy of the mechanical finesse of the hypothesis.
4. Zellweger's syndrome[41] is an inherited condition with abnormalities of the kidney, liver and brain. In the latter there is an incomplete disruption of neuronal migration, affecting especially neurons destined for cortical layers II and III. There is widespread gross convolutional disorder, with areas both of polymicrogyria and pachygyria. Histological analysis[42] reveals that in the polymicrogyric areas, there is a reduction in the number of cells in laminae II and III, and an increase in the number of cells (some ectopic) in laminae V and VI. In the pachygyric areas, there is a more marked reduction in laminae II and III: this is of such a magnitude that the morphological laminae V and VI come to lie 'just' [42] under the molecular layer, and in addition in these areas, there are even more ectopic neurons in these superficially displaced laminae. In both areas, there are large numbers of ectopic neurons in the subcortical white matter. If the model's predictions are applied

to these changes, then the morphological alterations seen should not occur: in particular the pachygyric areas should be at least normally convoluted if not actually polymicrogyric.

Thus the model of Richman *et al* cannot be supported in its original form. There are two alternatives, however. One is that the actual numbers of displaced neurons are such that the net effect would be predicted by the hypothesis if it could be adapted to a much smaller field of action. The other is that in fact the growth of the cells in laminae II and III in polymicrogyric areas is greater than that, overall, both of the superficially-displaced, ectopic cell-laden laminae V and VI in pachygyric areas and the subcortical heterotopic neuronal areas, thus leading to increased folding of the cortical ribbon in these areas as predicted by the model. Unfortunately, in this study[42] as in most studies, stereological techniques were not applied to quantitate cell numbers, nor were Golgi staining techniques used in an attempt to examine dendritic field changes in abnormally positioned neurons. In either case it is apparent that as it stands the model of Richman *et al* is unsupportable.

However, based on this model, epileptogenesis in dysmorphic brains has been ascribed to the malpositioning of the component neurons: given that the model is untenable can this still be assumed to be true?

NEURONAL MALPOSITIONING IS NOT NECESSARILY EPILEPTOGENIC

Richman *et al*'s model can explain GA in terms of differential laminar growth of malpositioned neurons, and misconnection needs then to be implicitly invoked as a result to explain epileptogenesis. However, this may be unsustainable:

1. In the mutant 'reeler' mouse, there is a well-studied, gross disruption of the normal cytoarchitecture[43]. There is complete laminar inversion of the structure of the cortex, such that the morphological and functional characteristics of layer VI cells are to be found in the most superficial layer and those of layer II cells, in the deepest layer. These mice, though markedly ataxic, may grow to maturity and breed but never have seizures. Connectivity, as far as has been examined, is not different to that of the normal cortex. Thalamic and callosal connections are normally distributed. Visuotopic co-ordinates in the primary visual representation are indistinguishable from those in the normal mouse, as essentially are single-cell recordings of the receptive fields of neurons in the visual cortex[43,44]. Thus normal cortical function seems largely to have been maintained despite the gross cytoarchitectonic disorder because normal connectivity has been undisturbed.
2. Similarly, McConnell[45] has produced many bizarre cortical disruptions in her studies of cortical development: none of these animals have had seizures.
3. Jensen and Killackey[46] disrupted neuronal migration in rats by irradiating foetuses at specific times during gestation. They identified cells in the resulting subependymal heterotopic CD as those destined for layer V, based both on chronological (birthdate) and morphological grounds. These cells were shown to retain their expected projectional targets to the spinal cord, despite their failure to migrate. This argues not only for an early commitment to projection, based probably on an early restriction of laminar fate, but also that malposition does not necessarily result in miswiring.
4. Human CD lesions may not necessarily be associated with epilepsy (which remains a clinical diagnosis). Thus, in a series of 31 patients with congenital bilateral perisylvian GA (thought to be polymicrogyric in nature on MR grounds and shown histologically in two cases), 13% had never had seizures (the age of these patients is not published, however)[47].
5. There are reports of patients with presumed subependymal or subcortical heterotopic grey matter demonstrated on MR scanning who are asymptomatic, even though they may be older than their related index cases who presented with epilepsy[48].
6. Barkovich *et al*[49] have shown, semi-quantitatively, that neuropsychological and clinical seizure severity assessments are worse for those patients with subcortical heterotopia than for those with subependymal heterotopia. In addition, patients with subcortical heterotopia are more likely to have overlying gyral abnormalities than are patients with subependymal heterotopia. That the grey matter is further removed from its normal position in subependymal heterotopia than in subcortical heterotopia is too simple an interpretation and again demonstrates that position is not all in the genesis of pathophysiology.

Thus there exists a large body of work, animal and human, observational and experimental, to show that malpositioned neurons are not necessarily functionally misconnected, nor lesions consisting of such neurons necessarily epileptogenic. Malpositioning or dysmorphogenesis and misconnection or epileptogenesis may be associated but are not necessarily causally related.

How then can neuronal positioning and connectivity and cerebral morphology be associated?

WIRING: THE IMPLICIT LINK

The volume of the cortex increases hugely during ontogeny. There is much evidence to suggest that the development of the neuropil is responsible for the growth of the neocortex. The maximum rate of increase in cortical tangential extent is concurrent with neuronal elaboration of secondary and tertiary dendrites, and is therefore postmigrational[26]. Cortical neuronal dendritic maturation is associated with the ingression of corticopetal afferents; gyral development occurs concurrently with synaptogenesis[16,26]. Volumetric histological analysis reveals that the majority of the cortical ribbon is composed of material other than neuronal cell bodies[50]. Comparative intergyral measurements reveal that, for example, layer 4 is thicker where the cortical sensory input is greater[39], although cell density in areas of different function is the same[51].

There is a parallel increase in the volume of the neocortex through phylogeny. This progressive growth, however, is limited primarily to the surface area of the cortex[52]. Thus from the bat to the human, cortical thickness varies from 0.6 to 5 mm, a single order of magnitude; the expansion of the surface area, however, is over five orders of magnitude. It has been proposed that this difference is due to biophysical constraints on the length of the apical dendrites of pyramidal cells[52–54]. A more important consideration, however, may be that if the thickness of the cortex were to increase, and neurons to maintain extensive dendritic expansions, then the overlap in the radial dimension that would of necessity follow would inherently limit the access to these very neurons of incoming axons whose number perversely would need to increase per tangential unit area of cortex as more neurons would require connection. In order to maintain the probable parallel nature of processing function in the cortex[55], this hurdle has been sidestepped by expansion tangentially with limited increase of the thickness of the cortex. This also implies that in conditions in which the thickness of the cortex is pathologically increased, if the number of neurons in the radial extent is also proportionately greater, then for these neurons to remain connected, their dendritic expansions must be attenuated, implying altered interneuronal connectivity.

It would seem therefore that expansion of the cortex, that occurs in its surface area rather than its depth, is due to the development of interneuronal connections: the wiring that constitutes the neuropil. This is implicit in Richman's model of morphogenesis but it is not overtly stated. There is also a considerable body of evidence, however, that demonstrates its importance as a primary agent in dysmorphogenesis. This will now be reviewed.

(MIS)WIRING AND (DYS)MORPHOGENESIS

1. Barron in 1950[56] reported one of the few experiments performed in order to examine the causes of gyrogenesis. He was able to destroy various parts of the foetal sheep brain and then to examine the brain after several more days of intrauterine development. He showed primarily that the neocortex, separated from all its projectional targets and corticopetal fibre inputs nevertheless developed gyri and sulci. He also showed that when thalamic input to the presumptive visual cortex was removed that this region of cortex was less well endowed with secondary gyri than its undeafferented contralateral homologue. When the developing hemispheres were transected in the coronal axis, the caudal portion degenerated; the fissural pattern of the anterior remnants differed from comparable areas on unoperated foetuses. There was no histological examination of the lesioned brains, limiting the usefulness of the study. In addition, the specificity of the effects of surgery cannot be vouchsafed (see below). Nevertheless, Barron showed that cortical folding was an intracortically-generated event, and also that altered connections within the cortex and from subcortical structures could on occasion alter the final shape of the cortex.
2. That interneuronal connectivity is morphogenetic is also shown and discussed by Goldman and Galkin[57]. They performed prenatal prefrontal corticectomies in primates and subsequently compared the gyral patterns thus altered with those in postnatally operated

controls. They were able to demonstrate that the gyral pattern was altered not only in the operated area, as might be expected, but also in distant regions (e.g. occipital lobe) of the same hemisphere and also contralaterally. Although they were able to exclude prolongation of neurogenesis and interference with neuronal migration as possible explanations for their findings, they could not be confident that the trauma of surgery had not affected the foetus in some ill-defined systemic way, such as through transient ischaemia. Against this possibility, however, was their finding of normal 'general cytoarchitectonic composition' in the distantly affected gyri. It should be remembered that the prefrontal cortex is primarily associational and known to project in the rhesus monkey to the occipital lobe. The adjacent precentral gyrus of the dorsolateral convexity was unaffected, however: this argues against a non-specific mechanical—or indeed, vascular—effect of surgery as such effects would be expected to be more dramatic next to the lesioned area than in distant areas. More importantly, the precentral gyrus, unlike the affected occipital gyri, is not an associational region and thus intracortical connectional changes arising from the lesioning of prefrontal cortex would not be expected to alter connectivity, or the morphology, in this syrus. This was discussed by Goldman-Rakic[58].

Despite the loss of cortex, no specific neurobehavioural consequence was demonstrable in the prenatally-operated monkeys as compared to those operated on postnatally, who had predictable performance deficits on formal testing. It would seem that lesions that affect the development of the prefrontal cortex produce distant gyral changes as a result of altered connections between these regions. Connectivity can therefore be morphogenetic in this situation; altered connections and neuronal function must also be invoked to explain the lack of any functional deficit in prenatally lesioned animals.

3. By manipulating corticothalamic input, Rakic[31] provided a further example of the morphogenetic potency of interneuronal connectivity. When performed in the first half of gestation, bilateral enucleation led to the development of gyri in the normally smooth occipital convexity. This was due to an expansion of adjacent associational cortex into the region normally accommodating input from the lateral geniculate nucleus, without significant excess cell death. Thus altered connectivity, both increased and reduced, produced a morphogenetic change. Spontaneous congenital anophthalmia is a rare malformation in humans; in one documented case[59], it was associated with a reduced surface representation of Brodmann area 17, the homologous receptive region in the human.
4. In a number of human CD with undoubted gyral abnormalities of the hemispheres, there is often associated dysgenesis of the corpus callosum[60,61]. This is indirect evidence of altered connectivity and demonstrates its association with dysmorphogenesis, though it does not establish a causal link between the two. Thus in the Aicardi syndrome[62] there is GA and associated agenesis of the corpus callosum. Barkovich *et al*[63] have shown that callosal abnormalities are associated with GA on imaging and state that the first finding should lead to a search for the second. The author's own work has shown that in a case of subependymal heterotopia (SEH) associated with GA and in two of macrogyria associated with attenuated white matter, there is a significant alteration in the midline cross-sectional area of the corpus callosum—which may be increased as well as reduced in area—arguing again for altered connectivity in association with CD.
5. Detailed study of the histopathology of polymicrogyria[64,65] reveals that there are no axons or dendrites crossing the area of cell loss in lamina V (primarily) that is held to be responsible for the GA. Nevertheless, neurons were present superficial to the scar and must therefore have been connected, as unconnected neurons do not seem to be able to survive in the adult cortex[66]. Given that there were not processes crossing the laminar necrosis of layer V, as one would expect for overlying neurons, then these neurons must have been abnormally connected—as well as being thrown into abnormal gyral configurations. In an experimental parallel of this situation, Jones *et al*[67] demonstrated the development of altered and abnormal connections in the rat neocortex after the ablation of precursor cells of layers II to IV.
6. McConnell[68] has argued that attempts to understand normal and abnormal adult cerebral structure and function are inevitably hampered by the ephemeral nature of structures used in embryogenesis for morphogenesis; these include the radial glial fibres believed to guide migrating neurons along their route and the subplate neurons that are

generated first in cortical development. Thalamic axons arrive at the developing cortex at an early stage, before neurons of the definitive cortical plate have migrated to their final positions, but do not form synapses with their eventual target neurons for a considerable time (possibly months in some primates). It is believed that in the interim, they may synapse on subplate neurons—certainly synapses are seen in the subplate and electrical synaptic activity has been recorded from the subplate[19]. Selective destruction of the subplate neurons[20] leads to subsequent miswiring. Although no comment on morphogenesis was made in this paper, altered connectivity is seen to occur as a result of prior-altered connections (between the subplate and thalamic axons), thus demonstrating both the importance of McConnell's caveat and the conceptual importance of connectivity on subsequent development.

There is, therefore, much evidence to suggest that interneuronal connectivity is morphogenetic, and that dysmorphogenesis may result from misconnection of neurons. What of epileptogenesis?

CONNECTIVITY AND EPILEPTOGENESIS

1. The presence of morphologically aberrant cells has been shown in CD in the few studies which have addressed this problem. Bordarier *et al*[69] examined the orientation of pyramidal neurons in agyric cortex post-mortem in a child with abnormality of chromosome 17. The cortex was four-layered. In the superficial neuronal layer, consisting of pyramidal cells and small round neurons, 80% of the pyramidal cells had a radial inversion such that their apical dendrites were directed centripetally rather than centrifugally. In the deeper neuronal layer such reversed orientation was not seen. This finding is consistent with a similar reversal seen with laminar inversion in the cortex of the reeler mutant mouse, and is compatible with the findings of Pinto Lord[70] that axons and dendrites grow most prolifically where the two meet. Unfortunately in this study, whilst neuronal abnormality has been demonstrated, no assessment of connectivity is possible.
2. In the report by Takada *et al*[71], however, dendritic development in agyric visual cortex was examined in two cases using Golgi staining. They showed that the visual cortex was considerably thicker than expected for the age of the patients (4200 and 5800 μm compared with 2000 for the controls). Unfortunately quantitation of cell numbers was not performed, so it is not possible to determine whether this implies that dendritic fields were necessarily attenuated as would be predicted (see above). However a limited number of neurons were studied in greater detail and a number of variables were quantified. Most interestingly, they were able to demonstrate a significant reduction in the total apical dendritic length, the number of orders of branching of apical dendrites, the number of branches themselves and their complexity for pyramidal neurons in both the superficial and deep cellular layers of the four-layered cortex in the older of their two cases. Abnormalities, when compared to age-matched controls, were also present but less dramatic for the younger of the two cases. Again, as the development of dendrites depends on the axonal microenvironment in which they find themselves[70], this finding argues for abnormal connectivity beyond a simple inversion of orientation, and more towards an extensive miswiring (quantitatively and possibly in terms of complexity). Sadly, there are very few similar quantitative analyses. In one qualitative report[65], changes in dendritic morphology and orientation were found in a polymicrogyric brain.

The above points beg the question of the causal nature of these changes. That misconnection (as manifested by altered dendritic expansion) is functionally significant and indeed causal in nature is shown by evidence from a number of sources.

3. Patients with Down's syndrome have an increased prevalence of epilepsy; histopathological analysis of the brain in this condition is of interest. Before the inevitable onset of dementia, the macroscopic appearance of the brain in Down's syndrome is completely normal. Extensive analysis at the microscopic level using conventional staining techniques is also normal. However, using the Golgi stain, Becker and his coworkers[72] have demonstrated extensive synaptic dysgenesis. There are also known to be electrophysiological abnormalities at the cellular level[73]. This strongly argues for the importance of neuronal integrity and interneuronal connectivity in the generation of dysfunction as well as showing that dysmorphogenesis need not accompany either misconnection or dysfunction. That such patients are also retarded to varying degrees

argues that particular patterns of misconnection, rather simply than its mere presence, are likely to be important. This aspect of the problem may prove least amenable to quantitative analysis.

4. Huttenlocher studied dendritic development in a small volume of the middle frontal gyrus obtained either at autopsy or operative biopsy from five severely retarded infants with seizures and compared the results quantitatively with development in controls and older individuals with retardation, some of whom also had seizures[74]. He used the Golgi technique to highlight dendritic morphology, but stated that the method would be too tedious to apply to large areas of the brain. Nevertheless, in this restricted area, he showed that the gross appearance of the brain was normal and that routine histological and electron microscopic analysis was also unremarkable, although details were not provided. On Golgi staining, however, he was able to identify a marked sparsity of the dendritic expansion in the infants, but not in the older patient group. This difference was quantifiable and occurred in all laminae, although only the results from layers III and V were presented. The length and branching complexity of both basal and apical dendrites were reduced, with a paucity of spines on the dendrites suggesting a reduced number of synapses. Abnormal findings were not apparent in the older, less severely retarded patients, and this was ascribed partly to the relative insensitivity of the technique. In four of five infants, brain size was also significantly reduced: based on the previously-discussed major contribution of the growth of the neuropil to cortical expansion, this is not an unexpected finding. The shortest interval between seizure onset and histological analysis was six months, although in one case the biopsy was obtained at twenty months following a 'few days' only of seizures (which are not described in any greater detail). Thus although the possibility exists that seizure activity may have produced the dendritic abnormalities, the absence of similar findings in the cortex of the older patients, who had had seizures for many years argues against this and rather for a causative role of the dendritic attenuation.

   At a more detailed structural level, Purpura[75] found abnormal dendritic spine morphology in cortical cells from three retarded infants with epilepsy, whose brains were macroscopically normal.

   Thus abnormal function (developmental decline and epilepsy) was probably caused in these cases by connectional abnormalities, without, it should be noted, gyral dysgenesis.

5. Ferrer *et al*[76] report the finding of abnormally-distributed and shaped local-circuit neurons, identified by immunostaining, in a surgically resected, macroscopically-normal specimen from the peri-Rolandic area. The dendritic expansions of these neurons were atypical for the morphology of their cell bodies, arguing for associated abnormalities of their connections to other neurons. Unfortunately, the electrophysiological characteristics of these neurons were not studied, although electrocorticographic evidence of epileptogenesis localized to the areas where abnormal neurons were common. The authors do not report whether the epilepsy partialis continua that afflicted the patient was stopped: we must presume that it was. Nevertheless, this report demonstrates the importance of neuronal connectional abnormalities in the genesis of epilepsy.
6. Experimental work involving the creation of a transient epileptic focus in the rat hippocampus[77] by the injection of cholera or tetanus toxins has shown that epileptogenesis is associated with electrophysiological and morphological changes in hippocampal pyramidal neurons without any alteration in their number or position in the hippocampus. Thus abnormal connectivity can produce abnormal function without the need to invoke abnormal neuronal position or dysmorphogenesis.

CONNECTIVITY: A MODIFIED HYPOTHESIS

In the light of the importance of connectivity, and the problems with the current overall model linking neuronal malpositioning with epileptogenesis, an alternative hypothesis is proposed.

This is that interneuronal connectivity, through neuropil growth, is the primary influence on morphogenesis and, independently, the substrate for function. Equally, misconnection is held responsible for abnormal function (epileptogenesis) and, independently, dysmorphogenesis, the latter only occurring if misconnection is extensive enough. The old and new hypotheses may be summarized diagrammatically thus:

Old

(Mal)Position → (Mis)Connection →

(Dys)Morphogenesis → (Dys)Function

New

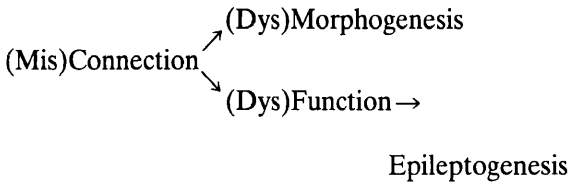

The new hypothesis may be further extended to include the phenomenon of neuronal malpositioning, which no longer occupies a position of determinative importance. It may, however, reflect an earlier insult resulting in both malpositioning and, independently, misconnection thus:

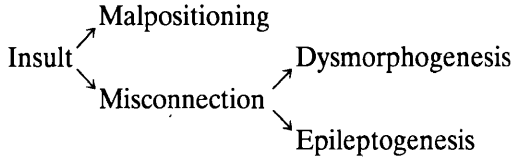

Many insults are known to be able to produce malpositioning or misconnection; how they act is not clear. In the 'reeler' mutant, for example, Pinto Lord and Caviness[78] have shown indirectly that there is an abnormal adhesion of neurons to radial glial fibres such that late migrating neurons are not able to pass between previously-migrated neurons which remain in stubborn contact with the glial guides. Thus, they pile up proximally and eventually the cortical laminar inversion characteristic of the reeler mutant is produced. Palmini *et al*[79] have proposed a model for neuronal malpositioning based on temporospatially distributed disturbances of glial guide-neuron adhesion. Neither Palmini nor Pinto Lord, however, are able to show whether the postulated patterns of disturbance of intercellular adhesion are neuronal or glial in origin—or even both.

Nevertheless, it is now clear that malpositioning of itself does not lead to misconnection, as the reeler mutant demonstrates. This would seem to argue for a neuronal cause for misconnection, rather than an extraneuronal cause, for example in the scaffolding or the glia. That in some cases of epilepsy, abnormal neurons are indeed found (e.g. focal cortical dysplasia, DNT) also suggests a primary neuronal abnormality causing misconnection. Abnormal multinucleated neurons have also been found in polymicrogyric brains[80] and in a case of unilateral megalencephaly associated with subcortical neuronal heterotopia, neuronal nuclear and nucleolar volumes, DNA and RNA were all increased[81]. A mutation in a homeotic developmental control gene (Small eye, a point mutation at the Pax-6 locus) is associated with delayed neuronal migration and impaired axonogenesis in the mouse[82]. A recent report has identified a gene defect in human subjects with some forms of lissencephaly[83]; the normal gene product has a significant homology to β-subunits of G proteins, which participate in signal transduction in pyramidal neurons and may be involved in growth cone collapse. Deletion of a neural cell adhesion molecule[84] and the involvement of neural NMDA receptors in cell migration[85] have also recently implicated the neuron centrally in the generation of abnormal brain structure.

Thus there would seem to be a primary neuronal role, whatever the actual cause, in malpositioning and misconnection.

IMPLICATIONS OF THE NEW HYPOTHESIS

1. Although intuitive and predictive of some of the morphological changes seen in various forms of CD, Richman *et al*'s model has been shown to be inadequate in certain cases. The new hypothesis, however, lends itself to a more robust modelling of gyrogenesis based primarily and explicitly on interneuronal connectivity. This model can also take into account other ontogenetic events, such as programmed cell death[66], not considered by Richman, but which may have marked effects on morphogenesis. In essence the model attempts to reproduce brain growth and morphogenesis assuming that interneuronal connectivity is the motive force in these processes. It employs new methodologies from the study of complexity in the prediction of the effect of iterative connectional changes between a large number of identical topologically non-overlapping units (representing neurons) whose individual growth is determined by connections and in turn determines the shape of the aggregate structure, the brain. Subtle alterations of connectivity can be modelled, and the new hypothesis could be tested more easily at a theoretical level: this model is more powerful than that of Richman *et al* because it is more detailed and flexible. Further details of this model cannot be included because of constraints of space (unpubl. res.).
2. The old supposition that misplaced neurons would necessarily be epileptogenic has been shown to be false; in any case it could not explain why lesions such as DNTs should be epileptogenic—based on morphological analysis only, it is not possible to say where dysplastic neurons in these (or any other) lesions should have been positioned. How-

ever, it has been shown that dysplastic neurons may have abnormal connections (see above). Thus it is conceivable that dysplastic neurons in DNTs are abnormally connected and therefore the lesion epileptogenic. Using Golgi staining and neuronal process-tracing techniques (e.g. with DiI), it should now be possible to determine whether this is indeed the case and thus provide (an interim, at least) explanation of the epileptogenic potential of DNTs.

3. DNTs also illustrate another aspect of the modified hypothesis. It is known that whilst the majority of patients who have surgical resection of their DNTs become seizure-free post-operatively, some do not. If dysplastic neurons in DNTs do represent a collection of misconnected neurons, then it is not unreasonable to suppose that their removal should also remove the focus of epileptogenesis. However, in some cases, the DNT may simply be a local marker of more extensive connectional disruption and thus its removal would not necessarily cure the epilepsy.

   Using volumetric MR data, quantitative measurements of the regional distribution of white and grey matter have been performed[86]. The statistical distribution of such measurements is narrow for neurologically normal controls and from them a normal range can be established for various volumetric and distributional parameters. Preliminary analysis of similar data for patients with DNTs has shown that there are no abnormalities (defined as volume or volume ratio measurements more than three standard deviations from the mean value for the controls) of grey or white matter volume distribution in the pre-operative MR scans of those patients who are seizure-free following the removal of their DNT. Patients who continue to have seizures despite the complete resection of their lesion (as shown by post-operative MR scans) had many abnormalities of volume distribution in their pre-operative scans, that were not apparent to unaided visual inspection of those scans and were outside the lesion. Given that the majority of the grey matter is neuropil, this finding suggests that there is extensive connectional abnormality in such patients (even if the proportion of grey matter occupied by neuropil is different in DNTs this still argues for altered connectivity in DNTs, worse for some than for others). That some of these connectional abnormalities are distant from the lesion makes it unlikely that focal resection of the lesion alone will render the patient seizure-free.
4. In general, patients with gyral anomalies are less likely to become seizure-free than, for example, patients with hippocampal sclerosis, when the visible lesion alone in each group is excised at operation. Current thinking ascribes this to a more extensive abnormality of cerebral structure in GA than can be seen by either the eye at operation or on MR scanning, but there is no published proof of this. Using the same methodology as was applied to DNTs above, it has been shown[86] that 18/18 patients with GA had abnormalities of regional volume distribution of grey or white matter, and that in 15/18 cases, such abnormalities lay outside the MR-visualized lesion. This provides evidence for the hypothesis that abnormalities of structure in the brains of patients with GA are extensive and would explain why the removal of the lesion alone would not necessarily render the patient seizure-free. Using the same technique, volumetric scans of ten patients with histologically-proven hippocampal sclerosis, all of whom had complete hippocampal resection on post-operative MR scans, were examined. None had any abnormalities of grey or white matter volume distribution and, to date, all are seizure-free post-operatively (minimum follow-up period twelve months). The hypothesis would predict that patients with GA would fare badly if their scan analysis revealed extralesional abnormalities and they were subjected to surgery: this is a falsifiable claim, thus ensuring that the new hypothesis is testable. Conversely, however, it should be made clear that the absence of such volumetric anomalies would not necessarily predict operative success!

As the application of MR techniques increases, it may become less likely still that patients with CD undergo surgical attempts to cure them of their epilepsy. It thus becomes more important that resected—and post-mortem—specimens are studied whenever possible using advanced histopathological techniques and quantitative Golgi analyses. Many of these methods can be applied to stored fixed specimens, and such analyses would constitute an important test of the hypothesis for patients with gyral abnormalities in particular and those without visible lesions in general.

It is likely however that this modified hypothesis is still a simplification of the real situation, as

to some extent is inevitable. McConnell[87] has performed transplantation experiments taking ventricular epithelium from rats of a given gestational age and implanting it into more developed cortex. The fate of the transplanted neurons appears only partly fixed at a given stage of development, and it is possible that the position of a neuron may affect its fate and, thus, its connectivity, if it finds itself in an abnormal position before it should. This is an artificial situation however, and it is not comparable to that obtaining in the conditions being considered here, as all the neurons have left the germinal epithelium by the time they are involved in a pathological situation. That such subtleties abound should not, however, be forgotten. Thus, for example, it is known that epileptic activity can itself alter interneuronal connectivity[88,89]: however the proposition here is that abnormal connectivity prior to the onset of epilepsy is responsible for abnormal morphogenesis and subsequent epileptogenesis (which may itself then further alter connectivity).

CONCLUSION

It is known that in certain cases of chronic partial epilepsy, underlying structural abnormalities of the brain are present and presumably responsible for the epilepsy. Richman *et al* attempted to relate one aspect of the structure of these brains, neuronal malpositioning, to another, cerebral dysmorphogenesis. Subsequently, the link was made to function and it was assumed that abnormal structure—in this case, abnormal neuronal positioning—was the cause of the abnormal function—epilepsy. With the use of magnetic resonance scanning, the presence of such lesions in the brains of patients with chronic partial epilepsy has been found increasingly more frequent, making this an important area of research given that resection of dysgenetic areas may on occasion cure patients of their epilepsy.

However, the validity of Richman's model has been questioned and found wanting. Whilst it remains likely that interneuronal connectivity is the primary cause of neocortical growth, as was implicit in their model, the model itself cannot explain other findings of abnormal morphogenesis associated with neuronal malpositioning, as for example found in Zellweger's syndrome.

In addition, the assumption that neuronal malpositioning was also epileptogenic has been challenged and found to be not necessarily correct. Malpositioned neurons may not be abnormally connected, nor do they always lead to dysmorphogenesis visible to the eye. Neither do dysgenetic lesions always result in epilepsy.

Instead, it is suggested that interneuronal connectivity is not only the primary force in morphogenesis, but that it is also responsible for visible dysmorphogenesis and, independently of the finding of abnormal shape, responsible also for abnormal function in the guise of epileptogenesis. Thus abnormal neuronal position and abnormal cerebral function are separable: their co-occurrence may reflect a common disruptive insult to neuronal maturation.

The hypothesis offers an explanation for dysmorphic abnormalities that are difficult to understand in Richman *et al*'s model and generates a model of cerebral morphogenesis that is more flexible and powerful. It also provides an explanation for the epileptogenic potential of dysgenetic lesions, such as DNTs. That abnormal function in this model can occur without the accompaniment of visibly abnormal structure could help to explain why resection of the visible lesion at surgery may not always lead to a cessation of seizure activity.

The hypothesis could be tested at a number of levels. Macroscopically, further correlation between the finding of abnormal connection parameters (e.g. altered relationships of corpus callosum areas to cortical volumes, or alterations of other surrogate measures of connectivity) and a poor surgical outcome would be a clinically important test. If shown to hold true, it might also become an important prognosticator of surgical outcome. At the histological level, the hypothesis could be tested by examining the numbers of neurons in dysgenetic lesions and by quantifying their connectivity using both Golgi staining and other new staining techniques. Lastly, the demonstration of abnormal neuronal functional interactions would test whether structural changes were associated with functional changes at the cellular level. This may help to unravel the mechanisms of epileptogenesis in some cases of chronic partial epilepsy: it is not inconceivable that this might also shed light on other epileptic syndromes and make more rational our care of those patients with refractory partial epilepsy.

ACKNOWLEDGMENTS

The author is supported by the Wellcome Trust and would like to thank Dr J.C.M. Porter.

REFERENCES

1. Richman, D.P., Stewart, R.M., Hutchinson, J.W. and Caviness, V.S. Jr. Mechanical model of brain convolutional development. *Science* 1975; **189**: 18–21.
2. Jacobson, M. *Developmental Neurobiology.* 2nd edition New York, Plenum Press, 1978.
3. Squier, M.V. Development of the cortical dysplasia of type II lissencephaly. *Neuropathology and Applied Neurobiology* 1993; **19**: 209–213.
4. Barth, P.G. Disorders of neuronal migration. *Canadian Journal of Neurological Sciences* 1987; **14**: 1–16.
5. Daumas-Duport, C. Dysembryoplastic neuroepithelial tumours. *Brain Pathology* 1993; **3**: 283–295.
6. Raymond, A.A., Halpin, S.F.S., Alsanjari, N. *et al.* Dysembryoplastic neuroepithelial tumour: features in 16 patients. *Brian* 1994; **117:** 461–476.
7. Taylor, D.C., Falconer, M.A., Bruton, C.J. and Corsellis, J.A. Focal dysplasia of the cerebral cortex in epilepsy. *Journal of Neurology, Neurosurgery and Psychiatry* 1971; **34**: 369–387.
8. Meencke, H. Neuron density in the molecular layer of the frontal cortex in primary generalised epilepsy. *Epilepsia* 1985; **26**: 450–454.
9. Raymond, A.A., Fish, D.R., Sisodiya, S.M., Alsanjari, N., Stevens, J.M. and Shorvon S.D. Abnormalities of gyration, heterotopia, fibrous sclerosis, focal cortical dysplasia, microdysgenesis, dysembryoplastic neuroepithelial tumor and dysgenesis of the anticortex in epilepsy: clinical electroencephalographic and neuroimaging features in 100 adult patients. *Brain* 1995; (in press).
10. Raymond, A.A., Cook, M.J.C., Fish, D.R. and Shorvon, S.D. Cortical dysgenesis in adults with epilepsy. In: *Magnetic Resonance Scanning and Epilepsy.* (Eds S.D. Shorvon, D.R. Fish, F. Andermann, G.M. Bydder, H. Stefan). New York, Plenum Press, 1993: 89–94.
11. Palmini, A., Andermann, F., Olivier, A., Tampieri, D. and Robitaille Y. Focal neuronal migration disorders and intractable partial epilepsy: results of surgical treatment. *Annals of Neurology* 1991; **30**: 750–757.
12. Jones, E.G. and Peters, A. (Eds). *Cerebral Cortex, Vol 1 Cellular Components of the Cerebral Cortex.* New York, Plenum Press, 1984.
13. *Gray's Anatomy.* 37th edition (Eds P.L. Williams, R. Warwick, M. Dyson and L.H. Bannister). Edinburgh, Churchill Livingston, 1989.
14. Caviness, V.S. Jr. Normal development of the cerebral neocortex. In: *Developmental Neurobiology, Nestlé Nutrition Workshop Series, Vol 12.* (Eds P. Evrard and A. Minkovski). New York, Vevey/Raven Press, 1989: pp. 1–10.
15. Marin-Padilla, M. Neurons of layer I: a developmental analysis. In: *Cerebral Cortex, Vol 1.* (Eds E.G. Jones and A. Peters). New York, Plenum Press, 1984: pp. 447–478.
16. Molliver, M.E., Kostovic, I. and Van der Loos H. The development of synapses in the cerebral cortex of the human fetus. *Brain Research* 1973; **50**: 403–407.
17. Williams, R.S. Abnormal development and destructive processes of the human brain during the first half of gestation. In: *Developmental Neurobiology, Nestlé Nutrition Workshop Series, Vol 12* (Eds P. Evarard and A. Minkowski). New York, Vevey/Raven Press, 1989: pp. 10–20.
18. Angevine, J.B. and Sidman, R.L. Autoradiographic study of cell migration during histogenesis of cerebral cortex in the mouse. *Nature* 1961; **192:** 766–768.
19. Shatz, C.J., Chun, L.L. and Luskin, M.N. The role of the subplate in the development of the mammalian telencephalon. In: *Cerebral Cortex, Vol 7* (Eds E.G. Jones and A. Peters). New York, Plenum Press, 1984: pp. 35–58.
20. Ghosh, A., Antonini, A., McConnell, S.K. and Shatz, C.J. Requirement for subplate neurons in the formation of thalamocortical connections. *Nature* 1990; **347**: 179–181.
21. Sarnat, H.B. Disturbances of late neuronal migration in the perinatal period. *American Journal of Diseases of Childhood* 1987; **141**: 969–980.
22. Peters, A. Classification of cortical neurons. In: *Cerebral Cortex, Vol 1* (Eds E.G. Jones and A. Peters). New York, Plenum Press, 1984: pp. 107–122.
23. Jones, E.G. Laminar distribution of cortical efferent cells. In: *Cerebral Cortex, Vol 1* (Eds E.G. Jones and A. Peters). New York, Plenum Press, 1984: pp. 521–554.
24. Rakic, P., Bourgeois, J., Eckenhoff, M.E., Zecevic, N. and Goldman-Rakic, P.S. Concurrent overproduction of synapses in diverse regions of the primate cerebral cortex. *Science* 1986; **232**: 232–235.
25. Marin-Padilla, M. Prenatal and early postnatal ontogenesis of the human motor cortex: a Golgi study. I. The sequential development of the cortical layers. *Brain Research* 1970; **23**: 167–183.
26. Chi, J.G., Dooling, C. and Gilles, F.H. Gyral development of the human brain. *Annals of Neurology* 1977; **1**: 86–93.
27. Ono, M., Kubik, S. and Abernathey, C.D. Atlas of the cerebral sulci. New York, Thieme Medical Publishers, Inc., 1990.
28. Jenkins, G. B. Contributions in Embryology. 1921; **13:** 41 (quoted in 1).
29. Walsh, C. and Cepko, C. Clonal dispersion in proliferative layers of developing cerebral cortex. *Nature* 1993; **362**: 632–635.
30. Tan, S. and Breen, S. Radial mosaicism and tangential cell dispersion both contribute to mouse neocortical development. *Nature* 1993; **362**: 638–640.
31. Rakic, P. Specification of cerebral cortical areas. *Science* 1988; **241**: 170–176.
32. Price, J. Organizing the cerebrum. *Nature* 1993; **362**: 590–591.
33. Rakic, P. Defects of neuronal migration and the pathogenesis of cotical malformations. *Progress in Brain Research* 1988; **73**: 15–37.
34. Meencke, H. and Veith, G. Migration disturbances in epilepsy. In: *Molecular Neurobiology of Epilepsy (Epilepsy Research Supplement 9)* (Eds J. Engel Jr., C. Wasterlain, E.A. Cavalheiro, U. Heinemann and G. Avanzini). Elsevier Science Publisher B.V. 1992: pp. 32–40.
35. Sarnat, H.B. Cerebral dysplasias as expressions of altered maturational processes. *Canadian Journal of Neurological Sciences* 1991; **18**: 196–204.
36. Sidman, R.L. and Rakic, P. Neuronal migration, with special reference to developing human brain: a review. *Brain Research* 1973; **62**: 1–35.
37. Armstrong, E., Curtis, M. and Buxhoeveden, D.P. *et al.* Cortical gyrification in the rhesus monkey: a test of the mechanical folding hypothesis. *Cerebral Cortex* 1991; **1**: 426–432.
38. Prothero, J.W. and Sundsten, J.W. Folding of the cerebral cortex in mammals: a scaling model. *Brain Behaviour and Evolution* 1984; **24**: 152–167.
39. Welker, W. Why does cerebral cortex fissure and fold? a review of determinants of gyri and sulci. In: *Cerebral*

Cortex, Volume 8B (Eds E.G. Jones and A. Peters). New York, Plenum Press, 1984: pp. 3–136.
40. Bok, S.T. *Histonomy of the Cerebral Cortex.* Amsterdam, Elsevier Publishing Company, 1959.
41. Della Giustina, E., Goffinet, A.M., Landrieu, P. and Lyon, G. A Golgi study of the brain malformation in Zellwéger's cerebro-hepato-renal disease. *Acta Neuropathologica (Berl)* 1981; **55**: 23–28.
42. Evrard, P., Caviness, V.S. Jr., Prats-Vinas, J. and Lyon, G. The mechanism of arrest of neuronal migration in the Zellweger malformation: an hypothesis based upon cytoarchitectonic analysis. *Acta Neuropathologica (Berl)* 1978; **41**: 109–117.
43. Caviness, V.S. Jr., Crandall, J.E. and Edwards, M.A. The reeler malformation. In: *Cerebral Cortex, Vol 7.* (Eds E.G. Jones and A. Peters). New York, Plenum Press, 1984: pp. 59–89.
44. Simmons, P.A., Lemmon, V. and Pearlman, A.L. Afferent and efferent connections of the striate and extrastriate visual cortex of the normal and reeler mouse. *Journal of Comparative Neurology* 1982; **211**: 295–308.
45. McConnell in discussion for chapters by Caviness, Williams and Evrard. In: *Developmental Neurobiology, Nestlé Nutrition Workshop Series, Vol 12.* (Eds P. Evrard and A. Minkowski). New York, Vevey/Raven Press, 1989: pp. 43–48.
46. Jensen, K.F. and Killackey, H.P. Subcortical projections from ectopic neocortical neurons. *Proceedings of the National Academy of Sciences, USA* 1984; **81**: 964–968.
47. Kuzniecky, R., Andermann, F. and Guerrini, R. The epileptic spectrum in the congenital bilateral perisylvian syndrome. *Neurology* 1994; **44**: 379–385.
48. Huttenlocher, P.R., Taravath, S. and Mojtahedi, S. Periventricular heterotopia and epilepsy. *Neurology* 1994; **44**: 51–54.
49. Barkovich, A.J. and Kjos, B.O. Gray matter heterotopias: MR characteristics and correlation with developmental and neurologic manifestations. *Radiology* 1992; **182**: 493–499.
50. Haug, H. Remarks on the determination and significance of the gray cell coefficient. *Journal of Comparative Neurology* 1956; **104**: 473–492.
51. Rockel, A.J., Hiorns, R.W. and Powell, T.P.S. The basic uniformity in structure of the neocortex. *Brain* 1980; **103**: 221–244.
52. Haug, H. Brain sizes, surfaces, and neuronal sizes of the cortex cerebri: a stereological investigation of man and his variability and a comparison with some mammals (primates, whales, marsupials, insectivores, and one elephant). *American Journal of Anatomy* 1987; **180**: 126–142.
53. Hofman, M.A. Size and shape of the cerebral cortex in mammals. *Brain Behaviour and Evolution* 1985; **27**: 28–40.
54. Hofman, M.A. The fractal geometry of convoluted brains. *Journal Hirnforschung* 1991; **32**(1): 103–111.
55. Eccles, J.C. The cerebral neocortex: a theory of its operation. In: *Cerebral Cortex, Vol 2* (Eds E.G. Jones and A. Peters). New York, Plenum Press, 1984: pp. 1–36.
56. Barron, D.H. An experimental analysis of some factors involved in the development of the fissure pattern of the cerebral cortex. *Journal of Experimental Zoology* 1950; **113**: 553–573.
57. Goldman, P.S. and Galkin, T.W. Prenatal removal of frontal association cortex in the fetal rhesus monkey: anatomical and functional consequences in postnatal life. *Brain Research* 1978; **152**: 451–485.
58. Goldman-Rakic, P.S. Morphological consequences of prenatal injury to the primate brain. *Progress in Brain Research* 1980; **53**: 3–19.
59. Bolton, J.S. Anophthalmia in a human fetus. *Philosophical Transactions of the Royal Society of London (Ser B)* 1900; **193**: 165.
60. Parrish, M.L., Roessmann, U. and Levinsohn, M.W. Agenesis of the corpus callosum: a study of the frequency of associated malformations. *Annals of Neurology* 1979; **6**: 349–354.
61. Billette de Villemeur, T., Chiron, C. and Robain, O. Unlayered polymicrogyria and agenesis of the corpus callosum: a relevant association? *Acta Neuropathologica (Berl)* 1992; **83**: 265–270.
62. Chevrie, J.J. and Aicardi, J. The Aicardi syndrome. In: *Recent Advances in Epilepsy, Vol 3* (Eds T.A. Pedley and B.S. Meldrum). Edinburgh, Churchill Livingston, 1986: pp. 189–210.
63. Barkovich, A.J. and Norman, D. Anomalies of the corpus callosum: correlation with further anomalies of the brain. *American Journal of Neuroradiology* 1988; **9**: 493–501.
64. Williams, R.S. The cellular pathology of microgyria. *Acta Neuropathologica (Berl)* 1976; **36**: 269–283.
65. Ferrer, I. A Golgi analysis of unlayered polymicrogyria. *Acta Neuropathologica (Berl)* 1984; **65**: 69–76.
66. Maxwell Cowan, W., Fawcett, J.W., O'Leary, D.D.M. and Stanfield, B.B. Regressive events in neurogenesis. *Science* 1984; **225**: 1258–1265.
67. Jones, E.G., Valentino, K.L. and Fleshman, J.W.J. Adjustment of connectivity in the rat neocortex after prenatal destruction of precursor cells of layers II–IV. *Developmental Brain Research* 1982; **2**: 425–431.
68. McConnell, S.K. Perspectives on early brain development and the epilepsies. In: *Molecular Neurobiology of Epilepsy (Epilepsy Research Suppl 9)* (Eds J. Engel Jr., C. Wasterlain, E.A. Cavalheiro, U. Heinemman and G. Avanzini). Elsevier Science Publishers B.V., 1992: pp. 183–191.
69. Bordarier, C., Robain, O., Rethore, M., Dulac, O. and Dhellemes, C. Inverted neurons in agyria. *Human Genetics* 1986; **73**: 374–378.
70. Pinto Lord, M.C. and Caviness, V.S. Jr. Determinants of cell shape and orientation: a comparative Golgi analysis of cell–axon interrelationships in the developing neocortex of normal and reeler mice. *Journal of Comparative Neurology* 1979; **187**: 49–70.
71. Takada, K., Becker, L.E. and Chan, F. Aberrant dendritic development in the human agyric cortex: a quantitative and qualitative Golgi study of two cases. *Clinical Neuropathology* 1994; **7**: 111–119.
72. Jagadha, V. and Becker, L.E. Dendritic pathology: an overview of Golgi studies in man. *Canadian Journal of Neurological Sciences* 1989; **16**: 41–50.
73. Becker, L.E. Synaptic dysgenesis. *Canadian Journal of Neurological Sciences* 1991; **18**: 170–180.
74. Huttenlocher, P.R. Dendritic development in neocortex of children with mental defect and infantile spasms. *Neurology* 1974; **24**: 203–210.
75. Purpura, D.P. Dendritic spine 'dysgenesis' and mental retardation. *Science* 1974; **186**; 1126–1128.
76. Ferrer, I., Pineda, M., Tallada, M. *et al.* Abnormal local-circuit neurons in epilepsia partialis continua associated with focal cortical dysplasia. *Acta Neuropathologica (Berl)* 1992; **83**: 647–652.
77. Traub, R.D., Jefferys, J.G.R. and Miles, R. Analysis of the propagation of disinhibition-induced after-discharges along the guinea pig hippocampal slice in vitro. *Journal of Physiology* 1993; **472**: 267–287.
78. Pinto Lord, M.C., Evrard, P. and Caviness, V.S. Jr.

Obstructed neuronal migration along radial glial fibres in the neocortex of the reeler mouse: a Golgi-EM analysis. *Developmental Brain Research* 1982; **4**: 379–393.

79. Palmini, A., Andermann, F., de Grissac, H. *et al.* Stages and patterns of centrifugal arrest of diffuse neuronal migration disorders. *Developmental Medicine and Child Neurology* 1993; **35:** 331–339.
80. De Leon, G.A. Observations on cerebral and cerebellar microgyria. *Acta Neuropathologica (Berl)* 1972; **20:** 278–287.
81. Manz, H.J., Phillips, T.M., Rowden, G. and McCullough, D.C. Unilateral megalencephaly, cerebral cortical dysplasia, neuronal hypertrophy, and heterotopia: cytomorphometric, fluorometric cytochemical, and biochemical analyses. *Acta Neuropathologica (Berl)* 1979; **45**: 97–103.
82. Schmahl, W., Knoedlseder, M., Favor, J. and Davidson, D. Defects of neuronal migration and the pathogenesis of cortical malformations are associated with Small eye (Sey) in the mouse, a point mutation at the Pax-6-locus. *Acta Neuropathologica (Berl)* 1993; **86**: 126–135.
83. Reiner, O., Carrozzo, R., Shen, Y. *et al.* Isolation of a Miller-Dieker lissencephaly gene containing G protein β-subunit-like repeats. *Nature* 1993; **364**: 717–721.
84. Tomasiewicz, H., Ono, K., Yee, D. *et al.* Genetic deletion of a neural cell adhesion molecule variant (N-CAM-180) produces distinct defects in the central nervous system. *Neuron* 1993; **11**: 1163–1174.
85. Komuro, H. and Rakic, P. Modulation of neuronal migration by NMDA receptors. *Science* 1993; **260**: 95–97.
86. Sisodiya, S.M., Free, S.L., Stevens, J.M., Fish, D.R. and Shorvon, S.D. Widespresd cerebral structural changes in patients with cortical dysgenesis and epilepsy. *Brain* 1995; (in press).
87. McConnell, S.K. and Kaznowski, C.E. Cell cycle dependence of laminar determination in developing neocortex. *Science* 1991; **254**: 282–285.
88. Represa, A., Jorquera, I., La Salle, G.L.G. and Ben-Ari, Y. Epilepsy induced collateral sprouting of hippocampal mossy fibers: does it induce the development of ectopic synapses with granule cell dendrites? *Hippocampus* 1994; **3:** 257–268.
89. Babb, T.L., Kupfer, W.R., Pretorius, J.K., Crandall, P.H. and Levesque, M.F. Synaptic reorganisation by mossy fibres in human epileptic fascia dentata. *Neuroscience* 1991; **42**: 351–363.